Extrachromosomal regulators of phenotypic heterogeneity in *Saccharomyces* species

LAURA ANN PETCH

Thesis submitted to the University of Kent for the degree of PhD in Genetics

DECLARATION

No part of this thesis has been submitted in support of an application for any degree or other qualification at the University of Kent, or any other University or Institution of learning.

L. A. Petch

August 2020

ACKNOWLEDGEMENTS

I would like to thank Professor Mick Tuite for the initial opportunity to work on '*Prion-mediated phenotypic heterogeneity in wild yeast'* as an undergraduate summer student; for without that summer I would not have discovered my passion for laboratory research. I would like to thank him for the opportunity to work on this PhD project, and for his outstanding support and guidance throughout. I would like to express my gratitude to him for inspiring me and always pushing me to achieve my best.

I want to thank my friends and colleagues in Kent Fungal Group and the School of Biosciences, who have helped me in so many ways and made my time in the laboratory one that I will cherish forever.

I would like to thank my Mum, my friends, and my best friends Natalie and Amber Petch, for their compassion and encouragement throughout. I thank them for listening to so many talk rehearsals when they may as well have been in a different language.

A very special mention must go to Nicholas Canavan, who entered my life towards the end of this PhD yet offered me nothing but love and endless support. I thank him for being my proof-reader, my Microsoft Word wizard, my cheerleader, my tear wiper, my coffee supplier, my personal chef, my motivation, and everything in-between. I thank him for always pushing me to be the best that I can be.

~

I dedicate the work in this thesis to my Dad, Albert Petch. With the last educational achievement he witnessed being my acceptance into grammar school at 11 years old, dedicating my PhD thesis to him 14 years later feels surreal. But with every moment of self-doubt, every feeling of loneliness, and every wish to give up, I am reminded of him. I am reminded of his pride in me. And I am reminded of his words: "you can only do your best."

It is always, all for you, Dad.

ABSTRACT

Phenotypic heterogeneity in the yeast *Saccharomyces cerevisiae* has input from both genetic and epigenetic determinants. In addition to changes in DNA sequence induced by mutagens and error-prone mechanisms, there are a variety of 'non-mutagenic' chemicals that can trigger inherited changes in phenotype. One such agent, guanidine hydrochloride (GdnHCl), can both generate mitochondrial *petite* mutants and also induce the loss of various prions from this yeast species. Prions are novel protein-based epigenetic determinants that undergo self-perpetuating, heritable changes in their structure, resulting in the aggregation of an alternative conformational form of a protein. To date, prions have been almost exclusively studied in laboratory-bred strains of *S. cerevisiae,* and the work in this thesis broadens the study to wild strains i.e. non-laboratory strains of *S. cerevisiae* and three related *Saccharomyces* species: *S. bayanus, S. mikatae* and *S. kudriavzevii.* The studies outlined here sought to answer two questions; whether the mechanism of *petite* induction by GdnHCl is the same as leads to prion loss i.e. by inhibition of the molecular chaperone Hsp104; and whether we can identify prion-associated traits in other *Saccharomyces* species by GdnHCl-mediated curing. To answer the first question, the use of *S. cerevisiae* mutants lacking either Hsp104 or the related mitochondrial chaperone Hsp78 ruled out inhibition of both of these proteins as the mechanism of *petite* induction by GdnHCl, as both mutants maintained mitochondrial function. Furthermore, GdnHCl also generates respiratory-deficient *petite* mutants in the three *Saccharomyces* species under test, and a detailed comparative analysis of the impact of GdnHCl on the ultrastructure and respiratory functions of mitochondria in these species is reported. The search for prion-related phenotypes in these *Saccharomyces* species uncovered the possible existence of one or more endogenous prion which may control phenotypic traits that impact on a cell's chance of survival in fluctuating environments. Finally, the ability of these genetically-related species to facilitate and perpetuate the formation of other amyloid-forming proteins; Alzheimer's disease associated protein Aβ42 and Huntingtin (Htt)-associated polyglutamine (polyQ) was analysed. The results obtained indicate that each of these species can propagate the amyloid forms of Aβ42 and polyQ, but these amyloid states are differentially impacted upon by the endogenous prion state of the host yeast species. The expansion of studies into alternate species of *Saccharomyces* has uncovered the possible existence of prions and prion-related phenotypes in these species; and provides considerable potential to develop more disease-relevant models in the future.

ABBREVIATIONS

Aβ	Amyloid-beta
ACMNPV	Autographa californica multiple nucleopolyhedrovirus
ADP	Adenosine diphosphate
Ant-A	Antimycin A
APOE -ε4	Apolipoprotein E ε4
APP	Alzheimer's Precursor Protein
ATP	Adenosine triphosphate
BLAST	Basic Local Alignment Sequence Tool
BSE	Bovine spongiform encephalopathy
C. albicans	*Candida albicans*
CEs	Constitutive escapers
CPrD	Candidate prion-forming domain
CJD	Creutzfelt-Jakob disease
DAPI	4′,6-diamidino-2-phenylindole
DIC	Differential interference contrast
dH_2O	Pure deionised water
ECL	Enhanced chemiluminescence
ER	Endoplasmic reticulum
EtBr	Ethidium bromide
ETS	Electron transport system
FCCP	Carbonylcyanidep-trifluoromethoxyphenylhydrazone
GdnHCl	Guanidine hydrochloride
GFP	Green fluorescent protein
GGM	Glycerol glucosamine medium
GPI	Glycophosphatidylinositol
HPLC	High performance liquid chromatography

HSV1	Herpes simplex virus type 1
Htt	Huntingtin
IDRs	Intrinsically disordered protein regions
IMS	Inner-membrane space
ISCMs	Inactivating stop codon mutations
LB	Luria Bertani
LiOAc	Lithium acetate
MAVS	Mitochondrial-antiviral protein
mPOS	Mitochondrial Precursor Over-Accumulation Stress
mtDNA	Mitochondrial DNA
MUSCLE	Multiple Sequence Comparison by Log-Expectation
NBD1	Nucleotide Binding Domain 1
NBD2	Nucleotide Binding Domain 2
NMD	Nonsense-mediated mRNA decay
nMT	Non-mitochondrial
OPR	Oligopeptide repeat sequence
PanOCT	Pangenome Ortholog Clustering Tool
PCR	Polymerase chain reaction
PFD	Prion-forming domain
PLAAC	Prion-Like Amino Acid Composition
PEG	Polyethylene glycol
PNM2	[*PSI*$^{+}$] no more
PPM	Phosphopeptidomannan
PolyQ	Polyglutamine
PrP	Prion protein
PrLD	Prion-like domain
PVDF	Polyvinylidene fluoride

QNR	Q/N rich region
S. bayanus/Sb	*Saccharomyces bayanus*
S. cerevisiae/Sc	*Saccharomyces cerevisiae*
SGD	*Saccharomyces* genome database
S. kudriavzevii/Sk	*Saccharomyces kudriavzevii*
S. mikatae/Sm	*Saccharomyces mikatae*
SS-DNA	Salmon sperm DNA
SSS	*Saccharomyces sensu stricto*
STREs	Stress-response elements
TE	Tris/HCl/EDTA
TET	Triethiltyn bromide
TTC	2,3,5-triphenyl tetrazolium chloride
USA	Ureidosuccinate
YEPD	Yeast extract peptone dextrose
YEPGal	Yeast extract peptone galactose
YEPG	Yeast extract peptone glycerol
YFP	Yellow fluorescent protein

CONTENTS

Chapter 1: Introduction

1. Chapter 1: Introduction

1.1. Prion proteins and their mechanisms of inheritance

Proteinaceous infectious particles, commonly known as prions, are misfolded structures of proteins that were initially described by Stanley Prusiner in 1982. Such proteins were found to consistently co-purify with scrapie infectivity, a rare degenerative disorder initially thought to be caused by slow viruses (Prusiner, 1982). The discovery of protease-resistant proteins in scrapie-infected brain tissue helped confirm the presence of a novel causative agent in a range of transmissible spongiform encephalopathies. Subsequently, prion proteins have been identified in mammals, fungi, and more recently bacteria and viruses (Tetz & Tetz, 2018), with the ability to undergo self-propagating, heritable conformational changes which alter homologous protein function thus leading to the evolution of diverse traits and in some cases, disease. The term 'prion' describes a protein that exists in multiple physically distinct states, for example a) a [*prion*$^{-}$] state displayed by an array of secondary structures with a soluble conformation associated with normal cellular activity, and b) a [*PRION*$^{+}$] state displayed by a stable conformational change that is enriched in β-structure and prone to aggregate into insoluble amyloid-like structures, associated with altered protein function.

The mechanism of prion inheritance is linked to the conformational change of the prion protein from a [*prion*$^{-}$] to a [*PRION*$^{+}$] state, and is described as the 'protein-only hypothesis' of prion formation and replication (Baskakov et al., 2002; Prusiner, 1982). This sporadic misfolding takes place when the [*PRION*$^{+}$] protein induces the same conformational change in other homologous prion protein molecules currently in the [*prion*$^{-}$] state, thus highlighting the infectious nature of the [*PRION*$^{+}$] protein (**Figure 1.1**).

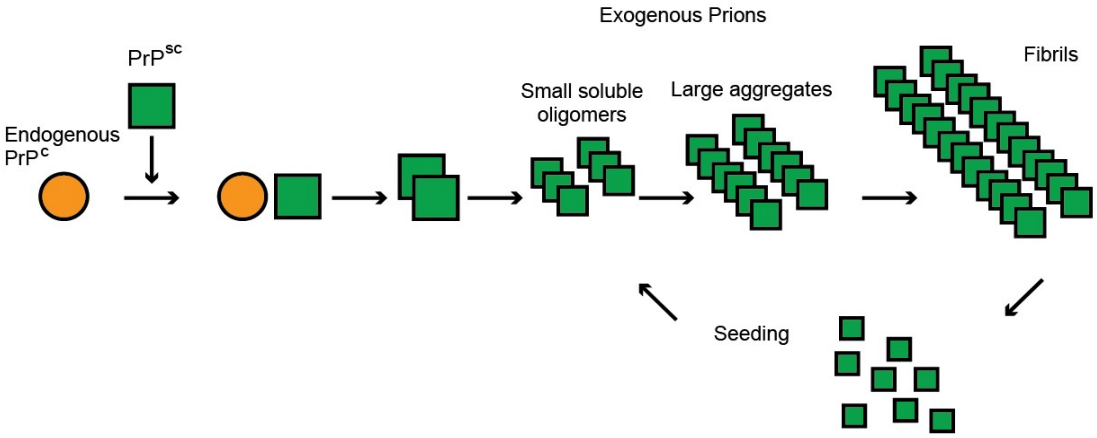

Figure 1.1: The mechanism of prion inheritance. The mechanism of prion inheritance is linked to the conformational change of the prion protein from a [*prion*$^{-}$] to a [*PRION*$^{+}$] state. This sporadic misfolding takes place when the [*PRION*$^{+}$] protein (labelled PrP^{Sc}) induces the same conformational change in other homologous prion protein molecules in the [*prion*$^{-}$] state (labelled endogenous PrP^{C}). This initial conformation change is followed by the aggregation event, in which the oligomers act as 'seeds' to recruit native proteins into the growing aggregate. Breaking of the aggregating fibrils is then required to generate new seeds, resulting in an exponential rise in amyloid formation.

Prions transmit phenotypes via self-propagating structures that are both active and dominant, while maintaining a common pathway of conversion, aggregation, and replication. The initial step is the formation of the first prion protein; a process which remains largely unclear but involves at least partial unfolding and misfolding of the protein into small oligomers (Tuite & Koloteva-Levin, 2004). This process is followed by the aggregation or elongation event, in which the oligomers act as 'seeds' or 'propagons' to recruit native proteins into the growing aggregate. Breaking of the aggregating fibrils is then required to generate new seeds, resulting in an exponential rise in amyloid formation (**Figure 1.1**).

In mammalian cells, prions are transmitted in a process termed 'seed spreading', whereby seeds exit the cell via exocytosis and bind to native prion molecules or receptor proteins found on the cell membrane in the brain. Following such binding, seeds are internalised via endocytosis of a

new cell, and travel along the axon to reach neighbouring cells via axon dendrite connections and nanotubes (Brundin et al., 2010). The exact mechanism of prion protein entry into the mammalian cytoplasm is yet to be defined. In unicellular organisms such as yeasts, a protein in the [*PRION*$^{+}$] state is transmitted from mother to daughter cell during mitosis and meiosis by the division of 'infected' cytoplasm between cells or spores. Newly synthesised prion proteins are then susceptible to [*PRION*$^{+}$] conversion by existing [*PRION*$^{+}$] molecules, thus maintaining the pool of [*PRION*$^{+}$] proteins that would otherwise be filtered out by replication.

1.2. Defining a prion protein

Defining a prion protein requires accurate identification, detection, isolation, and monitoring *in vivo*; allowing the many subtleties in their form to be distinguished. Recent research focuses on the generation of prion candidates using bioinformatics and genetic screening, but further evaluation involving molecular dynamics, biophysical modelling and composition-based prion propensity is required for the discovery of new prions. The activity of novel prions also requires an understanding of the key impacting factors such as localisation and interaction with other proteins. The following sections introduce well-established criteria required for a protein to be defined as a prion, with a primary focus on yeast prions.

1.3. Wickner's genetic criteria for a prion

Yeast prions have been described as "proteins acting as genes", with the ability to transmit phenotype both vertically to daughter cells and horizontally by cytoplasmic mixing to neighbouring cells (Wickner et al., 2013). In 1994, Wickner developed the main criteria that allow prions to be distinguished from nucleic acid-based determinants of phenotype in yeasts (Wickner, 1994) (**Figure 1.2**):

1. Expression of the gene encoding the prion protein must be essential to the establishment and maintenance of the [*PRION*$^{+}$] state.
2. The [*PRION*$^{+}$] phenotype is the same or similar to the phenotype of a mutant of that gene, and such mutants fail to propagate the prion. The relation of phenotype to mutant is true if

the prion produces effects as a result of protein inactivity, but not if it produces a novel or toxic effect, as seen for [*PIN*$^+$] (described in Section 1.6.2) and toxic variants of [*PSI*$^+$] and [*URE3*] (Wickner et al., 2013).

3. Mutagenic agents can reversibly eliminate the [*PRION*$^+$] state, and the same prion could rarely arise in this 'prion-cured' strain. The prion may still arise *de novo* at a very low frequency, as the corresponding prion protein is still being produced in the cell. The consequential [*prion*$^-$] cells can be returned to the [*PRION*$^+$] state by cytoplasmic transfer from a [*PRION*$^+$] strain. It is the reversibility, not the curing itself, which highlights the prion nature of the protein.
4. Over-expression of the prion protein in a [*prion*$^-$] cell can greatly increase the frequency with which the [*PRION*$^+$] state arises *de novo*. The more there is of the protein that is capable of changing to the [*PRION*$^+$] state, the more frequently the phenomenon will occur in a cell.

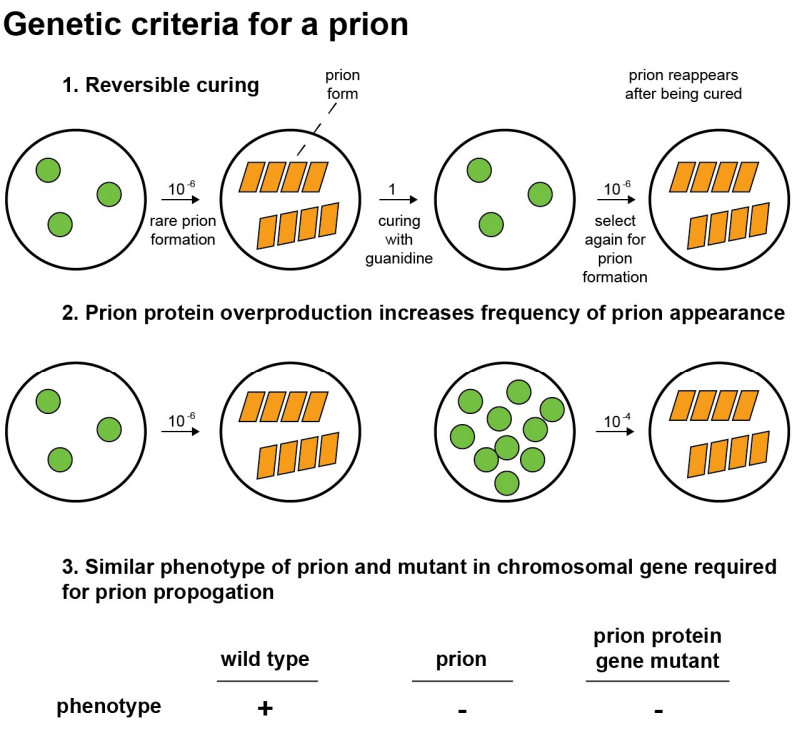

Figure 1.2: The genetic criteria required for a yeast or fungal prion. Both [*URE3*] and [*PSI*$^+$] follow all criteria outlined by Wickner; displaying prion-mediated phenotypes as a result of deficiency in the normal function of the corresponding protein (Taken from Wickner, 1994).

Some proteins have been described as prions without necessarily following all of Wickner's criteria because their phenotypes are due to a gain of function; examples include [*Het-s*] in *Podospora anserina* and [*PIN*$^+$] in *Saccharomyces cerevisiae* (Coustou et al., 1997; Derkatch et al., 2001) (see Sections 1.7.2 and 1.6.2 below). More recently, novel examples of protein-based inheritance have been described which show properties distinct to 'classical' prions; namely prion-like proteins and mnemons (Caudron & Barral, 2013) which also fail to meet all of Wickner's criteria. Such novel examples of protein-based inheritance cause a heritable phenotypic change in the cell following elevated protein levels and have no association with amyloid formation (see Section 1.9.2).

1.4. The prion-forming domain

The prion-forming capacity of a protein is reliant on the presence of a modular domain, typically longer than 60 amino acids in length and referred to as the prion-forming domain (PFD) (Ter-Avanesyan et al., 1993). In most prions discovered to date, the PFD is essential for the *de novo* manifestation and maintenance of the protein in the [*PRION*$^+$] state. Fusion of the PFD to an unrelated protein can confer the prion-forming capability to that non prion-forming protein. This property is illustrated by the fusion of Sup35 PFD with the unrelated rat glucocorticoid receptor, which results in both aggregation and inheritance of the fusion protein (Li & Lindquist, 2000). This newly created prion maintained the epigenetic nature of the original [*PSI*$^+$] prion and was subject to both induction and curing. However, the prion-mediated phenotype changed drastically with the phenotype of the [*PSI*$^+$] prion transformed from one affecting protein synthesis to one affecting the transcription of the rat glucocorticoid-regulated promoter. These findings confirm the protein-only nature of yeast prion inheritance, as the function domain of the protein attached to the PFD is solely responsible for determining the change in phenotype (Li & Lindquist, 2000).

1.4.1. Prion forming domains are amyloidogenic

Once converted into a [*PRION*$^+$] state, prion proteins have a highly infectious nature, with structural rearrangements that increase the abundance of β-strands; stretched out regions of

polypeptides, within the PFD; common in most yeast prions. When hydrogen bonds form between the main chain carbonyl group C=O of one β-strand and the -NH group of another, a major form of secondary structure known as the β-pleated sheet is formed. Typically, β-strands aligned in opposite or 'anti-parallel' directions are more stable, and stack upon one another to form unbranching polymers or fibrils, collectively named amyloid (**Figure 1.3**).

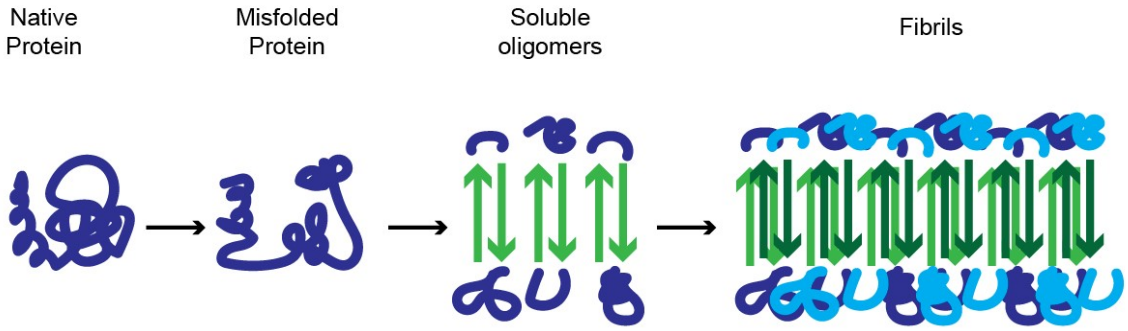

Figure 1.3: The formation of amyloid fibrils. Once converted into a [*PRION*$^{+}$] form, structural rearrangements increase the abundance of β-strands, seen in green. Typically, β-strands aligned in opposite or 'anti-parallel' directions are more stable, and stack upon one another to form unbranching polymers or fibrils, collectively named amyloid.

For example, following an initial lag period that is inversely correlated with protein concentration, the Sup35 PFD polymerises spontaneously, forming amyloid. The resulting fibrils of Sup35 display characteristics indicative of amyloid, including protease and heat resistance, β-rich structure, and binding to the dye Congo red (Glover et al., 1997; King et al., 1997). Further *in vitro* studies of the Sup35 PFD support the protein-only hypothesis of prion inheritance, as the introduction of sub-stoichiometric quantities of Sup35 into the cytoplasm of living yeast using a liposome transformation protocol greatly increases the rate of [*PSI*$^{+}$] appearance in yeast, as a result of self-propagating aggregates of cellular Sup35 (Sparrer et al., 2000).

The mechanism by which a PFD in the β-rich [*PRION*$^{+}$] form templates the conversion of other homologous PFDs to the same [*PRION*$^{+}$] conformation, thereby propagating the amyloid state, is yet to be determined. Segregation and structural analysis at the single-fibril level is required to

distinguish not only the possible link between amyloid structure and propagation, but also the link between amyloid structure and function. Single-fibril structural analysis would also help allow quantification of amyloid polymorphisms in heterogeneous populations, which may uncover differing biological activities between cells infected with the same amyloid sample. Structural characteristics have been shown to determine the replication rates of prion fibrils and consequently the phenotypic characteristics of Creutzfeldt-Jakob disease (Safar et al., 2015). This behaviour has also been implicated with numerous 'strains' of the Tau protein causing different pathologies in different regions of the brain (Kaufman et al., 2016), and is further implicated in Alzheimer's related Aβ peptides (Cohen et al., 2016) (see Section 1.8.2.4 below).

1.4.2. Many prion-forming domains are glutamine and asparagine rich

Initial bioinformatic screening to identify novel prion proteins relied on the use of common features of Sup35 and Ure2 as query sequences. Common features include the PFD; highly enriched for glutamine (Q) and asparagine (N) and lacking in hydrophobic and charged residues. Such bioinformatic approaches identified *RNQ1* as a possible prion encoding gene (Sondheimer & Lindquist, 2000) (Section 1.6.2). Mutagenesis studies of Sup35 revealed that mutations involving the replacement of Q/N residues with alternate charged residues blocks the addition of monomers to [*PSI*$^{+}$] aggregates in nearly all cases, and short, highly Q/N-rich segments within the Sup35 PFD were important for prion aggregate growth (Maclea & Ross, 2011).

Both Q and N are intrinsically linked through their structural similarity, possessing carboxamide as the side chain functional group (**Figure 1.4**). Carboxamide makes PFDs a rich source of hydrogen bonds, thought to contribute to interfacial electrostatic interactions between charged amino acids, thus promoting the formation of larger amyloid oligomers (Yun et al., 2007). As previously mentioned in Section 1.4.1, hydrogen bonds form between the main chain C=O of one β-strand and the N-H group of another, forming the β-pleated sheet. Carboxamide groups have

been labelled as ‘polar zippers’, which further increase the abundance of hydrogen bonds, which are then further stabilised by the binding of water molecules (Yun et al., 2007).

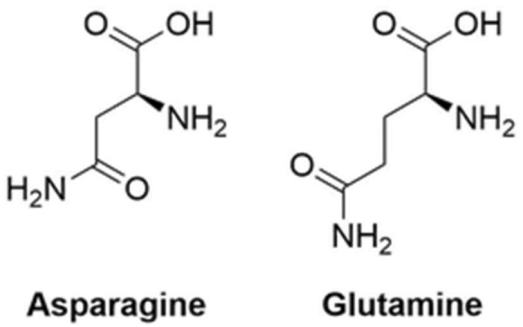

Figure 1.4: The chemical structure of asparagine and glutamine.

The crucial role that both glutamine and asparagine residues play in the aggregation driven by a PFD was shown using Sup35 mutants that are either poorly recruited into, or cause curing of, wildtype amyloids *in vivo.* Such mutations were mapped exclusively within a short glutamine/asparagine-rich region of Sup35, and all but one occur at polar residues (DePace et al., 1998). Furthermore, substituting these residues for charged residues resolubilises the associated protein and reverses the prion phenotype (Alberti et al., 2009).

Most prions identified to date share Q/N-richness as a common prion-associated characteristic. A notable exception is the PFD of HET-s, a protein of the fungus *Podospora anserina* further discussed in Section 1.7.2. Het-s has been shown to propagate as a prion in *S. cerevisiae*, and such yeast-derived propagons are infectious when introduced into *Podospora* (Taneja et al., 2007). These findings suggest that the observed Q/N-richness characteristic of most fungal prions is not a specific requirement of *S. cerevisiae*, and non-Q/N-rich prion proteins may exist in *S. cerevisiae* e.g. Mod5 and other yeast species. Moreover, the presence of the [*PIN*$^{+}$] prion enhances HET-s ring-like aggregate formation in *S. cerevisiae*, highlighting an interaction between Q/N-rich and non-Q/N-rich prions (Taneja et al., 2007).

1.4.3.Prion forming domains and the species barrier

The PFD confers a high degree of specificity to prion aggregation as demonstrated by a 'species barrier' during Sup35 prion replication. This 'barrier', which prevents cross-seeding between PFDs from different yeast species, was first observed when the PFD of Sup35 from *Candida albicans* was fused to the functional C domain of *S. cerevisiae* Sup35 and formed a prion, yet the presence of the *S. cerevisiae* Sup35 prion gene was notably required for continued propagation of the heterologous prion (Santoso et al., 2000). Such species specificity appears to be controlled by a 19-amino acid Q/N rich region at the N-terminus of ScSup35p. Substituting this region in the CaSup35p-PFD with amino acids 8-26 from ScSup35p was sufficient to confer species specificity to Sup35p polymerisation, now acting as wild type ScSup35p (Santoso et al., 2000). Similarly, Chernoff et al. (2000) found that the [*PSI*$^{+}$] state of the endogenous *S. cerevisiae* Sup35 could not be transmitted by expression of the heterologous Sup35p from *Pichia methanolica*, in the absence of the *S. cerevisiae* protein. However, Chernoff et al. (2000) later reported that over-expressing full length PmSup35p induced the prion form of ScSup35 at low levels, suggesting a bypass of species barrier with high-level overexpression of the heterologous PFD.

The PFD-associated species barrier of Sup35 was further studied in members of the *Saccharomyces* species, namely *Saccharomyces paradoxus* and *Saccharomyces bayanus.* All three Sup35 proteins formed prions in *S. cerevisiae,* although prions formed by such heterologous proteins were less stable than endogenous ScSup35p (Chen et al., 2007). Interestingly, all Sup35 proteins co-aggregated in *S. cerevisiae* cells, but cross-species prion transmission was asymmetric; ScSup35 could not co-aggregate in *S. bayanus* or *S. paradoxus* in almost all heterologous combinations. Such a decreased level of prion conversion provides evidence of a species barrier which occurs at the level of conformational transition, rather than with co-aggregation (Chen et al., 2007).

Chen et al. (2010) later noted that the ability of a heterologous PFD to either reproduce or switch the variant-specific prion pattern in species of *Saccharomyces* depends on both

sequence divergence, and the prion variant. In contrast with previous work, the PFD of *S. paradoxus* was shown to be sufficient for a strong transmission barrier for weak [*PSI*$^{+}$], yet only caused a slight decrease in transmission of strong [*PSI*$^{+}$] (Chen et al., 2010). Furthermore, Chen et al. (2010) concluded that individual amino acid substitutions within short amyloidogenic stretches of *S. bayanus* Sup35 PFD can drastically affect prion conversion. In *S. bayanus,* PFD length also appears to contribute to the species barrier, as length is significant in amyloid core formation, as well as correct alignment of interacting sequences in different amyloid units (Chen et al., 2010). The importance on furthering our understanding of the prion species barrier within *Saccharomyces* species will be further discussed in Section 1.10.

1.5. The [*PRION*$^{+}$] state depends on interactions with chaperones

In yeast, the infectious nature of the prion protein relies on the exploitation of molecular chaperones; commonly responsible for the refolding and stabilisation of proteins following exposure to stress. Such molecular interactions rely on substrate specificity, and/or a specific localisation within the cell, to function. The discovery that continued propagation of [*PSI*$^{+}$]; the prion form of the translation termination factor Sup35 (Section 1.6.1) is reliant on Hsp104 for its maintenance a) provided support for the prion hypothesis, and b) highlighted that [*PSI*$^{+}$] is a result of a Sup35 misfolding event (Chernoff et al., 1995). The critical role of Hsp104 in prion propagation is necessary for all amyloid-based yeast prions, with the exception of few yeast prions, namely [*ISP*$^{+}$] and [*GAR*$^{+}$] (Brown & Lindquist, 2009; Rogoza et al., 2010). In the case of [*ISP*$^{+}$], a lack of Hsp104 dependency may be due to the difference in [*ISP*$^{+}$] localisation, with formation of foci in the nucleus as opposed to cytoplasmic foci formed by most yeast prions (Rogoza et al., 2010).

Hsp104 plays a key role in prion propagation by passing the chain of aggregated protein through a central pore formed by the hexameric Hsp104, thus denaturing the protein and allowing it to renature (Lum et al., 2004). Millimolar concentrations of guanidine hydrochloride (GdnHCl) cure [*PSI*$^{+}$] by reversibly inhibiting the prion propagation and disaggregase activity of Hsp104, through

a direct target of amino acid residue 184 (Jung et al., 2002; Ness et al., 2002). This suggests that Hsp104 actively fragments Sup35 prion fibrils, creating new seeds or propagons thus increasing the availability of 'recruiting' ends (Chernoff et al., 1995; Glover et al., 1997). The severance of the prion amyloid is therefore blocked by GdnHCl-associated inhibition of Hsp104, preventing the generation of new seeds that can be passed on to daughter cells, thus filtering out prions by replication (Byrne et al., 2007; Eaglestone et al., 2000; Ness et al., 2002; Satpute-Krishnan et al., 2007). In support of this, a dominant ATPase-negative mutant of Hsp104 is unable to maintain [*PSI*$^{+}$] (Chernoff et al., 1995). Remarkably, the *Candida albicans* orthologue of Hsp104 can replace all functions of ScHsp104 in an *S. cerevisiae* null mutant, but CaHsp104 function is resistant to GdnHCl (Zenthon et al., 2006).

Overexpression of Hsp104 also inhibits formation of the [*PSI*$^{+}$] prion, and was originally thought to over-fragment Sup35 fibrils (Chernoff et al., 1995). In more recent years, Hung and Masison (2006) showed that mutations within, or total deletion of the N-terminal domain of Hsp104 does not affect prion propagation or heat shock tolerance, but eliminates the ability of Hsp104 overexpression to cure [*PSI*$^{+}$] (Hung & Masison, 2006). Interestingly, Ness et al. (2017) showed that Hsp104 overexpression creates [*psi*$^{-}$] cells by malpartition of [*PSI*$^{+}$] propagons between mother and daughter cells during cell division. Furthermore, in conditions of overexpression, Hsp104 does not interfere with the incorporation of newly synthesised Sup35 into fibrils, nor with the multiplication of propagons as numbers decline while growing in the presence of GdnHCl (Ness et al., 2017).

Prion propagation and overproduction curing of [*PSI*$^{+}$] by Hsp104 also requires contributions from other molecular chaperones, namely members of the Hsp70 family and their co-chaperones; the Hsp40 family (Lazarev et al., 2017; Newnam et al., 1999). Co-chaperone Sti1 which interacts with Hsp90, Hsp70 and Hsp104 is also required for overproduction curing (Moosavi et al., 2017), and radicicol-mediated curing of Hsp90 blocks Hsp104 curing (Reidy & Masison, 2010). The requirement of co-chaperones was also shown by Reidy, Miot and Masison (2012), who suggested that ClpB, the *Escherichia coli* homolog of Hsp104, can only propagate the yeast

prions [*PSI*$^{+}$], [*PIN*$^{+}$] or [*URE3*] when replaced with Hsp104 and *E.coli* Hsp70 (DnaK), but not when replaced with Hsp104 alone (Reidy et al., 2012).

1.6. Prion proteins of *Saccharomyces cerevisiae*

Although prions do not cause disease in yeast, they manifest themselves as heritable cytoplasmic elements with a mechanism of inheritance that operates at the level of protein conformation rather than nucleotide sequence. Yeast prions therefore provide a model system for studying mechanisms of amyloid formation and propagation that are applicable to mammalian diseases.

1.6.1. Translation termination: Sup35p and the [*PSI*$^{+}$] prion

[*PSI*$^{+}$] is the most extensively studied yeast prion and has formed the basis of much of prion biology research. Initially discovered by Brian Cox; [*PSI*$^{+}$] was found to be a non-Mendelian genetic element of *S. cerevisiae* with a clear enhancement of nonsense codon suppression (Cox, 1965). In a yeast cell-free translation system, addition of 20% [*psi*$^{-}$] lysate to a [*PSI*$^{+}$] lysate was sufficient to prevent detectable nonsense suppressor activity (Tuite et al., 1983). The [*psi*$^{-}$] 'factor' inhibiting suppression activity was found to be ribosome-associated and was thought to be involved in translation termination and inactivated in a [*PSI*$^{+}$] cell (Tuite et al., 1987).

[*PSI*$^{+}$] was subsequently identified as the prion form of the yeast Sup35 protein that was found to be necessary for the propagation of the [*PSI*$^{+}$] prion (Wickner, 1994; Cox et al 1994; Ter-Avanesyan et al., 2014). Conformational conversion of Sup35 to its proposed prion form was shown to reduce the functional pool of Sup35 available for translation termination, resulting in the nonsense suppressor phenotype associated with the [*PSI*$^{+}$] prion (Cox et al., 1994). The initial connection between Sup35 and [*PSI*$^{+}$] was made following Sup35 over-expression studies, which caused significant growth defects in a [*PRION*$^{+}$] but not in a [*prion*$^{-}$] state, and induced the *de novo* appearance of [*PSI*$^{+}$] in a [*psi*$^{-}$] cell (Chernoff et al, 1992; Ter-Avanesyan et al., 1993).

Sup35/eRF3 is an essential protein (Stansfield et al., 1995) composed of 3 regions; an N-terminal domain (the modular prion-forming domain), the highly charged middle (M)-domain, and the C-terminal region containing a GTPase domain. Sup35 is an essential component of the translation termination complex in eukaryotic cells; mediating the termination of translation upon arrival of a stop codon (UAA, UAG or UGA) in the ribosomal A-site with another essential protein Sup45/eRF1 (Stansfield et al., 1995; Zhouravleva et al., 1995). In the presence of a stop codon, Sup45 associates with the ribosome, and Sup35 is thought to bind to Sup45 to promote a better positioning within the ribosome (Stansfield et al., 1995). The Sup35 C-terminal GTPase domain is then responsible for release of the polypeptide from the peptidyl-tRNA at the ribosomal P site (Zhouravleva et al., 1995). The efficiency of stop-codon recognition by the Sup35/Sup45 complex is sensitive to both nucleotide sequence surrounding the stop codon, and the relative abundancies of both proteins (Zhouravleva et al., 1995). Deletion of the *SUP35* gene results in total loss of cell viability (Ter-Avanesyan et al., 1993). Interestingly, cells remain viable when Sup35 is present in its aggregated prion form, but a measurable defect in translation termination is apparent, thus suggesting only a partial loss of protein function, or a small pool of the soluble form remains and is sufficient for protein function (Byrne et al., 2009).

In [*PSI*$^{+}$] cells, the termination defect is widely used to confirm the presence of the prion. As previously mentioned, [*PSI*$^{+}$] was discovered as a trait which gave rise to enhancement of nonsense suppression whereby suppression of nonsense mutations such as the *ade1-14* nonsense (UGA) allele restores function to the encoded gene product. The red pigmented colonies formed by an *ade1-14* mutant are a result of a defect in adenine biosynthesis, and [*psi*$^{-}$] cells thus require adenine for growth on defined medium (**Figure 1.5**).

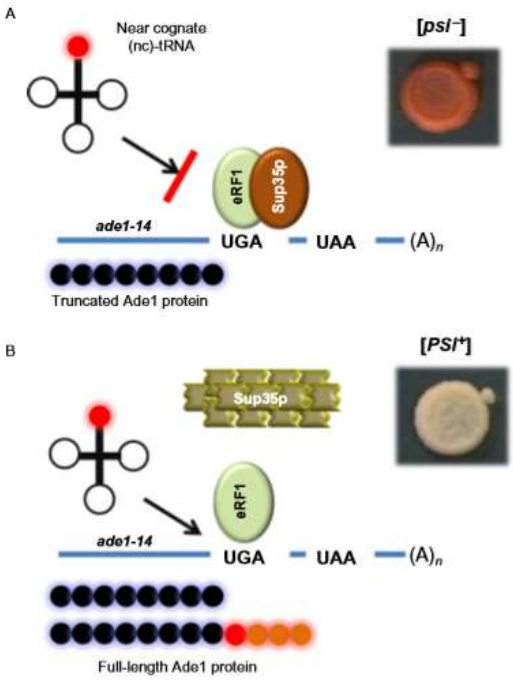

Figure 1.5: The [*PSI*⁺] prion causes a defect in translation termination in *S. cerevisiae*. Panel A: Translation termination in *ade1-14* prion-free cells is mediated by the interaction between Sup35 and Sup45 (eFR1), giving rise to red colonies. Panel B: In [*PSI*⁺] *ade1-14* cells Sup35 is mostly present in its [*PRION*⁺] state. Reduced translation termination results in the synthesis of functional *ADE1* gene product, thus restoring the 'wild-type' colony phenotype. The balance of truncated and full-length protein defines the efficiency of nonsense suppression. Taken from Tuite (2013).

1.6.2.[*PSI*⁺] inducibility: Rnq1p and the [*PIN*⁺] prion

Initial studies into the role of Sup35 demonstrated that curing of the [*PSI*⁺]-associated phenotype using guanidine hydrochloride resulted in two distinct populations of prion-free cells; a) cells in which Sup35 overexpression would re-induce a [*PSI*⁺] state, and b) cells where Sup35 overexpression was not sufficient for the re-induction of [*PSI*⁺] (Derkatch et al., 1997). The remarkable difference between these two populations was [*PSI*⁺] inducibility, and a strain was found to be either [*PSI*⁺]-inducibility positive ([*PIN*⁺]), or negative ([*pin*⁻]). The ability of this [*PIN*⁺]-associated trait to appear in strains lacking the Sup35 PFD led to the suggestion that [*PIN*⁺] was a novel yeast prion, which interacts with, but is not a variant of [*PSI*⁺] (Derkatch et al., 1997). Much like [*PSI*⁺], [*PIN*⁺] showed non-Mendelian inheritance and is dependent on the molecular chaperone Hsp104, but unlike most yeast prions, the [*PIN*⁺]-associated phenotype produces a gain-of-function for the prion protein; providing a necessary template for the *de novo* formation of

[*PSI*$^{+}$] in cells overexpressing Sup35 (Derkatch et al., 2001). The presence of [*PIN*$^{+}$] also facilitates the *de novo* appearance of other yeast prions, namely [*URE3*] (Derkatch et al., 2001) and the *de novo* aggregation of polyglutamine-expanded yeast proteins (Meriin et al., 2002) (see Section 1.8.2.1). Despite several theories to explain how [*PIN*$^{+}$] may mediate *de novo* [*PSI*$^{+}$] formation, the 'direct seeding model' developed by Derkatch et al*.,* (2001) appears to be the most likely. This highlights [*PIN*$^{+}$] as a 'universal nucleating factor'; providing an origin on which the seeds of a yeast prion can convert soluble forms of the heterologous protein into a [*PRION*$^{+}$] state, thus stabilising and promoting spontaneous conversion (Derkatch et al., 2001).

Recent findings by Villali et al*.,* (2020) suggest an unrelated role for [*PIN*$^{+}$] after seed formation; promoting the amplification of Sup35 amyloid rather than its clearance, by directly competing with Hsp104 thus limiting its disassembly activity of Sup35 amyloid (Villali et al., 2020). Mathematical models and *in vivo* experiments also linked the persistence of Sup35 amyloid to the conformationally-defined size of the Sup35 seed (Villali et al., 2020).

In a gene candidate analysis, deletion of the non-essential cellular *RNQ1* gene cured cells of the [*PIN*$^{+}$] phenotype thereby identifying Rnq1p as the protein determinant of [*PIN*$^{+}$] (Derkatch et al., 2001). Further analysis of Rnq1p highlighted a C-terminal domain highly enriched for glutamine (Q) and asparagine (N) residues, identifying the protein as a 'prion-forming protein' with a prion-like domain required for the switch to a transmissible prion form (Sondheimer & Lindquist, 2000). The Rnq1 protein was also shown to be aggregated in a [*PIN*$^{+}$] strain, but not in a [*prion*$^{-}$] strain (Derkatch et al., 2001). Fundamental research by Patel and Liebman (2007) further highlighted Rnq1 as the determinant of [*PIN*$^{+}$], as fibrils formed from the PFD of Rnq1 were able to induce the [*PIN*$^{+}$] phenotype when transformed into a [*pin*$^{-}$] yeast strain (Patel & Liebman, 2007).

The sequence of Rnq1p and its PFD became an intriguing area of study due to its highly polymorphic nature. Various strains of *S. cerevisiae* possess *RNQ1* alleles with numerous polymorphisms clustered to three regions within the PFD, with distinct deletions or insertions which alter the abundance of glutamine residues within Rnq1 (Kelly et al., 2012; Resende et al.,

2003). An increase in the number of glutamine residues increases the likelihood of aggregation, and particularly the neurodegenerative nature of polyglutamine diseases (Meriin et al., 2002) (see Section 1.8.2.1).

Interestingly, genetic screening revealed at least eleven other proteins that can give rise to the [*PIN*$^+$] phenotype when overexpressed, including Cyc8 and Swi1 both of which can form prions in their own right (see Section 1.6.4) (Derkatch et al., 2001). Lsm4; responsible for mRNA processing and turnover, and Nup116; responsible for nuclear transport were also highlighted as likely prion candidates in this genetic screen (Alberti et al., 2009). More recently, overexpression of Lsm4 has been shown to eliminate [*PSI*$^+$], [*URE3*] and [*RNQ*$^+$] prions by forming amyloid *in vivo,* and the Q/N-rich region of this protein was revealed as being responsible for such prion loss (Oishi et al., 2013).

1.6.3. Nitrogen catabolism: Ure2p and the [*URE3*] prion

When grown on a rich source of nitrogen such as ammonia, yeast cells repress the transcription of genes needed for using poor nitrogen sources. Ure2p mediates such nitrogen catabolite repression by blocking the positive transcription regulator, Gln3p. Dal5p, a transporter for the poor, but useable, nitrogen source allantoate is also regulated by Ure2p. Ureidosuccinate (USA) is an intermediate in uracil biosynthesis with similar structure to allantoate, making it a suitable substrate for uptake by Dal5p. Therefore, *ure2* mutants can take up ureidosuccinate (labelled the "USA1 phenotype") on ammonia containing media, whereas wild type cells cannot (named the "USA2 phenotype") (Wickner, 1994). [*URE3*] was first identified as a genetic element which causes the defective control of nitrogen catabolism (and the USA1 phenotype), and was later discovered to be the prion form of Ure2p (Wickner, 1994). Edskes, Gray and Wickner (1999) found that as a GFP fusion, Ure2p is aggregated in cells carrying the [*URE3*] prion, but evenly distributed in [*ure3*$^-$] cells cured by guanidine hydrochloride, thus highlighting the self-propagating aggregation of Ure2 (Edskes et al., 1999). The properties of [*URE3*] show great similarities to

[*PSI*$^{+}$], which also relies on the aggregation of a previously misfolded protein and does not segregate in accordance with Mendel's 1st and 2nd laws of inheritance.

Maintenance of [*URE3*] also relies on the molecular chaperone Hsp104; indicated by elimination when grown on GdnHCl (Moriyama et al., 2000). [*URE3*] was found to be transmissible via cytoduction but was no longer transferred in this way when in the absence of Hsp104. Interestingly, unlike the [*PSI*$^{+}$] prion, [*URE3*] was not eliminated by Hsp104 overproduction (Moriyama et al., 2000). However, overproduction of nucleotide exchange factor Sse1p cures strains of [*URE3*] (Kryndushkin & Wickner, 2007). Sse1p promotes the release of ADP from molecular chaperone Hsp70 (Ssa1), in turn allowing ATP to bind, impacting the balance of binding, release and refolding activities of Hsp70. On complete loss of Sse1, Ssa1 was found in a continuous ADP-bound state, thus blocking the addition of new monomers to the [*URE3*] fibril and further highlighting the requirement of Hsp70 in [*URE3*] propagation (Kryndushkin & Wickner, 2007).

1.6.4. Chromatin remodelling: Swi1p and the [*SWI*$^{+}$] prion

The accessibility of genes, their regulatory sequences and control of gene expression is altered by reversible modifications of DNA structure, such as the packaging of DNA into chromatin by association with histones. The basic repeating structural and functional unit of chromatin is the nucleosome, and disruption of the nucleosome is caused by protein complexes such as the SWI/SNF complex in eukaryotes (the BAF complex in mammals) (Saha et al., 2006). Cells use the SWI/SNF complex to remodel chromatin so that relevant regions of the DNA can be made accessible for control of gene expression, and this process requires the energy of ATP hydrolysis, in one of three ways; a) nucleosome remodelling which alters the interactions of histones within the nucleosome to expose required regions of DNA; b) nucleosome sliding to a different position on the DNA exposing required regions of DNA; and c) nucleosome displacement which dissociates the nucleosome from one DNA molecule to another (Saha et al., 2006).

In *S. cerevisiae,* the SWI/SNF complex is composed of at least 11 subunits, and one of these subunits; Swi1p, regulates the transcriptional activity of ~6% of total genes (Saha et al., 2006). Null mutants of SWI/SNF are viable, but display phenotypes of slow growth, reduced mating-type switching and an inability to use non-fermentable carbon sources. In mammals, mutations in the Snf5 homolog, Ini1, are associated with reduced levels of tumour suppression (Saha et al., 2006).

In *S. cerevisiae,* Swi1p has been shown to convert to the [*SWI*$^{+}$] prion without Swi1p overexpression, indicating the probability of this event occurring naturally in the cell. Such prion conversion displays a partial loss-of-function phenotype of the SWI/SNF complex. Further resemblance to other yeast prions is the dependency of [*SWI*$^{+}$] propagation on Hsp104, indicated by a loss of [*SWI*$^{+}$] on *HSP104* deletion or GdnHCl-mediated Hsp104 inhibition. Moreover, [*SWI*$^{+}$] is dominantly and cytoplasmically transmitted, forms aggregates in the cell, and components of the SWI/SNF complex have high glutamine and asparagine content (Du et al., 2008). Such observations led to the discovery of [*SWI*$^{+}$] as an endogenous prion and epigenetic regulator of protein conformation in *S. cerevisiae* (Goncharoff, Du and Li, 2018).

1.6.5. Transcription regulation: Sfp1p and the [*ISP*$^{+}$] prion

The Sfp1p protein is a transcription factor containing at least two functional zinc-finger domains and is the global regulator of the expression of ~10% of yeast genes, including those that encode ribosomal proteins and other components of translational machinery (Marion et al., 2004). The function and nuclear targeting of Sfp1p is regulated by TORC1 phosphorylation, as part of the rapamycin (TOR) signalling pathway (Marion et al., 2004). Sfp1p belongs to a group of asparagine-enriched proteins and was initially detected in its prion form as a non-chromosomal anti-suppressor in strains containing specific *sup35* nonsense suppressor mutations. It was noted that strains containing [*ISP*$^{+}$] expressed the dominant non-suppressor phenotype, whereas the [*isp*$^{-}$] derivative displayed the suppressor (i.e. stop-codon read-through) phenotype (Rogoza et al., 2010). A *sfp1*Δ deletion strain shows the irreversible loss of [*ISP*$^{+}$], and although the prion form is associated with a non-suppressor phenotype, the *sfp1*Δ does not display this same

phenotype. A lack of [*ISP*$^{+}$] phenotype observed in the *sfp1*Δ strain may be because a) cytosolic [*isp*$^{-}$] does not interact with the nonsense suppressor, or b) the [*ISP*$^{+}$] prion accumulates in the nucleus and may sequester the nucleocytoplasmic protein with nonsense-suppressor activity (Rogoza et al., 2010).

The observed behaviours of the [*ISP*$^{+}$] prion appear to differ from other well-established yeast prions, with a higher spontaneous prion conversion rate at around 1.0 x 10^{-4} per cell per generation, compared to 1.0 x 10^{-6} per cell per generation for [*PSI*$^{+}$]. Moreover, an Sfp1-GFP fusion in an [*ISP*$^{+}$] strain formed nuclear localised foci (Rogoza et al., 2010). Interestingly, neither deletion nor overproduction of Hsp104p influenced the propagation of [*ISP*$^{+}$], suggesting the absence of dependence on Hsp104 as a molecular chaperone (Rogoza et al., 2010).

1.6.6.Overriding glucose repression: Pma1p, Std1p and the [*GAR*$^{+}$] prion

When grown on medium containing 2% glycerol and 0.05% glucosamine (GGM), certain mutant yeast cells arise that do not follow Mendelian patterns of inheritance and the underlying genetic determinant of this trait was later recognised as the [*GAR*$^{+}$] prion (Brown & Lindquist, 2009). [*GAR*$^{+}$] leads to an override of the preference of carbon source and provides yeast with a gain-of-function resistance to the monosaccharide glucosamine, in contrast with wild type [*gar*$^{-}$] cells which specialise in glucose metabolism. Glucosamine is structurally similar to glucose, and therefore gives a strong signal that glucose is present in the culture, triggering glucose repression. Cells that acquire [*GAR*$^{+}$] can circumvent this repression and grow well on GGM (Jarosz, Lancaster, et al., 2014).

Much like other yeast prions, [*GAR*$^{+}$] produces ‘strong’ and ‘weak’ phenotypes, displaying either robust or moderate growth on GGM respectively. Both laboratory yeast strains and strains derived from unique ecological niches display such phenotypes, which are stably inherited from one generation to the next (Brown & Lindquist, 2009). On the other hand, several characteristics of the [*GAR*$^{+}$] trait distinguish it from other well-established yeast prions including the lack of amyloid

fibril formation, and the association of two protein components with the [*GAR*$^+$] trait. One of these proteins, the nuclear transcription factor Std1p, when overexpressed in yeast causes a new heritable state of carbon utilisation. Such protein overexpression indicated that Std1p is the determinant of the [*GAR*$^+$] prion and is not simply a dynamic regulator of glucose repression (Brown & Lindquist, 2009). Strikingly, the prion phenotype of [*GAR*$^+$] cells did not mimic a loss-of-function phenotype of Std1p, and Δ*std1* cells continued to grow on GGM, suggesting Std1p is not the sole determinant of the [*GAR*$^+$] prion. Furthermore, [*GAR*$^+$] propagation continued in Δ*std1* cells, highlighting that this transient inducing agent is not required for [*GAR*$^+$] maintenance. Moreover, gene expression profiling studies identified a 40-fold downregulation of the Std1p-regulated hexose transporter Hxt3p as the only transcriptional difference between [*GAR*$^+$] and [*gar*] cells. Despite Hxt3p downregulation found in a [*GAR*$^+$] state, glucose uptake was not decreased, and Δ*hxt3* cells did not lose the glucose-repression phenotype of [*GAR*$^+$] (Brown & Lindquist, 2009).

Leading on from this, membrane-bound protein pump Pma1p was labelled as a propagating agent which physically interacts with Std1p in [*GAR*$^+$] formation, and attenuation of Pma1p activity is a contributing factor to the [*GAR*$^+$] state (Brown & Lindquist, 2009). Substitution of the essential *S. cerevisiae PMA1* with the *S. bayanus* or *S. paradoxus* orthologue blocked [*GAR*$^+$] propagation (Brown & Lindquist, 2009). Transient overexpression of either *PMA1* or *STD1* was shown to be sufficient in establishing a heritable conversion to the [*GAR*$^+$] state, and once established, either protein was sufficient for propagation. Δ*std1* cells carrying a deletion in the N-terminus of *PMA1* are unable to propagate [*GAR*$^+$] suggesting the formation of a Pma1p/ Std1p complex in [*GAR*$^+$] cells which is no longer detectable in [*gar*] cells (Brown & Lindquist, 2009).

The [*GAR*$^+$] trait can also be differentiated from other well-established yeast prions by its reliance on alternative molecular chaperone Hsp70, as opposed to Hsp104 (Brown & Lindquist, 2009). Propagation of [*GAR*$^+$] continued in Δ*hsp104* cells, following *HSP104* overexpression, and in cells cured by GdnHCl indicating that Hsp104p is not required for the inheritance of [*GAR*$^+$].

In contrast, cells lacking Hsp70 proteins Ssa1 and Ssa2 lost the ability to grow on GGM, and a transient change in chaperone proteins was sufficient to reversibly cure cells of [*GAR*$^{+}$] (Brown & Lindquist, 2009). [*GAR*$^{+}$] variants of wild *S. cerevisiae* strains also lose their ability to grow on GGM following inhibition of Hsp70, further highlighting both the role of Hsp70 in [*GAR*$^{+}$] propagation and the potential impact of originating in diverse ecological niches on the *de novo* acquisition of [*GAR*$^{+}$] (Jarosz, Lancaster, et al., 2014).

In [*gar*$^{-}$] cells, glucose is utilised as the sole carbon source and is metabolised and fermented into high levels of ethanol, which is known to inhibit the growth of bacteria. In contrast, the [*GAR*$^{+}$] state creates a bacteria-friendly environment by reducing the ethanol output by >50%, and this state is initially triggered by a chemical messenger secreted by bacteria in close proximity to the yeast, indicated by green dots in **Figure 1.6** (Jarosz, Brown, et al., 2014). This bacteria-friendly environment was initially displayed in arrested wine fermentations with a particularly strong capacity for [*GAR*$^{+}$] induction, suggesting both the low ethanol and high residual sugar content of the environment.

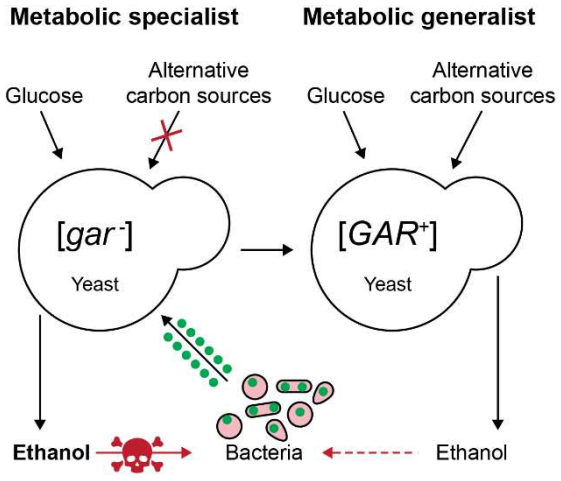

Figure 1.6: Cross-kingdom communication rewires yeast metabolism. In [*gar*] cells, glucose is the primary carbon source and is fermented to high levels of ethanol, inhibitory to bacterial growth. However, some bacterial species can secrete a chemical messenger (green dots) that induces the [*GAR*$^{+}$] state, resulting in an override in the preference of carbon source. Consequently, yeast cells become metabolic generalists with the ability to use alternative carbon sources in the presence of carbon source, leading to a reduction in ethanol levels which favours bacterial growth.

A bacterially-secreted chemical messenger was determined by growth of hundreds of generations on YEPG without direct selective pressures from either glucosamine or bacteria, following initial contamination of *Staphylococcus hominis*. In such conditions, yeast retained their ability to circumvent glucose repression, indicating that the chemical messenger secreted by *S. hominis* had induced a stable [*GAR*$^{+}$] trait, and did not simply influence the metabolism of nearby yeast cells (Jarosz, Brown, et al., 2014). This cross-kingdom chemical interaction was not exclusive to *S. hominis,* as 30% of evolutionarily and ecologically diverse bacteria tested had the capacity to secrete a diffusible factor which allowed yeast to grow on GGM (Jarosz, Brown, et al., 2014).

More recently, the bacterially secreted chemical messenger was identified as lactic acid by activity guided fractionation and reversed-phase high performance liquid chromatography (HPLC) of *S. gallinarum* and *L. innocua* extracts, which caused yeast cells to heritably bypass glucose repression on exposure (Garcia et al., 2016). Given that environmental conditions can greatly affect the amount of lactic acid produced by bacteria, various concentrations were tested to determine the optimum for [*GAR*$^{+}$] induction. Robust reversal of glucose repression was observed in yeast grown on GGM with concentrations of L- or D-lactic acid ranging from 0.025% up to 0.625%, albeit in a concentration-dependent manner. Interestingly, 1% lactic acid caused strong induction of [*GAR*$^{+}$] yeast, such that nearly all cells in the population grew into large colonies on GGM. Addition of 0.05% lactic acid did not increase growth on YEPD alone, eliminating the possibility that the yeast simply metabolise lactic acid.

Lactic acid also induces [*GAR*$^{+}$]-associated phenotypes in *Dekkera bruxellensis;* a fungus with ~200 million years of evolutionary distance from *S. cerevisiae*. *D. bruxellensis* strains exposed to concentrations of lactic acid within the physiological range produced by bacteria (0.02%) grow robustly on GGM. Colonies selected from such conditions were propagated for ~75 generations on YEPD and streaked onto GGM, indicating the heritable trait of circumventing glucose repression in each case (Garcia et al., 2016).

The ability of *D. bruxellensis* cells to circumvent glucose repression was significantly reduced following growth on GGM supplemented with the Hsp70 inhibitor myricetin, at concentrations that do not significantly affect growth on YEPG alone (Garcia et al., 2016). This suggests that the [*GAR*$^{+}$]-like traits that arise spontaneously or are induced by bacteria in this species depend strongly on the activity of Hsp70 chaperones (Garcia et al., 2016). In conclusion, bacterial production of lactic acid can heritably convert neighbouring fungi from metabolic specialists to generalists, even across a vast evolutionary distance.

1.7. Prions found in other species

1.7.1. Mammalian PrP^{Sc}

In 1982, Stanley Prusiner proposed that a protease-resistant protein, PrP, was responsible for scrapie; a well-established neurodegenerative disease of sheep that was both clinically and pathologically similar to several neurodegenerative disorders in humans (Prusiner, 1982). Prusiner suggested that it was in fact an isoform of PrP that was infectious, and went on to highlight the importance of identifying the replication mechanisms involved with this protein. He also stated that the emergence of prions may be in response to evolutionary pressure and as protection against degradation by the immune system (Prusiner, 1982).

The analysis of infected brain homogenate led to the identification of a 27-30 kDa portion of normal, cellular PrP (labelled PrP^{C}) which could undergo a conformational change from an α-helical to a β-sheet structure, and this modified isoform of PrP^{C} was labelled PrP^{Sc} (Pan et al., 1993) (**Figure 1.7**). The PrP sequence contains five variant octapeptide coding repeats in the N-terminus that are well conserved across mammals (Goldfarb et al., 1991) and these mediate the ability to bind copper and zinc at physiologically relevant concentrations (Pan et al., 2001). The ability of these repeats to bind metal ions may be significant as a 50% reduction in copper and elevated zinc and manganese levels has since been detected in the brains of patients with Creutzfelt-Jakob disease (CJD) (Pan et al., 2001).

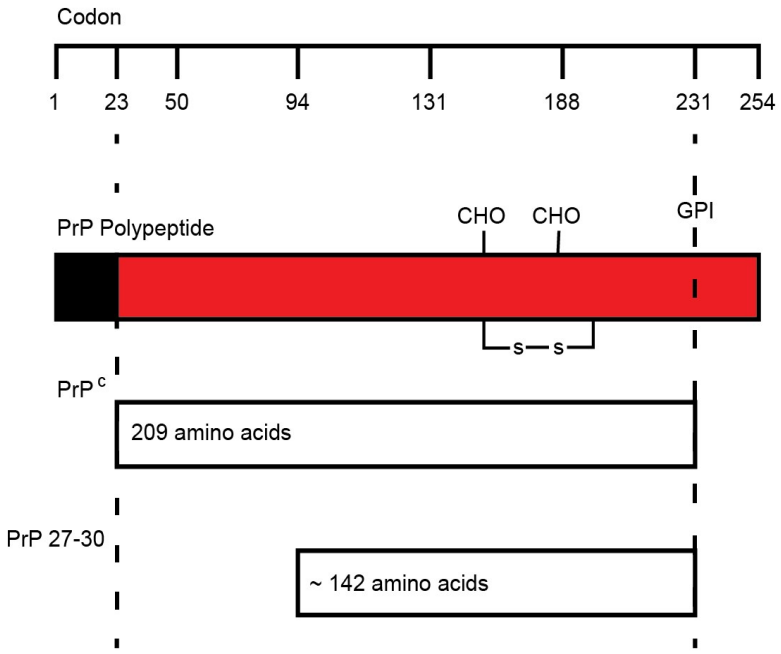

Figure 1.7: The PrP polypeptide is 254 residues long and is processed as shown, resulting in a 209 residue PrP molecule. Proteolysis of PrP^{Sc} generates a 142 residue fragment (PrP 27-30).

Both isoforms of PrP are tethered to the surface membrane of a glycophosphatidylinositol (GPI) anchor and are found in lipid rafts which are membrane domains rich in both sphingolipid and cholesterol. The presence of PrP in such domains implicates a role in signal transduction, cholesterol transport and the regulation of receptor trafficking (Madore, 1999). A GPI-anchored version of Sup35 (see Section 1.6.2) was expressed in neuronal cells which were later exposed to pre-formed Sup35 fibrils. Remarkably, the Sup35p-GPI fusion was found to self-propagate and form protease-resistant aggregates, implicating a key role of the GPI-anchor in PrP infectivity. PrP is the only known protein involved in a misfolding disease that possesses a GPI anchor (Speare et al., 2010). In more recent years, evidence has emerged that PrP is not sufficient for infectivity alone as a phospholipid component which affects the specificity of infectivity is also required (Deleault et al., 2012; Kim et al., 2010).

PrP also appears to be involved in developmental processes of the central nervous system (Hu, 2008), and has been recognised as a high affinity cell surface receptor for soluble amyloid-β peptide (Aβ) (Laurén et al., 2009) (see Section 1.8.2.4). An absence of PrP^C or the use of PrP^C antibodies block Aβ binding, inhibits Aβ-specific obstruction of potentiation and rescues synaptic plasticity (Laurén et al., 2009). Thus, PrP^C was identified as a mediator of Aβ-induced synaptic dysfunction, and PrP^C-specific chemical inhibitors may have therapeutic potential for Alzheimer's disease (Laurén et al., 2009).

Collectively, the transmissible spongiform encephalopathies (TSEs) of scrapie, bovine spongiform encephalopathy (BSE), kuru and Creutzfelt-Jakob disease (CJD) are labelled as 'prion diseases' which can either a) occur sporadically, b) be inherited following mutations in the PrP gene, or c) can be transmitted through 'infected' material. Symptoms of inherited CJD include dementia and deterioration of coordinated movement, and analysis of CJD-infected brain tissue shows PrP^{Sc} in the form of amyloid plaques, spongiosis and neuronal loss. As with many yeast prions, various prion 'strains' of PrP^{Sc} occur with differing structural versions of the PrP^{Sc} isoforms, leading to a diverse range of disease symptoms and PrP^{Sc} deposit patterns in the brain.

1.7.2. The [HET-s] prion in the fungus *Podospora anserina*

Podospora anserina is a filamentous fungus that grows as a multicellular network of hyphae, which fuse to other cells for communication and homeostasis in a process called anastomosis. Such hyphal fusion can also occur between different individuals to form heterokaryons, which describes the mixing of genetically different nuclei within the cytoplasm of a hyphal fusion cell (Glass et al., 2000). The viability of heterokaryons depends on the genetic composition at heterokaryon (*het*) loci, and rejection of the heterokaryon is known as vegetative incompatibility (Rizet, 1952). All of the 9 *het* genes are represented by one of at least 2 polymorphic alleles (Rizet, 1952). In particular, the *het-s* locus encodes a prion-forming protein, and it is the prion state of the encoded HET-s protein that determines the outcome of the heterokaryon reaction between the *het-s* and a *het-S* strain, assuming there are complementarities at all other *het*-loci

(Coustou et al., 1997). In the prion form [Het-s], vegetative incompatibility occurs, whereas the hyphal fusion survives if the HET-s protein is in the non-prion state [Het-s*] (Coustou et al., 1997).

1.7.3. Plant Arabidopsis [*LD*$^+$]

With regards to biological memory, plant flowering has been an intriguing focus due to its unique regulation; a process involving memorising and integrating environmental conditions previously experienced. Using the highly developed computational programme Prion-Like Amino Acid Composition (PLAAC), prion domains were identified in nearly 500 plant proteins (Chakrabortee, Kayatekin, et al., 2016). More specifically, the prion-forming capacity of three *Arabidopsis* prion candidates involved in flowering was investigated using yeast as a model, as the function of such prion-forming domains (PFDs) can be confirmed using complementation of a known yeast PFD. All three proteins aggregated and formed SDS-resistant assemblies, although only the PFD of Luminidependens; a protein of the autonomous flowering pathway, could stably and heritably adopt both a soluble and insoluble prion conformation (Chakrabortee, Kayatekin, et al., 2016). Remarkably, LDPrD fully functionally replaced the prion-domain functions of Sup35 (Chakrabortee, Kayatekin, et al., 2016) In contrast with well-established yeast prions, [*LD*$^+$] was not removed by GdnHCl-mediated inhibition of Hsp104, and did not form high-molecular weight amyloids, as visualised using GFP fusions. Instead, [*LD*$^+$] formed low-molecular weight oligomers and was shown to rely on both Hsp90 and Hsp70 for propagation; similar to the behaviour of the non-amyloid forming [*GAR*$^+$] prion (Chakrabortee, Kayatekin, et al., 2016). These results indicate the evolutionarily conservation of prion-like conformational switches, and the significance of such switches in a variety of common biological processes.

1.7.4. Amoeba *Dictyostelium discoideum* Q/N-rich proteome

The use of bioinformatics has revealed that *Dictyostelium discoideum,* a soil-dwelling amoeba, is an organism with the highest content of putative prion-like proteins so far investigated. Despite a seemingly high aggregation-prone proteome, prion-like proteins Htt-Q103 and Sup35 remained soluble and innocuous to *D. discoideum* (Malinovska et al., 2015). However, impairment of

molecular chaperones such as Hsp100 by heat stress or specific inhibitors leads to the formation of cytosolic, cytotoxic aggregates of these prion-like proteins. This suggests a distinct role of cytosolic molecular chaperones in protein aggregation. Interestingly, prion-like proteins can accumulate in the nucleus to be degraded by the ubiquitin-proteasome network, highlighting the evolutionary adaptation of *D. discoidseum* to allow efficient regulation of the high number of aggregation-prone proteins in its proteome (Malinovska et al., 2015).

1.7.5. Bacterial Clostridium botulinum (Cb-Rho)

Using the probability-based Markov algorithm to model randomly changing systems, ~60,000 bacterial genomes were screened for proteins containing candidate prion-forming domains (cPrDs). The *Clostridium botulinum* transcription termination factor Rho, a highly conserved hexameric helicase which terminates transcription by RNA polymerase, was identified as a candidate containing a cPrD (Hochschild & Yuan, 2017). Rho was also found to assemble into amyloid aggregates using an *E. coli*-based secretion assay used to detect extracellular amyloid, and formed amyloid-like material when fused to yellow fluorescent protein (mYFP) (Hochschild & Yuan, 2017). The significance of the cPrD was further highlighted by a lack of amyloid-associated mYFP in variants lacking the cPrD and by the fully functional substitution of the Sup35 PrD with *Cb*-Rho cPrD. Yeast cells containing the *Cb*-Rho cPrD fused to Sup35 displayed a [*PSI*$^{+}$] phenotype with propagation dependant on the chaperone Hsp104, indicating the infectious properties of *Cb*-Rho aggregates introduced into yeast once produced in bacteria (Hochschild & Yuan, 2017). The identification of *Cb*-Rho as a bacterial prion-forming protein establishes protein-based inheritance in the bacterial domain, and specifically highlights the significance of cPrDs in Rho proteins of bacteria that represent at least six phyla. Typically, the switch to the prion state leads to a reduced or loss of function phenotype, but it must be noted that such mutations often facilitate the survival of bacteria in fluctuating environments, and bacterial prions therefore give rise to increased epigenetic diversity.

1.7.6. Viral AcMNPV LEF-10

It had previously been reported that LEF-10; a protein essential for viral DNA replication and gene expression in the double-stranded DNA virus Autographa californica multiple nucleopolyhedrovirus (AcMNPV), can form SDS-resistant, high-molecular weight aggregates (Nan et al., 2019). More recently, it was suggested that the nuclei of LEF-10-EGFP induced the soluble protein to adopt the insoluble, aggregated form resulting in repression of late gene expression, indicating the prion-like behaviours of LEF-10. Much like the described findings of Chakrabortee, Kayatekin et al. (2016) and Hochschild and Yuan (2017), the PFD of yeast Sup35 was replaced with LEF-10, with the fusion protein exhibiting a [*PSI*$^{+}$] phenotype. The resulting 'prion' was labelled [*LEF*$^{+}$]. Furthermore, the reliance of [*LEF*$^{+}$] propagation on Hsp104 in yeast was confirmed using both GdnHCl-mediated curing and *HSP104* gene deletion, resulting in [*lef*] cells, further highlighting the similarities of [*PSI*$^{+}$] and [*LEF*$^{+}$] requirements for maintenance (Nan et al., 2019).

Confirmation of the first virus-derived prion extends current knowledge of prion proteins into non-cellular life forms, thus providing evidence for their widespread occurrence in nature. Following on from the early suggestion that a combination of both herpes simplex virus type 1 (HSV1) and carriage of apolipoprotein E ε4 (APOE -ε4) allele is a strong risk factor for Alzheimer's disease (Itzhaki et al., 1997), further studies should focus on the idea that novel virus-derived prions can trigger the biogenesis of prion-related diseases in mammals following viral infection.

1.7.7. A recent hunt for ancient prions

More recently, novel amyloid-forming proteins have been identified in two of the oldest evolutionary lineages; Archaea and Cyanobacteria. Bioinformatic screens of NCBI's protein database predicted prion-like proteins by PLAAC (Chakrabortee, Kayatekin, et al., 2016) and identified prion candidates across all three domains of life (Zajkowski et al., 2019). This may suggest the presence of prion-like proteins in our last universal common ancestor. Further studies are required to characterise the amyloid properties of the 11 confirmed archaeal and 3 confirmed

cyanobacterial prion candidates, as well as uncovering the ability of such proteins to seed to amyloid form and transmit phenotypic traits (Zajkowski et al., 2019).

1.8. The biological significance of prions

1.8.1. Prion-mediated phenotypic heterogeneity

The initial identification of prions being associated with certain mammalian neurodegenerative disorders characterised these proteins as causative agents of disease, yet the subsequent identification of prions in yeast implied that the correlation between prions and disease was not the full story. In particular, naturally-occurring prions in yeast have been found to promote heritable changes in protein conformation and function that can lead to the evolution of diverse new traits and survival in fluctuating environments i.e. are potentially beneficial rather than detrimental. For example, the [*PSI*$^{+}$] prion in yeast can lead to a growth advantage of cells under stressful conditions, allowing greater rates of stress adaptation (True & Lindquist, 2000).

In recent years, it has become more apparent that yeast prions represent a level of epigenetic control of certain cellular processes, but questions remain as to whether such control is coordinated with genotype, especially given the role that many yeast prions play in transcriptional processes. It also raises the question of whether a network of prion-specific interactions occur within the cell. Beneficial phenotypes associated with [*PSI*$^{+}$] are not seen in all [*PSI*$^{+}$] strains tested (True & Lindquist, 2000), indicating that the host cell genotype plays a significant role in phenotype, without overriding the underlying translation termination defect (Tuite, 2013). The presence of inactivating stop codon mutations (ISCMs) present in both lab and wild strains of *S. cerevisiae* could explain how different genotypes can modulate [*PSI*$^{+}$]-dependant phenotypes, thus highlighting the interplay between epigenetic and genetic makeup within a strain (Fitzpatrick et al., 2011). Such interplay can give rise to a range of prion-mediated phenotypes (Tuite, 2013).

1.8.2. Prion-associated toxicity

1.8.2.1. [*PIN*$^+$] as a toxic amyloid model

Studies of glutamine expansion diseases have revealed the toxic aggregation and impact of polyglutamine-rich proteins on cellular physiology, also highlighting glutamine as an aggregation-prone amino acid. Models focussing on chains of glutamine residues i.e. polyglutamine – polyQ – tracts, suggest that glutamines possess random coiled coil conformations in the presence of highly soluble carriers, which destabilise on expansion, thus promoting aggregation and the formation of β-sheets (Masino et al., 2002).

Huntingtin molecules with expanded polyQ are more prone to aggregate into intracellular inclusion bodies, and overexpression of the yeast prion protein Rnq1 (Section 1.6.2) has also been shown to promote inclusion body formation (Meriin et al., 2002). Moreover, Rnq1 in its [*PIN*$^+$] prion state is essential for polyQ aggregation (Meriin et al., 2002). Interestingly, Hsp104 can also affect polyQ toxicity either via a) the direct modulation of polyQ aggregates or b) the indirect modulation of prions that interact with polyQ aggregation. Similar to most yeast prion proteins, defects in Hsp104 function can lead to the inhibition of seeding of polyQ aggregates (Meriin et al., 2002).

Moreover, mutant Htt-GFP (see Section 1.8.2.2) expressed in a yeast cell co-localises with Hsp104 and is continuously and directly removed from the inclusion body formed (Aktar et al., 2019). In yeast cells expressing Htt-72Q and lacking either *HSP104* or *RNQ1;* no inclusion bodies, GFP aggregates or liquid assemblies form, further highlighting the role of these proteins in Htt-polyQ associated toxicity (Aktar et al., 2019). In contrast, deletion of the proline-rich region in the amino-terminal region of Htt by-passes the requirement of Hsp104 for aggregate formation, and overexpression of Hsp104 or Hsp70 rescues growth defects in cells without resolving inclusions (Dehay & Bertolotti, 2006). Interestingly, aggregates formed by toxic proteins and cured by chaperones are physically distinct from aggregates formed by toxic proteins (Dehay & Bertolotti, 2006).

1.8.2.2. Polyglutamine-associated toxicity: Huntington's disease

In all known polyglutamine-associated diseases, a loss of neuronal cells in the brain results in progressive deterioration of muscle coordination (Harjes & Wanker, 2003). Despite the similarity of disease-symptoms, the only sequence similarity in the polyQ expanded proteins is within the polyQ tract, which plays a role in polyQ-associated toxicity.

Huntington's disease was first described as an autosomal dominant disease by George Huntington in 1872, and is a progressive neurodegenerative disorder caused by the expansion of the polyglutamine tract in the *HTT* gene (also referred to as the *IT-15* gene). Expansion of the number of repeated trinucleotides (CAG; codon for Gln) within exon-1 of Htt leads to a loss of neuronal cells and results in uncoordinated body movements, neuropsychiatric abnormalities and dementia. The critical threshold for glutamine expansion before pathological changes occur is 35-40 glutamines, and a repeat of 60 or more CAG units leads to a diagnosis of juvenile Huntington's. Interestingly, the longer the polyQ expansion, the more severe the disease symptoms and the earlier the onset (Norremolle et al., 1994). The Htt protein lacks sequence homology with any other known protein in eukaryotes and is expressed in nearly all tissues. Htt proteins are found in the nucleus and cytoplasm of neurons in the CNS, but also associate with mitochondria, Golgi apparatus and the endoplasmic reticulum (Harjes & Wanker, 2003).

Disease onset occurring at a 35-40 glutamine expansion implies a molecular or functional barrier controlled by polyglutamine tract length, regardless of protein identity or flanking sequence. However, differences between polyglutamine diseases highlight that the toxic nature and length of the polyglutamine tract is not the only factor influencing disease pathology. Analysis of the affected protein's identity, cellular localisation and flanking sequences may help to uncover possible mechanisms for disease progression and reveal cellular components with potential as therapeutic targets.

Differences in amino acids flanking the polyQ regions influence the specific toxic nature of each

polyQ expansion protein in a yeast cell. The commonly used FLAG-epitope (DYKDDDK) at the terminus of Htt- exon 1 causes non-toxic polyQ proteins to increase in toxicity, whereas the endogenous carboxyl-terminal polyproline region of Htt-exon 1 convert toxic polyQ proteins into non-toxic ones (Duennwald et al., 2006). Furthermore, different flanking sequences can direct polyQ misfolding to at least two morphologically distinct types of polyQ aggregate; “tight and benign” or “amorphous and toxic” (Duennwald et al., 2006). Interestingly, Peskett et al (2018) showed that aggregates of Htt- exon1 exist in both distinct liquid-like and solid-like forms, and lengthening of the polyQ tract is sufficient to drive such assembly formation. In a yeast model, time-lapse movies of aggregation events show the presence of liquid-like assemblies driven by the polyQ and proline-rich regions of Htt-exon1. Such assembly formation is thought to require Rnq1 as cells lacking the *RNQ1* gene display weak fluorescent polyQ assemblies (Peskett et al., 2018). Furthermore, observations of mutant Htt-GFP expressed in a yeast cell suggest that such assemblies move randomly and grow through the collision and coalescence of small aggregative particles (Aktar et al., 2019).

1.8.2.3. Genetic modifiers of polyQ-mediated toxicity

Upf proteins 1, 2 and 3 are involved in the nonsense-mediated mRNA decay (NMD) pathway; responsible for degradation of aberrant mRNA transcripts that carry premature termination codons, preventing synthesis of harmful C-terminally truncated proteins (Wang et al., 2001).

In Upf-deficient mutants, mRNA transcripts containing premature termination codons are stabilised. More specifically, the Upf1 protein is an ATP-dependant RNA helicase located in the cytoplasm, forming a complex with both Upf2 (also localised in the cytoplasm and rich in acidic amino acid residues) and Upf3 which localises to the nucleus and is rich in basic amino acid residues (Mendell & Dietz, 2008). Both eRF1 (Sup45) and eRF3 (Sup35) interact with Upf proteins in yeast, and *UPF* gene deletions promote nonsense suppression (Wang et al., 2001).

Findings reported in this thesis imply a role of Upf proteins in disease-associated amyloid aggregation.

Like the Upf proteins, further genetic modifiers have been found to play a role in disease-associated amyloid aggregation. Deletion of *BNA4* in the tryptophan degradation pathway, and *SCP160* involved in translation elongation efficiency prevent polyQ-mediated cytotoxicity in a [*PIN*$^+$] background (Cheng et al., 2018; Giorgini et al., 2005). Additionally, genome-wide analyses in yeast have identified fourteen genes, that, when deleted, result in elevated polyQ toxicity (Papsdorf et al., 2015). *UGO1, ATP15* and *NFU1* all encode mitochondrial proteins and damage to the mitochondrial network is seen in polyQ-intoxicated cells (Papsdorf et al., 2015). Moreover, non-fermentative growth is inhibited in yeast cells expressing polyQ proteins. This implies a connection between polyQ-mediated toxicity and mitochondrial functionality (Papsdorf et al., 2015).

1.8.2.4. Amyloid-associated toxicity: Alzheimer's disease

Amyloid-β peptide (Aβ) is a 40-42 amino acid proteolytic fragment of the Alzheimer's Precursor Protein (APP), generated by β- and γ- secretases (Goedert & Spillantini, 2006). The most common Aβ fragment is Aβ40, however mutations in *APP* or the γ- secretase network results in increased Aβ42 production which is a more hydrophobic peptide. Aβ42 is the predominant causative agent of Alzheimer's disease, causing β-amyloid oligomerization and the formation of β-amyloid deposits (Goedert & Spillantini, 2006). Such deposits; namely plaques, are found in the extracellular space of the brain, compared to intracellular β-amyloid found in the secretory pathway, the cytosol, and the mitochondria (LaFerla et al., 2007).

Yeast models have been used extensively to evaluate the cellular consequences of both extra and intracellular β-amyloid, which can be stabilised in yeast by the fusion to protein tags (Bharadwaj et al., 2008; Von Der Haar et al., 2007). Despite a high turnover, Aβ42 fusion proteins are reported to be non-toxic to yeast, although Aβ42-GFP expression causes a slight decrease in growth rate and induces the heat shock response (Caine et al., 2007). Von Der Haar et al. (2007) showed that both Aβ40 and Aβ42 peptides can mediate aggregation of yeast prion protein Sup35 when they replace the endogenous PFD. However, such Sup35-Aβ42

fusions form aggregates that are qualitatively different from [*PSI*$^{+}$] prions in their requirements for maintenance and propagation (Von Der Haar et al., 2007).

Further studies by D'Angelo et al*.,* (2013) also expressed Aβ42-GFP expression proteins in *S. cerevisiae,* and established a system in which Aβ enters the secretory pathway, moves to the plasma membrane and thus becomes cytotoxic. Aβ also crosses membranes and targets the mitochondria in the cell (D'Angelo et al., 2013). However, the level of toxicity depends on the form of Aβ expressed, with an arctic mutant ($A\beta_{ARC}$) being more toxic than the wild type Aβ42 (D'Angelo et al., 2013). Furthermore, the level of Aβ-induced cytotoxicity also depends on the presence of proteins involved in protein trafficking pathways, namely PICALM; encoding phosphatidylinositol-binding clathrin assembly protein in mammals (D'Angelo et al., 2013). The PICALM yeast homologues; AP180 proteins (Wendland & Emr, 1998) increase Aβ toxicity in *S. cerevisiae* (D'Angelo et al., 2013).

Interestingly, treatment of cells with the Hsp104 inhibitor, GdnHCl stimulates Aβ42-GFP oligomerisation, however deletion of the *HSP104* gene inhibits oligomerisation of this fusion protein. This suggests an interaction of Hsp104 with Aβ42-GFP, which may protect the protein from disaggregation and degradation (Bagriantsev & Liebman, 2006).

Studies must therefore address how yeast cells are able to tolerate, detoxify and maintain Aβ42; and whether the presence of a prion protein or specific molecular chaperone facilitates aggregation, and impacts Aβ42 polymer size and structure. In addition, the Sup35-Aβ42 fusion model may be used to identify novel compounds that can modify Aβ42-associated aggregation.

1.9. Alternative mechanisms of protein inheritance in *Saccharomyces cerevisiae*

The ongoing study of yeast prions has led to a general acceptance of the existence and biological impact of protein-based inheritance and the field is continuing to widen. A fairly novel example of protein-based inheritance is the concept of 'prion-like' proteins; proteins which show no diagnostic sequence or biochemical feature of known *S. cerevisiae* prions, but which have similar non-Mendelian laws of segregation (Chakrabortee, Byers, et al., 2016). In a screening of ~5300 proteins of *S. cerevisiae*, 46 were found to cause a heritable phenotypic change following elevated protein levels, and such phenotypes were retained once expression returned to normal. Many of the observed phenotypes had no associated amyloid-forming protein. Further prion-like behaviours were investigated through reliance on the molecular chaperones Hsp104, Hsp70 and Hsp90 and proteins that did not require such chaperone activity, yet caused the emergence of a beneficial new trait were labelled as prion-like (Chakrabortee, Byers, et al., 2016). Although such studies resulted in the discovery of several novel prion-like proteins, stress levels which induced such prion-associated phenotypes were engineered. Such stress was caused by protein overexpression, specifically causing aggregation and protein insolubility. The question which needs to be addressed is whether a natural signal can trigger such an epigenetic trait.

1.9.1. Stress granules

Although the molecular mechanisms underlying the form and function of such granules remain unclear, it is thought that stress granules cause a range of morphological changes (Hou et al., 2011). Such morphological changes take place in response to cellular stimuli such as stress or viral infection, and an example is an altered structure of the nucleolus (Courchaine et al., 2016). In such adverse conditions, the stress granules are able to assemble and disassemble in the cell. It is thought that stress granules contain RNA-binding proteins, as well as factors which stall translation (Courchaine et al., 2016). Many of the RNA-binding proteins in such stress granules contain prion-like domains (PrLD) consisting of intrinsically disordered regions thought to be recruited to stress granules to elicit formation via liquid-liquid phase separation (Baer & Ross, 2020). Prion-like domains that are recruited to such stress-induced assemblies require specific amino acid composition as shown by the efficient stress granule formation following synthetic

prion-like domain (Baer & Ross, 2020). Similarly, serine-arginine (SR) protein kinase Sky1; responsible for mRNA splicing regulation and RNA transport, has been established as a novel regulator of stress granule dynamics in *S. cerevisiae* (Shattuck et al., 2019). As previously discussed, the PrLD of Sky1 plays a definitive role in such stress granule formation, although the exact interaction of the PrLD within the stress granule remains to be defined.

1.9.2. Mnemons

Several studies have demonstrated that *S. cerevisiae* has an intrinsic ability to maintain 'biological memories' as exemplified by the Whi3 mnemon. Haploid yeast exist in two mating types; **a** cells which secrete the pheromone a factor and **α** cells which secrete α factor. Using pheromone receptors, cells of the opposite mating types sense each other's presence, which in turn leads to a series of activation pathways to promote successful mating. Caudron and Barral (2013) showed that yeast exposed to mating pheromones for an extended period without experiencing successful mating become refractory to this signal, and continue to divide in both the presence and absence of such a signal. Cells were found to 'memorise' such unproductive mating attempts, and so the refractory state is maintained throughout the life span of the cell (Caudron & Barral, 2013). It was suggested that this refractory state of the cells is caused by the super assembly and inactivation of the mRNA binding protein Whi3, which in turn allows the expression of the normally inhibited Cln3; a G1 cyclin involved in cell cycle progression. Much like prion proteins, such conformational change is counteracted by the molecular chaperone Hsp70, but interestingly this trait is only stable in mother cells over many divisions, and is not inherited by daughter cells (Caudron & Barral, 2013). Thus, Whi3 was labelled as a 'mnemon', a protein establishing memory through conformational change. This therefore leads to the question of whether other proteins exist in the form of mnemons in both unicellular and multicellular organisms. This existence could uncover alternative forms of memory, and encode the cell state used in previous environmental conditions (Caudron & Barral, 2013).

More recently it was reported that ($Whi3^{mnem}$) is strongly associated with the endoplasmic reticulum (ER) membranes, and only confined in the mother cell by the presence of membrane

diffusion barriers at the bud neck (Caudron et al., 2020). Interestingly, defects in this diffusion barrier facilitates (Whi3^{mnem}) propagation in a mitotically stable manner, similar to prions. However, neither induction or curing of the [*PSI*$^{+}$] prion is affected by whether diffusion barriers are present or not. Thus, (Whi3^{mnem}) is a self-templating state, whose anchorage to the ER membranes maintains its confinement in the mother cell, preventing prion-like infectious propagation (Caudron et al., 2020). Furthermore, yeast cells can acquire a mitotically stable refractory state to pheromone, recently termed constitutive escapers (CE). Such a phenotypic state has been shown to mimic a loss of function of Whi3 and requires the prion-like domain of Whi3 (Caudron et al., 2020). This further highlights Whi3 as a dominant, inactive, self-templating prion form in CE variants, and indicates a promising case for the identification of novel prions in yeast.

1.10. *Saccharomyces* species

As described in Section 1.4.3, prions are poorly transmitted between species due to the presence of a "species barrier". This phenomenon was first recognised in scrapie prion transmission between sheep and goats, which adopted an extended incubation period when compared to intra-species transmission (Cuille and Chelle, 1939). The notion of a species barrier to prion transmission has been studied in members of the evolutionarily-related species of *Saccharomyces*.

*Saccharomyces s*pecies are a complex of at least seven species ranging from key industrial and laboratory species, to those that remain in geographically limited environmental ranges (Borneman & Pretorius, 2014). Near complete genome sequences and a collection of genetically marked haploid strains of *S. bayanus, S.kudriavzevii* and *S. mikatae* have allowed comparison to the genomes of *S. cerevisiae* and *S. paradoxus* (**Figure 1.8**). Such comparison has given us insight into species-specific gains and losses, and provides a valuable toolset for comparative studies of gene function, metabolism, prions, and key evolution events (Scannell et al., 2011).

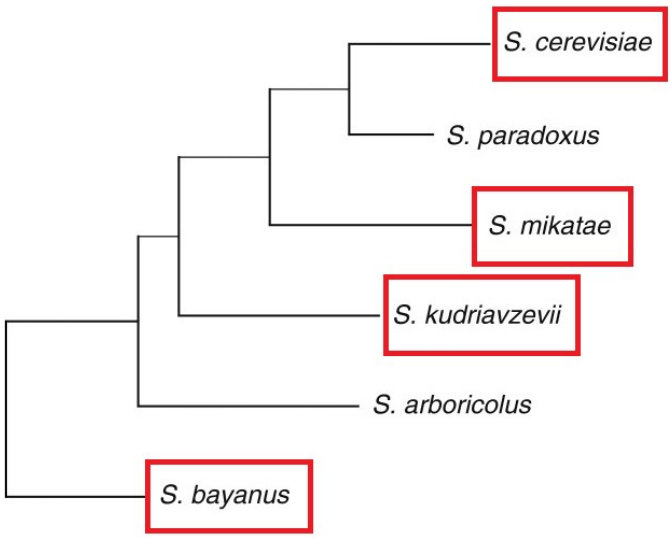

Figure 1.8: The phylogenetic tree of *Saccharomyces* species. The phylogenetic relationships among members of the *Saccharomyces* genus. Red boxes denote the *Saccharomyces* species used throughout this study.

The species barrier for prion transmission has been studied in *Saccharomyces* species, highlighting a decreased level of prion conversion between species (Chen et al., 2007). It is clear that sequence divergence at a single nucleotide level, the physical interaction of heterologous proteins between different species and prion variants all contribute to the cross-species species barrier. Whether a link exists between % amino acid sequence divergence of the heterologous PFD and the effectiveness of such a barrier remains to be established (Bruce & Chernoff, 2011).

Moreover, it remains unclear whether well-established prion proteins of *S. cerevisiae,* namely Sup35 and Ure2, can transform into their stable prion conformations in the native cellular context of non-*cerevisiae* species (Afanasieva et al., 2011; Edskes et al., 2009). Also, among *Saccharomyces* species, the Rnq1 sequence is significantly more divergent across the whole molecule, yet a transmission barrier for the Rnq1 prion between members of *Saccharomyces* has yet to be investigated experimentally (Harrison et al., 2007). In a study of 21 different yeast species only 9 appeared to encode a Rnq1 orthologue,

suggesting that the RNQ1 gene is missing from some fungal genomes (Harrison et al., 2007). This leaves a distinct gap in the knowledge of whether a) the RNQ1 gene exists in the evolutionarily-related species of *S. cerevisiae,* b) if present, whether Rnq1 can convert into its prion derivative in other *Saccharomyces* species, and c) whether Htt-polyQ expansion proteins can become cytotoxic in these species.

A requirement for further investigation also lies in the presence of other prion-like proteins in this group of yeasts and specifically those prions considered as molecular memory devices. One example is the search for Lsb2; a stress-inducible cytoskeleton-associated protein, which forms a metastable prion in response to high temperature, and possession of an amino acid substitution required for Lsb2 prion formation coincides with acquisition of increased thermotolerance in *Saccharomyces* species evolution (Chernova et al., 2017). Remarkably, only *S. paradoxus* and *S. cerevisiae,* characterised by increased optimal growth temperature, contain the N residue at position 213 required for Lsb2 prion formation, compared to the more distantly related *S. mikatae* and *S. bayanus.* Therefore Lsb2 prion formation in response to heat stress coincides with yeast adaptation to grow at higher temperatures, connecting prion formation in *Saccharomyces* to the cellular response to environmental stresses (Chernova et al., 2017).

1.11. The *Saccharomyces cerevisiae* clade

The reduced levels of prion discovery in non-domesticated strains of *S. cerevisiae* have been used to support the argument that prions have a detrimental impact on the host, and a strong selective pressure against their retention in a natural environment (Nakayashiki et al., 2005). More specifically, it has been suggested that more than half of [*PSI*$^{+}$] variants observed are lethal or highly pathogenic, in contrast with the ‘mild’ variants usually studied (McGlinchey et al., 2011). Thus, the idea that certain prions cause ‘disease-like’ states in yeast may provide us with an answer as to why there are lower levels of ‘naturally-occurring’ prions in a natural environment.

Leading on from this, many of the fungal prions discovered so far have been in laboratory-bred strains and have been labelled as potential ‘laboratory artifacts’ that arise through cultivation of fungal cells under conditions far removed from the environment in which they would have evolved

in (Tuite, 2013). 'Unnatural' lab environments include short-term storage at 4^{o}C or long-term storage at -80^{o}C, each creating possible selective pressures on the cell population (Tuite, 2013). The *de novo* formation of many yeast prions in the lab could have been induced by chemical pressures or unnatural protein overexpression which otherwise may not occur in a natural environment and therefore certain yeast prions would not have existed in a natural yeast population. It is therefore important to use non-domesticated strains of the *S. cerevisiae* clade to establish whether fungal prions are present in these strains, and whether any naturally-occurring prions can be transferred between closely or distantly related species.

In contrast, many of the studies already focussing on the use of wild strains of *S. cerevisiae* have suggested that prions are not artefacts of culturing under laboratory conditions. Great care is taken to maintain the wild character of such strains and comparative growth of archived strains and their well-studied derivatives shows no difference (Halfmann et al., 2012). Studies show that prions can be advantageous in the strain's natural ecological niche as exemplified in the strain *Sc.* #5672 where presence of the [*PSI*$^{+}$] prion in this strain caused a clear growth advantage on synthetic grape must, a medium that mimics conditions of early wine fermentation (Halfmann et al., 2012).

Phenotypic analysis in undefined wild strains of the same species also allows us to acknowledge the presence of the pan-genome; the concept of 'accessory' non-conserved genes across strains of the same species which contribute to intra-specific variability (McCarthy & Fitzpatrick, 2019). The core *S. cerevisiae* genome contains 4900 gene models, conserved across 100 strains tested, accounting for 85% of the total species pan-genome (**Figure 1.9**). The remaining genes are either duplicates of core gene models conserved across one or more strain, accessory genes missing a syntenic orthologue in only one other strain, or singletons; a gene carried by a unique chromosome in the sample. Overall, accessory genes which differ between strains make up 14.9% of the pan-genome in *S. cerevisiae* (McCarthy & Fitzpatrick, 2019) **(Figure 1.9**).

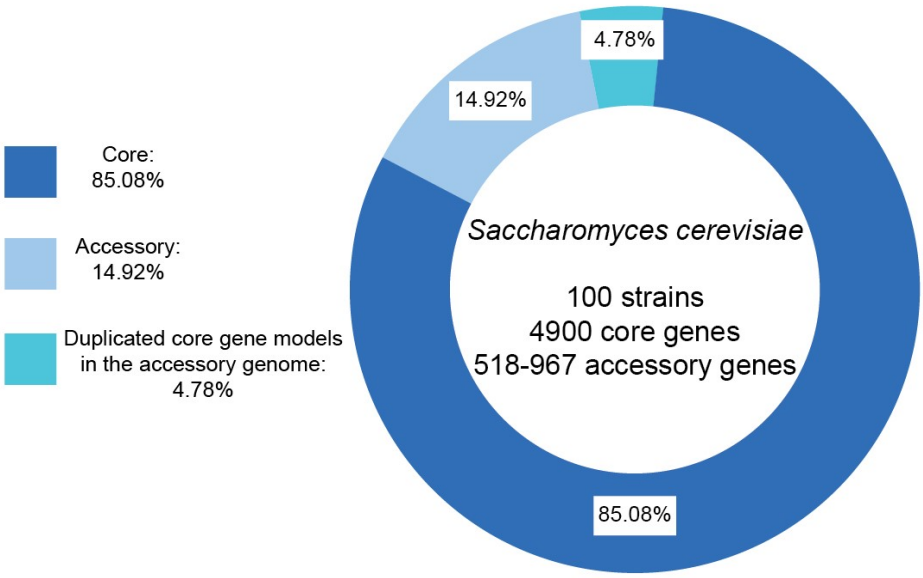

Figure 1.9: The pan-genome of *Saccharomyces cerevisiae*. The ring represents the total number of gene models in the pan-genome, expressed as a proportion of total pan-genome size. Coloured sections denote the core genes, accessory genes, and duplicated core gene models in the accessory genome. Labelled % add up to >100%, as duplicated core gene models have been accounted for both in the accessory genome, and as duplicates.

Using the Pangenome Ortholog Clustering Tool (PanOCT), the intraspecific variability of each gene has been investigated (McCarthy & Fitzpatrick, 2019). Focusing on such variability on a gene-to-gene level rather than studying the pan-genome based on families of related gene models meant that both the conservation and distribution of a biological function can be observed. Not only do such analyses account for loss of micosynteny between fungal strain genomes, the extent of core genome content duplication occurring within fungal accessory genomes can also be established (McCarthy & Fitzpatrick, 2019). Functionally, core genomes are enriched for housekeeping processes, whereas accessory gene models are found within clusters in the terminal and subterminal regions of genomes and are enriched for processes that may be implicated in antimicrobial resistance (McCarthy & Fitzpatrick, 2019).

Further studies using BLASTP searches of the systematic mutation set available on *Saccharomyces* Genome Database (SGD) showed that less than 20% of the genes in the *S.*

cerevisiae S288C genome are essential for growth while 962 of the 1031 predicted gene models with an inviable knockout phenotype are within the core *S. cerevisiae* genome. On the other hand, a significant proportion of gene models within the *Sc.* S288C accessory genome are associated with a viable knockout phenotype, which may reinforce the more variable nature of accessory genomes, relative to core genomes (McCarthy & Fitzpatrick, 2019).

The variable nature of accessory genomes between different strains of the same species highlights the importance of studying strains of the *S. cerevisiae* clade on both a genotypic and phenotypic level. Such differences infer that many prions and prion variants may remain to be discovered in these strains, each with different impacts on host growth and behaviour in a wide range of habitats.

1.12. Aims of the project

The aims of this research project initially focused on exploring extrachromosomal regulators of phenotypic heterogeneity in both *Saccharomyces* species and members of the *S. cerevisiae* clade using GdnHCl to generate potentially prion-free strains of these yeasts. As well as the loss of prions from *S. cerevisiae*, GdnHCl causes the generation of mitochondrial *petite* mutants. Therefore the answers to two related questions were sought: (1) is the mechanism of *petite* induction by GdnHCl the same as leads to prion loss i.e. by inhibition of the molecular chaperone Hsp104?; and (2) can we identify prion-associated traits in other *Saccharomyces* species by GdnHCl-mediated curing? Analyses of well-established yeast prion proteins Sup35 and Rnq1 were also undertaken in *Saccharomyces* species, with the aim of investigating the potential impact of minor differences in amino acid sequences within the PFD on cross-species prion transmission. Finally, the ability of these genetically related species to facilitate and perpetuate the formation of other amyloid-forming proteins has also been examined, with a focus on the Alzheimer's disease associated protein Aβ42 and Huntingtin (Htt)-associated polyglutamine (polyQ). The behaviour of these amyloidogenic proteins was investigated, focussing on the impact of the prion state of the microbial host.

Chapter 2: Materials and Methods

2. Chapter 2: Materials and Methods

Safety Information:

Risk assessments including COSHH were carried out for all required procedures, involving the use of hazardous chemicals or equipment. All work involving genetically modified organisms and pathogens were performed in an ACDP category two laboratory.

2.1. Media used for the culture of *Saccharomyces cerevisiae, Saccharomyces bayanus, Saccharomyces mikatae, Saccharomyces kudriavzevii and Escherichia coli*

Unless otherwise stated, all media and sterile solutions were sterilised by autoclaving at 121 ^{o}C, 15 lb/sq.in for 11 mins in a Prestige Medical benchtop autoclave.

2.1.1. Water used in study

Pure deionised water (dH_2O) was produced by Thermo Scientific Barnstead NanoPure Diamond water system.

2.1.2. Yeast extract, peptone, dextrose (YEPD) medium

Table 2.1: Ingredients required for YEPD (Complete) media.

Ingredients	**Amount per litre**
Glucose	20 g
Yeast Extract (Difco)	10 g
Bactopeptone (Difco)	20 g
dH_2O	Up to 1 L final volume

For solid medium, Granulated Agar (Difco) was added to a final concentration of 2 % w/v prior to autoclaving.

2.1.3. Prion curing with guanidinium salts

For prion curing and the continued inhibition of Hsp104p, guanidine hydrochloride (Sigma) was added to YEPD medium after autoclaving to a final concentration of 5 mM from a 6 M stock solution in dH_2O.

2.1.4. Inhibition of Hsp90 with radicicol

For Hsp90 inhibition, radicicol (Sigma) was added to the appropriate medium after autoclaving to a final concentration of 10 µg/ml, from a 5 mg/ml stock solution in dH_2O.

2.1.5. Generating *petite* mutants with ethidium bromide and guanidinium salts

For the generation of respiratory-deficient *petite* mutants, ethidium bromide (Sigma) was added to the appropriate medium after the medium had been autoclaved, to a final concentration of 10 µg/ml, from a stock solution of 10 mg/ml in dH_2O. Guanidine hydrochloride and guanidine thiocyanate were also used for the generation of *petite* mutants, added to the appropriate medium after autoclaving to a final concentration of 5 mM, from a stock solution of 6 M in dH_2O. *Petite* mutants were confirmed by a lack of growth on YEPG (See Section 2.1.6).

2.1.6. Yeast extract, peptone, 3 % glycerol (YEPG) medium

Table 2.2: Ingredients required for YEPG medium

Ingredients	Amount per litre
Glycerol (100 %)	30 ml
Yeast Extract (Difco)	10 g
Bactopeptone (Difco)	20 g
dH_2O	Up to 1 L final volume

Glycerol (100 %) is added to the medium after autoclaving. For solid medium, Granulated Agar (Difco) was added to a final concentration of 2 % w/v prior to autoclaving.

2.1.7. Synthetic dextrose (Minimal) medium

Table 2.3: Basic requirements for synthetic dextrose (minimal) media.

Ingredients	Amount per litre
Glucose	20 g
Yeast Nitrogen Base (without amino acids, with ammonium sulphate – Difco)	6.7 g
dH_2O	Up to 1 L final volume

For solid medium, Granulated Agar (Difco) was added to a final concentration of 2 % w/v prior to autoclaving. To select for yeast cells carrying plasmid DNA the relevant nutritional marker was selected for by adding Yeast Synthetic Complete Drop-Out Media Supplement (Formedium) prior to autoclaving, lacking the appropriate amino acid. For uracil drop-out media, 1.9 g per litre was added.

2.1.8. Galactose induction (YEPGal) medium

Table 2.4: Ingredients required for galactose induction media.

Ingredients	Amount per litre
Galactose	20 g
Yeast Nitrogen Base (without amino acids, with ammonium sulphate – Difco)	6.7 g
dH_2O	Up to 1 L final volume

For solid medium, Granulated Agar (Difco) was added to a final concentration of 2 % w/v prior to autoclaving. To select for yeast cells carrying plasmid DNA the relevant nutritional marker was selected for by adding Yeast Synthetic Complete Drop-Out Media Supplement (Formedium) prior to autoclaving, lacking the appropriate amino acid. For uracil drop-out media, 1.9 g per litre was added.

2.1.9. Complete medium with variable carbon source

Table 2.5: Ingredients required for complete media with variable carbon source.

Ingredients	Amount per litre
Carbon source (dextrose, galactose, sucrose, fructose, maltose)	20 g
Yeast Nitrogen Base (without amino acids, with ammonium sulphate – Difco)	6.7 g
dH_2O	Up to 1 L final volume

For solid medium, Granulated Agar (Difco) was added to a final concentration of 2 % prior to autoclaving.

2.1.10. Glycerol glucosamine medium (GGM)

Table 2.6: Basic requirements of glycerol glucosamine media, prior to autoclaving.

Ingredients	Amount per litre
Glycerol (100 %)	20 ml
Yeast Extract (Difco)	10 g
Bactopeptone (Difco)	20 g
dH_2O	Up to 1 L final volume

After autoclaving, 0.05 % D-[+]-glucosamine hydrochloride (Sigma) was added from a 1 % stock filter sterilised in dH_2O. For solid medium, Granulated Agar (Difco) was added to a final concentration of 2 % w/v prior to autoclaving. For control GGM, glycerol (100 %) was replaced with glucose 20 g per litre.

For the induction of the [*GAR*$^+$] prion, sodium D-lactate (sigma) was added to the medium prior to autoclaving to give final concentrations of 0.025 %, 0.625 % and 1.25 %.

2.2. Luria Bertani (LB) media for the culture of *Escherichia coli*

Table 2.7: Ingredients required for Luria Bertani (LB) media.

Ingredients	Amount per litre
Bactotryptone (Difco)	10 g
Yeast Extract (Difco)	5 g
Sodium Chloride	10 g
dH_2O	Up to 1 L final volume

For solid medium, Granulated Agar (Difco) was added to a final concentration of 2 % w/v prior to autoclaving. To select for ampicillin resistant transformants of *E. coli*, ampicillin was added to a

final concentration of 100 µg/mL after the medium had been autoclaved, from a 100 mg/mL stock solution in dH_2O, filter sterilised.

2.3. Incubation conditions for the culture of *Saccharomyces cerevisiae, Saccharomyces bayanus, Saccharomyces mikatae, Saccharomyes kudriavzevii*

All strains of *Saccharomyces cerevisiae, Saccharomyces bayanus and Saccharomyces mikatae* were grown at 30 ^oC unless otherwise indicated, with constant shaking at 200 rpm for liquid cultures. All strains of *Saccharomyces kudriavzevii* were grown at room temperature (~24 ^oC), with constant shaking on a rolling mixer for liquid cultures.

2.4. Incubation conditions for the culture of *Escherichia coli*

All strains of *Escherichia coli* were incubated at 37 ^oC, with constant shaking at 200 rpm for liquid cultures.

2.5. Growth and viability analysis of *Saccharomyces* strains

2.5.1. Automated growth rate analysis

A single colony of yeast was inoculated into 5 ml of the relevant medium for overnight growth. Cell density was determined by absorbance at OD 600, and the appropriate volume of overnight culture was used to inoculate 1ml of fresh media in a sterile 24-well plate (Greiner) to a final OD 600 ~0.1 units. A BMG Labtech FLUOstar OPTIMA plate reader was used to measure growth rate of the culture with the following settings:

- double orbital shaking mode

- 3 mM diameter shaking width
- 1837 second cycle time
- 600 nm excitation
- 400 nm shaking frequency
- 30 secs additional shaking time before each cycle
- 0.5 sec positioning delay

The strain doubling time was determined using the following calculation: time in minutes was plotted against OD600 values using Microsoft Excel, and then an exponential trend-line was applied to the graph along with the trend-line equation. The natural logarithm of 2 was divided by the equation x value to give the doubling time in minutes.

2.5.2. Growth analysis on different carbon sources

Strains were grown overnight in 5 ml YEPD complete media (see Section 2.1.2). Cells from a 500 µl aliquot were pelleted by centrifugation at 13,000 rpm for 30 secs at room temperature, washed in 500 µl sterile dH_2O, pelleted and resuspended again. An aliquot of the washed cells was used to establish a 5x fold dilution series in water, before a 96 well replica-plater was used for spotting onto complete agar medium containing various carbon sources (see Section 2.1.9). Plates were incubated at 30 ^oC for 2-3 days or until growth was present (~24 ^oC for *S. kudriavzevii*).

2.5.3. Methylene blue staining of yeast cells

Strains were grown overnight in 5 ml YEPD complete media (see Section 2.1.2). Cells from a 200 µl aliquot were then centrifuged at 13,000 rpm for 30 secs at room temperature and mixed with 200 µl 0.1% (w/v) methylene blue solution. Stained cells were immediately visualised by loading in a haemocytometer, and images were captured on a Huawei P20 Pro using the Lictin Cell Phone Microscope Adapter.

2.6. *Saccharomyces cerevisiae* strains used in this study

Table 2.8: Saccharomyces cerevisiae strains used in this study.

Strain	Genotype	Source
BY4741	*MATα his3Δ1 leu2Δ0 met15Δ0 ura3Δ0*	(Brachmann et al., 1998)
74D-694	*MATa ade1-14, trp1-289, his3Δ-200, ura3-52, leu2-3, 112*	(Patino et al., 1996)
BY4743	*MATa/α; his3D1/his3D1; leu2D0/leu2D0; met15D0/MET15; LYS2/lys2D0; ura3D0/ura3D0*	(Brachmann et al., 1998)
DBVPG6044 (3983)	*Mat α, ho::HygMX, ura3::KanMX-Barcode*	(Cubillos et al., 2009)
YPS128 (3903)	*Mat α, ho::HygMX, ura3::KanMX-Barcode*	(Cubillos et al., 2009)
Y12 (3913)	*Mat α, ho::HygMX, ura3::KanMX-Barcode*	(Cubillos et al., 2009)
UWOPS 03.461.4 (3923)	*Mat α, ho::HygMX, ura3::KanMX-Barcode*	(Cubillos et al., 2009)
DBVPG6765 (3883)	*Mat α, ho::HygMX, ura3::KanMX-Barcode*	(Cubillos et al., 2009)
SX1	Genetically undefined*	(Wang et al., 2012)
SX2	Genetically undefined*	(Wang et al., 2012)
SX6	Genetically undefined*	(Wang et al., 2012)
BJ6	Genetically undefined*	(Wang et al., 2012)
BJ20	Genetically undefined*	(Wang et al., 2012)
BJ14	Genetically undefined*	(Wang et al., 2012)

HN11	Genetically undefined*	(Wang et al., 2012)
HN14	Genetically undefined*	(Wang et al., 2012)
HN15	Genetically undefined*	(Wang et al., 2012)
HN16	Genetically undefined*	(Wang et al., 2012)
FJ7	Genetically undefined*	(Wang et al., 2012)
HN2	Genetically undefined*	(Wang et al., 2012)

*Preliminary studies were carried out with genetically undefined wild strains of *S. cerevisiae,* discovered in remote parts of the planet ranging from rotten tree bark in primeval forests to fruit in secondary forests in Northern and Southern China.

2.7. *Saccharomyces cerevisiae* strains from the Yeast Knock-Out Collection (http://www.openbiosystems.com/GeneExpression/Yeast/YKO/) used in this study

BY4741 (*Mat a his3Δ1 leu2Δ0 met15Δ0 ura3Δ0*) derivatives with the *kanMX4* gene inserted in the place of indicated gene:

Table 2.9: Saccharomyces cerevisiae strains from the knockout collection used in this study.

Hsp104Δ	*hsp78Δ*	*hsp82Δ*	*upf1Δ*	*upf2Δ*	*upf3Δ*

2.8. *Saccharomyces* strains used in this study

Table 2.10: Strains of *Saccharomyces* used in this study.

Strain	Genotype	Source
S.bayanus JRY9194*	*MATa hoD::loxP his3 lys2 ura3*	C.T.Hittinger (Scannell et al., 2011)
S.bayanus JRY9195*	*MATα hoD::loxP his3 lys2 ura3*	C.T.Hittinger (Scannell et al., 2011)

S.mikatae JRY9183	*MATa hoD::NatMX trp1D::HygMX ura3D::HygMX*	C.T.Hittinger (Scannell et al., 2011)
S.mikatae JRY9184	*MATα hoD::NatMX trp1D::HygMX ura3D::HygMX*	C.T.Hittinger (Scannell et al., 2011)
S.kudriavzevii JRY9185	*MATa hoD::natMX ura3D0*	C.T.Hittinger (Scannell et al., 2011)
S.kudriavzevii JRY9188	*MATα hoD::natMX trp1D0 ura3D0*	C.T.Hittinger (Scannell et al., 2011)

For long term storage, 500 µl of each strain was mixed with 500 µl 80 % glycerol and stored at -80 ºC until required. Strains streaked on solid media were stored at 4 ºC until required.

* Within the species *Saccharomyces bayanus*, a natural subgroup; *Saccharomyces uvarum* was identified, with unique characteristics making it clearly distinguishable from other species of *Saccharomyces* (Rainieri et al., 1999). This species is often referred to as *S. bayanus var uvarum*. In 1999, it was reported that strain CBS 7001 is a standard *S. uvarum* strain, with a fully sequenced genome and auxotrophic mutants being derived from it (Rainieri et al., 1999). In this study, *S. bayanus* JRY9194 and *S. bayanus* 9195 are used; derived from this CBS 7001 type strain. In line with the description by Scannell *et al*. (2011) from which these strains were obtained, both *S. bayanus* JRY9194 and JRY9195 will be referred to as *S. bayanus*, despite being derived from strain CBS 7001 earlier labelled as *S. uvarum.*

2.9. *Escherichia coli* strains used in this study

Table 2.11: E. coli strains used in this study.

Strain	Genotype
DH5α	F-*deoR endA1 recA1 relA1 gyrA96 hsdT17(rk-mk+) phoAsupE44 thi-1 Δ(lacZYA-argF)U169 Φ80δlacZΔM15*

For long term storage, 500 µl of each strain was mixed with 500 µl 80 % glycerol and stored at -80 ^{o}C until required. Strains streaked on solid media were stored at 4 ^{o}C until required.

2.10. Plasmids used in the study

Table 2.12: DNA plasmids used in this study.

Plasmid	Description	Selectable Markers[a]	Source
pKA291 pVT100U-mt GFP (PCG50)		2 µ, *URA3*	Campbell Gourlay (University of Kent)
p6442-*SUP35NM-GFP*	*SUP35NM* region with C-terminal *GFP* tag under the control of the *CUP1* promoter	2 µ, P_{CUP1}, *URA3*	T. Serio Lab
pAG426-*RNQ1-GFP*	*RNQ1* ORF, C-	2 µ, P_{GAL1} *URA3*	Gemma Staniforth (University of Kent)

	terminal *GFP* tag		
pYES2-Htt-25Q	25Q-huntingtin fragment expressed with *GFP* tag under the control of the GAL-promoter	2 µ, P_{GAL1} *URA3*	Y Chernoff (Meriin et al., 2002)
pYES2-Htt-97Q	97Q-huntingtin fragment expressed with *GFP* tag under the control of the GAL-promoter	2 µ, P_{GAL1} *URA3*	Y Chernoff (Meriin et al., 2002)
GAL72Q+ProGFPp416	*HTT* region with C-terminal *GFP* tag	P_{GAL1} *URA3*	Addgene plasmid # 15582 ; http://n2t.net/addgene:15582 ; RRID:Addgene_15582
GAL46Q+ProGFPp416	*HTT* region with C-terminal *GFP* tag	P_{GAL1} *URA3*	Addgene plasmid # 15581 ; http://n2t.net/addgene:15581 ; RRID:Addgene_15581
pBEVY-GU-Aβ-mNeonGreen		2 µ, P_{GAL1} *URA3*	Nadejda Koloteva-Levine (University of Kent)
pBEVY-GU-mNeonGreen		2 µ, P_{GAL1} *URA3*	Nadejda Koloteva-Levine (University of Kent)

[a] **selectable markers** for transformation used:

URA3: uracil biosynthesis gene from *Saccharomyces cerevisiae*

2.11. Oligonucleotide primers

Table 2.13: Oligonucleotide primers used in this study.

Primer	Sequence 5' → 3'
Hsp104_Whole_F	TAGCCAAGCGTTACTTGCCA
Hsp104_Whole_R	TGGATCATGGAGTTGGCACC
KanMX_104_Insert_F	GGCGCAAACTTATGCAACCT
KanMX_104_Insert_R	AGAACCTCAGTGGCAAATCCT
Hsp78_Whole_F	GGGACGCTGAAAGAGCTGAA
Hsp78_Whole_R	AATAGCAGCAATGGCCTCGT
KanMX_78_Insert_F	GCATCGCGTTTGAATAGGGG
KanMX_78_Insert_R	TAATTTTTGCTTCGCGCCGT
UPF1_Whole_F	TGACAGGATGCAAGACGCAT
UPF1_Whole_R	CAGCACCAACACATGTGCAA
KanMX_UPF1_Insert_F	AGGCATCGTTTTAACGCACAC
KanMX_UPF1_Insert_R	TCAGAAACAACTCTGGCGCA
UPF2_Whole_F	TGGAGCAAACTGCCAGTGTAT
UPF2_Whole_R	TCCCAGTGAGCTTTCCGAAC
KanMX_UPF2_Insert_F	CGAATTGATGGAGCCTGCTT
KanMX_UPF2_Insert_R	GATTGTCGCACCTGATTGCC
UPF3_Whole_F	TGCTACCTCCAAATTTGACTGC
UPF3_Whole_R	TCACCAGTTCCAACCAGCTC
KanMX_UPF3_Insert_F	AGGAAAGGAAAACCTACTGAGGG
KanMX_UPF3_Insert_R	TCAGAAACAACTCTGGCGCA
KanMX_Whole_F	GGCAATCAGGTGCGACAATC
KanMX_Whole_R	GATCCTGGTATCGGTCTGCG

All oligonucleotide primers were synthesised by Eurofins MWG Operon. The primers were stored as 100 pmol/µL stock solutions in sterile MilliQ water at -20 ^{o}C until required.

2.12. Introduction of DNA into host cells

2.12.1. Transformation of *Saccharomyces* species using the lithium acetate method

Using a sterile inoculating loop, a fresh colony of yeast was picked and inoculated into 5ml of appropriate medium and incubated overnight at 30 ^{o}C with shaking (~24 ^{o}C for *S.kudriavzevii*). 1 ml of the fresh overnight culture was harvested by benchtop centrifugation at 13,000 rpm for 20 sec at room temperature. The supernatant was decanted and the pellet was resuspended in the following reagents added sequentially: 240 µl of polyethylene glycol (PEG)-4000 (50 % w/v), 36 µl of 1 M LiOAc, 10 µl of freshly denatured single-stranded carrier DNA (salmon sperm DNA, 10 mg/ml), 5 µl of plasmid DNA (up to 1 ug), and 34 µl of sterile dH_2O. The transformation mix was vortexed at full speed for 1 min before incubating at 30 ^{O}C for 30 min (~24 ^{o}C for *S. kudriavzevii)*, followed by incubation at 42 ^{o}C for 30 min. Cells were harvested by benchtop centrifugation at 3,000 rpm for 2 min at room temperature. Following centrifugation, the supernatant was decanted and the pellet resuspended in 1 mL YEPD medium and left at room temperature overnight. This media was decanted, and cells were resuspended in 300 µl of sterile dH_2O prior to plating 50-200 µl on the appropriate synthetic complete drop-out selection medium. Plates were incubated at 30 ^{O}C for 3-4 days, and the transformants subsequently re-streaked onto fresh synthetic complete drop-out selection medium, as appropriate.

2.12.2. Optimised transformation of *Saccharomyces* species using the lithium acetate method

Cells from an overnight culture were resuspended in 50 ml YEPD and grown to a density of 0.7-1.0 OD_{600}. Cells were harvested by centrifugation at 4000 rpm for 5 mins and resuspended in 10 ml sterile water (purchased from Sigma: W4502-1L and autoclaved). Cells were harvested again, resuspended in 1 ml sterile water and transferred to a 1.5 ml Eppendorf tube. The cells were harvested again by centrifugation at 5000 rpm for 1 minute and resuspended in 1.5 ml freshly prepared sterile TE/LiOAc prepared from 10 x concentrated stocks (giving a final dilution v/v of 1^{TE}: 1^{LiOAc}: 8^{dH2O}).

Components of TE/LiOAc: 10x LiOAc = 1 M LiOAc (adjusted to pH 7.5 with dilute acetic acid), 10 x TE (0.1 M Tris/HCL, 0.01M EDTA [pH 7.5]

A 50 µl aliquot of cells were harvested again, resuspended in 200 ul TE/LiOAc and mixed with 5 µl plasmid DNA and 5 µl of ssDNA. 300 µl of freshly prepared sterile 40% PEG 4000 prepared from stock solutions (giving a final dilution vol/vol of 1^{TE}: 1^{LiOAc}: 8^{PEG}) was added. The cells were then incubated for 30 mins at 30 ^{o}C with constant agitation.

Components of 40 % PEG solution:

50 % PEG 4000 (filter sterilised), 10 x TE, 10 x LiOAc

84 ul undiluted DMSO was added to each sample, and cells were incubated at 42 ^{o}C for 15 mins. Following the addition of 800 µl sterile H_2O, cells were collected by centrifugation at 13000 rpm for 10 secs, and resuspended in 1ml YEPD for 2-3 hrs at 30 ^{o}C (~24 ^{o}C for *S. kudriavzevii*). The media was decanted, and cells were resuspended in 300 µl of sterile dH_2O prior to plating 50-200 µl on the appropriate synthetic complete drop-out selection medium. Plates were incubated at 30 ^{O}C for 3-4 days, and the transformants subsequently re-streaked onto fresh synthetic complete drop-out selection medium, as appropriate.

2.12.3. Transformation of *Saccharomyces* species using electroporation

A single colony of yeast was used to inoculate 100 ml of YEPD complete medium and incubated overnight at 30 ^{o}C with shaking (~24 ^{o}C for *S. kudriavzevii*). 100 ml of culture was harvested by centrifugation at 5000 rpm for 2 mins, resuspended in TELiDTT (using fresh DTT) (filter-sterilised), and incubated at room temperature for 1 hr.

Components required for TELiDTT: 10 ml 10 x TE, 10 ml 1 M LiOAc, 1 ml 1 M DTT, dH2O up to 100 ml final volume.

The cell suspension was centrifuged at 5000 rpm at 4 °C for 5 mins, sequentially washed in 25 ml ice-cold water and then 10 ml 1 M sorbitol. Samples were harvested again at 5000 rpm at 4 °C for 5 mins, resuspended in 100 µl ice cold 1 M sorbitol and kept on ice. For electroporation, 40 µl of cell suspension was placed in a pre-chilled 1.5 ml Eppendorf tube along with ~5 ng plasmid DNA. The mixture was incubated on ice for 5 mins, transferred to an electroporation cuvette, placed in an electroporation chamber and pulsed at 1.5 kV, 25 µFD and 200 ohms. 1 ml 1 M sorbitol was immediately added to the sample and was mixed by inversion. 100 µl of each sample was plated on the appropriate selective medium with the addition of 1 M sorbitol, and incubated at 30 °C for 2-5 days until growth was observed.

2.12.4. Transformation of *Escherichia coli* with plasmid DNA

The appropriate purchased competent bacterial strain (see Section 2.9) was removed from -80 °C storage and thawed on ice. The cells were mixed gently by flicking the tube and 50-100 µL of cells were transferred to a pre-chilled 1.5 ml Eppendorf tube. Up to 5 µl of plasmid DNA (≤1 µg) was added to the cell suspension per 50 µl of competent cells, and the tube was gently swirled to mix. The transformation mix was incubated on ice for 30 mins before 45 secs heat-shock at 45 °C and returned to ice for a further 2 mins. The transformation reaction was diluted with 900-950 µl of LB medium (Table 2.7) and incubated at 37 oC for 1 hr, with shaking at 200 rpm. Between 50-200 µl of the mixture was plated on LB agar plates containing 100 µl ampicillin (Table 2.7), and the plates were incubated at 37 oC overnight.

2.13. DNA Methods

2.13.1. Extraction and small-scale purification of plasmid DNA from *Escherichia coli*

5 ml LB medium with 100 µg/ml ampicillin (see Section 2.2) was inoculated with a single colony of *E.coli* bearing the plasmid of interest and grown overnight at 37 ^{o}C with shaking. Cells were harvested by centrifugation at 13,000 rpm for 10 min at room temperature and the supernatant decanted. The resulting pellet was used to isolate the required plasmid DNA using a Qiagen QIAprep Spin Miniprep Kit according to manufacturer's instructions. The DNA was eluted with 50 µl of the EB buffer provided with the Qiagen QIAprep Spin Miniprep Kit.

2.13.2. Separation of DNA by agarose gel electrophoresis

DNA fragments were separated by electrophoresis on 1 % (w/v) agarose gel when the fragments were expected to be greater than ~1 kb in length. For samples containing fragments of a smaller size (<1 kb) a 1.5 % (w/v) agarose gel was used. The analytical gels were made with Molecular Biology Grade agarose (Sigma) and were melted in 1x TAE buffer in a microwave oven for 2 mins at full power.

Components of 1 x TAE buffer: 4.84 g Tris Base per 1 L, 1.14 mL Glacial Acetic Acid per 1 L, 2 mL 0.5 M EDTA (pH 8.0), milli-Q water up to 1 L.

The molten liquid agarose was cooled to ~50 °C before 5 µL of Sybr-Safe DNA stain (ThermoFisher) per 50 ml of gel was added. The gel solution was poured into a gel forming cassette and placed in an electrophoresis tank once solidified. 1x TAE buffer was added in sufficient quantity to cover the gel surface by 2-3 mm. DNA samples were prepared by adding 1/5 of a volume of 6x blue loading dye (Promega) to the samples and loaded into the wells of the gel. For plasmid DNA preparations and PCR products, 5 µl of samples were loaded. Electrophoresis was carried out at 100 V until the bands had migrated the desired distance ~1 cm from the end of the gel. The DNA fragments were visualised by short wavelength (312 nm) UV transillumination wearing appropriate PPE.

2.13.3. Extraction and purification of genomic DNA from *Saccharomyces* species

A single yeast colony was used to inoculate 300 µl of Yeast Cell Lysis Solution supplied in the Yeast Genomic DNA Purification Kit (MasterPure), before incubation at 65 °C for 15 min. Samples were placed on ice for 5 min, and 150 µl of MPC Protein Precipitation Reagent (MasterPure) was added. Samples were mixed by gentle vortexing, and cellular debris was pelleted by centrifugation in a microcentrifuge at room temperature for 10 min at ≥ 10,000 rpm. The supernatant was mixed with 500 µl isopropanol in a clean 1.5 ml Ependoorf tube, and DNA was pelleted at room temperature by centrifugation for 10 min at ≥ 10,000 rpm. The supernatant was removed, and the pellet containing the DNA was washed with 70 % (v/v) ethanol. The remaining DNA was suspended in 35 µl TE Buffer.

Components required for TE Buffer: 10 mM Tris-HCl, 1 mM EDTA (pH 8.0)

2.13.4. Polymerase Chain Reaction (PCR) amplification of specific DNA

PCR was performed using the Roche "High Fidelity PCR System" and a Techne TC-3000 thermal cycler. Either 1.5 µl of mini-prep plasmid DNA (see Section 2.10) or 1 µl of yeast genomic DNA (see Section 2.13.3) was used as the source of the DNA template. The following reagents were mixed on ice in a thin-walled 0.2 ml thin-walled Eppendorf PCR tube (Table 2.14)

Table 2.14: Reagents required for PCR amplification of DNA.

Reagent	**Volume Added**	**Final Concentration**
High Fidelity Buffer (10x) with 15 ml $MgCl_2$	5 µl	(1.5 ml $MgCl_2$)
dNTP mix, 10 mM each dNTP	1 µl	200 µM each dNTP
Forward Primer 100 pmol/µl	1 – 5 µl	300 nM
Reverse Primer 100 pmol/µl	1 – 5 µl	300 nM
Template DNA	1 – 5 µl	0.1 – 250 ng
High Fidelity Enzyme Mix	1 µl	3.4 U/reaction
Sterile Milli-Q water	Up to 50 µl	

The contents of the tube were mixed thoroughly by vortexing and placed in the thermal cycler. The cycling programme used was specifically tailored to the size of the DNA being amplified and to the primers being used (Table 2.13). A 5 µl aliquot of the PCR product was run on an agarose gel (see Section 2.13.2) and the remainder stored at -20 ^{o}C until required.

2.14. Protein Methods

2.14.1. Separation of proteins by SDS-polyacrylamide gel electrophoresis (SDS-PAGE)

SDS-polyacrylamide gel electrophoresis (SDS-PAGE) was performed with precast gels using NuPAGE 10 % Bis-Tris gels with NuPAGE MOPS SDS running buffer, according to manufacturer's instructions. An Invitrogen X-Cell SureLock gel tank was used, and the gel was typically run at 200 V for 50 mins.

2.14.2. Preparation of cell-free lysates for western blot analysis

A single colony of the desired strain was used to inoculate 10 ml of appropriate liquid medium. The culture was grown overnight at 30 ^{o}C (~24 ^{o}C for *S. kudriavzevii*) with constant shaking. This starter culture was then used to inoculate a further 10 ml of appropriate medium to an OD600 of 0.1. Depending on the strain being studied, a wash step was carried out prior to sub-culturing. This wash step included harvesting cells by centrifugation at 3,000 rpm for 5 min at room temperature, decanting the supernatant and resuspending the pellet in sterile water. Two further wash steps were carried out, and the sub-culture was then incubated at 30 ^{o}C until an OD600 of 0.4-0.6 was reached. Certain strains were resuspended in a 2 % galactose induction medium (Table 2.4) and incubated for a minimum of 3 hrs. The OD600 of each culture was measured and a volume equivalent to 4.0 OD600 units was removed and placed into a separate tube. The cells were harvested for 5 min at 3,000 rpm and the cell pellet was resuspended in 200 µl of lysis buffer.

Components of Western Blotting Lysis Buffer:

100 mM NaOH, 0.05 M EDTA, 2 % SDS, 2 % β-mercaptoethanol

The cell suspension was incubated at 90 °C for 10 mins, before 5 µl of 4 M acetic acid was added and the suspension was vortexed for 30 secs. The cell suspension was incubated at 90 °C for a further 10 mins. For cultures intended for western blot analysis, 50 µl loading buffer was added.

Components required for western blotting loading buffer*:* 0.25 M Tris- HCl (pH 6.8), 50% glycerol, 0.05 % bromophenol blue.

Protein concentration for each sample was determined using an Eppendorf Biophotometer at 280 nm, and 50 µl of a 1 µg/µl preparation was made by diluting an adequate volume of sample in the sample buffer. 15 µl of the preparation was loaded onto an SDS-PAGE gel (see Section 2.14).

2.14.3. Preparation of cell-free lysates for sedimentation analysis

A single colony of the desired strain was used to inoculate 10 ml of appropriate liquid medium. The culture was grown overnight at 30 °C (~24 °C for *S. kudriavzevii*) with constant shaking. This starter culture was then used to inoculate a further 10 ml of appropriate medium to an OD600 of 0.1. Depending on the strain being studied, a wash step was carried out prior to subculturing. This wash step included harvesting cells by centrifugation at 3,000 rpm for 5 min at room temperature, decanting the supernatant and resuspending the pellet in 200 µl sterile water. Two further wash steps were carried out, and the sub-culture was incubated at 30 oC until an OD600 of 0.4-0.6 was reached. Certain strains were resuspended in a YEPGal medium (see Section 2.1.8) and incubated for a minimum of 3 hrs. The OD600 of each culture was measured and a volume equivalent to 4.0 OD600 units was removed and placed into a separate tube. The cell suspension was transferred to a 1.5 ml microcentrifuge tube to which 50 µl lysis buffer and an equal volume of glass beads (diameter 425-600 µm) was added. Cells were lysed by vortexing 4 times for 30 secs, with 30 secs on ice in each interval. 100 µl of lysis buffer was then added and the resuspension briefly vortexed.

Components of sedimentation analysis lysis buffer: 1 x PBS, 100 mM NaCl, 2 mM PMSF, Protease Inhibitor Tablet (Sigma).

The tubes were immediately placed on ice and centrifuged for 3 min at 8,000 rpm in a pre-cooled centrifuge at 4 ^{o}C. 80 µl of supernatant was carefully pipetted to a clean pre-chilled tube, and 40 µl of this was transferred to a 1ml Beckman thick-walled polycarbonate tube. This tube was then placed into a pre-chilled TLA.100 rotor and centrifuged at 50,000 rpm for 15 mins at 4 ^{o}C in a Beckman Optimax ultracentrifuge machine. The remaining 40 µl represented the total (T) lysate fraction. The 40 µl of supernatant collected from the polycarbonate tube following ultracentrifugation represented the soluble (S) lysate fraction and this was transferred to a pre-chilled 500 µl micro-centrifuge tube. A 40 µl aliquot of lysis buffer was used to resuspend the pellet in the polycarbonate tube and this suspension represented the pellet (P) lysate fraction, which was also transferred to a pre-chilled tube. To each fraction, 20 µl of sample buffer was added and the samples boiled for 5 mins at 100 oC before loading 15 µl of each onto an SDS-PAGE gel (see Section 2.14).

2.14.4. Staining of SDS-PAGE gels

After electrophoresis, proteins within a gel were visualised following a 1hr incubation with Coomassie stain, followed by a 1hr incubation with de-stain, and then an overnight de-staining step in fresh de-stain solution at room temperature.

Components required for Coomassie stain*:* 40 % (v/v) Methanol, 20 % (v/v) Glacial Acetic Acid, 0.1% (w/v) Coomassie Brilliant Blue R250.

Components required for de-stain: 10 % (v/v) Methanol and 10 % (v/v) Acetic Acid.

2.14.5. Western blot analysis of SDS-PAGE gels

Proteins were separated on the basis of molecular mass by SDS-PAGE (see Section 2.14). The wells and bottom edge of the gels were removed using a gel knife and the gel was then incubated in transfer buffer. Six pieces of Whatmann 3 mm paper (Thermo Fisher) were cut to approximately the same size as the gel (~30 mm x 30 mm) and soaked briefly in transfer buffer immediately prior to blotting. One piece of PVDF Polyvinylidene fluoride (PVDF) membrane (Thermo Fisher) was activated in 100 % methanol for 1 minute with agitation.

Components required for western blotting transfer buffer: 0.29 % (w/v) Glycine, 0.58 % (w/v) Tris-HCl, 0.037 % (w/v) SDS, 20 % Methanol.

Two pieces of blotting paper were placed on the anode plate of a Trans-Blot Semi-Dry Transfer cell (BioRad), followed by the PVDF membrane, the polyacrylamide gel, and the final two pieces of blotting paper. To ensure that there were no significant air bubbles present between layers, a roller was used to remove any excess air. The cathode plate was place on top and the apparatus was connected to a power supply. A voltage of 10V was applied for 1 hr. Upon completion of the semi-dry transfer the PVDF membrane was removed for use in the immunoblotting procedure (see Section 2.14.6).

2.14.6. Immunoblotting procedure

Following on from the semi-dry transfer protocol, the PVDF membrane was placed in 6 ml of blocking solution in a clean polyethylene terephthalate box and incubated with shaking for 1 hr at room temperature. The membrane was briefly washed twice with TBS/T, placed in 15-20 ml of blocking solution containing the appropriate concentration of primary antibody (Table 2.16), and incubated at 4 ^{o}C overnight with shaking.

Components of western blotting blocking solution:

5 % (w/v) Dried Skimmed Milk (Oxoid), TBS/T (Tris Buffered Saline and 0.2 % Tween 20 [Sigma])

Following overnight incubation, the PVDF membrane was carefully removed and washed 3 times with TBS/T for 5 mins. After completion of the wash phases, the PVDF membrane was placed in fresh blocking solution containing an appropriate concentration of secondary antibody (Table 2.16) and incubated at room temperature with shaking. The PVDF membrane was then washed with TBS/T as previously undertaken after the primary antibody straining.

2.14.7. ECL detection (Enhanced Chemiluminescence)

The PVDF membrane was placed in a clean polyethylene terephthalate box and the ECL solutions (Table 2.15) were mixed in a 1:1 ratio. The TBS used to incubate the PVDF membrane was discarded and the ECL solution was added and the PVDF membrane incubated for 1 min with constant agitation. The ECL solution was then discarded and the membrane removed and placed in a Saran wrap. The membrane was placed into the SYNGENE G:BOX gel doc system and blots were visualised. The GeneSys Software (Version 1.6.5.0) was used to visualise blots and a Synoptics 6MP camera was used to capture images.

Table 2.15: Components required for ECL solutions 1 and 2.

Solution	**Components**	**Amount up to 5ml**
ECL Solution 1	250 mM luminol 3-aminophthalhydrazide (Fluka No. 09253)	50 µl
	90 mM p-coomaric acid (Sigma No C9008)	22 µl
	1 M Tris.HCl (pH 8.5)	500 µl
	dH_2O	Up to 5 ml final volume
ECL Solution 2	30 % hydrogen peroxide	3.2 µl
	1 M Tris.HCl (pH 8.5)	500 µl
	dH_2O	Up to 5 ml final volume

2.14.8. Semi-Denaturating Detergent Agarose Gel Electrophoresis (SDD-AGE analysis)

The yeast cultures were grown in appropriate medium until OD600 ~4 prior to lysis, which was then performed using the glass bead method (see Section 2.14.3) in PEB buffer.

Components of SDD-AGE PEB Buffer: 25 mM Tris-HCl (pH 7.5), 50 mM KCl, 10 mM $MgCl_2$*$6H_2O$, 1 mM EDTA-Na, Complete Protease Inhibitor Tablet (Sigma).

Once the crude lysate was obtained, cell debris was removed using a 3 min spin at 8000xg (4^{o}C). Lysate obtained in this way is turbid with a total protein concentration of 3-10 mg/ml, measured using a Biophotometer. 1.5 % w/v agarose was melted in 1xTAE, and 10 % w/v SDS was added drop by drop to the molten agarose to avoid solidification, giving a final concentration of 0.1 % SDS. The gel was cast in a 6 x 8 x 0.6cm electrophoresis casting chamber. Before loading the gel, samples containing ~80 µg of lysate protein were incubated in sample buffer at 42 oC for 5 mins. Samples were then run in a horizontal gel chamber in 1 x TAE + 0.1 % SDS at a constant voltage of 125 V.

Components required for SDD-AGE sample buffer: 60 mM Tris-HCL (pH 6.8), 5 % glycerol, 2 % SDS, 0.05 % bromophenol blue.

Once the gel had run to ~1cm from the end of the gel, the wells and bottom edge were removed using a gel knife. Nine pieces of Whatmann 3 mm paper (Thermo Fisher) were cut to approximately the same size as the gel and soaked in transfer buffer T immediately prior to blotting. One piece of PVDF membrane (Thermo Fisher) was activated in 100 % methanol for 1 minute with agitation.

Components required for SDD-AGE Transfer Buffer T: 20 mM Tris-base, 200 mM glycine, 0.1% SDS, 15 % Methanol.

The proteins were transferred from the agarose gel onto PVDF membrane using semi-dry transfer (see Section 2.14.5) and a voltage of 10 V was applied for 1 hr. Upon completion of the semi-dry transfer the PVDF membrane was removed for use in the immunoblotting procedure (see Section 2.14.6)

2.14.9. Antibodies used in study

Table 2.16: Antibodies used in study.

Antibody	Host	Dilution
Anti-Sup35p (MT50)	Rabbit	1:5000
Anti-Hsp104p 34A	Rabbit	1:5000
Anti-Rnq1p	Rabbit	1:5000
Anti-PGK	Rabbit	1:5000
Anti-rabbit (HRP) (Secondary)		1:5000

2.15. Mitochondrial dysfunction assays

2.15.1. 2,3,5-triphenyl tetrazolium chloride (TTC) overlay assay

2,3,5-triphenyl tetrazolium chloride (TTC) is reduced from a colourless pigment to an insoluble red pigment by the activity of the mitochondrial respiratory chain (Ogur et al., 1957) and can therefore be used as an indicator of respiratory proficiency. A single colony of the yeast strain to be tested was used to inoculate the appropriate medium and grown as an overnight culture. These cultures were then diluted 1:50,000 in sterile dH_2O and 200 µl plated onto the appropriate medium. Plates were incubated for 2-3 days at 30 ^oC (~24 ^oC for *S. kudriavzevii*) until colonies were well formed. TTC at 0.2 % w/v was dissolved in 0.067 M Sodium Phosphate buffer (pH 7.0) containing 1.5 % granulated agar (Difco), and ~10 ml of the solution per plate was overlaid on the yeast colonies. Following a 1-2 hr incubation at room temperature, colony colour was noted and plates were scanned for record.

2.15.2. High resolution respirometry

The Oroboros O2K Oxygraph High Resolution Respirometer was used to determine the consumption of O2 from mitochondria, and Datlab 4 software was used for the analysis of the data generated. Calibration of the instrument was carried out by loading 2 ml PBS into both 2 ml capacity chambers, maintained overnight at 30 ^{o}C. Cells from an overnight liquid culture were counted using a Neubauer haemocytometer and diluted to a cell density of 10^6 cells/ml into 3 ml of an appropriate medium lacking glucose. 2 ml of each diluted culture was inserted into one of the two chambers to ensure each chamber was full. The chamber stoppers were inserted into position and any residual liquid culture was aspirated away. The exact cell concentration was then entered into the Datlab4 software for an accurate oxygen flux/unit sample (cell) reading. For the analysis of mitochondria, a series of drugs that target the electron transport chain were introduced into the chamber using clean syringes. The sequence of drug addition is outlined below, with a 5 minute interval left between each.

Respirometry drugs:

The following compounds were used to evaluate respiration in yeast cells:

- Triethiltyn bromide (TET) (Sigma-Aldrich) (0.2 mM final concentration from a 50 mM stock solution in DMSO)
- Carbonylcyanidep-trifluoromethoxyphenylhydrazone (FCCP) (Fluka) (0.012 mM final concentration from a 12 mM stock solution in ethanol)
- Antimycin A (AntA) (Sigma-Aldrich) (0.002 mM final concentration from a 2 mM stock solution in ethanol)

2.16. Microscopy

2.16.1. Sample preparation

Strains from an overnight yeast culture were sub-cultured into a fresh appropriate selective medium and induced for plasmid expression where necessary (2.1.8). Analysis was performed on both stationary-phase and log-phase cells. A suitable aliquot of culture was pelleted by a 30 second centrifugation at 13,000 rpm, washed once with 1ml 1xPBS, harvested again and resuspended in an appropriate volume of 1xPBS (20-200 µl). For visualisation, a 5 µl aliquot was spotted onto a microscope slide.

2.16.2. Cell counting using a haemocytometer

A 10 µl cell suspension was pipetted under the coverslip of the Neubauer haemocytometer and cells within a 25 square region (equivalent to 1 mm^2) were counted and multiplied by 10^4 to determine the cell number per ml of the sample. Any dilution of the sample prior to counting was factored into the final cell number/ml. For greater accuracy, a minimum number of 5 chambers were counted and the average cell count was used to determine final cell number.

2.16.3. 4′,6-diamidino-2-phenylindole (DAPI) staining of yeast cells

A suitable aliquot (0.2 – 1 ml) of log-phase cells were pelleted by a 30 second centrifugation at 13,000 rpm. Cells were resuspended in 0.5 ml 1xPBS buffer, and 1.5 µl of DAPI (6x concentration). Cells were incubated in the dye for ~30 mins, with occasional gentle agitation. Cells were then harvested as before, and the cell pellet resuspended in an appropriate volume of PBS (20 – 200 µl). A 5 µl aliquot was spotted onto a microscope slide for visualisation.

2.16.4. Hoechst staining of yeast cells

Cells from an overnight culture were pelleted by centrifugation at 13,000 rpm for 30 secs and fixed in 70 % (v/v) ethanol. Cells were washed with PBS and stained with 0.1-1 µg/ml of Hoechst 33342 (Sigma-Aldrich) (using a 10mg/ml stock solution in dH2O) for 20 mins. Cells were washed again in PBS, and a 5 µl aliquot was mounted onto a microscope slide for visualisation.

2.16.5. Light and Fluorescent Microscopy

All yeast cell samples were visualised using an Olympus MT20 fluorescence microscope connected to a PC running CellR software (Manufacturer: Soft Imaging System). For the visualisation of fluorescent yeast cells, an Olympus 1x81 inverted microscope was used. The light source was provided by a Cool LED pE4000 illumination system. All images were captured using an Andor's Zyla 4.2 PLUS sCMOS camera. The acquisition software used for visualisation was Micro Manager version 1.4.22 (Manufacturer: µManager). A single drop of Olympus Immoil-F30CC immersion oil was applied to the surface of the cover slip and an Olympus 60 x objective lens (NA = 1.35) was used to locate cells within a sample. An Olympus 100 x objective lens (NA = 1.4) was used to visualize individual cells. Cells with GFP-tagged proteins were analysed using the GFP channel with excitation/emission wavelengths of 488/512 nm. Differential Interference Contrast (DIC) images were taken using a halogen light source with identical settings to GFP imaging. To ensure images were representative of the whole population each microscopy experiment was repeated in triplicate and ~20 pictures were taken per sample. The counting of cells was conducted by eye from images generated.

2.16.6. ImageJ processing of microscope images

The images to be merged were opened in ImageJ FIJI software (Manufacturer: National Institute of Health). The images were first converted to 32-bit type and then saved in .jpeg or .png format.

2.17. Bioinformatics

2.17.1. DNA Sequence analysis

Sequence alignment of gene sequences (nucleotide and amino acid sequences) was carried out in BLAST (Basic Local Alignment Sequence Tool, NCBI). Further analysis for percentage of amino acid sequence similarity between species was carried out using MUSCLE (Multiple Sequence Comparison by Log-Expectation, EMBL-EBI). Intrinsic disordered protein regions of the *RNQ1* gene were predicted in all species using IUPred2 (Walsh et al., 2015). IUPred2 predicts global structural disorder that encompasses at least 30 consecutive residues of the protein.

2.18. Statistical Analysis

The Analysis ToolPak was added into Microsoft Excel as a statistical add-in. Using this data analysis pack, the statistical significance of evidence was quantified by calculation of the p-value, and error bars on all graphs denote standard deviation. By using the 't-Test: Paired Two Sample for Means' tool, statistics were performed on both the biological replicates and technical replicates of each experiment. When the p-value was less than the significance level of 0.05 labelled as *, or 0.01 labelled as **, the null hypothesis was rejected and the difference between the two means was deemed significant.

Chapter 3: Analysing [*PSI*$^{+}$] and [*RNQ*$^{+}$] prions in *Saccharomyces* species

3. Chapter 3: Analysing [*PSI*$^+$] and [*RNQ*$^+$] prions in *Saccharomyces* species

3.1. Introduction

In recent years, research on the well-established yeast prions [*PSI*$^+$] and [*RNQ*$^+$] has been predominantly focussed on laboratory strains of *Saccharomyces cerevisiae,* with very little known about the existence of endogenous [*PSI*$^+$] and [*RNQ*$^+$] prions in non-domesticated strains of *S. cerevisiae,* or in other closely-related species of *Saccharomyces*. The failure to find certain prions in non-domesticated strains of *S. cerevisiae* has contributed to the argument that prions have a detrimental impact on the host, and further highlights a strong selective pressure against their retention in cells growing in a natural environment (Nakayashiki et al., 2005).

In contrast, the prion-forming ability of Sup35 in other species of yeast may imply an evolutionary value of [*PSI*$^+$] formation in organisms such as *Candida albicans, Candida maltose, Debaromyces hansenii* and *Kluyveromyces lactis* (Edskes et al., 2014). However, prion formation in these species was at a much lower frequency than observed in *S. cerevisiae*, and [*PSI*$^+$] formation could not take place in a number of other fungal species. This highlights that the prion-forming ability of Sup35 may not be a conserved trait, and is instead a side effect of a protein domain conserved for an alternative role (Edskes et al., 2014). Su and Harrison (2019) examined the conservation of sequence and of prion-like composition for collections of prion-forming proteins and prion-like proteins from *S. cerevisiae.* They showed that the prion-like status of a protein is conserved for around half the set of prion-formers at the level of *Saccharomycetes,* but the sequences of PFDs seem to evolve more quickly than other domains of prion-like proteins. An increase in mutation rate may be linked to the acquisition of functional roles of PFDs (Su & Harrison, 2019).

Distinct amino acid sequence changes produce barriers to the transmission of [*PSI*$^+$] within *S. cerevisiae* and between other species of yeast (Chen et al., 2007; Edskes et al., 2009). Most species transmission barriers occur as a result of amino acid substitutions in the PFD, however deletions in the *C. albicans* Sup35 M-domain; a region with non-prion function, leads to an

intraspecies transmission barrier (Edskes et al., 2014). Such sequence alterations may have been selected to increase prion resistance in scenarios where [*PSI*$^{+}$] and other prions are severely toxic to a cell (McGlinchey et al., 2011). Moreover, despite a high level of sequence divergence across the Rnq1 protein in *Saccharomyces* species, the possibility of a species barrier for [*PIN*$^{+}$] prion formation is yet to be determined (Harrison et al., 2007).

Near complete genome sequences of *Saccharomyces* will therefore allow comparisons to the *S. cerevisiae* genome, and give insight into species-specific gains, losses, and key evolution events (Scannell et al., 2011). This chapter provides an analysis of the sequences of the *SUP35* and *RNQ1* genes in different *Saccharomyces* species and highlights the potential impact of minor differences in amino acid sequences within prion-forming domains on cross-species prion transmission. Western blot analysis is then used to detect the presence or otherwise of Sup35 and Rnq1 prion proteins in several different *Saccharomyces* species and the propensity of these species to promote the aggregation of the *S. cerevisiae* cross-species barriers examined by expression of ScSup35-GFP and ScRnq1-GFP fusion proteins in four different *Saccharomyces* species.

3.2. A bioinformatic overview of *SUP35* and *RNQ1* genes in all species of *Saccharomyces*

3.2.1. Sequence alignment of *SUP35* and *RNQ1* in *Saccharomyces* species

Amino acid sequence homology of the proteins encoded by the *SUP35* and *RNQ1* genes was inferred using a combination of sequence similarity scores and sequence identity scores. Sequence similarity was predicted in BLAST using a scoring matrix BLOSUM62, to find high-scoring hits that may not match exactly but are similar. BLAST does not take into account gaps in this process, meaning there is potential to miss significant similarities present in the database (Koski & Golding, 2001). Sequence identity also fails to take gaps into account, and scores all amino acids present as one continuous sentence. Therefore, scores of both similarity and identity were considered to predict sequence homology. All sequences were manually aligned and analysed using MUSCLE (Multiple Sequence Comparison by Log-Expectation,

EMBL-EBI) as similarity spread out over an entire domain is likely to be more biologically significant than short, nearly exact matches. Thus, only sequences with >60% homology were inferred as similar, as sequences which share significant similarity are homologous, but many homologous sequences do not share significant similarity.

Sequence comparison of *SUP35* in the species examined revealed a significant degree of amino acid conservation **(Figure 3.1**). Both *S. bayanus* and *S. mikatae* had high percentages of *SUP35* sequence homology to *S. cerevisiae*, but slightly lower similarity when compared to each other. The scores of *S. kudriavzevii* could not be considered, as *SUP35* was only accessible as an incomplete shotgun sequence. In shotgun sequencing, segments of amino acids that are available are often grouped together using a chain termination method to create reads (Harrison & Zimmerman, 1984). Multiple overlapping reads for the target DNA are obtained by several rounds of fragmentation and overlapping, producing inaccurate results and possible false positives of sequence similarity.

A)

Species	No. of amino acids	Predicted molecular weight
S. cerevisiae SUP35	686 aa	76 kDa
S. bayanus SUP35	668 aa	74 kDa
S. mikatae SUP35	535 aa	60 kDa

B)

	S. cerevisiae	*S. bayanus*	*S. mikatae*
S. cerevisiae		92.33	92.34
S. bayanus	92.33		89.21
S. mikatae	92.34	89.21	

Figure 3.1: Sequence comparison of *SUP35*. Panel A: The number of amino acids in *SUP35*, along with the predicted molecular weight for each *Saccharomyces* species. **Panel B:** Alignment of each species of *S accharomyces* shows a high percentage of *SUP35* sequence homology. The sequence of *S. kudriavzevii* was only available as an incomplete shotgun sequence and therefore could not be estimated.

Analysis of the *RNQ1* sequence between species of *Saccharomyces* demonstrated that conservation of amino acid composition of the protein is maintained (**Figure 3.2**). High percentages of sequence homology are seen between *S. cerevisiae, S. mikatae* and *S. kudriavzevii*. A lower, but still significantly high sequence homology is seen between *S. cerevisiae* and *S. bayanus*, but this lower percentage may simply be down to the more distant relationship between the two species. These results suggest that the composition of Rnq1 in *S. cerevisiae* i.e. rich in both glutamine and asparagine residues, is significant for Rnq1 function as it is conserved in the other *Saccharomyces* species, and that these conserved residues have evolved from a common ancestor.

A)

Species	No. of amino acids	Predicted molecular weight
S. cerevisiae RNQ1	405	42
S. bayanus RNQ1	391	41
S. mikatae RNQ1	395	41
S. kudriavzevii RNQ1	405	42

B)

	S. cerevisiae	*S. bayanus*	*S. mikatae*	*S. kudriavzevii*
S. cerevisiae		87.99	91.47	90.15
S. bayanus	87.99		86.4	86.63
S. mikatae	91.47	86.4		87.82
S. kudriavzevii	90.15	86.63	87.82	

Figure 3.2: Sequence comparison of *RNQ1.* Panel A) The number of amino acids in *RNQ1*, along with the predicted molecular weight for each *Saccharomyces* species**.** **Panel B)** Alignment of each species of *Saccharomyces* shows a high percentage of *RNQ1* protein sequence homology.

3.2.2. Analysing the similarity of the Prion-Forming Domain of Sup35 in all *Saccharomyces* species

The N-terminal domain of Sup35 is essential for the *de novo* manifestation and maintenance of the [*PSI*$^{+}$] prion (Li & Lindquist, 2000) and has been labelled the prion-forming domain (PFD), outlined in Chapter 1, Section 4.1. The exact function of the middle M-domain of Sup35 remains unclear, although the substitution for this domain for the charged regions from two other proteins created variants that acquired prion states, albeit with different properties (Liu et al., 2002). One M-domain variant was soluble in both the [*PRION*$^{+}$] and [*prion*$^{-}$] states, curable by GdnHCl, but not curable by genetic modifications of *HSP104*. An alternate variant could only maintain the [*PRION*$^{+}$] state in the presence of the wild-type protein, highlighting the impact of the M-domain on [*PSI*$^{+}$] formation regardless of the same N-terminal prion-determining region (Liu et al., 2002). On the other hand, the C-terminal domain is essential for the translation termination activity of the protein (Ter-Avanesyan et al., 1993) (**Figure 3.3**).

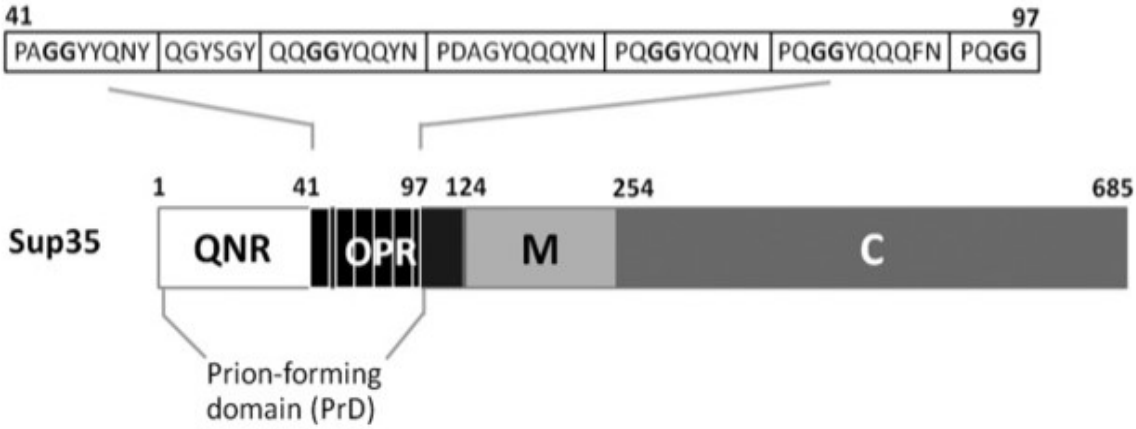

Figure 3.3: **The Sup35 protein of *Saccharomyces cerevisiae* consists of three distinct regions: an N-terminal prion-forming domain containing a Q/N-rich tract (QNR) and a consensus oligopeptide repeat sequence (OPR); a middle (M) domain; and the functional C-terminal domain (C), taken from Josse et al., (2012).**

In *S. cerevisiae,* the N-terminal prion-forming domain resides between residues 1 and 97, which consists of two distinct regions: a Q/N rich region (QNR, residues 1-40) and a series of

oligopeptide repeats (OPR, residues 41-97) (Jossé et al., 2012) (**Figure 3.3**). The QNR region forms the core of amyloid Sup35, whereas the OPR is essential for continued propagation of the [*PRION*$^{+}$] state (DePace et al., 1998; Krishnan & Lindquist, 2005). Unlike the Q/N-rich region of the PFD, the presence of oligopeptide repeats is not recognised as a diagnostic feature of a yeast prion. The impact of primary sequence on prion-like properties in a protein therefore remains to be fully understood (Jossé et al., 2012).

Although conservation of the prion properties of Sup35 exists between species of *Saccharomyces* there is an inability of these yeasts to transmit the infectious prion state (Chen et al., 2007). This 'species barrier' reflects the inability of Sup35 molecules from the different *Saccharomyces* species to co-aggregate with the *S. cerevisiae* Sup35, which is essential for transmission of the [*PSI*$^{+}$] prion state (Kushnirov et al., 2000). Kushnirov et al. (2000) also suggest that the Sup35 N-terminal domain plays a key role in the observed species barrier, thus the sequence of the PFD was compared between each species. Interestingly, it is thought that the asparagine-rich nature of the PFD arose in early *Saccharomycetes* evolution, with *Saccharomycetes* displaying a distinctive trend for population sizes of prion-like proteins (An et al., 2016). Throughout the evolution of *Saccharomycetes,* the likelihood of increasing numbers of N residues and a tendency to form more poly-N tracts led to the expansion of the prion phenomenon. This stands in comparison with other fungi such as *Eurotiales,* which have much fewer Q/N-rich proteins highlighting a greater intolerance for amyloid-forming proteins (An et al., 2016).

The percentage similarities of the PFDs of Sup35 of *S. bayanus, S. mikatae* and *S. kudriavzevii* compared to *S. cerevisiae* are 78%, 89% and 86% respectively. The Sup35 PFD of *S. mikatae* aligns with *S. cerevisiae* with no gaps, whereas *S. kudriavzevii* Sup35 PFD has one gap (**Figure 3.4).** As expected the species with the highest difference in PFD similarity is the most distantly related *S. bayanus*, which lacks one oligopeptide repeat and has two single-residue insertions (**Figure 3.4**). The transmission of prions between species may therefore be inhibited due to a high sensitivity to small differences in PFD amino acid sequence.

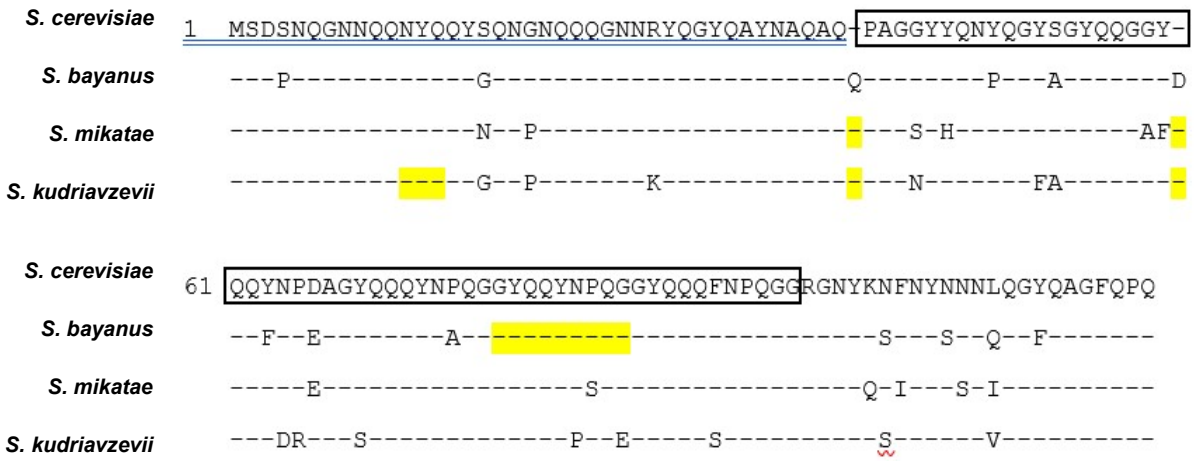

Figure 3.4: Sequence alignment of Sup35 PFDs of each species of *Saccharomyces*. Letters shown depict differences in amino acid residues compared to the sequence of Sup35 PFD in *S. cerevisiae.* Gaps are shown as yellow highlighted dashes, and boxes highlight the oligonucleotide repeats in *S. cerevisiae*.

The minimum region essential for propagation of [*PSI*$^+$] in *S. cerevisiae* is assumed to be the first 57 residues of Sup35; encompassing all Q/N-rich regions and the first two OPRs (Osherovich et al., 2004). Substitutions Q33K and A34K within a previously uncharacterised oligopeptide repeat of Sup35; namely the *sup35-M0* allele, destabilised the fibril structure and eliminated the formation of [*PSI*$^+$] with high efficiency (Danilov et al., 2019), further highlighting this region as important for [*PSI*$^+$] maintenance (DePace et al., 1998). These findings stand in agreement with previous work by Paul et al. (2015), who suggested that both low levels of natural selection and small-scale mutations within the Sup35 PFD will result in aggregation-prone proteins, as a small number of mutations are sufficient in causing aggregation (Paul et al., 2015). Two to seven rationally designed point mutations introduced into four yeast Q/N-rich domains with no detectable aggregation activity promoted such activity in two of the domains, and prion activity in the remaining domains. This highlights the possibility of these non-aggregating domains being a few mutations away from becoming aggregating-domains (Paul et al., 2015). Specifically, **Figure 3.4** highlights a substitution from G to A in a key oligonucleotide repeat in the *S. mikatae* PFD. Further work is thus required in order to confirm whether *S. mikatae* Sup35 has the ability to form the [*PSI*$^+$] prion in the presence of this amino acid substitution.

3.2.3. Predicting the Intrinsic Disordered Protein Regions of Rnq1 in all species of *Saccharomyces*

The PFD of Rnq1 in *S. cerevisiae* has four distinct QN-rich regions (**Figure 3.5**) and one of these regions is usually sufficient to maintain a heritable aggregated state *in vivo*, as well as transmission of the [*PIN*$^+$] prion state to daughter cells (Kadnar et al., 2010). Specifically, amino acids 132-405 are thought to define the prion-forming domain (Sondheimer & Lindquist, 2000). Sondheimer and Lindquist (2000) also show that Rnq1153-405 can form a stable prion when fused to Sup35 lacking the [*PSI*$^+$] PFD. This indicates that the fusion of prion-determining regions with different functional proteins can produce a new prion, whose functions can be switched on or off in a heritable manner (Sondheimer & Lindquist, 2000).

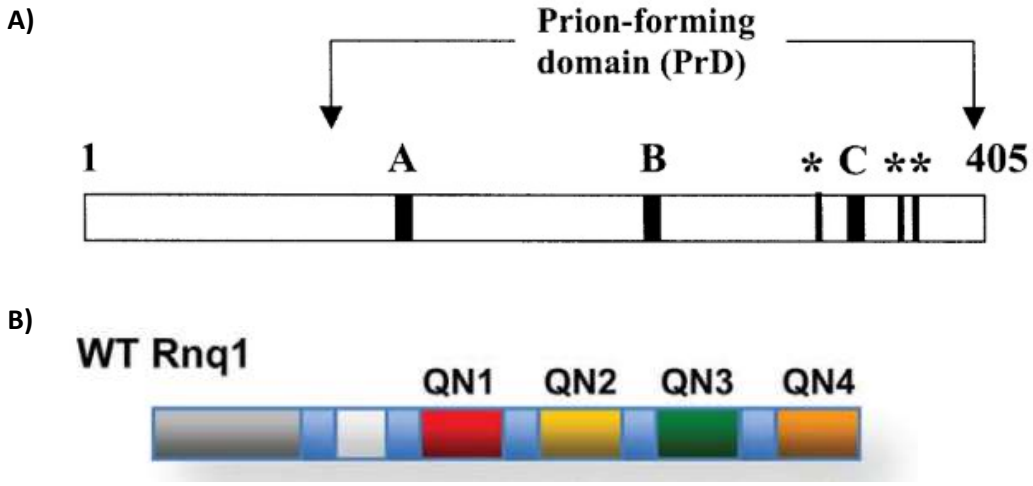

Figure 3.5: The PFD of Rnq1 in *S. cerevisiae*. Panel A) The sequence of *S. cerevisiae* Rnq1 indicating the location of the prion-forming domain, defined by Sondheimer and Lindquist (2000), and the location of the polymorphic regions A, B and C, adapted from Resende et al., (2003). **Panel B)** Each of the Q/N-rich regions QN1, QN2, QN3 and QN4 are seen in red, yellow, green and orange respectively, and can all transmit the prion state (taken from Kadnar et al., 2010).

An increase in glutamine abundance in a protein is associated with an increased tendency to aggregate and is also linked to neurodegenerative pathology in polyglutamine diseases (Meriin et al., 2002). Therefore, differences in the QN-rich regions of Rnq1 between different species of *Saccharomyces* would be predicted to alter a) the frequency with which [*PIN*$^+$] can arise, b) the induction of other prion proteins to undergo conformational changes into their prion state, and c)

the induction of heterologous polyglutamine protein aggregation. As the function of Rnq1 remains unclear, it is possible that both aggregation and interaction with alternative aggregation-prone proteins is key to its function (Kadnar et al., 2010). More recently, Villali et al*.,* (2020) offered an unrelated role for [*PIN*$^{+}$] after seed formation; promoting amplification rather than clearance of Sup35 amyloid by directly competing for Hsp104 binding, thus titrating its activity (Villali et al., 2020). It is now thought that the size of the Sup35 nucleation seed links to amyloid persistence; interactions with [*PIN*$^{+}$], and successful transition between prion states.

As described in Chapter 1, Section 4.1, PFDs are biased towards residues that balance disorder propensity and prion propensity, such as Q and N (Pierce et al., 2005). Such residues are strongly associated with intrinsic disorder, and are highly overrepresented in the Sup35, Rnq1 and Ure2 PFDs (Toombs et al., 2010). Thus, it is well-established that intrinsically disordered protein regions (IDRs) play a critical role in the formation of many yeast prions, but further analysis is required to distinguish the level of IDR conservation in proteins of *Saccharomyces.*

IUPred2 (Walsh et al., 2015) was used to identify IDRs which lack a stable monomeric structure within the Rnq1 protein of each species of *Saccharomyces.* Dupace et al*.,* (1998) showed that prion protein Sup35 contains intrinsically disordered Q/N rich segments, but such regions are yet to be published in Rnq1. Establishing IDRs in the Rnq1 protein of each species may act as a diagnostic feature for prion propensity. Each residue in each Rnq1 sequence was scored between 0 and 1, corresponding to the probability of the given residue being part of a disordered region. An IDR is predicted as a structural disorder encompassing at least 30 consecutive residues of the target protein (Walsh et al., 2015). The PFD of Rnq1 in *S. cerevisiae* is depicted in **Figure 3.6** with consistent high scores close to 1, highlighting this region as one that is intrinsically disordered. The predictions for IDRs in all other *Saccharomyces* Rnq1 proteins are highly consistent with the PFD of Rnq1 in *S. cerevisiae,* suggesting region homology between species, and the predicted propensity of these species to perpetuate the [*PIN*$^{+}$] prion.

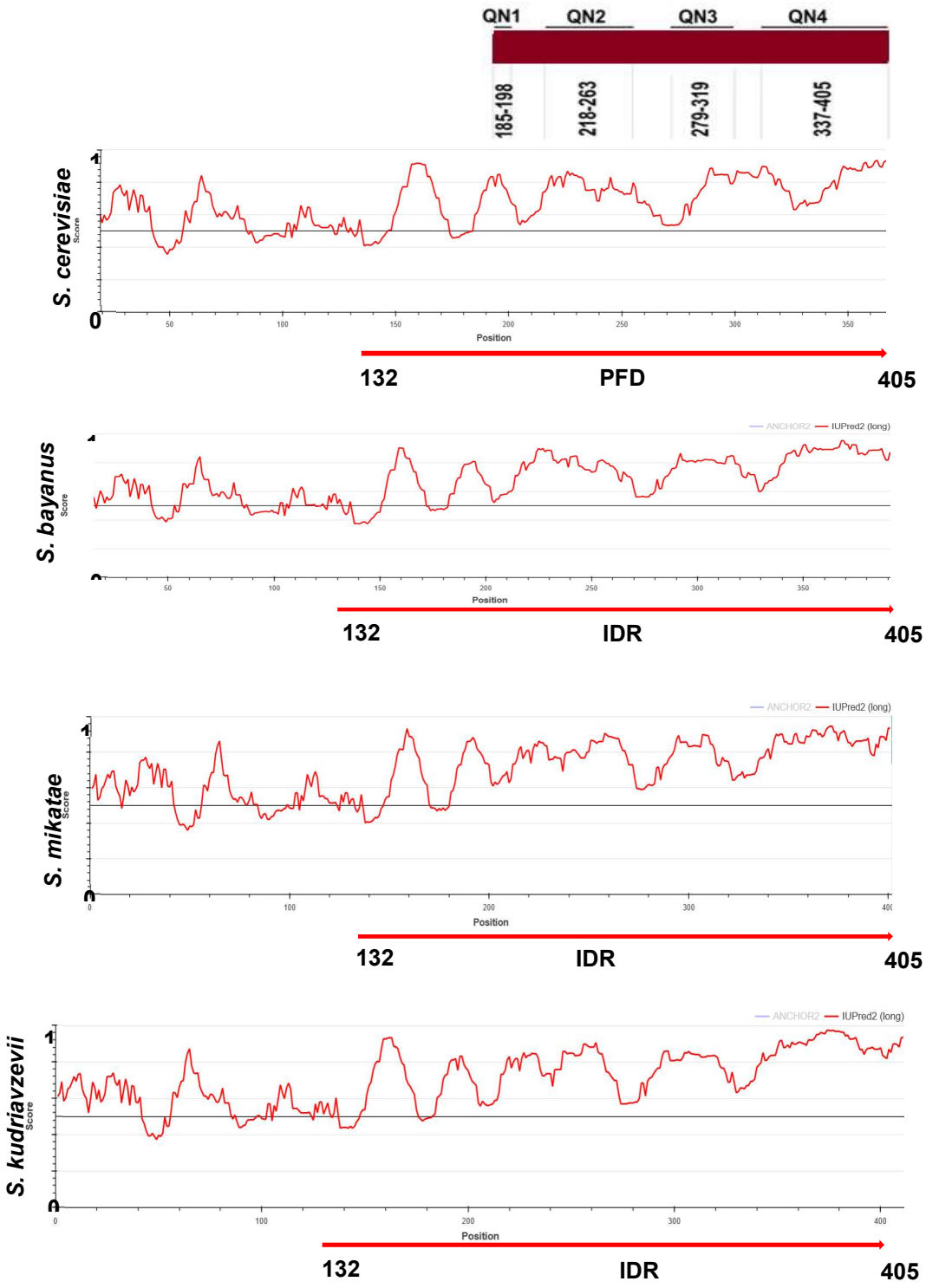

Figure 3.6: IUPred2 predictions of Intrinsic Disordered Regions of Rnq1 across all species. Each graph is based on assigning a score between 0 and 1 to each residue, corresponding to the probability of the given residue being part of a disordered region. The Rnq1 PFD in *S. cerevisiae* is between aa 132-405, and the predicted IDRs of Rnq1 are predicted and labelled at the same point in each species. The Four Q/N-rich regions in the *S. cerevisiae* Rnq1 PFD are indicated, adapted from Kadnar et al., (2010).

3.3. Detecting endogenous prion proteins Sup35 and Rnq1 in all *Saccharomyces* species

3.3.1. Western blot analysis of Sup35 and Rnq1 in *Saccharomyces species*

Endogenous prion proteins Sup35 and Rnq1 were detected in all species of *Saccharomyces* by western blot analysis using a polyclonal antibody raised against the Sup35 protein from *S. cerevisiae*, as described in Materials and Methods (Section 2.14.9). Both Rnq1 and Sup35 were detected at sizes larger than predicted despite being are in line with the *S. cerevisiae* control (**Figure 3.8**). *S. mikatae* Sup35 appeared at a molecular weight much higher than expected, with the bioinformatic sequence analysis suggesting its size as 60kDa. However, the similarity in molecular weight of each protein in each species further supports the protein homology between each species (Section 3.2). The presence of a lower molecular weight band observed in lanes of *S. cerevisiae* and *S. mikatae* must also be noted. Two bands may indicate a specific protein cleavage product, highlighting a specific sequence recognised by endonucleases that is not presenting in *S. bayanus* or *S. kudriazvevii*. Successful probing with the target antibody may therefore uncover subtle differences in the *Sup35* protein between species of *Saccharomyces.* The levels of 3-PhosphoGlycerate Kinase (Pgk1p), an essential protein of known molecular weight, were also detected in each yeast strain as a control (**Figure 3.7**).

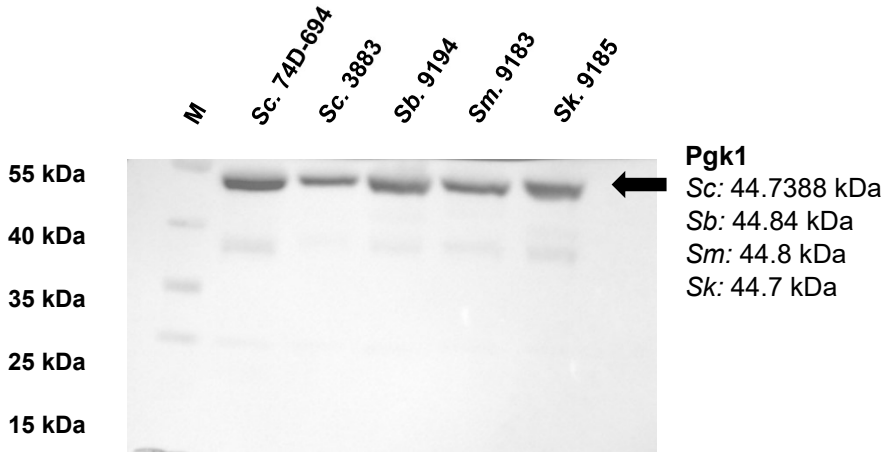

Figure 3.7: Western blot analysis of Pgk1 in all species shows the protein at the expected molecular weight. This experiment was repeated three times and a representative data set is shown.

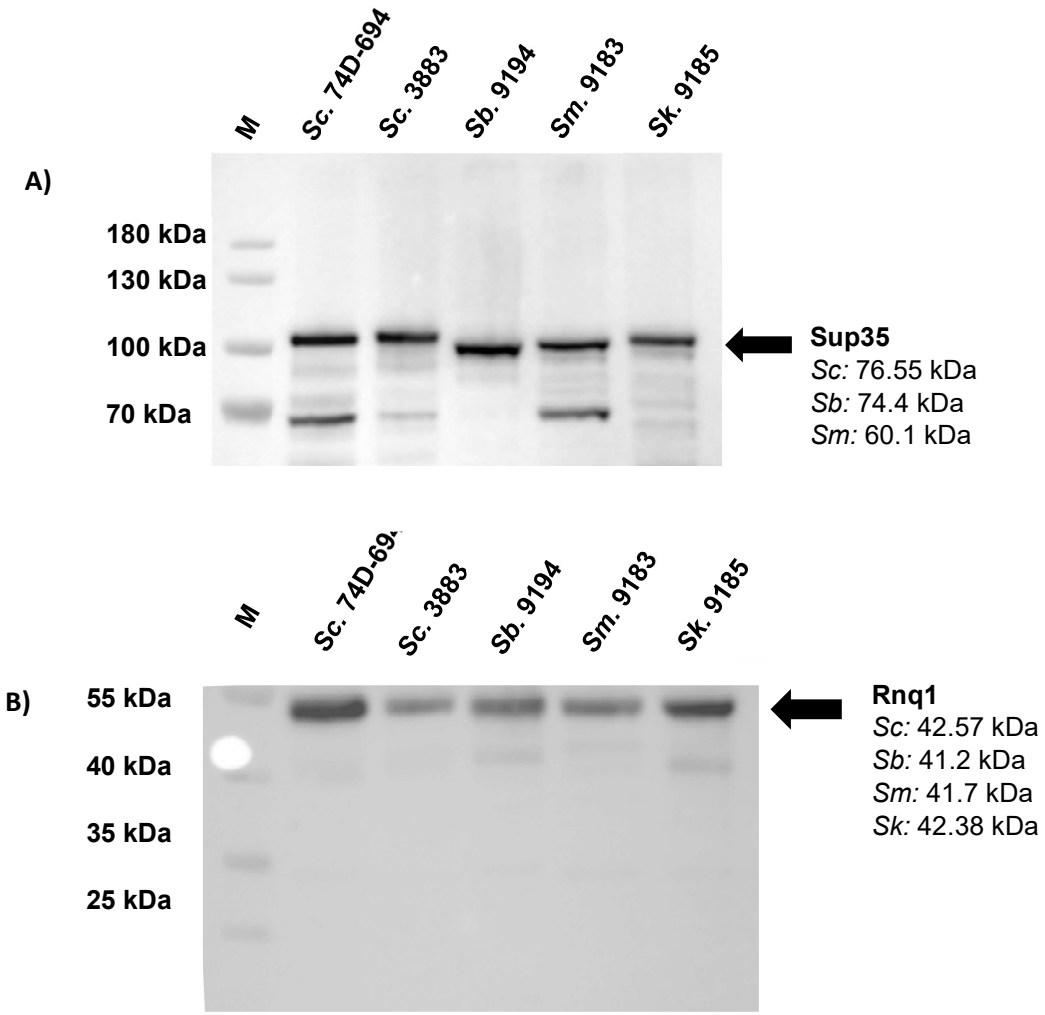

Figure 3.8: Western blot analysis of Sup35 and Rnq1 in all species. Panel A) Western blot analysis of Sup35 in all species shows the protein at molecular weight slightly higher than expected. **Panel B)** Western blot analysis of Rnq1 in all species shows the protein at a molecular weight higher than expected. All bands are seen in line with the *S. cerevisiae* control. This experiment was repeated three times and a representative data set is shown.

3.3.2. Western blot analysis of Sup35 and Rnq1 in the *Saccharomyces cerevisiae* clade

Endogenous prion proteins Sup35 and Rnq1 were also detected in all species of the *Saccharomyces cerevisiae clade* by western blot analysis. Both proteins were detected at molecular weights slightly higher than expected, although the bands remained in line with the *S. cerevisiae* laboratory control. There was no significant difference in the observed molecular weights of each protein in each strain (**Figure 3.9).**

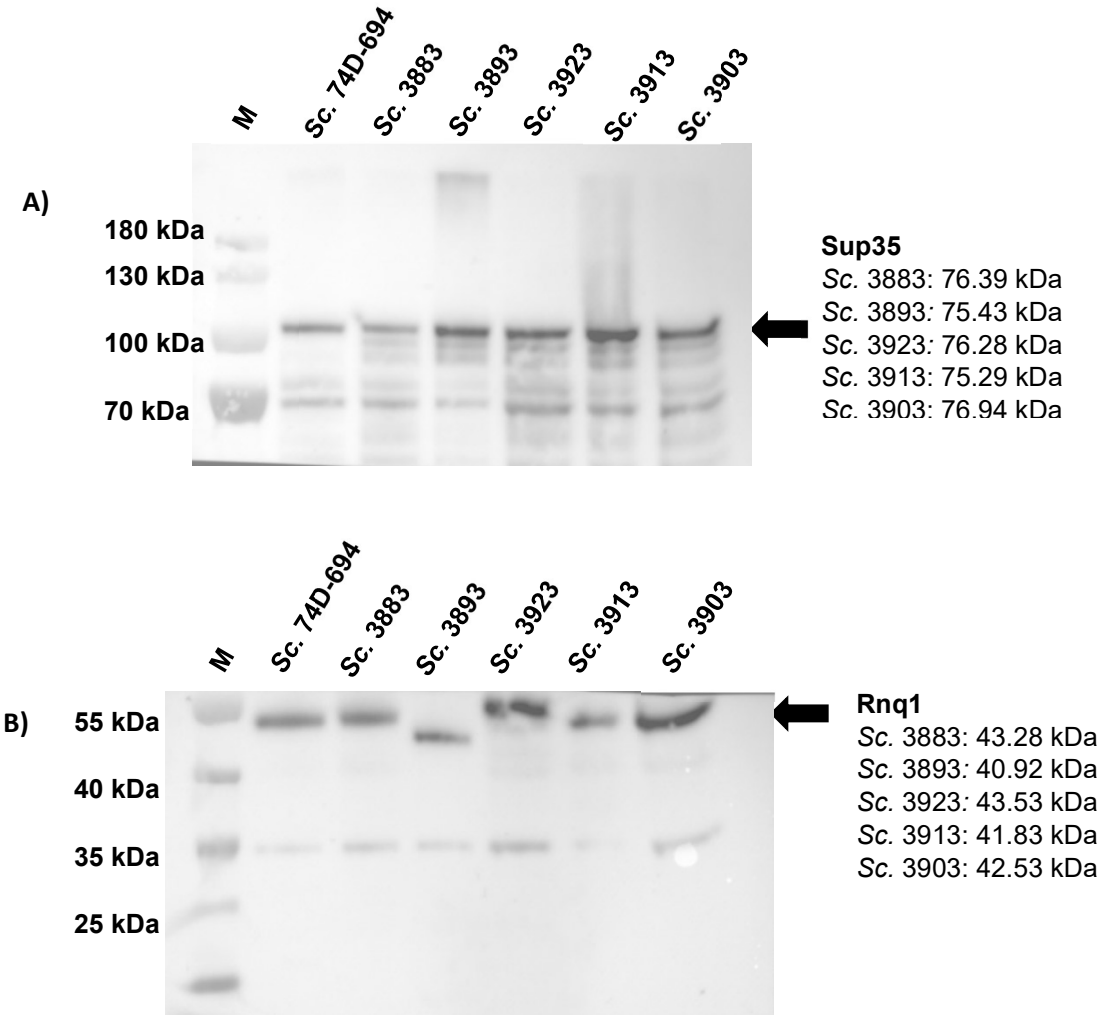

Figure 3.9: Western blot analysis of Sup35 and Rnq1 in all *S. cerevisiae* strains. Panel A) Western blot analysis of Sup35 in all species shows the protein at the a molecular weight slightly higher than expected. **Panel B)** Western blot analysis of Rnq1 in all species shows the protein at a molecular weight higher than expected. All bands are seen in line with the *S. cerevisiae* laboratory control. This experiment was repeated three times and a representative data set is shown.

Further analysis of potential aggregated forms of Sup35 and Rnq1 was carried out using sedimentation analysis, a method used to quantify the proportion of either Sup35 or Rnq1 in soluble and higher molecular weight aggregated [*PRION*$^{+}$] states by ultracentrifugation (Ness et al., 2002). Preliminary work included the preparation of [*PRION*$^{+}$] and [*prion*$^{-}$] cell extracts to provide total (T), soluble (S) and pellet (P) fractions according to both Sup35 and Rnq1 sedimentation protocols in all species of *Saccharomyces,* although it is an incomplete analysis and further repeats are required (data not shown). In contrast, semi denaturing agarose gel electrophoresis (SDD-AGE) analysis was also carried out to allow specific separation of SDS-resistant polymers of yeast prion proteins based on molecular weight. However, this data is also an incomplete analysis, lacking the *S. cerevisiae* [*psi*$^{-}$] control (**Figure 3.10**). The SDD-age profile for non-domesticated *S. cerevisiae* control strain, and species of *Saccharomyces* are comparable to the wild-type [*PSI*$^{+}$] control strain, with SDS-resistant aggregates, albeit at a range of aggregate sizes. None of the strains tested showed monomeric material, despite being expected for the *S. cerevisiae* [*psi*$^{-}$] control strain, thus highlighting a requirement for repeats. Nevertheless, these results may indicate the ability of *Saccharomyces* species to form prion polymers, albeit with different polymer size distribution. The high molecular weight SDS-resistant aggregated material should also be compared to *Sc.* [*PSI*$^{+}$] controls in strong and weak prion variants, to identify the potential impact on aggregate size. These methods provide a means to assess both aggregate size and proportion of aggregated versus soluble material in a cell population (Ness et al., 2002; Patino et al., 1996).

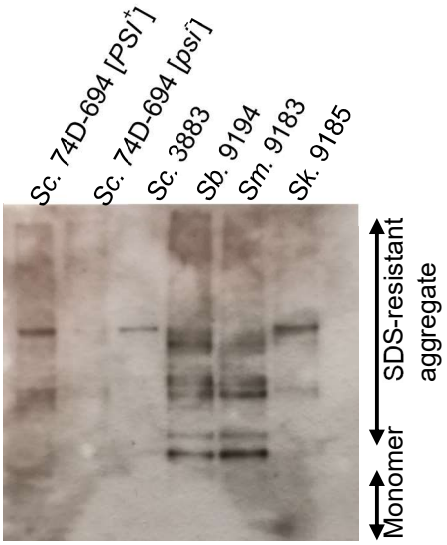

Figure 3.10: SDD-AGE analysis of Sup35 in species of *Saccharomyces*. SDD-AGE analysis of Sup35 in the different species suggests an ability to form prion polymers, but further repeats with [*psi*-] controls are required.

3.4. Analysing the expression of ScSup35-GFP and ScRnq1-GFP in all species of *Saccharomyces*

The aggregation of Sup35, indicative of the [*PSI*+] state in *S. cerevisiae,* can be observed microscopically by fusing the protein to Green Fluorescent Protein (GFP), the resulting plasmid being called p6442-SUP35NM-GFP (Patino et al., 1996). Specifically, the C-domain of Sc-Sup35 that is not required for aggregation has been replaced with GFP. The fusion protein was therefore expressed in all *Saccharomyces* species under the control of the *CUP1* copper-inducible promoter. In a [*PSI*+] state, GFP would be expected to coalesce into multiple bright foci in cells, compared to diffuse fluorescence one would expect to see evenly distributed throughout a [*psi*-] cell.

The expression of p6442-SUP35NM-GFP in [*PSI*+] *S. cerevisiae* produced bright foci in both log and stationary phase cells, as previously reported (Patino et al., 1996). Interestingly, all other species of *Saccharomyces* produced diffuse fluorescence, indicative of a [*psi*-] state, but this may provide evidence for the species barrier highlighted by Chen et al., (2007). Their work

demonstrated that Sup35 from *S. bayanus* formed a prion in *S. cerevisiae,* although prions formed by such heterologous proteins were less stable than endogenous ScSup35p (Chen et al., 2007). *S. bayanus* Sup35 co-aggregated in *S. cerevisiae* cells, but cross-species prion transmission was asymmetric in almost all heterologous combinations. Further analyses of the species barrier in other members of the *Saccharomyces* focused on the transmission of [*PSI*$^{+}$] from *S. cerevisiae* Sup35 to hybrid Sup35 proteins with PFDs from such species. All hybrid Sup35 proteins could adopt the prion formation in *S. cerevisiae,* but could not readily adopt the prion form from the [*PSI*$^{+}$] prion of *S. cerevisiae* (Afanasieva et al., 2011). Furthermore, *S. bayanus* displayed changes in both cell size and shape in response to expression of fluorescent proteins, while *S. kudriavzevii* displayed high levels of cell flocculation, but very low levels of fluorescence (**Figure 3.11**).

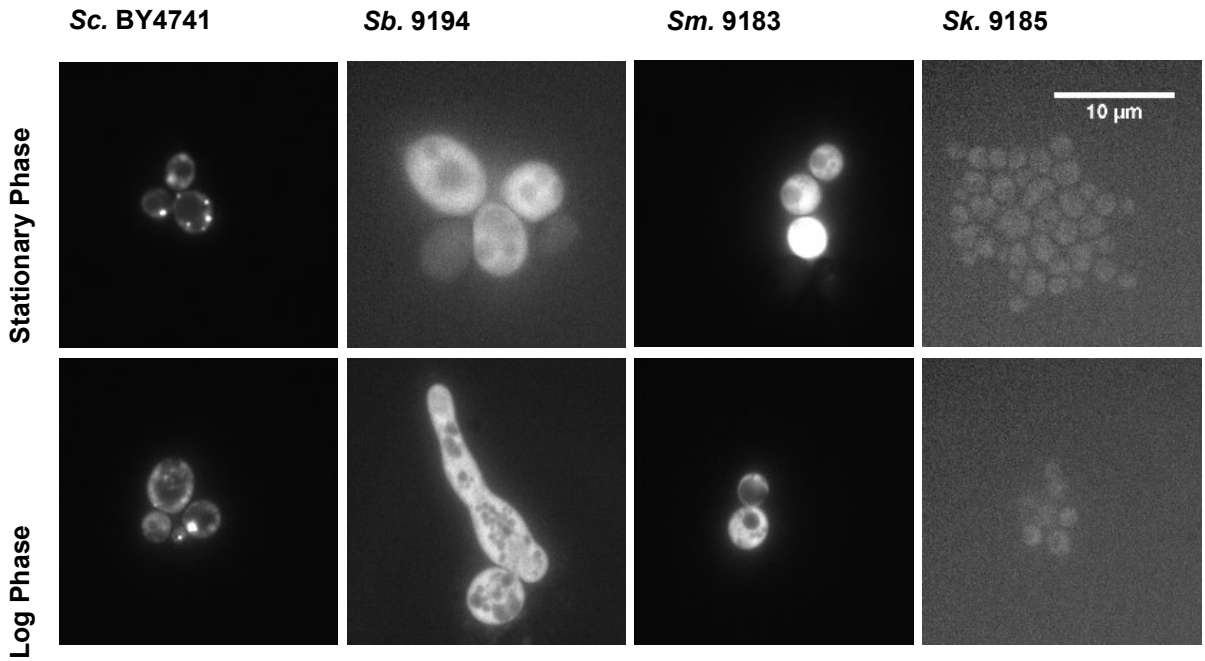

Figure 3.11: ScSup35-GFP forms fluorescent foci in [*PSI*$^{+}$] cells of *S. cerevisiae*, but not in other *Saccharomyces* species. Images shown were taken by fluorescent microscopy at 100x magnification during both log and stationary phases of growth, following induction with copper for 4 hours. Each strain was visualised in three independent biological experiments, and a data set representative of at least 200 cells per visualisation is shown. The scale bar represents 10 µm.

As with Sup35, the joining of a GFP-tagged Rnq1 fragment to endogenous Rnq1-based prion aggregates can be visualised by the formation of fluorescent GFP foci. The plasmid pAG426-

RNQ1-GFP that expresses a Rnq1-GFP protein under the control of the *GAL1* promoter was introduced into each *Saccharomyces* species. In an endogenous [*PIN*$^{+}$] state, ScRnq1-GFP forms bright fluorescent foci in *S. cerevisiae* (Patel & Liebman, 2007). In contrast, in a [*pin*$^{-}$] state, the fluorescence is diffuse across the cell. In *S. cerevisiae,* foci indicative of [*PIN*$^{+}$] were present as expected in this strain, but in all other species, fluorescence was again diffuse across all cells, indicating the possibility by a species barrier. Harrison et al*.,* (2007) expressed that a species barrier for the formation of the Rnq1 prion is yet to be demonstrated experimentally in members of *Saccharomyces,* although Kelly et al*.,* (2012) showed even in wild strains of *S. cerevisiae,* Rnq1 polymorphisms create a small transmission barrier. These polymorphisms include premature stop codon alleles that cannot propgate the [*PIN*$^{+}$] prion from the reference allele, several small deletions, and point mutations (Kelly et al., 2012). A change in vacuole size was also seen across all species (**Figure 3.12**).

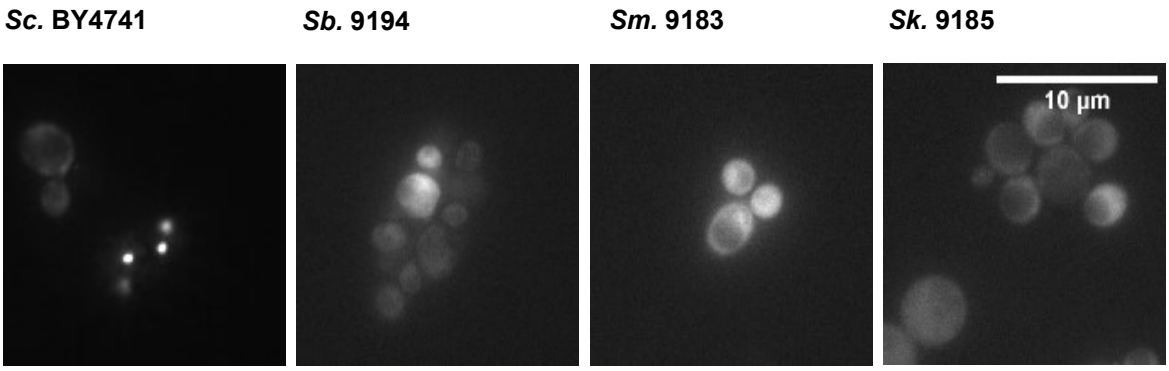

Figure 3.12: ScRnq1-GFP forms fluorescent foci in *S. cerevisiae*, but not in any other *Saccharomyces* species. Images were taken by fluorescent microscopy at 100x magnification during both log and stationary phases of growth, following induction with galactose for 3 hours. Each strain was visualised in three independent biological experiments, and a data set representative of at least 200 cells per visualisation is shown. The scale bar represents 10 µm.

To confirm that the fluorescent foci visualised in *S. cerevisiae* was indicative of both endogenous [*PSI*$^{+}$] and endogenous [*PIN*$^{+}$], all cells were treated with GdnHCl. GdnHCl causes reversible inhibition of the chaperone activity of Hsp104 which is necessary for endogenous prion propagation (Tuite et al., 1981). Exposure to millimolar concentrations of GdnHCl therefore generates prion-free cells. Following GdnHCl curing, fluorescent foci indicative of the [*PRION*$^{+}$]

state of *S. cerevisiae* were no longer detectable (**Figure 3.13**), confirming previous findings on the endogenous prion state of the strain.

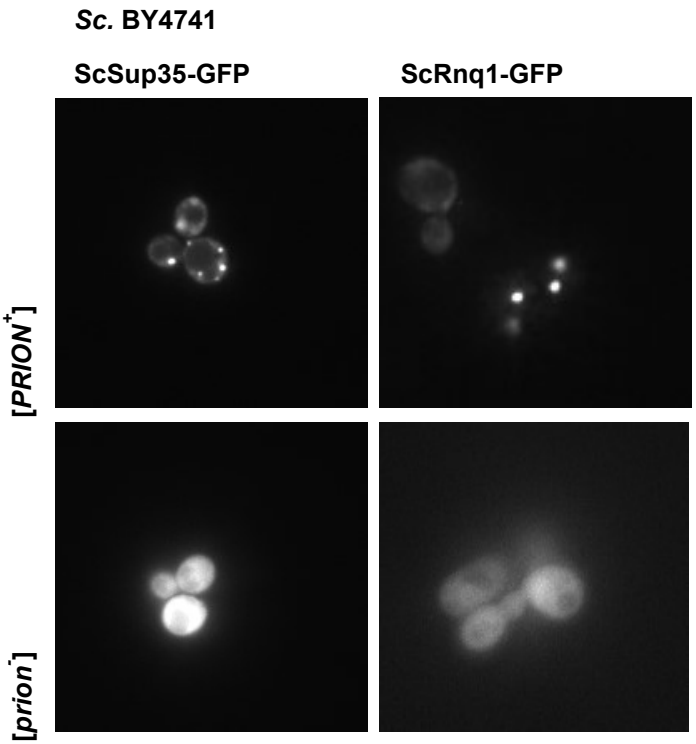

Figure 3.13: Fluorescent foci indicative of [*PSI*$^+$] and [*RNQ*$^+$] are replaced with diffuse fluorescence following curing with 5mM GdnHCl. Images were taken by fluorescent microscopy at 100x magnification following induction with copper for 4 hours or galactose for 3 hours, for expression of ScSup35-GFP and ScRnq1-GFP respectively. Each strain was visualised in three independent biological experiments, and at least ~200 cells per condition were visualised.

3.5. Discussion

The inability of other *Saccharomyces* species to form fluorescent GFP foci following expression of either ScSup35-GFP and ScRnq1-GFP may not be indicative of an endogenous [*prion*$^-$] state, but instead the presence of a cross-species prion transmission barrier (Chen et al., 2007). Impairment of cross-species prion transmission was originally detected in *Saccharomyces* using both complete Sup35 proteins and chimeric constructs with heterologous PFDs. All Sup35 proteins co-aggregated in *S. cerevisiae* cells, but cross-

species prion transmission was asymmetric in almost all heterologous combinations (Chen et al., 2007). This decreased level of prion transmission may demonstrate that the prion species barrier can be controlled in ways other than the physical association of heterologous proteins, such as the level of conformational transition. Further work by Chen et al. (2007) revealed that naturally occurring polymorphisms in the non-QN-rich region of Sup35N generate prion transmission barriers, and such barriers are not directly proportional to sequence divergence (Chen et al., 2010). Cross-species transmission barriers of Rnq1 were also shown to be generated by deletions of the QN-rich regions in Rnq1, with each region sufficient in maintaining the transmission of the [*PIN*$^+$] prion into daughter cells (**Figure 3.5**) (Kadnar et al., 2010). The data discussed highlights that the identity of specific sequences, not the overall level of PFD homology is essential for prion transmission.

To further explore the possibility of cross-species prion transmission barrier preventing seeding of the ScSup35 and ScRnq1 proteins it will be necessary to construct Sup35-GFP and Rnq1-GFP fusion proteins with *SUP35* and *RNQ1* from each *Saccharomyces* species. Asymmetry of cross-species prion transmission was detected by inefficient prion transfer from *S. cerevisiae* to *S. bayanus,* but efficient prion transfer in the opposite direction (Chen et al., 2010) (described in Chapter 1, Section 1.4.3). This shows that focussing predominantly on *S. cerevisiae* prion transmission neglects the possibility of efficient prion transmission between other species of *Saccharomyces,* further highlighting the requirement for future work. Cross-species transmission barriers can also be analysed by cytoduction experiments where cells of *Saccharomyces* strains are exposed to non-homologous [*PSI*$^+$] and [*RNQ*$^+$] seeds using cytoplasm exchange. Cytoduction was successfully used to transmit [*URE3*] from one strain to another by cytoduction, using cytoplasmic mixing without nuclear fusion (Wickner, 1994).

As previously mentioned, analysis of the species barrier in other members of *Saccharomyces* focused on the transmission of [*PSI*$^+$] from *S. cerevisiae* Sup35 to hybrid Sup35 proteins with PFDs from such species. Hybrid Sup35 genes were created from *S. cerevisiae SUP35* by replacing the N-terminal domain (residues 1-120) with the corresponding region from heterologous *SUP35* genes. All hybrid Sup35 proteins could adopt the prion formation in

S. cerevisiae, but could not readily adopt the prion form from the [*PSI*$^{+}$] prion of *S. cerevisiae* (Afanasieva et al., 2011). Expression of the hybrid Sup35 proteins in *S. cerevisiae* [*PSI*$^{+}$] cells also resulted in the frequent loss of the native prion. Interestingly, all hybrid Sup35 proteins displayed different patterns of interaction with the native [*PSI*$^{+}$] prion, at levels of copolymerisation, acquisition of the prion state and induced prion loss. Such patterns of interaction also appeared to be linked to the variant of the [*PSI*$^{+}$] prion, and in some cases expression of the hybrid Sup35 proteins caused the loss of [*PSI*$^{+}$]. For weak [*PSI*$^{+}$], variants in the presence of Sup35-bay or Sup35-mik, produced [*psi*$^{-}$] cells at frequencies up to 24%, compared to no detectable [*PSI*$^{+}$] loss in the presence of the Sup35-kud hybrid (Afanasieva et al., 2011). Further analyses of the presence of a species barrier for the transmission of [*PSI*$^{+}$] must therefore focus on the impact of the prion variant.

Chapter 4: The impact of guanidine hydrochloride on genetic and epigenetic determinants in *Saccharomyces* species

4. Chapter 4: The impact on guanidine hydrochloride on genetic and epigenetic determinants in *Saccharomyces species*

4.1. Introduction

Mitochondria are self-replicating, DNA-containing organelles which are not essential to yeast cells grown in the presence of a fermentable carbon source but are required when the only carbon source is a non-fermentable one. Structural changes to mitochondrial DNA (mtDNA) can be caused by a wide range of chemical agents, providing a means to study the structure, function, and replication of mtDNA. One well-established example of an mtDNA-based mutation is the *petite* mutation, typically causing respiratory deficiency at a spontaneous frequency of ~1% per generation (Goldring et al., 1970). The *petite* mutation is irreversible and maintained in succeeding generations, often carried by a cytoplasmic factor such as mtDNA. The *petite* phenotype is characterised by a small yeast colony size when grown on fermentable carbon sources such as glucose, and an inability to grow on non-fermentable substrates such as lactate or glycerol (Goldring et al., 1970).

In addition to changes in nuclear or mitochondrial DNA sequence induced by chemical and physical mutagens in *S. cerevisiae*, there are a variety of 'non-mutagenic' chemicals that result in inherited changes in cytoplasmic determinants such as mitochondrial DNA or prions. One example, is guanidine hydrochloride (GdnHCl) which generates mitochondrial *petite* mutants in *S. cerevisiae* (Juliani et al., 1973), as well as inducing the loss of [*PSI*$^{+}$] (Tuite et al., 1981) and other prions from this yeast species (Edskes et al., 1999). In *S. cerevisiae* the efficiency of GdnHCl to induce *petite* mutants is comparable to the efficiency of ethidium bromide, and occurs even when cell growth does not, indicating that even parent cells are transformed into *petites* by GdnHCl (Juliani et al., 1973).

The observation that GdnHCl can induce *petite* mutants in all species of *Saccharomyces* (Section 4.2) led us to question whether the mechanism of *petite* induction by GdnHCl is the

same as leads to prion loss i.e. by inhibition of the molecular chaperone Hsp104, or through an Hsp104-independent mechanism. The results described in this chapter provide a detailed comparative analysis of the impact of GdnHCl on the ultrastructure and respiratory functions of mitochondria in all species, and details whether mutants of *S. cerevisiae* lacking either Hsp104 or the related mitochondrial chaperone Hsp78 (Leonhardt et al., 1993) are able to maintain mitochondrial function, thereby exploring the role of these proteins in the mechanism of *petite* induction by GdnHCl.

4.2. The frequency of spontaneous and GdnHCl-induced *petite* mutants in *Saccharomyces* species

The initial aim was to measure the frequency of spontaneous and GdnHCl-induced *petite* mutants in all species of *Saccharomyces,* in order to verify that all species were susceptible to GdnHCl prior to exploring prion curing. Following growth on YEPD with increasing concentrations of GdnHCl (0-5mM), the 2,3,5-triphenyl tetrazolium chloride (TTC) assay was used as an indicator of respiratory proficiency (Chapter 2). TTC is reduced by the activity of a fully functioning mitochondrial respiratory chain from a colourless pigment to an insoluble red one (Ogur et al., 1957).

In both laboratory and wild strains of *S. cerevisiae,* a linear increase in the percentage of *petite* mutants was observed following treatment with increasing concentrations of GdnHCl (**Figure 4.1**). This observation was also made in all species of *Saccharomyces.* It was noted that fewer GdnHCl-induced *petite* mutants were observed in *S. mikatae,* but a reduced sensitivity to GdnHCl has frequently been noted in this species (**Figure 4.2**).

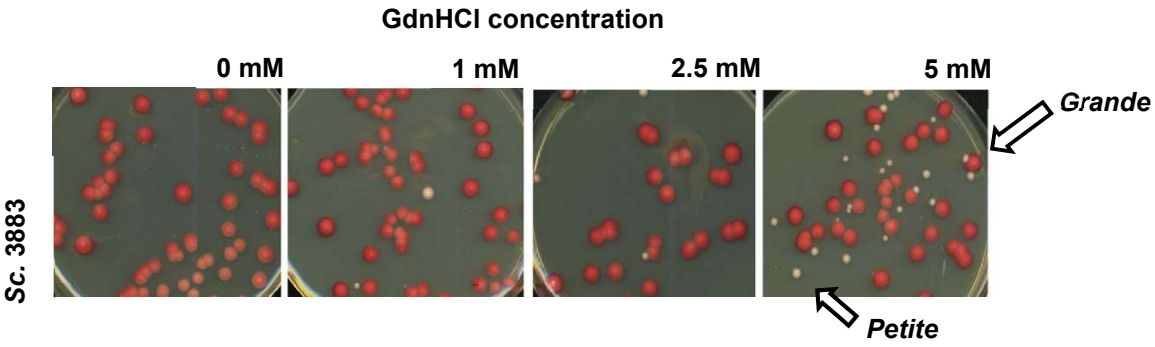

Figure 4.1: The induction of petite mutants in *S. cerevisiae* following treatment with increasing concentrations of GdnHCl. *Petites* were identified by the TTC overlay assay. TTC is reduced by the activity of a fully functioning mitochondrial respiratory chain from a colourless pigment to an insoluble red one. Red cells are respiratory efficient, compared to petite white mutants.

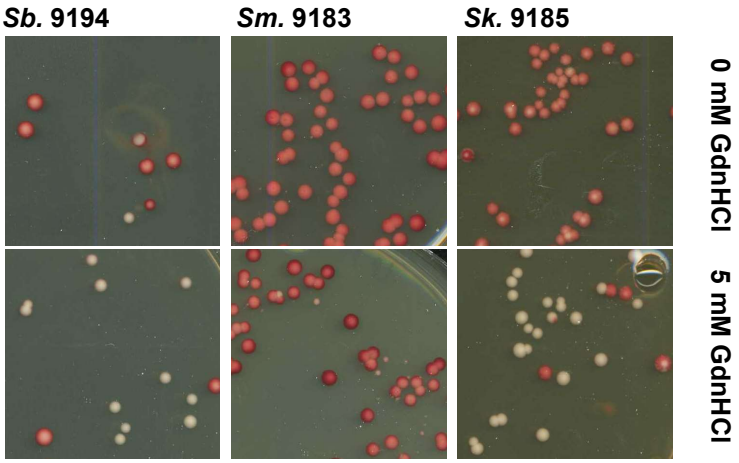

Figure 4.2: The induction of petite mutants in *Saccharomyces* species following treatment with GdnHCl. *Petites* were identified using the TTC overlay assay. TTC is reduced by the activity of a fully functioning mitochondrial respiratory chain from a colourless pigment to an insoluble red one. Red cells are respiratory efficient, compared to *petite* white mutants.

A percentage increase in *petite* mutants was observed following exposure to GdnHCl in all species of *Saccharomyces* (**Figure 4.3**). Interestingly, the frequency of spontaneous *petite* mutants in *S. bayanus* at a given concentration of GdnHCl was much higher than in other species. No spontaneously occurring *petite* mutants were observed in ~600 untreated cells of *S. mikatae,* suggesting the evolution of a robust network of mitochondrial proteins within this species. The status of all *petite* mutants in each species was confirmed by a lack of growth on glycerol, by restreaking ~30 *petite* mutants. These data confirm that GdnHCl is also able to induce *petite* mutants in each of the *Saccharomyces* species tested.

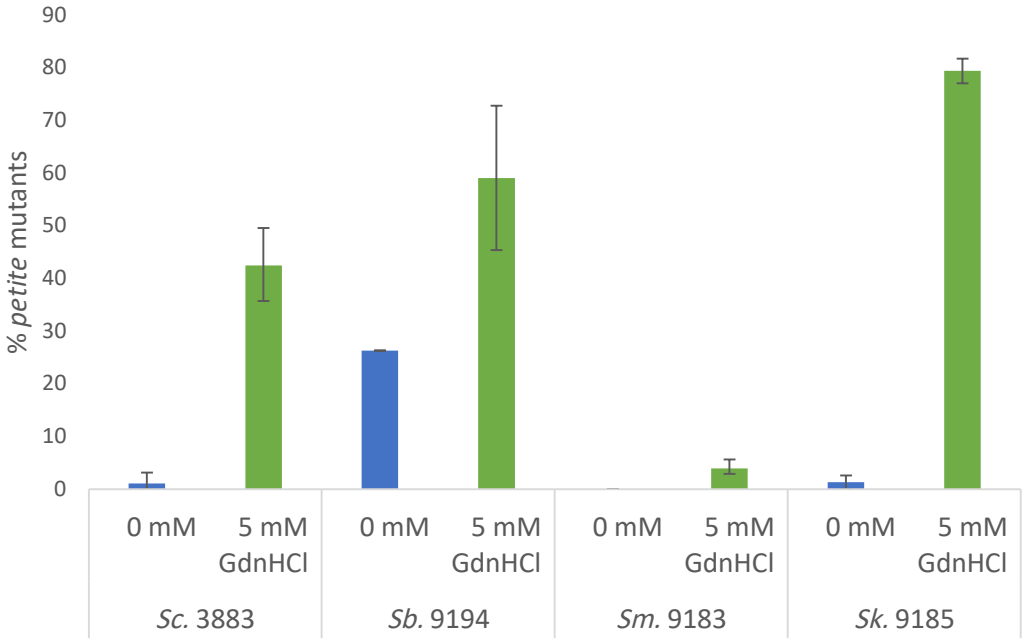

Figure 4.3: The frequency of petite mutants in *Saccharomyces* species increases following exposure to 5 mM GdnHCl. The percentage of petite mutants was calculated by counting the number of respiratory deficient (white) colonies observed in a total of ~250 colonies, taken across three biologically independent TTC overlay assays. The dataset presents an average of these results.

4.3. GdnHCl causes an increase in cell flocculation in *S. kudriavzevii*

Following the induction of *petite* mutants in *S. kudriavzeveii* by GdnHCl, the TTC overlay assay revealed colonies with uneven, scattered pigment. Not only did the degree of TTC reduction vary from pink to red pigment between colonies; red, pink and white spots were also observed within a single colony, indicating cells that are activating respiration in defined regions within a single colony. These observed phenotypes in *S. kurdriavzevii* were both stable and reproducible following treatment with GdnHCl.

To further explore the nature of this unusual phenotype, a loopful of cells from each of the red, pink and white colonies was visualised using differential interference contrast (DIC) microscopy, which revealed an increased level of flocculation in cells that are respiratory-deficient (**Figure 4.4**). In liquid culture, flocculation of *S. kudriavzevii* was readily apparent in the form of 2-3 mm spherical pellets, but such flocculation increased following treatment with GdnHCl and was not reversed using sonication. Flocculence has been reported to be regulated by mating type, with diploids showing a lower level of flocculation than haploids in this species (Scannell et al., 2011), although a haploid strain was used here and there was no indication of a change in ploidy following exposure to GdnHCl.

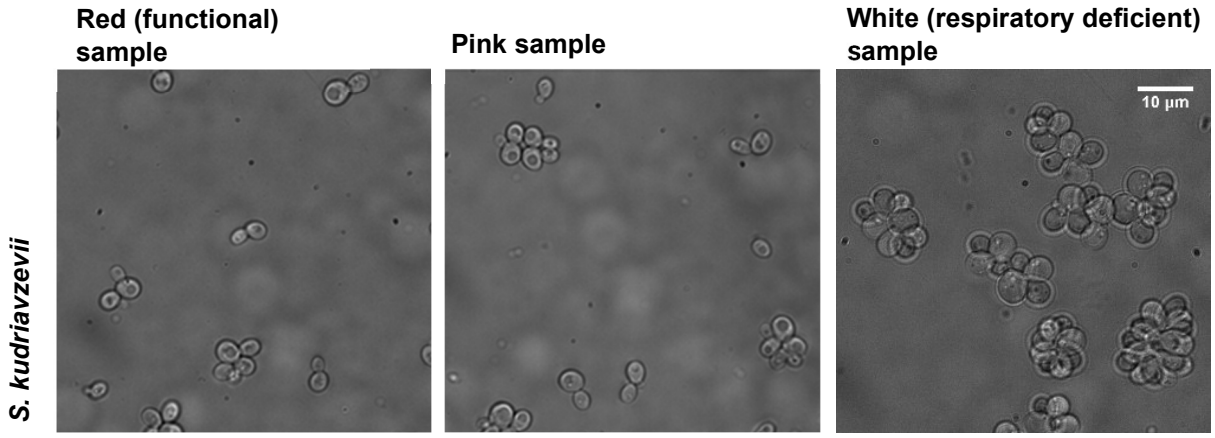

Figure 4.4: Flocculation of *S. kudriavzevii* increases in petite mutants generated by GdnHCl. Images were taken using DIC microscopy at 100x magnification and visualised in three independent biological experiments. A dataset representative of ~200 cells or 200 'flocs' is shown.

In all species of *Saccharomyces,* flocculation is controlled by the expression of *FLO1, FLO5, FLO8, FLO9* and *FLO10* genes, and such expression can be influenced by pH, temperature, carbon source and ethanol concentration (Soares, 2011). Additionally, *S. kudriavzevii* has a number of genetic alterations, particularly the PDC6 gene which is replaced by a pseudogene; responsible for pyruvate decarboxylase and its expression is induced by sulphur limitation. This highlights that this species may have experienced selective pressure to alter alcohol metabolism, and in turn, flocculation capacity (Scannell et al., 2011).

The link between mitochondria and flocculation remains unclear, as our data disagrees with literature previously published. For example, Acta et al. (1980) initially reported that defects in the inner mitochondrial membrane of *petite* mutants resulted in changes in cell adhesion. However, it was suggested that defective mitochondria in *petite* mutants caused a decrease in the ability of cells to flocculate, which is most likely linked to mitochondria regulating the permeability of the cell (Acta et al., 1980). Similarly, [*rho*^{o}] mutants of *S. cerevisiae* showed fewer biologically active glycoproteins in the form of peripheral phosphopeptidomannans (PPMs), which are ligands of lectins crucial for flocculation (Iung et al., 1999).

Alternatively, the link between mitochondria and flocculation may be via an activation in MAPK signalling, triggering flocculation in *S. cerevisiae* and in our case, *S. kudriavzevii* (Patrick Rockenfeller, University of Witten, personal communication). It remains to be established whether the observed increase in flocculation in *S. kudriazvevii* was due to an increase in *petite* mutants, or a more direct interaction between GdnHCl and the cell wall.

4.4. The impact of GdnHCl exposure on mitochondrial DNA and the ultrastructure of mitochondria in *Saccharomyces* species

4.4.1. Impact on nuclear DNA

Following the demonstration of an increase in the frequency of *petite* mutants in all species of *Saccharomyces* after treatment with GdnHCl, the impact of GdnHCl exposure on mtDNA and nuclear DNA was investigated at an ultrastructural level. In live yeast, Hoechst dye treatment showed bright nuclear DNA in *Saccharomyces* species indicating intact nuclear DNA and no clear differences were observed (**Figure 4.5**).

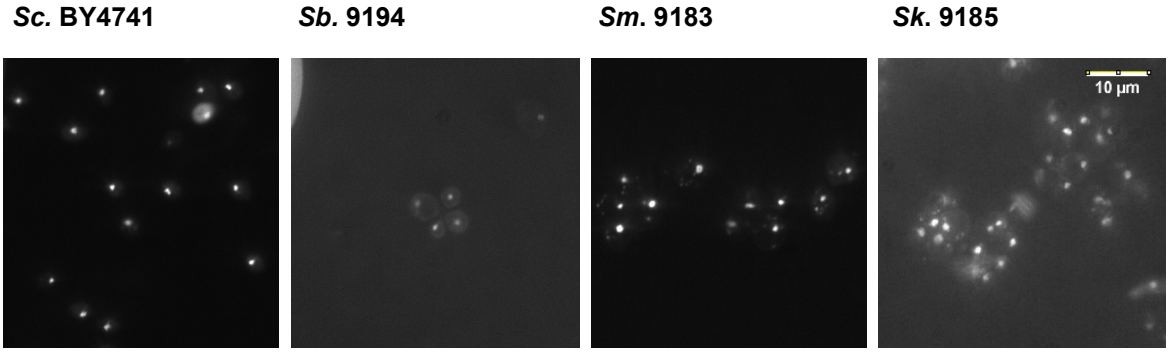

Figure 4.5: Visualisation of DNA in species of *Saccharomyces* using Hoechst dye. Cells of each species were visualised using fluorescent microscopy at a magnification of 100x, following Hoechst staining and three wash steps with PBS. Each strain was visualised in three independent biological experiments, and a dataset representative of at least 200 cells is shown. The scale bar represents 10 µm.

4.4.2. Analysis of the morphology of mitochondria in *Saccharomyces* species

The morphology of mitochondria was visualised in the *Saccharomyces* species using a plasmid encoded with mitochondrial matrix-directed green fluorescent protein (GFP). The plasmid expressed GFP fused in frame to a *Neurospora crassa*-derived leader sequence, taken from a mitochondrial ATPase subunit protein. This leader sequence interacts with the TOM and TIM complexes in both the mitochondrial outer and inner membranes (Westermann & Neupert, 2000), thus directing the GFP into the matrix as if it was an ATPase subunit protein

(Westermann & Neupert, 2000). Once in the matrix, the leader sequence is cleaved and the mitochondria are visualised as bright, fluorescent, tubular structures at the periphery of the cell.

Although subtle differences in the morphology of mitochondria were observed between the *Saccharomyces* species, treatment with GdnHCl caused no apparent structural changes in *petite* mutants of any of the species (**Figure 4.6**). The mitochondria of *S. cerevisiae* appeared fragmented as opposed to long tubular structures as expected. The mitochondria of *petite* mutants of *S. mikatae* could not be visualised following treatment with GdnHCl, as the frequency of *petite* mutants was so low in this species, that none were available for transformation.

Ethidium bromide (EtBR) can efficiently induce *petite* mutants at a comparable frequency to that seen for GdnHCl in *S. cerevisiae. Petite* mutants generated by treatment with 10 µg/ml ethidium bromide often lack mitochondrial DNA and are referred to [*rho*^{o}] mutants, in contrast to [*rho*$^{-}$] mutants which contain non-functional, mutated mtDNA (Nagley & Linnane, 1970).

Using mitochondrial matrix-directed GFP, the mitochondrial morphology of EtBr-induced *petite* mutants was also visualised in all species. The mitochondria of *S. cerevisiae* remained in a more fragmented state than the long, tubular structures expected, and the mitochondria of EtBr-treated *S. mikatae* appeared to be less bright than the wildtype control. This may indicate a reduced= plasmid uptake of these cells. Overall, there were no observed difference in the mitochondrial morphology of any of the *Saccharomyces* species following treatment with EtBr, and there were no difference in the morphology of mitochondria in GdnHCl-induced or EtBr-induced *petite* mutants (**Figure 4.6**).

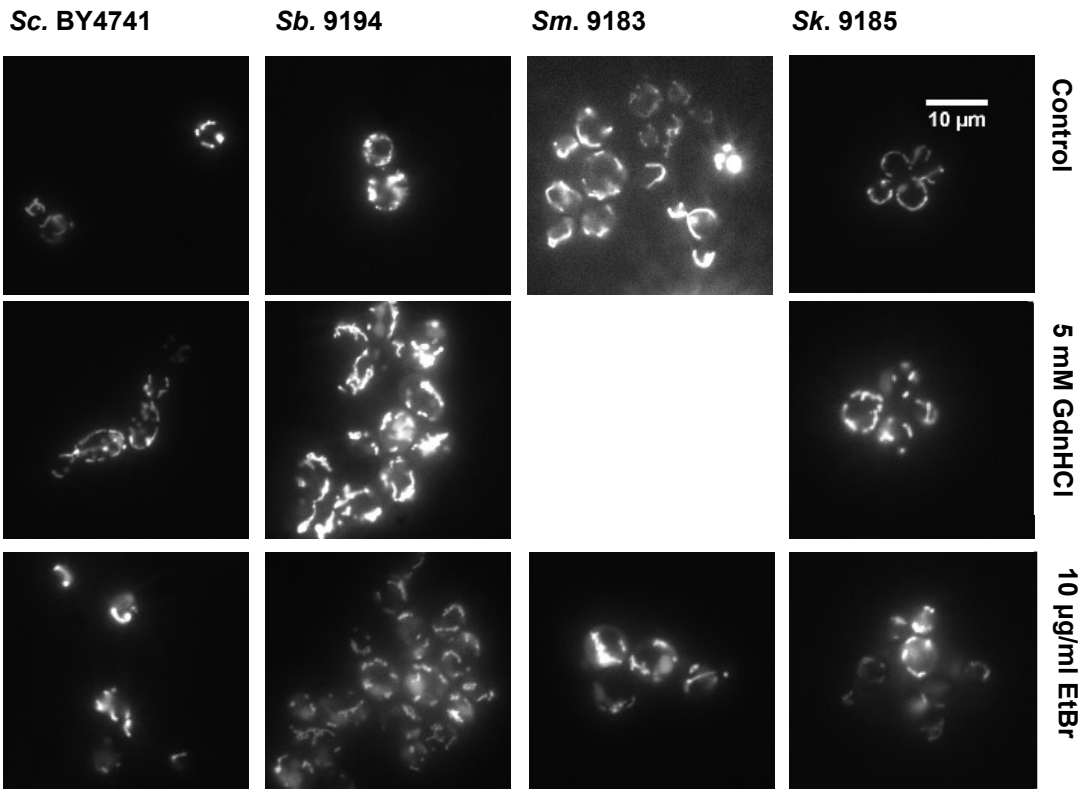

Figure 4.6: Visualisation of mitochondrial morphology following GdnHCl-induced or Etbr-induced petite generation using a mitochondrial matrix-directed GFP. Cells of each species were visualised using fluorescent microscopy at a magnification of 100x. Each strain was visualised in three independent biological experiments, and at least ~200 cells per condition were studied. The scale bar represents 10 µm. The mitochondria of GdnHcl-induced petite mutants of *S. mikatae* could not be visualised, as the frequency of *petite* mutants was so low in this species cells could not be selected for transformation.

4.4.3. Analysis of mitochondrial DNA

The nature of the *petite* status induced by GdnHCl was confirmed with 4',6-diamidino-2-phenylindole (DAPI) staining, a fluorescent dye which binds strongly to adenine-thymine rich regions in DNA such as those found in yeast mtDNA. In all wildtype cells of *S. cerevisiae, S, bayanus* and *S. mikatae,* cytoplasmic DAPI staining was observed, indicative of mtDNA (**Figure 4.7**). Only nuclear signal was revealed in *S. kudriavzevii* wildtype cells, suggesting the absence of detectable amounts of mtDNA and the possibility of this species being '*petite* negative'. In '*petite* negative' yeasts, several species form small, irregular-shaped microcolonies, compromising a few to several thousand cells, visible only under the microscope (Fekete et al.,

2007). Confirming the absence of mtDNA in selected *petite* colonies using DAPI staining may therefore indicate nuclear *petites* (pet) or mitochondrial (mit)$^-$ cells (Chen & Clark-Walker, 1999).

Following treatment with GdnHCl, no mtDNA could be observed in most cells of *S. cerevisiae, S. bayanus* or *S. kudriavzevii,* confirming the [*rho*^{o}] phenotype, comparable to the indicated percentages of *petite* frequency observed in these strains. DAPI staining did reveal the presence of mtDNA in GdnHCl-treated *S. mikatae,* further highlighting the reduced sensitivity to GdnHCl and concomitant low frequency of *petite* mutants in this species (**Figure 4.7**). Alternatively, intact mtDNA in this species may demonstrate that the DNA modification that occurred as a result of exposure to GdnHCl behaved as if a "sensitive site" i.e. target for the action of GdnHCl had been removed.

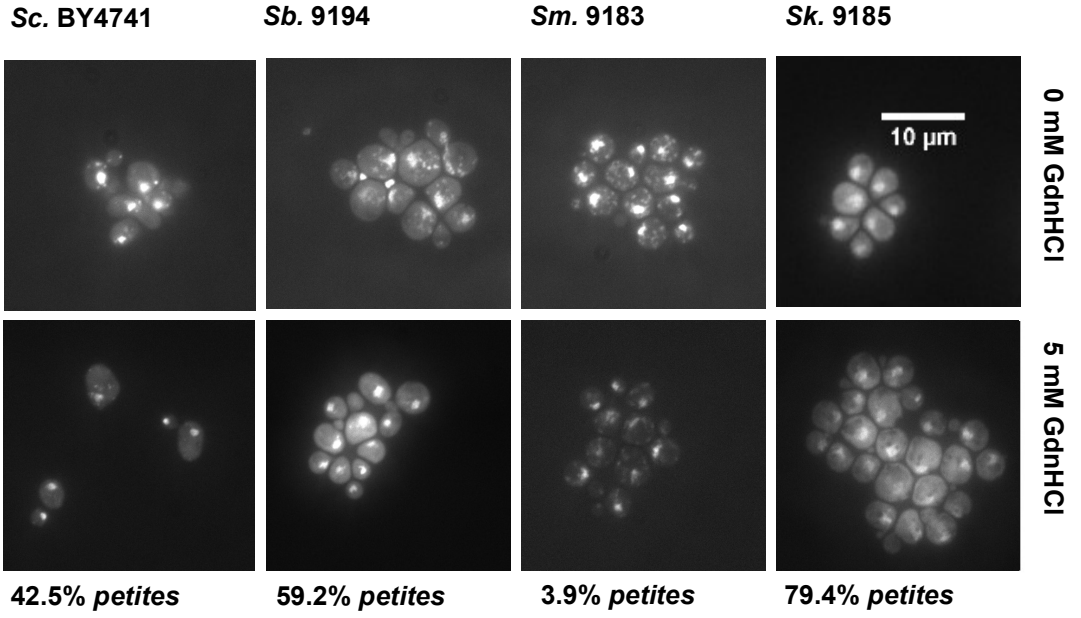

Figure 4.7: Visualisation of DAPI stained cells in *Saccharomyces* species following treatment with GdnHCl. Cells of each species were visualised using fluorescent microscopy at a magnification of 100x, following staining with fluorescent dye DAPI. Each strain was visualised in three independent biological experiments, and at least ~200 cells per condition were studied. Percentages indicate the frequency of GdnHCl-induced petite mutants in each species. The scale bar represents 10 µm.

4.5. Investigating the target of GdnHCl for the induction of *petite* mutants

The observation of GdnHCl treatment inducing *petite* mutants in several different *Saccharomyces* species led us to further investigate the mechanism of such *petite* induction by this chaotropic agent. As previously mentioned, GdnHCl inhibits the ATPase activity of the molecular chaperone Hsp104 to induce the loss of various prions from yeast (Ness et al., 2002). This led us to question whether the mechanism of GdnHCl in *petite* induction is the same as leads to prion loss or is Hsp104 independent.

One scenario is that GdnHCl targets an alternative molecular chaperone to generate *petite* mutants. One strong candidate for such a target is another heat shock protein, namely Hsp78. Hsp78 is a disaggregase located in the mitochondrial matrix with similar activity to the cytosolic Hsp104. Hsp78 was originally described by Leonhardt et al., (1993), and its chaperone function was further verified by Röttgers et al., (2002). Much like its bacterial homologue ClpB, Hsp78 is thought to be involved in the reactivation of aggregated proteins, in cooperation with another molecular chaperone Hsp70 (Reidy et al., 2012). It has been assumed that Hsp70 is responsible for the initial binding and stabilisation of imported misfolded substrate proteins, releasing them to Hsp78 for direct degradation in an ATP-dependent reaction (Röttgers et al., 2002). When Hsp70 levels are depleted, Hsp78 also appears to represent a salvage pathway, capable of substituting for a mitochondrially-located Hsp70 activity in protein translocation and the initial stabilisation of proteins (Schmitt et al., 1995). Consequently, both the role and location of Hsp78 in *S. cerevisiae* made this protein a likely candidate that mediated GdnHCl-induced and *petite* generation.

4.5.1. A bioinformatic overview of *HSP104* and *HSP78* genes in *Saccharomyces* species

DNA sequences of *HSP78* and *HSP104* were manually aligned in order to investigate any key differences in domains and significant residues, as similarity throughout entire domains is likely to be more biologically significant than nearly exact matches (**Figure 4.8**). As members of the AAA+ protein family, both Hsp78 and Hsp104 have ATPase type Nucleotide Binding Domain 1

(NBD1) and Nucleotide Binding Domain 2 (NBD2) in common. NBD1 is responsible for the ATPase activity of each chaperone, and NBD2 is required for oligomerisation (Abrahão et al., 2017). In comparison to Hsp104, Hsp78 has a truncated N-terminus making it a shorter protein (811 aa) than Hsp104 (908 aa). Interestingly, the N-terminus is responsible for substrate binding in Hsp104 and other homologues (Abrahão et al., 2017).

Sequence similarity scores and sequence identity scores were calculated between *HSP104* in different *Saccharomyces* species, and between *HSP78* in the same *Saccharomyces* species in order to assess sequence homology. Sequence similarity was calculated in BLAST (Koski & Golding, 2001), followed by manual alignment and comparison of percentage homology using MUSCLE (EMBL-EBI). Sequences with >60% similarity are inferred as showing significant similarity (Koski & Golding, 2001) .

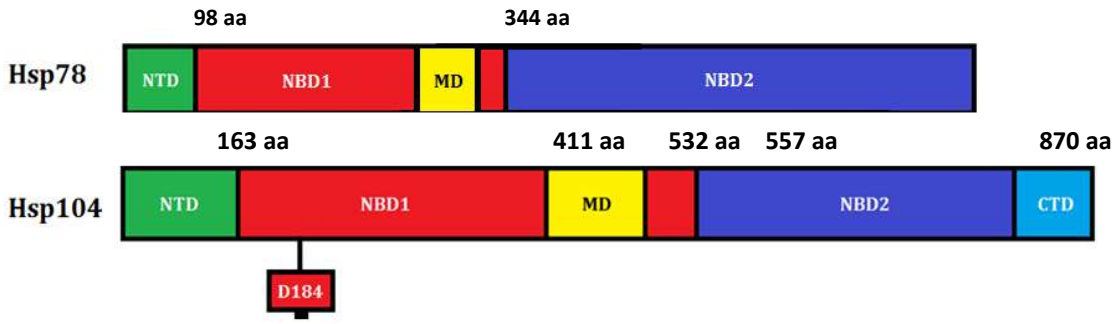

Figure 4.8: A schematic of domain organisation of Hsp104 and Hsp78 in *S. cerevisiae*. Key domains nucleotide binding domain 1 (NBD1) and nucleotide binding domain 2 (NBD2) are labelled in each protein. The N-terminal domain (NTD) and middle domain (MD) are also labelled for comparison. Amino acid residue 184 (D184) was identified as the target of GdnHCl by Jung et al (2002), and is also labelled.

The comparison of *HSP104* sequences revealed a significant level of similarity in all species, bar *S. kudriavzevii* (**Figure 4.9**). A high degree of amino acid conservation in *HSP104* was observed between *S. cerevisiae, S. bayanus* and *S. mikatae.* The scores of *HSP104* sequence homology could not be calculated for *S. kudriavzevii,* as this particular gene sequence was only accessible as an incomplete shotgun sequence.

A)

Species	No. of amino acids	Predicted molecular weight
S. cerevisiae HSP104	908	102
S. bayanus HSP104	908	102
S. mikatae HSP104	908	102

B)

	S. cerevisiae	*S. bayanus*	*S. mikatae*
S. cerevisiae		97.25	99.01
S. bayanus	97.25		97.03
S. mikatae	99.01	97.03	

Figure 4.9: A comparison of *HSP104* in all species. Panel A: The number of amino acids in *HSP104*, along with the predicted molecular weight for each *Saccharomyces* species**. Panel B:** Alignment of *HSP104* gene sequences in *Saccharomyces* species. The sequence of *S. kudriavzevii* was only available as an incomplete shotgun sequence and therefore could not be estimated.

Analysis of the homology of the *HSP78* amino acid sequence between the *Saccharomyces* species revealed that conservation of amino acid composition of the protein is maintained (**Figure 4.10**). High percentages of sequence homology are seen between all species, with the highest sequence homology seen between *S. bayanus* and *S. kudriavzevii* at a percentage of 96.01%. The high sequence homology reflects the close evolutionary relationship between these species as seen with Hsp104. The *HSP78* sequence of *S. mikatae* was only available as a 128 amino acid stretch, thus accurate sequence comparisons could not be estimated.

A)

Species	No. of amino acids	Predicted molecular weight
S. cerevisiae HSP78	811	91
S. bayanus HSP78	811	91
S. kudriavzevii HSP78	810	91

B)

	S. cerevisiae	*S. bayanus*	*S. kudriavzevii*
S. cerevisiae		94.54	93.33
S. bayanus	94.54		96.01
S. kudriavzevii	93.33	96.01	

Figure 4.10: A comparison of *HSP78* in all species. Panel A: The number of amino acids in *HSP78*, along with the predicted molecular weight for each *Saccharomyces* species. **Panel B:** Alignment of *HSP78* gene sequences in *Saccharomyces* species. The *HSP78* sequence of *S. mikatae* was only available as a 128 amino acid stretch, thus accurate sequence comparisons could not be estimated.

4.5.2. Analysis of the target residue of GdnHCl in both Hsp104 and Hsp78

GdnHCl cures yeast prions by inactivating Hsp104 by blocking its critical ATPase activity (Ness et al., 2002). An independent screen to identify mutations in *S. cerevisiae* that affect [*PSI*$^{+}$] formation characterised amino acid residue 184 as the target of GdnHCl. Mutations in *HSP104* at this site affected both prion propagation and the ability of GdnHCl to eliminate [*PSI*$^{+}$] further highlighting its importance in both processes (Jung et al., 2002). Residue D184 is conserved

among Hsp100 proteins and is located at the N-terminal end of NBD1 in Hsp104 (**Figure 4.8**). There is no equivalent residue in NBD2 of Hsp104 (Jung et al., 2002).

Sequence comparison and alignment of Hsp104 and Hsp78 between each species revealed the conservation of residue D184 in both proteins in *Saccharomyces* species, bar *S. mikatae,* as the *HSP78* sequence of was only available as a 128 aa stretch (**Figure 4.11**). The overall conservation of this residue among species a) confirms the ability of GdnHCl to target Hsp104 in all species of *Saccharomyces* and b) supports the hypothesis that GdnHCl could target Hsp78 and this in turn may be responsible for *petite* mutant generation.

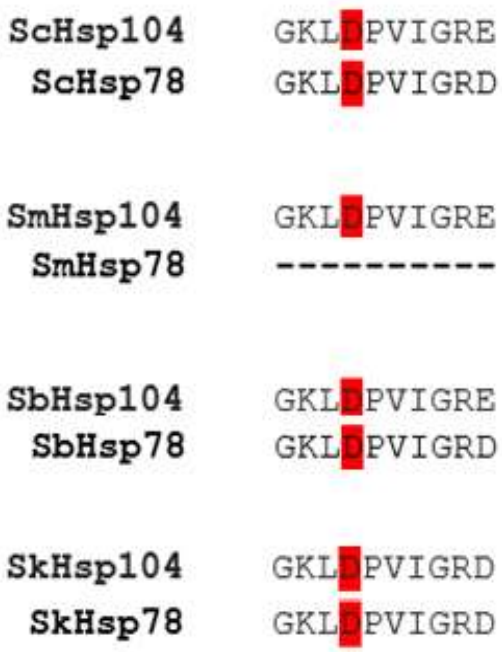

Figure 4.11: Alignment of amino acid sequence spanning the D184 residue of ScHsp104. The target residue D184 of GdnHCl is highlighted in red in each protein, and gaps for *S. mikatae* are shown as dashes, as *HSP78* was only available as a 128 amino acid stretch, thus accurate sequence comparisons could not be estimated.

4.6. Petite induction by GdnHCl in Δ*hsp78* and Δ*hsp104* mutants of *S. cerevisiae*

The role of both Hsp104 and Hsp78 in *petite* generation by GdnHCl was evaluated by deletion of the non-essential *HSP104* and *HSP78* genes. These two strains, constructed in the haploid strain of *Sc.* BY4741 were available from the BY4741 knockout collection (see Materials and Methods, section 2.7)

Prior to their use it was felt to be important to confirm that the strains obtained contained the desired gene knockout. Using polymerase chain reaction (PCR) DNA amplification, the gene knockouts of *HSP104* and *HSP78* in BY4741 were confirmed as follows. In each knockout the *kanMX4* gene had been inserted in the place of each indicated gene. Primers were designed to specifically target and therefore confirm (1) the presence or absence of either *HSP104* or *HSP78* in both the wildtype and knockout derivative of *Sc.* BY4741; (2) the presence or absence of *kanMX4* in the place of each indicated gene in both the wildtype and knockout derivative; and (3) the presence or absence of the *kan*MX4 gene in the correct orientation and correct point of insertion (see **Figure 4.12**). Both Δ*hsp78* and Δ*hsp104 S. cerevisiae* knockouts were confirmed by gel electrophoresis, detecting PCR products of the expected sizes (**Figure 4.12**).

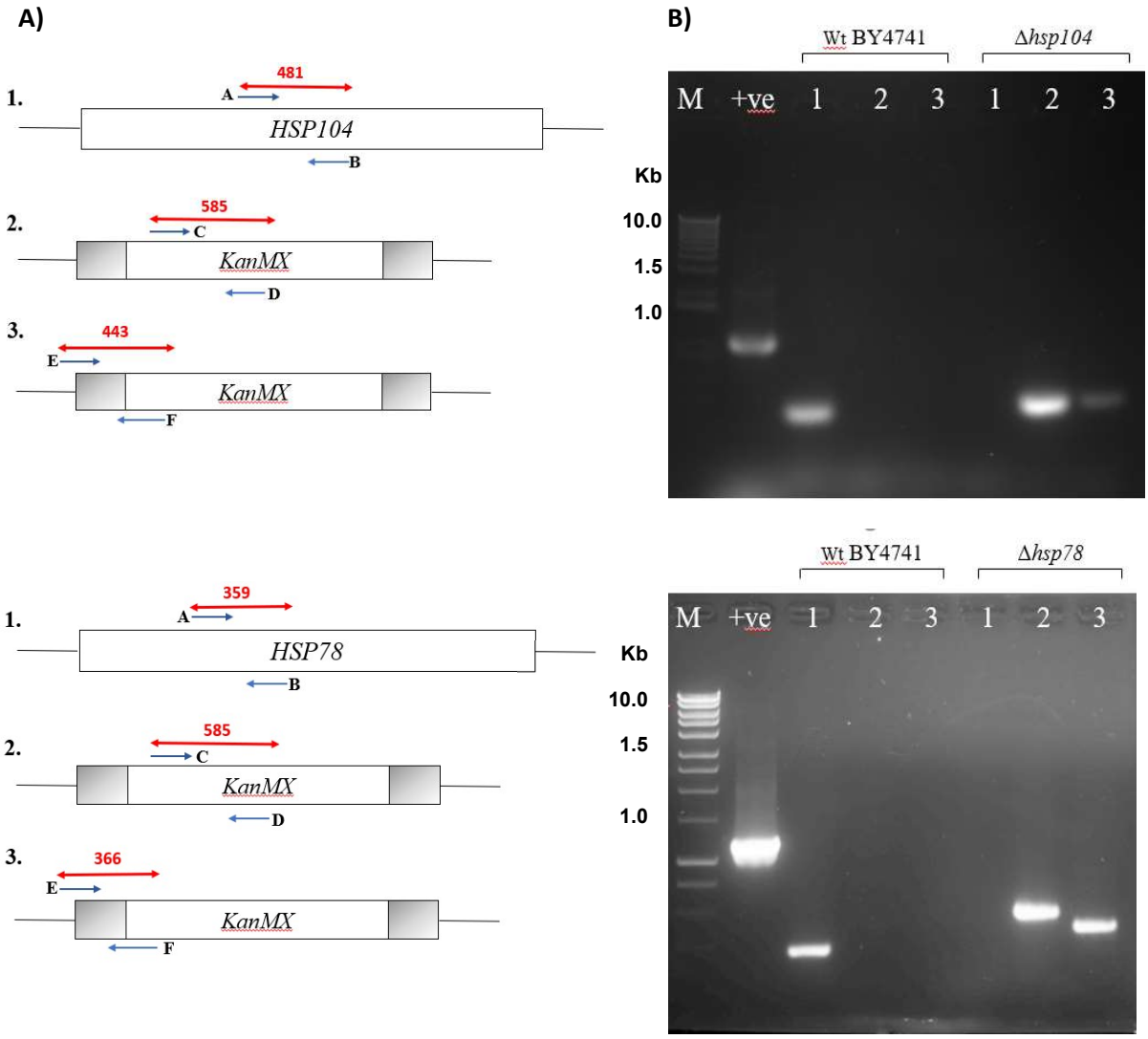

Figure 4.12: PCR DNA amplification of *S. cerevisiae* gene knockouts of *HSP104* and *HSP78.* **Panel A)** The strategy used to confirm the gene knockouts of *HSP104* and *HSP78* in *Sc* strain BY4741. 1. indicates the region targeted to confirm the presence or absence of either *HSP104* and *HSP78*. 2. indicates the region targeted to confirm the presence or absence of *kanMX4* in the place of each indicated gene. 3. indicates the presence or absence of the *kanMX4* gene in the correct orientation and point of insertion. Labelled letters indicate the starting point of each primer, and numbers in red indicate the predicted size of PCR product required to confirm both *Δhsp78* and *Δhsp104 S. cerevisiae* knockouts. **Panel B**) Agarose gel analysis of PCR products. Visualised bands are indicative of PCR products at the expected sizes. 1) confirms the presence of *HSP104* or *HSP78* in the wildtype control respectively, but not in the *Sc. Δhsp104* or *Sc. Δhsp78* 2) confirms the presence of *kanMX4* in the place of *HSP104* or *HSP78* in *Sc. Δhsp104* or *Sc. Δhsp78* respectively, and 3) confirms the presence of *kanMX4* in the correct orientation and point of insertion in *Sc. Δhsp104* and *Sc. Δhsp78* respectively.

4.6.1.Growth analysis of *Sc.* Δ*hsp78* and *Sc.* Δ*hsp104*

Each knockout strain of *Sc.* BY4741 and the wildtype control were grown in complete medium containing glucose as the sole carbon source, and YEPG containing glycerol as the sole carbon source to determine the frequency of *petite* mutants in these strains. Each condition included the addition of GdnHCl over a range of 0- 8 mM. The growth of each strain was analysed using the multi-well plate reader in two biologically independent experiments, each time in triplicate. The data reflect the average of all experiments.

In both the Δ*hsp78* and Δ*hsp104 Sc.* knockouts, the doubling time reduced following the addition of 8mM GdnHCl in YEPD (**Figure 4.13**). This was not the case for wildtype *Sc.* BY4741, suggesting that these two mutants show a greater sensitivity to GdnHCl compared to the wild-type. In YEPG however, the doubling time of each strain increased significantly following the addition of GdnHCl (**Figure 4.13**). As *petite* mutants are unable to grow using glycerol as a sole carbon source, the observed slower doubling time may be consistent with a higher number of GdnHCl-induced *petite* mutants in the growing culture.

The slowest doubling time was apparent in the Δ*hsp78 Sc.* knockout (**Figure 4.13**). Such results may suggest that the highest number of GdnHCl-induced *petite* mutants are seen in this strain, despite the absence of the *HSP78* gene, and that Hsp78 is not required for mitochondrial function and/or maintenance. An increase in GdnHCl-induced *petite* mutants would suggest that the target of GdnHCl is still present and functioning in this mutant strain i.e. Hsp78 is not the target for GdnHCl in *petite* generation.

The observed similar doubling time for *Sc.* BY4741 and its Δ*hsp104* derivative in YEPG + 8mM GdnHCl **(Figure 4.13)** would suggest that a similar number of GdnHCl-induced *petite* mutants are generated in each of these strains, in both the presence and absence of the *HSP104* gene. This would be consistent with there being an alternative target of GdnHCl in *petite* induction. However, it remains unclear whether an increase in doubling time reflects impaired of delayed cell growth, or the death of cells within the population studied. Alternatively, it may simply be that

the growth of all strains is delayed when using glycerol rather than glucose as a carbon source, rather than the generation of *petite* mutants and therefore a complete lack of growth.

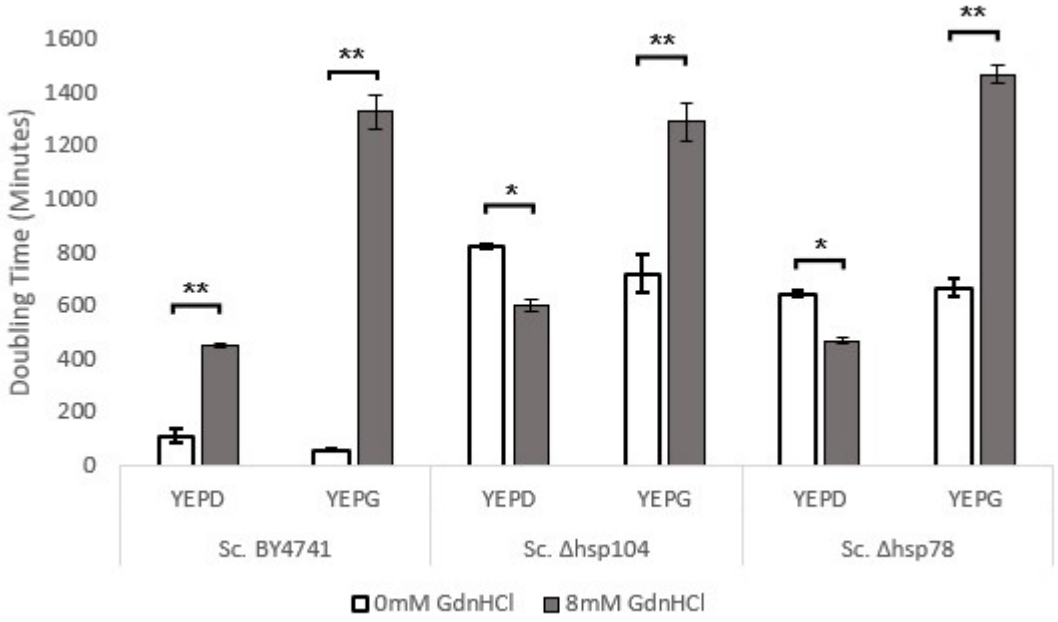

Figure 4.13: Doubling times of all strains grown in YEPD and YEPG containing 8 mM GdnHCl. All species show a significant increase in doubling time when grown in YEPG + 8 mM GdnHCl. The graph represents three biological replicates each containing two technical repeats. Error bars denote Standard Deviation. Paired two-tail t-tests were carried out on both biological and technical replicates: *p<0.05, **p<0.01.

The results of the growth experiment indicated a slower or impaired level of growth in all strains, and a delay in reaching diauxic shift following the additions of varying concentrations of GdnHCl when compared to growth in glycerol alone. It is unclear whether this impaired growth is a direct result of increasing concentrations of GdnHCl, or reflects an increase in GdnHCl-induced *petites* in each strain.

In the wildtype *Sc.* BY4741, growth was impaired with the addition of GdnHCl (**Figure 4.14**). There is an extremely low level of growth observed in YEPG + 8 mM GdnHCl, suggesting an increase in the number of *petite* mutants that are unable to grow in this condition. This

would further suggest that in this control strain, the target of GdnHCl for the generation of *petite* mutants is still functional.

The growth profile of the *Sc. Δhsp104* strain showed a reproducible delay in reaching diauxic shift in each addition of GdnHCl (**Figure 4.14**). Some growth was still observed in YEPG with the addition of 8mM GdnHCl. Growth of the remaining population in this condition suggest a lower level of *petite* mutants present in this strain suggesting that the target for GdnHCl in *petite* generation is absent. The growth profile of the *Sc. Δhsp78* strain revealed impaired growth in each addition of GdnHCl, and almost a complete absence of growth in YEPG + 8 mM (**Figure 4.14**). This may indicate a higher level of GdnHCl-induced *petite* mutants in this growth condition, highlighting that the target of GdnHCl is still present and the target of GdnHCl in *petite* generation is not Hsp78. The most direct way to test the hypotheses described above is to determine *petite* induction directly.

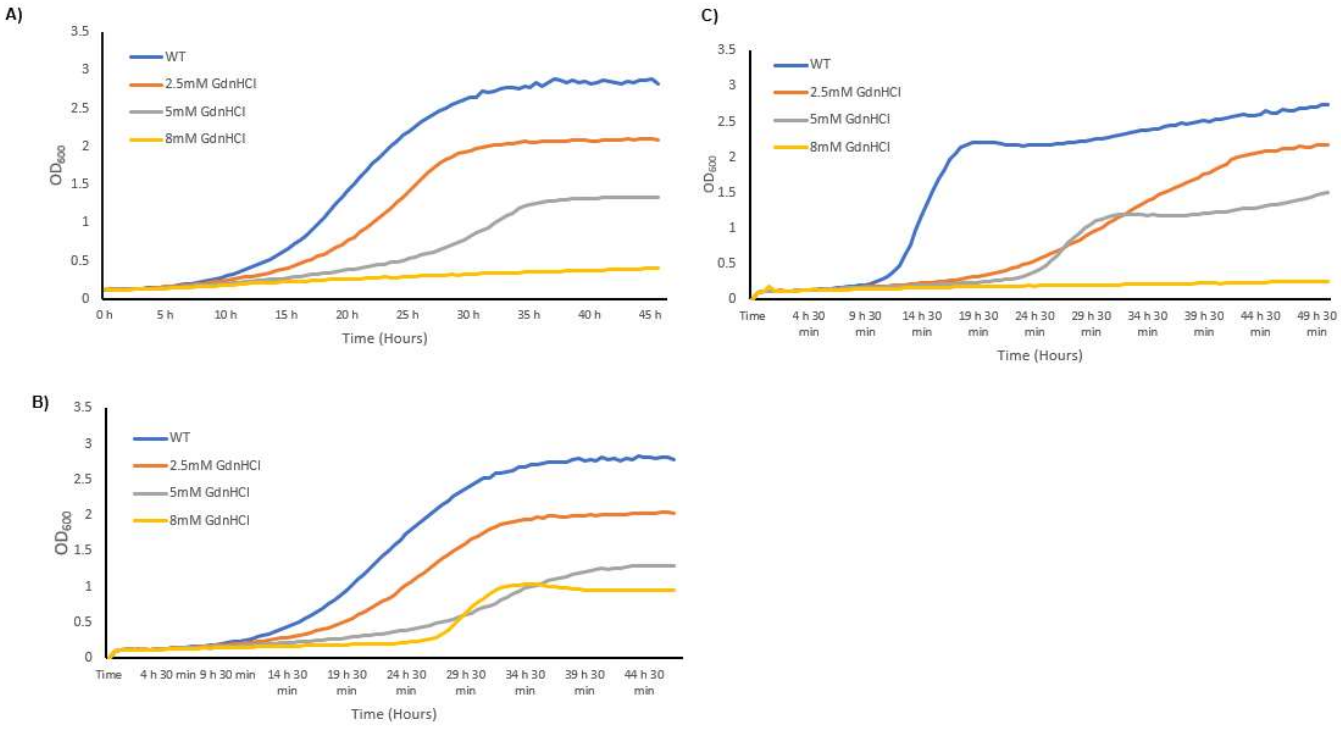

Figure 4.14: The growth profiles of **Panel A)** *Sc.* BY4741 in glycerol with different concentrations of GdnHCl, **Panel B)** *Sc.* BY4741 *Δhsp104* in glycerol with different concentrations of GdnHCl, and **Panel C)** *Sc.* BY4741 *Δhsp78* in glycerol with different concentrations of GdnHCl. Each graph represents three biological replicates containing two technical triplicates.

4.6.2. The frequency of spontaneous and induced *petite* mutants in Δ*hsp78* and Δ*hsp104* of *S. cerevisiae*

The frequency of spontaneous, GdnHCl-induced and EtBr-induced *petite* mutants was determined in Δ*hsp78* and Δ*hsp104* knockouts of *S. cerevisiae,* to further investigate the target of GdnHCl in *petite* mutant generation. Following growth on YEPD with concentrations of GdnHCl up to 5 mM or 10 μg/ml EtBr, the TTC assay was used as an indicator of respiratory proficiency and the percentage of *petites* after each treatment was calculated.

In wildtype *Sc.* BY4741, *Sc.* Δ*hsp78* and *Sc.* Δ*hsp104,* a significant percentage increase was observed in GdnHCl-induced *petite* mutants when compared to the frequency of non-induced *petites* (**Figure 4.15**). Interestingly, the highest level of GdnHCl-induced *petite* mutants was seen in *Sc.* Δ*hsp78.* This would suggest that in the absence of *HSP78,* the target of GdnHCl for *petite* induction remains, further supporting the findings reported in Section 4.6 above implying that Hsp78 is not the target.

A statistically significant increase in GdnHCl-induced *petite* mutants was also seen in *Sc.* Δ*hsp104,* compared to both the spontaneous frequency of *petite* mutants in this strain, and the frequency of GdnHCl-induced *petite* mutants in wildtype *Sc.* BY4741 (**Figure 4.15**). This suggests that in the absence of Hsp104*,* GdnHCl is targeting an alternative protein for *petite* mutant generation as suggested by the findings reported in Section 4.6. Alternatively, it may indicate the presence of a 'salvage pathway' for GdnHCl-induced *petite* generation in cells lacking the primary target i.e Hsp104. The status of all *petite* mutants as described was confirmed by a lack of growth on glycerol.

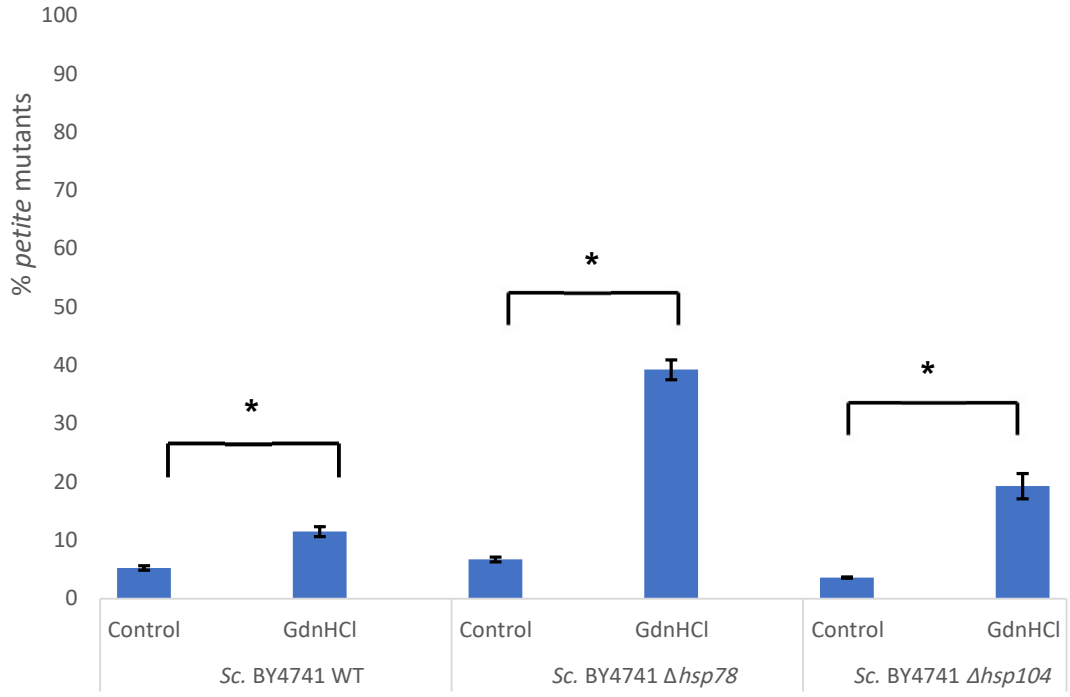

Figure 4.15: The frequency of *petite* mutants in *Sc.* BY4741 and *Sc.* knockouts *Δhsp78* and *Δhsp104* following treatment with 5 mM GdnHCl. The percentage of *petite* mutants was calculated by counting the number of respiratory deficient (white) colonies observed in a total of ~250 colonies, taken across three biologically independent TTC overlay assays, each with two technical replicates. The dataset presents an average of these biological replicates and these technical replicates, and error bars denote Standard Deviation. Paired two-tail t-tests were carried out on both biological and technical replicates: *p<0.05.

A statistically significant increase in the frequency of EtBr-induced *petite* mutants was observed in wildtype *Sc.* BY4741, *Sc.* Δ*hsp78* and *Sc.* Δ*hsp104,* compared to the frequency of spontaneous *petite* mutants in each of these strains (**Figure 4.16**). The percentage of EtBr-induced *petite* mutants were observed at a frequency above 80% in each strain, with little difference observed between strains. This would suggest that 10 µg/ml is sufficient in *petite* generation in each strain despite the absence of either Hsp104 or Hsp78. It has previously been reported that EtBr induces *petite* mutants at a comparable frequency to GdnHCl in *S. cerevisiae* (Nagley & Linnane, 1970). In the strains under study here, EtBr appeared to be much more efficient in *petite* generation than GdnHCl.

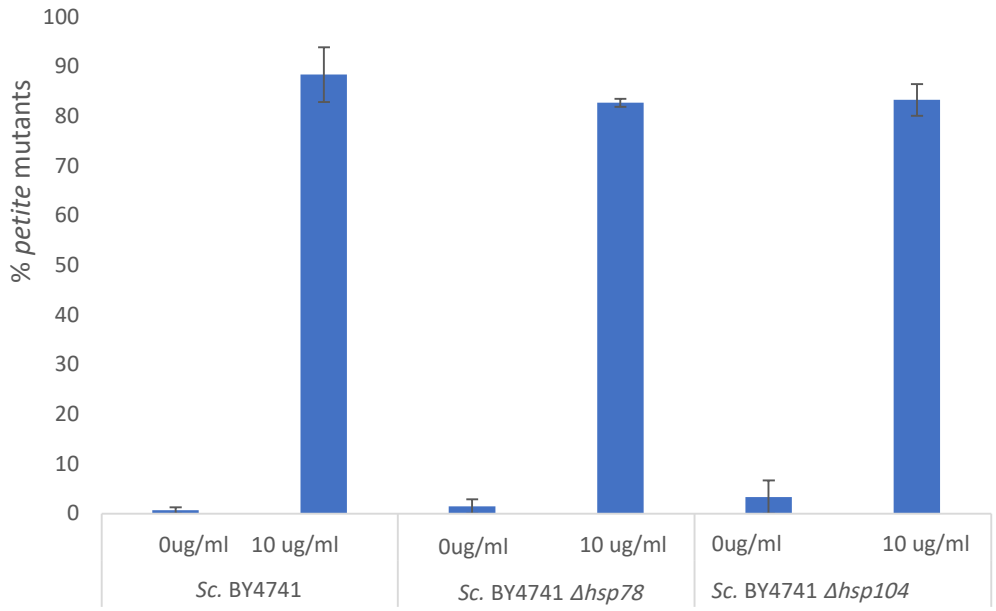

Figure 4.16: The frequency of *petite* mutants in *Sc.* BY4741 and *Sc.* knockouts *Δhsp78* and *Δhsp104* following treatment with 10 µg/ml EtBr. The percentage of *petite* mutants was calculated by counting the number of respiratory deficient (white) colonies observed in a total of ~250 colonies, taken across three biologically independent TTC overlay assays, each with two technical replicates. The dataset presents an average of these biological replicates and these technical replicates, and error bars denote Standard Deviation.

4.6.3. DNA and mitochondria in Δ*hsp78* and Δ*hsp104* knockouts of *S. cerevisiae*

To further investigate the target of GdnHCl in *petite* mutant generation and the increase in GdnHCl-induced *petite* mutants in both knockout derivatives of *Sc.* BY4741, the impact of GdnHCl on mtDNA and nuclear DNA was explored at an ultrastructural level. Hoechst staining of DNA showed bright intact nuclear DNA in all strains when visualised using fluorescent microscopy, and no obvious differences between strains (**Figure 4.17**).

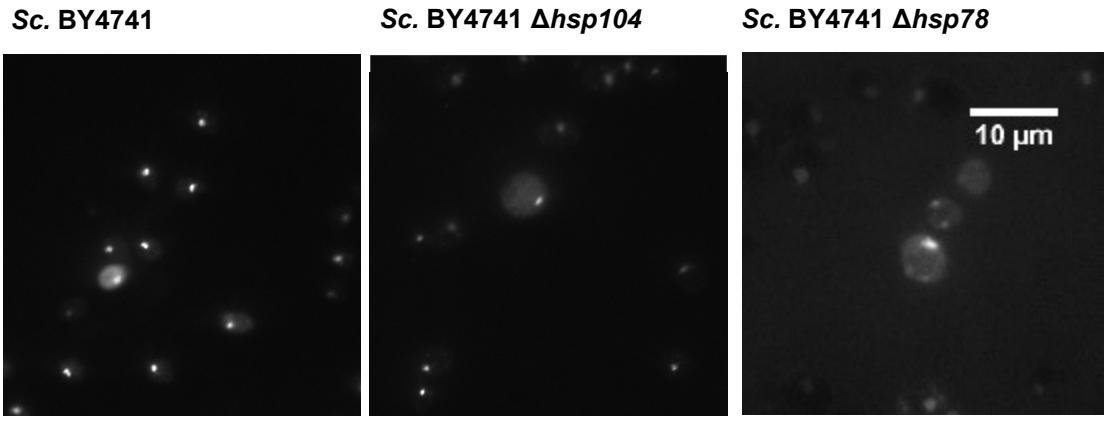

Figure 4.17: Visualisation of DNA in *Δhsp104* and *Δhsp78 Sc.* BY4741 using Hoechst dye. Cells of each species were visualised using fluorescent microscopy at a magnification of 100x, following Hoechst staining and three wash steps with PBS. Each strain was visualised in three independent biological experiments, and at least ~200 cells were visualised in each condition. The scale bar represents 10 µm.

The mitochondria of *Sc.* BY4741, *Sc.* Δ*hsp78* and *Sc.* Δ*hsp104* were examined at an ultrastructural level using mitochondrial-matrix direct GFP as described in Section 4.6.3 above. When observing mitochondrial shape and size, no differences were observed between each of the strains (**Figure 4.18**). As previously found, the mitochondria of the wildtype strain appeared to be fragmented as opposed to long, tubular structures. In both *Sc.* BY4741 and its Δ*hsp78* derivative, the mitochondria appeared to be bright and at the periphery of the cell. This was also the case for the mitochondria in the majority of *Sc.* Δ*hsp104* cells, but overall the fluorescence levels were detectably lower. When comparing all cells expressing the mitochondrial matrix-directed GFP to the same cells visualised using DIC, it is interesting to note that the mitochondria are not fluorescing in all cells of each sample. This may be indicative of inefficient DNA transformation and a reduced uptake of the plasmid across the population, or loss of the plasmid as its maintenance is not being selected for.

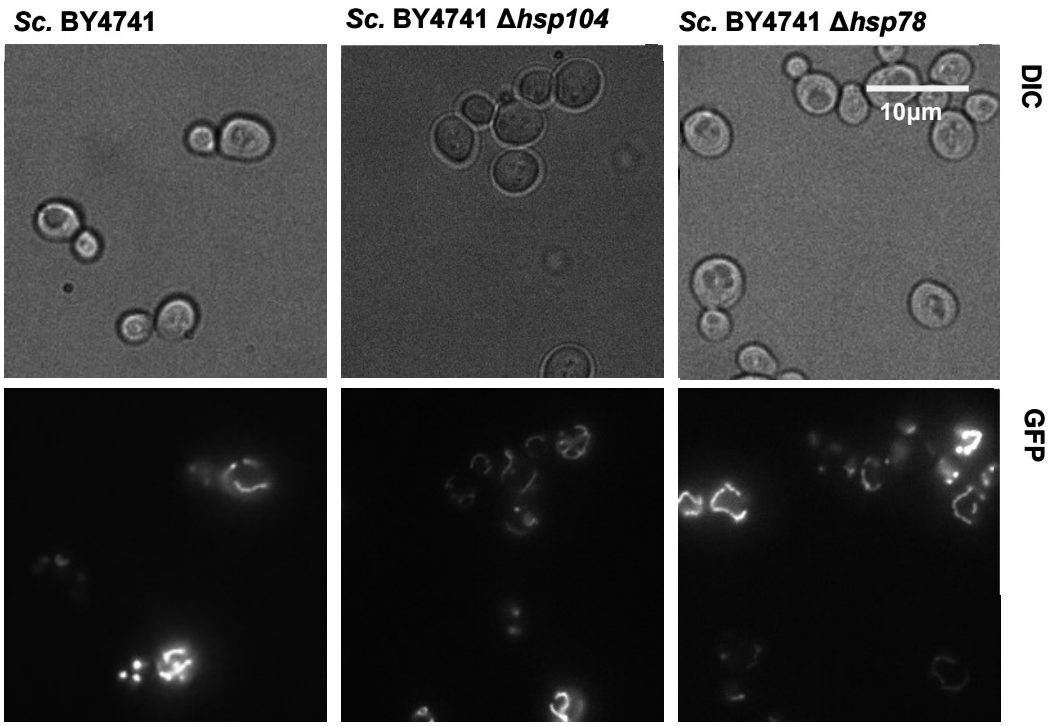

Figure 4.18: Visualisation of mitochondrial morphology following GdnHCl-induced *petite* generation using a mitochondrial matrix-directed GFP. Cells of each species were visualised using both DIC and fluorescent microscopy at a magnification of 100x following the expression of mitochondrial matrix-directed GFP, and the same cells can be seen in each condition. Each strain was visualised in three independent biological experiments, and at least ~200 cells were visualised in each condition. The scale bar represents 10 µm.

DAPI staining was used to confirm the *petite* status of all GdnHCl-treated cells of BY4741 and its Δ*hsp78* and Δ*hsp104* derivatives. Prior to treatment with GdnHCl, both nuclear and cytoplasmic DAPI staining was visible in all strains, indicative of the presence of mtDNA (**Figure 4.19**). Following GdnHCl-induced *petite* generation, only a nuclear signal was observed in all strains, highlighting the absence of mtDNA and confirmation of the [*rho*^{o}] phenotype (**Figure 4.19**). Both confirmation of *petite* status using DAPI and the percentage of GdnHCl-induced *petite* mutants in each strain further highlights the ability of GdnHCl to generate *petite* mutants even in the absence of Hsp104 and Hsp78*,* implying an alternative target of GdnHCl in the generation of *petite* mutants. Alternatively, it may be that in the absence of one protein, the other 'replaces' its function, and it would therefore be of value to assess the frequency of *petite* generation and the impact of GdnHCl in a double knockout of *HSP78* and *HSP104.*

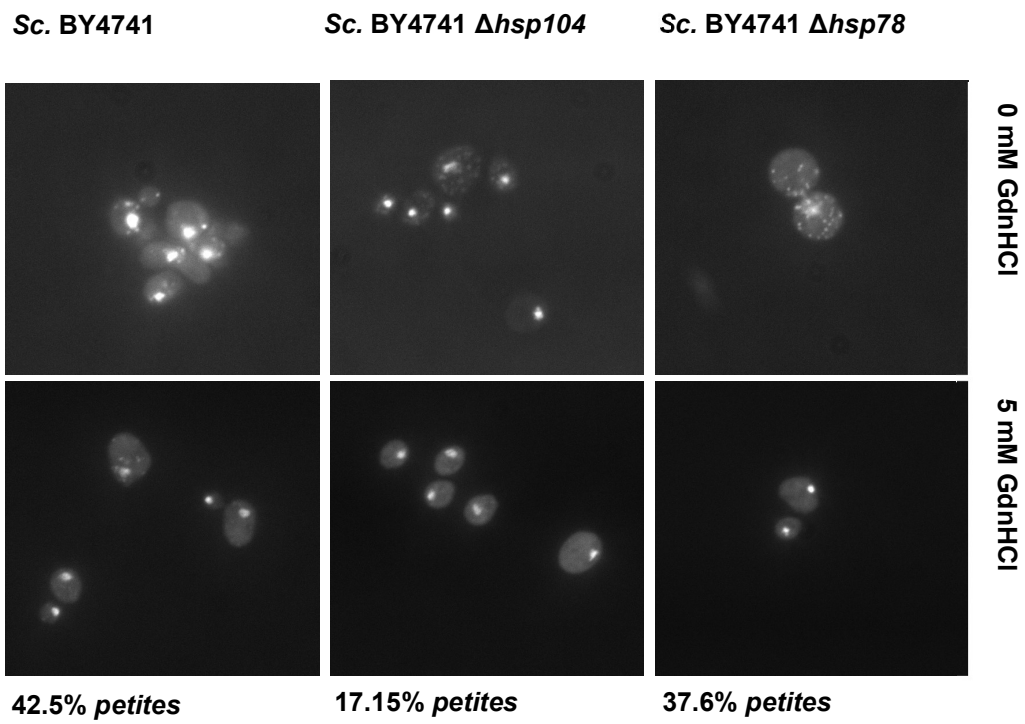

Figure 4.19: Visualisation of DAPI stained cells in *Saccharomyces* species following treatment with GdnHCl. Cells of each species were visualised using fluorescent microscopy at a magnification of 100x, following staining with fluorescent dye DAPI. Each strain was visualised in three independent biological experiments, and at least ~200 cells were visualised in each condition. Percentages indicate the frequency of GdnHCl-induced petite mutants in each strain.

4.7. The impact of GdnHCl on the respiratory functions of mitochondria in wildtype *S. cerevisiae, Sc.* Δ*hsp78* and *Sc.* Δ*hsp104* knockouts

Although the findings described above clearly indicate that GdnHCl generates *petite* mutants in *Sc.* BY4741, *Sc.* Δ*hsp78* and *Sc.* Δ*hsp104* knockouts, the specific target of GdnHCl in such *petite* induction remains unclear. While GdnHCl appeared to have no detrimental impact on the ultrastructure of mitochondria in all strains, it was also felt important to assess the activity of the mitochondria following GdnHCl treatment. This was achieved using a high-resolution respirometer to analyse oxygen consumption by three strains, *Sc.* BY4741, *Sc.* Δ*hsp78* and *Sc.* Δ*hsp104* knockouts, in the presence and absence of 2.5 mM GdnHCl. A lower concentration of

GdnHCl was chosen as cells are known to show a higher sensitivity to chemical agents using this method. Oxygen consumption was measured as O_2 flow per specific unit sample (cell). The drugs triethiltyn bromide (TET), carbonylcyanide p-trifluoromethoxyphenylhydrazone (FCCP), and antimycin A (AntA) were used to investigate the function of individual components of the mitochondrial respiratory chain (**Figure 4.20**).

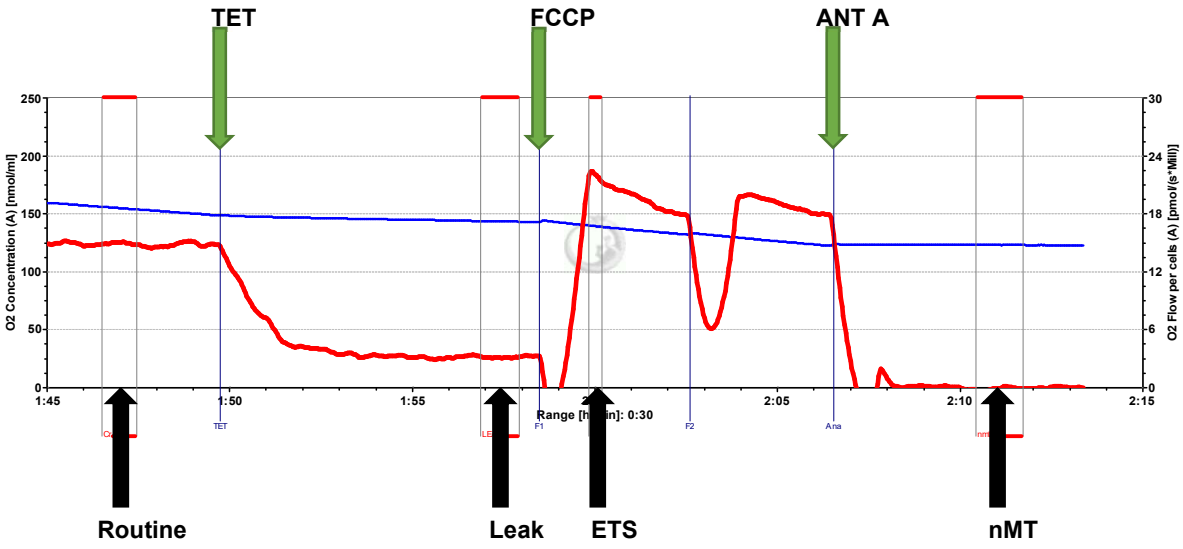

Figure 4.20: A typical respirometry profile generated from the Oroboros oxygraphy-2k to indicate the changes in routine respiration following drug addition. The red trace is indicative of the oxygen flux per unit sample (pmol/s*Mill), and the blue line represents oxygen concentration in the sample. Each black arrow indicates the steady state oxygen flux (Routine respiration), the induced mitochondrial resting state (Leak), the maximal capacity of the electron transport system (ETS) and the non-mitochondrial oxygen flux (nMT). The addition of each drug is represented by green arrows, with triethiltyn bromide (TET) inducing leak respiration, Carbonylcyanidep-trifluoromethoxyphenylhydrazone (FCCP) inhibiting ATP synthase and therefore allowing maximal electron transport through the ETS and Antimycin A (AntA) inhibiting the ETS.

In each respirometry experiment, the routine state of respiration for each strain was first established. Following the addition of GdnHCl to YEPD cultures of each strain, the routine level of respiration was found to be significantly reduced indicative of a direct impact of GdnHCl on overall respiration in all strains (**Figure 4.21**). A difference between routine respiration in *Sc.* Δ*hsp78* and *Sc.* Δ*hsp104* was also observed.

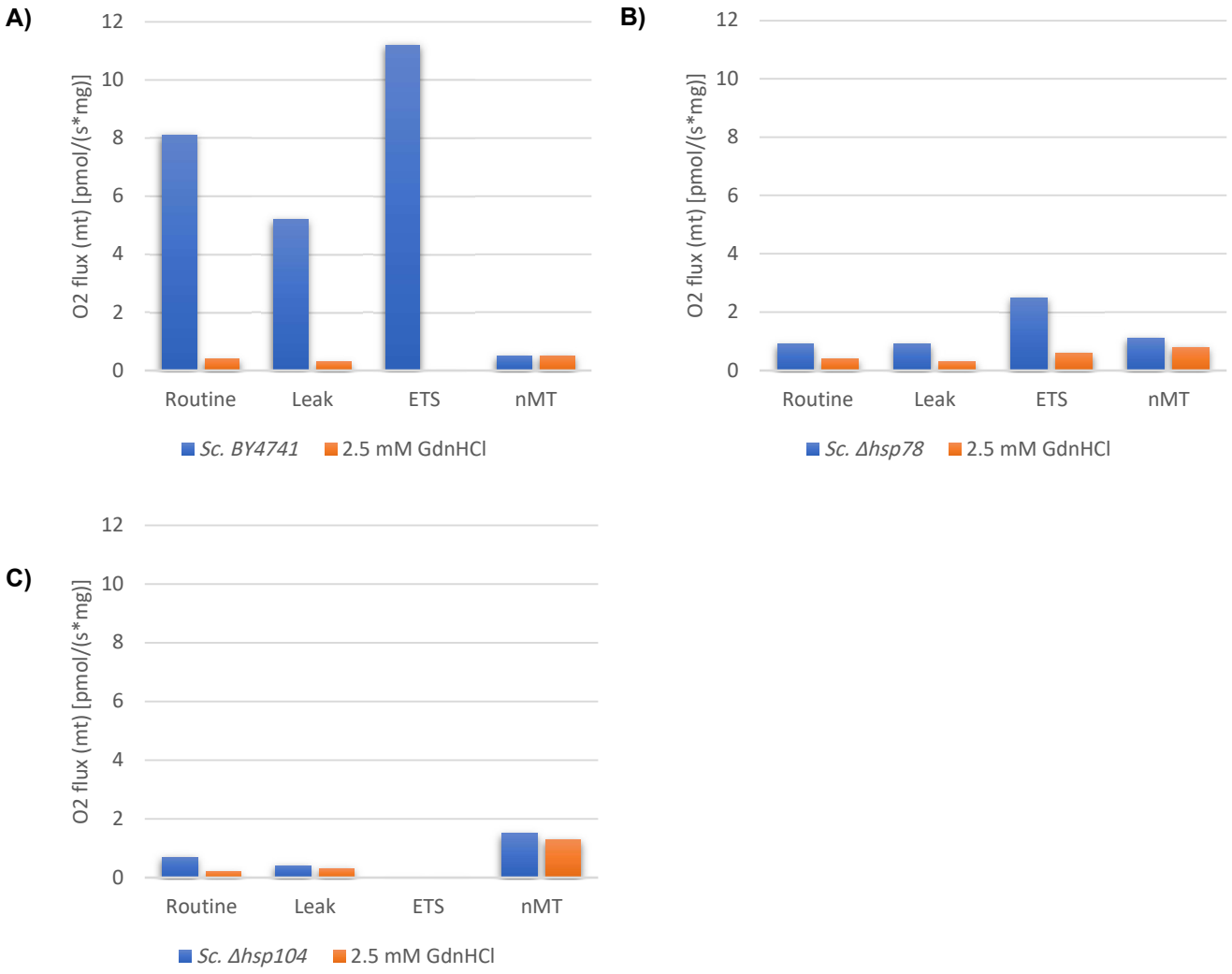

Figure 4.21: The routine, leak, ETS and NMT oxygen flux values for A) Sc. *BY4741*, **B)** *Δhsp78* and **C)** *Δhsp104* with and without the addition of 2.5 mM GdnHCl. The results shown represent the average values generated from 3 biological repeats, each with two technical replicates.

The 'leak' level of respiration was then measured following the addition of the drug TET, which inhibits ATP synthase complex V (Pious & Hawley, 1972). ATP synthase produces ATP by pumping protons across the mitochondrial inner-membrane space (IMS) into the mitochondrial matrix. Inhibition of this pathway leads to the accumulation of protons within the IMS, resulting in protons returning to the matrix independent of ATP synthase. The results is an overall inhibition of the movement of electrons through the electron transport chain, representing an integral control mechanism of ATP synthase. The addition of TET therefore indicates the free movement of

protons independent of the proton pump and is thus labelled 'leak' respiration. The addition of GdnHCl caused a significant decrease in leak respiration in all strains (**Figure 4.21**). Prior to the addition of GdnHCl, a higher level of respiration which occurs independently of ATP synthase proton pumping activity was observed. A decrease in leak respiration in all strains following the addition of GdnHCl may instead imply that a TET-induced drop in respiration did not take place. This would indicate that oxygen consumption and electron movement already occur independently of ATP synthase under these conditions thus showing that following the addition of GdnHCl, ATP is not synthesised i.e. uncoupled respiration.

The maximal capacity of the electron transport system (ETC) was measured following the addition of the uncoupling agent FCCP. FCCP forms pores in the IMM making it permeable, allowing the free flow of protons across it. This results in the disruption of the membrane potential provided by the proton gradient, allowing the ETC to function at its maximal potential. Therefore, the higher the ETS detected, the higher the capacity of the ETC. FCCP thus abolishes the link between the respiratory chain and the phosphorylation system usually observed in intact mitochondria. In both *Sc.* BY4741 and *Sc.* Δ*hsp78,* the ETS was higher than the routine level of respiration following the addition of FCCP, indicating functional mitochondria capable of making ATP (**Figure 4.21**). In both *Sc.* BY4741 with the addition of GdnHCl, and *Sc.* Δ*hsp104* knockouts with and without GdnHCl, the level of ETS is completely abolished (**Figure 4.21**). Thus in cells treated with GdnHCl and/or lacking a functional Hsp104, the overall capacity of the ETS was reduced and the mitochondria non-functional.

Finally, the level of non-mitochondrial (nMT) respiration was measured following the addition of Ant A. AntA inhibits cytochrome C reductase (complex III), preventing the transfer of electrons. Complex III is the third phase in the ETC and causes oxidation at the Qi site. Inhibition at this specific site therefore prevents re-oxidation by oxygen, and any oxygen consumption detected after the addition of AntA is therefore of nMT origin. A high level of nMT was detected in the *Sc.* Δ*hsp104* strain, mimicking the high level of nMT observed in all three strains under test following the addition of GdnHCl. This would suggest that without a functional Hsp104 in *Sc.* BY4741, the

function of mitochondria ceases. Hsp104 therefore appears to be the target of GdnHCl in *petite* generation (**Figure 4.21**).

Individual components of the ETC were further analysed to identify whether a specific component was affected by the addition of GdnHCl. These components were analysed by comparing the oxygen flux ratios between the Routine and ETS (R/E) and the Leak and ETS (L/E). The R/E defines how close to the maximal capacity the mitochondria are functioning during routine respiration. Moreover, the closer the R/E ratio is to 1, the closer to maximum capacity the ETS is working in the strain (**Figure 4.22**). *Sc.* BY4741 showed a high R/E, which could not be calculated following the addition of GdnHCl due to a complete lack of ETS. A reasonably high R/E was also observed in *Sc.* Δ*hsp78*, which increased following the addition of GdnHCl. This may suggest that the mitochondria were not functioning at their maximum capacity prior to GdnHCl treatment. In this case, an increase in R/E may suggest more uncoupling of the ETC, an increase in ADP driven respiration or a limitation of the ETC components. Finally, no R/E could be calculated for *Sc.* Δ*hsp104,* as the ETS was completely abolished.

To determine whether a high R/E was due to uncoupled respiration, the L/E was also calculated. The closer the L/E to 1, the higher the levels of uncoupled respiration that are occurring independently of ATP synthase (**Figure 4.22**). Uncoupled respiration is not transformed into energy by phosphorylation of ADP. In *Sc.* BY4741, the L/E is relatively low, which suggests a relatively low level of uncoupled respiration. As the mitochondria in these wildtype cells are functioning close to their maximal capacity, we can conclude that these cells are neither necrotic or apoptotic. The impact of GdnHCl on L/E in *Sc.* BY4741 could not be assessed due to a lack of ETS. An increase in the L/E following the addition of GdnHCl in *Sc.* Δ*hsp78* implied an increase in uncoupled respiration. As with R/E, L/E could not be calculated for *Sc.* Δ*hsp104,* as the ETS was completely abolished.

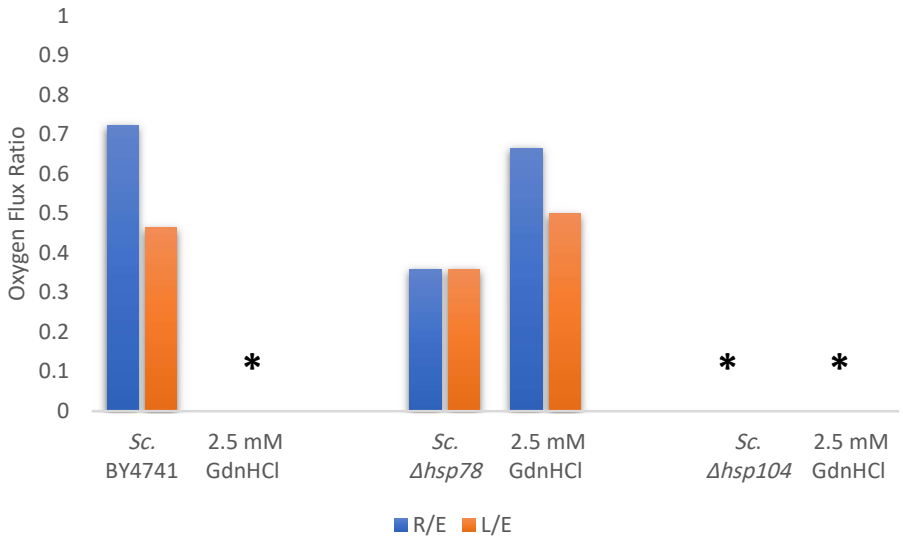

Figure 4.22: The oxygen flux ratios between the Routine and ETS (R/E) and the Leak and ETS (L/E) are shown for all strains with and without the addition of 2.5 mM GdnHCl. * indicates complete abolishment of the ETS in that condition and therefore no ratio calculation was possible. The results shown represent the average of three biological repeats, each with two technical replicates.

In conclusion, it is evident that both a loss of Hsp104 and treatment with GdnHCl completely abolishes mitochondrial respiration. GdnHCl stops respiration completely in both *Sc.* BY4741 and in *Sc.* Δ*hsp78*, but has little to no effect in *Sc.* Δ*hsp104* because the mitochondria are already in a suppressed state in this strain. Therefore, it was concluded that Hsp78 is not the target of GdnHCl in respiratory-deficient *petite* mutant generation.

The direct impact of GdnHCl on Hsp104 could be further established by a time point analysis, where the activity of mitochondria is measured at specific time points following the addition of GdnHCl. This would allow the production of a timeline between the addition of GdnHCl and the generation of *petite* mutants. Furthermore, the frequency of *petite* mutants in each of the respiratory deficient strains should be calculated by taking samples directly from the respirometer and plating these samples on glycerol. The levels of mitochondrial activity both in wildtype cells

and following the addition of GdnHCl should also be analysed in all species of *Saccharomyces,* to provide a complete story for the role of GdnHCl in petite generation.

4.8. Discussion

Both a loss of Hsp104 activity and treatment with GdnHCl causes mitochondrial suppression in *S. cerevisiae.* The same reduction in mitochondrial activity in each of these conditions is consistent with Hsp104 being the target of GdnHCl that leads to the generation of *petite* mutants. *Petite* mutants can also be generated during the translation of proteins that are relocated into the mitochondria, further implying that the target of GdnHCl does not have to be mitochondria-based. In turn, it is possible that such mutants restrict the levels of protein available to the mitochondria, and Hsp104 may be associated with such a mechanism. It has been suggested that Hsp104 regulates redox states within the cell. In *hsp104*Δ cells for example, mitochondria lose both membrane integrity and control of the electron transport chain, thus resulting in a higher level of intracellular ROS (Ueom et al., 2003).

An alternative explanation for the role of Hsp104 in *petite* generation could be the formation of an mPOS (Mitochondrial Precursor Over-Accumulation Stress) response. When stressed, mitochondria may face inefficient protein import, resulting in reduced cell fitness by disruption of the proteostatic network in the cytosol (Coyne & Chen, 2018). mPOS is characterised by the accumulation of toxic unimported mitochondrial proteins in the cytosol. When under stress, the yeast cell will upregulate suppressor genes which likely alleviate mPOS by reducing protein synthesis, thus leading to reduced protein misfolding and increased protein turnover. When a cell's capacity to stabilise the proteome is exceeded, these proteins accumulate in the cytosol, in turn generating an mPOS response and decreasing cell viability. Defects in many pathways including mutations in mt-protein import machinery, IMM protein misfolding and mt-DNA mutations may cause an mPOS response. Therefore, it is likely that mitochondrial damage does not directly target the core protein import machinery, but is still sufficient in compromising mt-protein import and causing cell death (Coyne & Chen, 2018). This may signify that GdnHCl targets

Hsp104, which in turn causes an mPOS response resulting in the formation of *petite* mutants. This hypothesis must be tested by confirming the presence of an mPOS response, using antibodies that target specific proteins which accumulate in the cytosol, for example Aac2; encoding the major isoform of adenine nucleotide translocase involved in ATP/ADP exchange across the IMM (Wang et al., 2008)

The experimental findings reported in this Chapter strongly suggest that Hsp78 is not directly impacted in GdnHCl-induced *petite* generation. Although the link between Hsp78 and GdnHCl-induced *petite* generation may not be direct, studies by others suggests that Hsp78 may still play a role in thermotolerance and stress protection. For example, under extreme heat stress, *hsp78*Δ cells lose all respiratory function (Röttgers et al., 2002).

Interestingly, GdnHCl still induces *petite* mutants in *S. cerevisiae* in the absence of Hsp104*,* highlighting the possibility of an alternative target of GdnHCl in *petite* generation. It is therefore likely that Hsp104 acts as the primary target of GdnHCl, but that an alternative protein plays a role in salvaging the pathway of *petite* mutant generation in the absence of this protein. Hsp70 would be a likely candidate for GdnHCl-induced *petite* induction, in the absence of Hsp104 since the integrity of the mitochondrial genome and a sufficient mitochondrial membrane potential necessary for efficient protein import requires at least one of Hsp70 and Hsp78 (Moczko et al., 1995). Moczko et al*.,* also (1995) suggest that Hsp78 only becomes important in situations where the activity of mt-Hsp70 is limiting, and Hsp78 may simply provide an additional component of the mitochondrial system of chaperone proteins. *Petite* mutant generation and a strongly reduced mitochondrial membrane potential may be indicative of a specific role of Hsp78 in the import of preproteins under conditions of impaired mt-Hsp70 function (Moczko et al., 1995). These findings imply that a similar interaction may be the case between GdnHCl and Hsp70, which is only significant when Hsp104 function is impaired.

Chapter 5: The impact of natural genetic variation on protein aggregation in *Saccharomyces* species

5. Chapter 5: The impact of natural genetic variation on protein aggregation in *Saccharomyces* species

5.1. Introduction

Haploid strains of *S. cerevisiae* can facilitate and perpetuate the formation of a range of heterologous, amyloid-forming proteins including the Alzheimer's disease-associated protein Aβ42 (Goedert & Spillantini, 2006) and Huntingtin (Htt)-associated exon 1 of the huntingtin protein (Htt) with a range of glutamine (Q) expansions e.g. Htt-97Q (Norremolle et al., 1994). The impact of disease-associated Htt-97Q on growth and viability of *S. cerevisiae* had been demonstrated previously including the ability of these proteins to cause toxicity and form aggregates indicative of amyloids (Masino et al., 2002). No studies of these heterologous proteins expressed in other species belonging to *Saccharomyces* have been reported to date.

In order to gain an understanding of the impact of expressing either Aβ42 or Htt-97Q in other genetically-related species of *Saccharomyces*, two other species of the *Saccharomyces* were used; namely *S. bayanus* and *S. mikatae*. *S. kudriavzeveii* was eliminated from this study as the plasmids used to express the amyloidogenic proteins were based on the *GAL1* promoter and hence require induction with galactose. The strains of *S. kudriavzeveii* used in this project have a non-functional *GAL* gene network of pseudogenes (Scannell et al., 2011).

In addition, one genetically marked wild strains of *S. cerevisiae* (Cubillos et al., 2009) was used in a parallel study representing a diverse ecological niche. As mentioned in Chapter 1, Section 1.11, the variable nature of accessory genomes between different strains of the same species may uncover different impacts of amyloid-forming proteins on host growth and behaviour. Alternate laboratory strain of *S. cerevisiae*, namely 74D-694 and *Sc.* BY4741 were also used throughout this chapter. The full list of yeast species/strains used in this study is provided in Materials and Methods.

The initial aim of this work was to determine whether each of these species can generate and propagate the amyloid forms of Aβ42 and polyQ, and if so, the impact these amyloid-forming proteins have on growth and viability of the host. However, this also required an investigation into whether the behaviour of these amyloidogenic proteins was impacted upon by the prion state of the host yeast species. For example, in *S. cerevisiae*, Htt-Q97 is only toxic if the strain contains an endogenous [*PIN*$^+$]-like prion (Meriin et al., 2002). Initially, Meriin et al*.,* (2002) showed that deficiencies in molecular chaperons Sis1 and Hsp104 inhibited the seeding of polyQ aggregates. Since Hsp104 is required for prion maintenance in yeast, this suggested a role for prions in polyQ aggregation and toxicity (Meriin et al., 2002).

To determine whether cell growth and toxicity of Aβ42 or Htt-97Q in these other strains and species was dependent on a [*PIN*$^+$]-like prion or another endogenous prion, the function of the endogenous molecular chaperone Hsp104 was impaired by chemical inhibition. This would block the propagation of any Hsp104-dependent prion states although one cannot rule out that Hsp104-independent prions may also exist in these strains/species. Creating such 'prion-free' cells would thus allow us to determine whether the impact of expression of Htt-Q97 has the same requirements in all species as in *S. cerevisiae*, whether the other genetically-related species of *S. cerevisiae* have a [*PIN*$^+$]-like prion and whether Aβ42 also relies on an endogenous prion for aggregation and/or toxicity.

5.2. Impact of expression of Htt-97Q in *Saccharomyces* species

Laboratory strains of *S. cerevisiae*, a genetically-marked wild strain of *S. cerevisiae* and strains of *S. bayanus* and *S. mikatae* were each transformed with pYES2-based plasmids expressing either Htt-25Q (which acts as the control) and Htt-97Q. In each case the transformed cells had the target Htt-Q25/97 sequence under the control of the regulatable promoter *GAL1*. Expression of the target gene was induced by transferring cells from a glucose-based medium into a medium containing galactose as the sole carbon source. The growth of each strain was then analysed

using the multi-well plate reader in two independent experiments, with each time point in triplicate. The data reflect the average of all of these experiments.

5.2.1.Htt-Q97 aggregation impacts growth of all species of *Saccharomyces*

When induced with galactose, the expression of Htt-97Q resulted in a slight but statistically significant increase in doubling time relative to the growth of all strains transformed with the plasmid but not induced for expression, in the glucose-based control medium (i.e. SD-ura), (**Figure 5.1**). The doubling time of all strains induced for expression of Htt-97Q was also statistically different to the doubling time of all strains expressing Htt-25Q as a control. This result suggests that expression of Htt-97Q in all strains and species tested inhibits cell growth although it is unclear whether this reflects an impaired rate of cell growth or an increase in cell death within the Htt-Q97 expressing population.

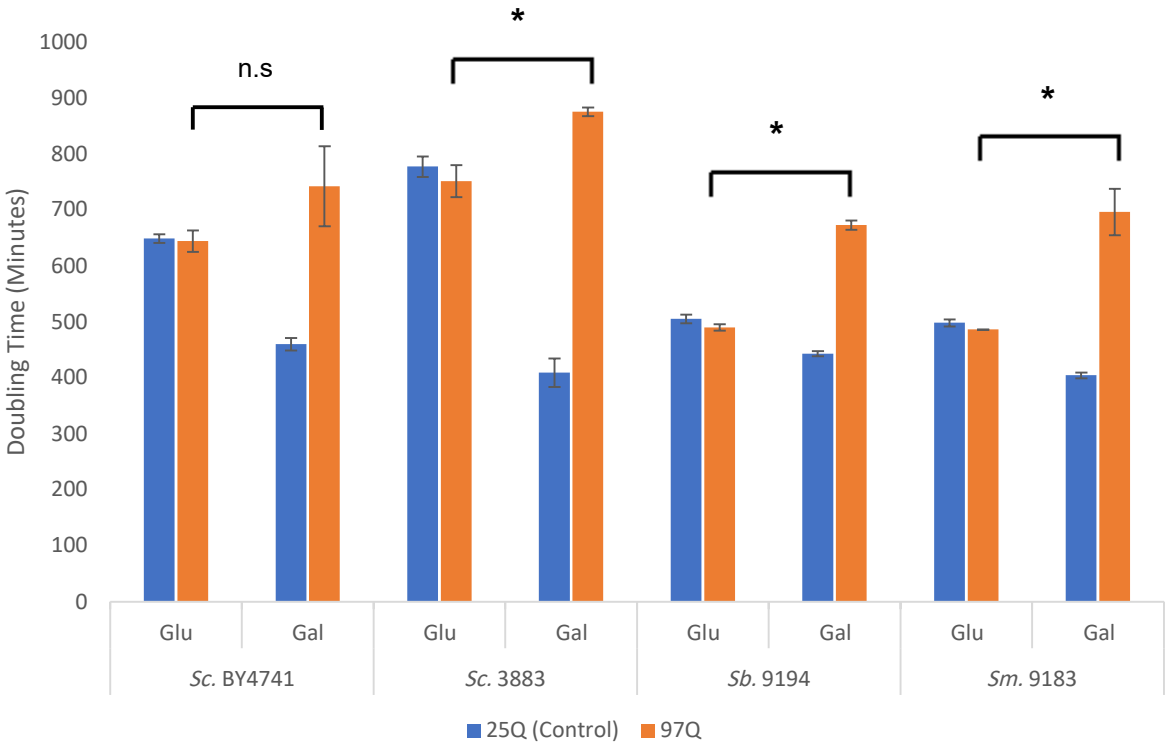

Figure 5.1: Doubling times following the induction of Htt-25Q and Htt-97Q expression. All species show an increase in doubling time when induced with galactose to express Htt-97Q. The data reflects the average of three biological repeats, each with two technical replicates. Statistics were performed on both the biological and technical replicates. Error bars denote standard deviation. Paired two tail T-tests were carried out: *p<0.05, n.s = not significant.

As previously shown in *S. cerevisiae* by Meriin et al. (2002) (Meriin et al., 2002), Htt-97Q has a toxic effect on the cell, resulting in an increased doubling time as was observed for the two strains of *S. cerevisiae* and two *Saccharomyces* species tested here (**Figure 5.1**). Overlaying the growth curves for the different strains growing on SD-Ura+Gal i.e. expressing Htt-97Q, revealed a difference in growth profile when compared to the typical growth profile of *Saccharomyces* species (detailed in Chapter 6) (**Figure 5.2**). Diauxic shift refers to the stage of growth where cells undergo dramatic metabolic changes, following the exhaustion of a fermentative carbon source. At this stage, cells prepare for post-diauxic respiratory growth where they consume the by-product of fermentative growth, ethanol (**Figure 5.2**).

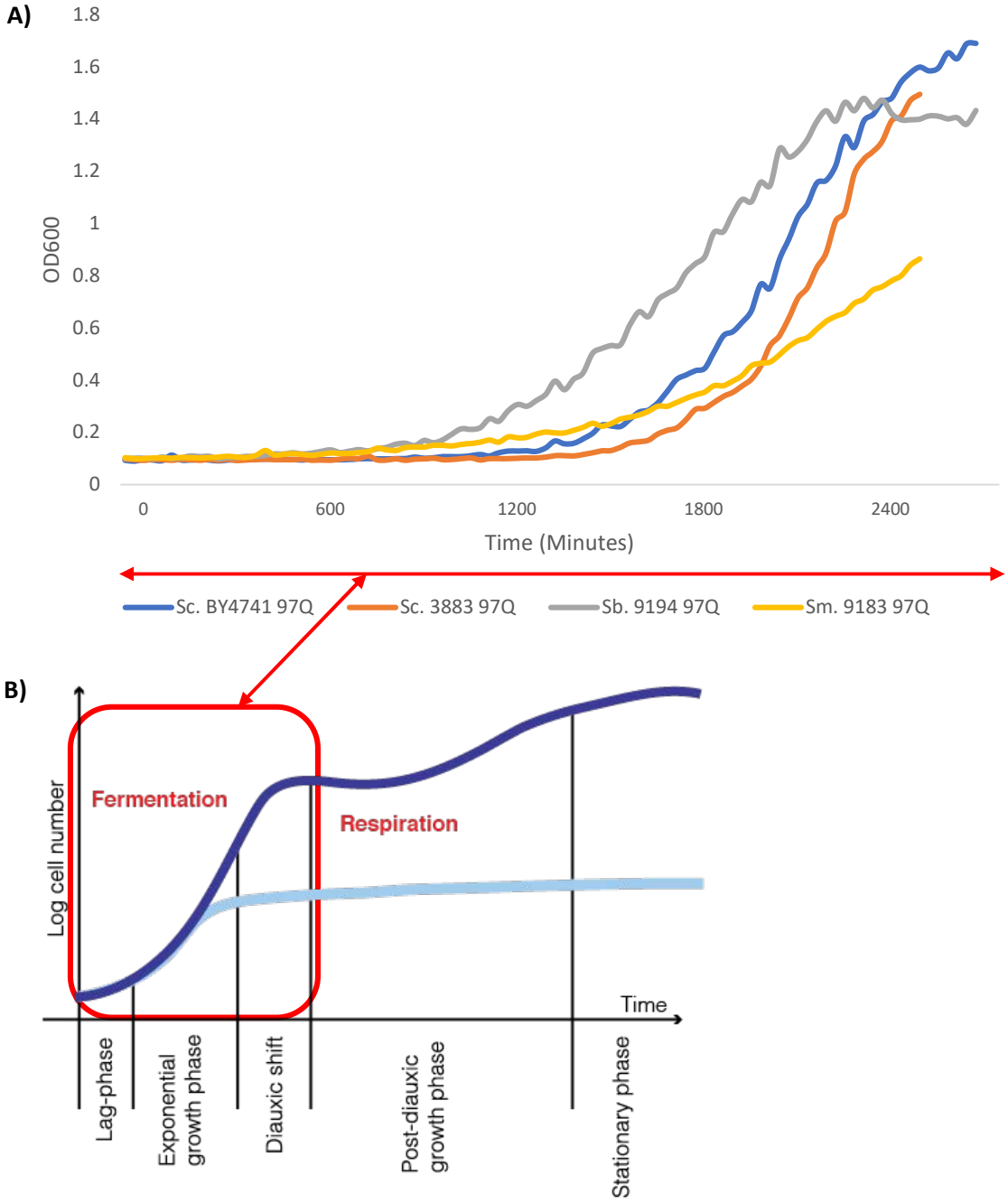

Figure 5.2*:* Growth profile of yeast strains expressing Htt-97Q. Panel A) Cell growth was monitored following Htt-97Q expression in *Saccharomyces* species. **Panel B**) A 'typical' growth curve for *S. cerevisiae* indicating the growth stages seen within a typical growth profile (taken from Smets et al., 2010).

The data indicate that expression of Htt-97Q has a detrimental impact on the growth of all strains and species tested as evidenced by a reduced growth rate. This is indicative of cell toxicity linked directly to the synthesis of Htt-Q97. However, the data do not extend into further stages of growth such as post-diauxic growth or stationary phase growth and so it was not possible to comment on the impact Htt-97Q has on the entire growth profile of each strain.

5.3. Aβ42 aggregation impacts optimal growth of all species of *Saccharomyces*

Laboratory strains of *S. cerevisiae*, a genetically-marked wild strain of *S. cerevisiae* and strains of *S. bayanus* and *S. mikatae* were each transformed with pBEVY-GU-based plasmids expressing either Aβ42 fused in frame to mNeonGreen or mNeonGreen alone as control. mNeonGreen is a fluorescent protein that can be used to observe localisation and aggregation in the yeast cell (Shaner et al., 2013). The growth of each strain was analysed in two independent experiments, each time in triplicate, and the data shown reflects the average of these experiments.

When expressing Aβ42, all strains bar *S. mikatae* showed a statistically significant increase in doubling time compared to the strains expressing mNeonGreen alone as controls (**Figure 5.3**). This suggests that the expression of Aβ42 in all strains causes an impairment or delay in cell growth, and a possible reduction in cell population size indicative of cell death.

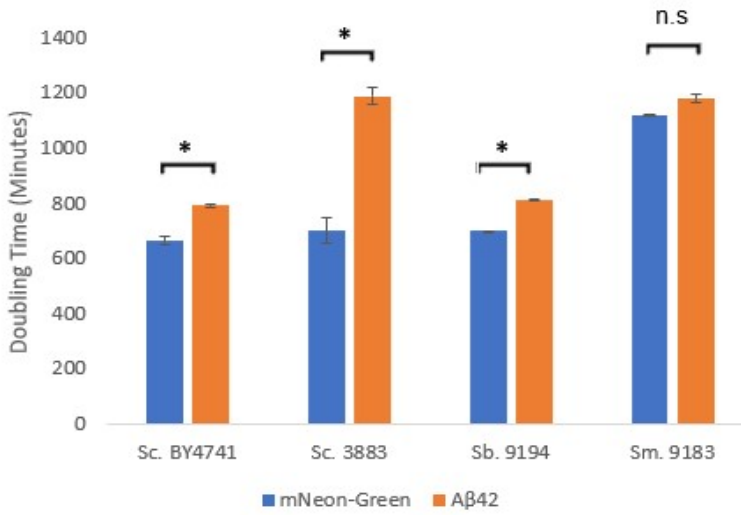

Figure 5.3: The doubling times of all strains as a consequence of induction of mNeonGreen and Aβ42 expression. The data reflects the average of three biological repeats, each with two technical replicates. Statistics were performed on both the biological and technical replicates. Error bars denote standard deviation. Paired two tail T-tests were carried out: *p<0.05, n.s = not significant.

An increase in doubling time in most strains expressing Aβ42 may suggest a negative effect on cell growth rate, and a level of toxicity in the cell caused by the Aβ42 moiety. A notable difference between the observed growth profiles of *Sc.* BY4741 and *Sb.* 9194 were observed when compared to their 'typical' growth profile (See Chapter 6). However, when comparing the growth curves of all strains expressing Aβ42, it was evident that there was little difference in the growth profiles of *Sc.* 3883 and *Sm.* 9183 (**Figure 5.4**).

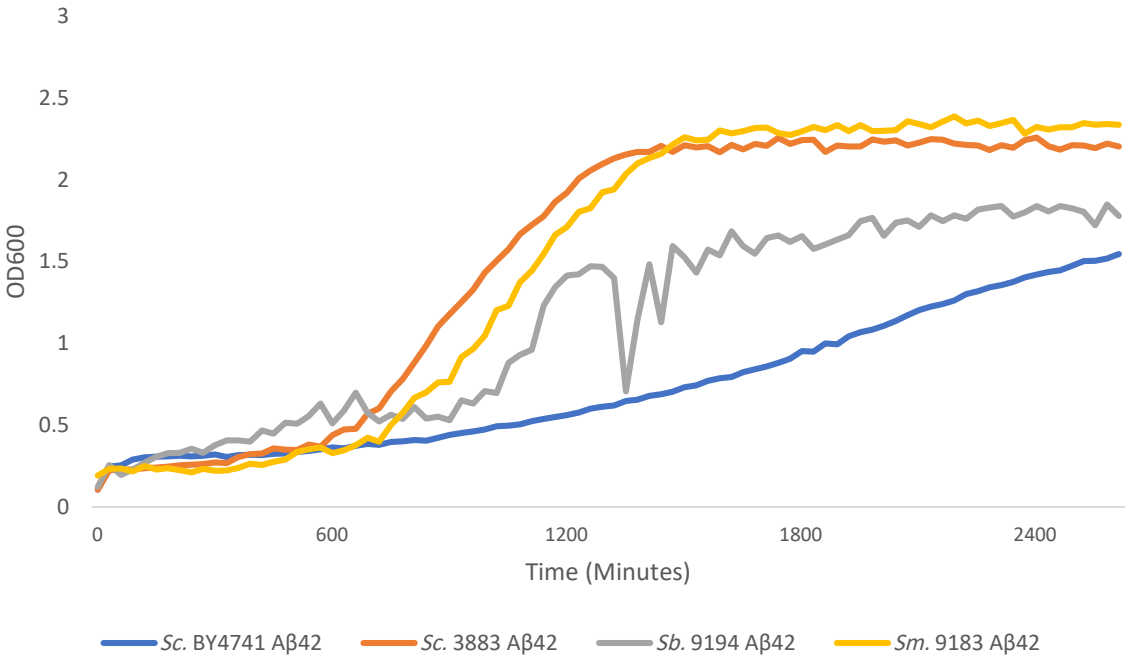

Figure 5.4: Growth profile of strains as a consequence of Aβ42 expression. This data represents an average of two biological repeats, each with three technical replicates.

The data suggest that the impact of expressing Aβ42 intracellularly on cell growth is inconsistent both within and between species of *Saccharomyces*. As with the expression of Htt-97Q, and particularly in the cases of *Sc*. BY4741 and *Sb*. 9194, without data extending further into the stages of growth it is not possible to comment on whether Aβ42 is detrimental to the cell. Caine et al*.,* (2007) showed that Aβ42 fusion proteins are non-toxic to yeast, although Aβ42-GFP expression caused a slight decrease in growth rate (Caine et al., 2007) which is inconsistent with the observed effect with *S. mikatae*. In the case of the other three yeast strains/species examined where there was a statistically significant change in growth rate, and a small but reproducible increase in doubling time of strains expressing Aβ42 suggesting some impairment of growth when cells expressed Aβ42-mNeonGreen.

5.4. Disease-associated Htt-97Q has minimal impact on the growth of diploid *S. cerevisiae* BY4743

All strains of all species previously tested here were haploid yeast strains, but both Aβ42 and Htt-Q97 are mainly studies in diploid organisms (Caine et al., 2007; Meriin et al., 2002). Consequently we next examined the effects of expression of these two amyloid-forming proteins in the diploid laboratory strain *Sc.* BY4743. The strain was therefore transformed with either pYES2-25Q or pYES2-97Q and expression induced as described above. The growth of BY4743 was analysed in biological triplicate across two independent experiments, and all data shown reflects the average of these experiments (**Figure 5.5**).

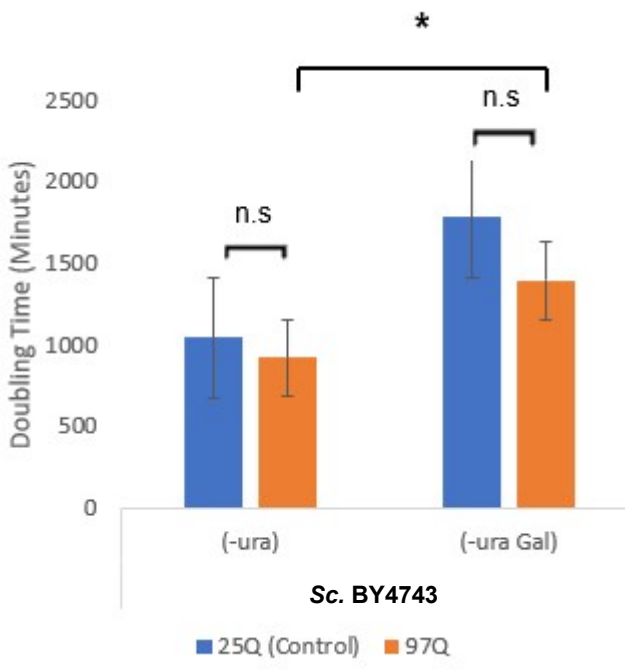

Figure 5.5: The doubling time of diploid strain BY4743 expressing either Htt-25Q or Htt-97Q. *Sc.* BY4743 expressing Htt-25Q and Htt-97Q suggests an increase in doubling time from control media to -ura Galactose. The data reflects the average of three biological repeats, each with two technical replicates. Statistics were performed on both the biological and technical replicates. Error bars denote standard deviation, paired two tailed tests were carried out: *p<0.05, n.s. = not significant.

When transferred to a galactose-based medium, BY4743 expressing Htt-97Q showed a significant increase in doubling time compared to growth in control medium SD-ura, when the strain was not induced for plasmid expression (**Figure 5.5**). In contrast with the results seen in the haploid version *Sc.* BY4741 (**Figure 5.1**), the doubling time of BY4743 expressing Htt-97Q reduced when compared to the expression of Htt-25Q, although these results were not statistically significant.

In contrast with the findings displayed in **Figure 5.2**, the expression of Htt-25Q and Htt-97Q in *Sc*. BY4743 showed no effect on growth profile (**Figure 5.6**). The results of the growth experiment indicate that the expression of Htt-Q97 has no significant impact on growth rate or the ability of the cells to transition through all expected growth stages.

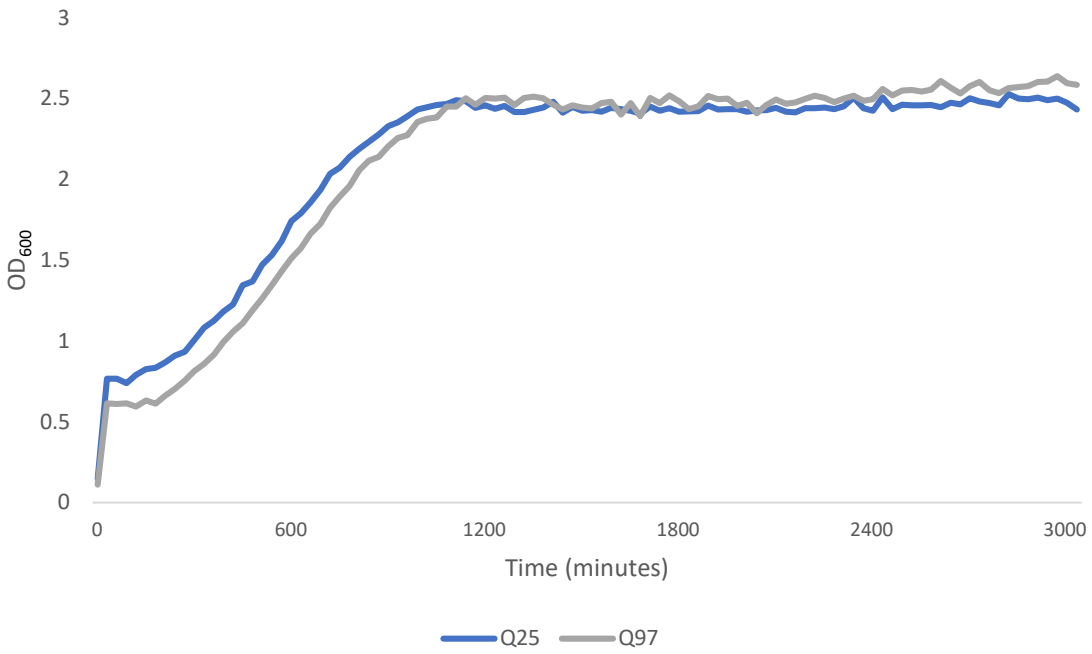

Figure 5.6: Growth profile of *Sc.* BY4743 cells expressing Htt-Q25 or Htt-97Q. This data represents an average of two biological repeats, each with three technical replicates.

5.5. Impact of expression of Htt-Q97 on cell viability of various yeast strains and species

The impact Htt-Q97 has on the viability of the various strains and *Saccharomyces* species was next investigated by determining cell viability using two different approaches; indirectly by use of a vital stain and directly by measuring the number of cells able to form a colony.

5.5.1. Assessing impact of Htt-Q97 expression indirectly using methylene blue staining

Previous studies have suggested that Htt-Q97 causes both aggregation and toxicity in *S. cerevisiae* (Meriin et al., 2002). To better understand the underlying mechanism of cell toxicity caused by Htt-Q97, and to differentiate a cytocidal effect from a cytostatic one, yeast cell viability was first measured by determining the percentage of observable cells in a population that take up a vital stain such as methylene blue (Matthews, 1914). Consequently, following the expression of Htt-Q97 or Htt-Q25 as a control, in the laboratory strains of *S.cerevisiae*, wild strain of *S. cerevisiae*, strains of *S. bayanus* and strains of *S. mikatae*, cells were stained with methylene blue and immediately visualised. While living cells have an active dehydrogenase system which

reduce methylene blue, dead cells cannot reduce the stain and therefore remain blue (Matthews, 1914) (**Figure 5.7**).

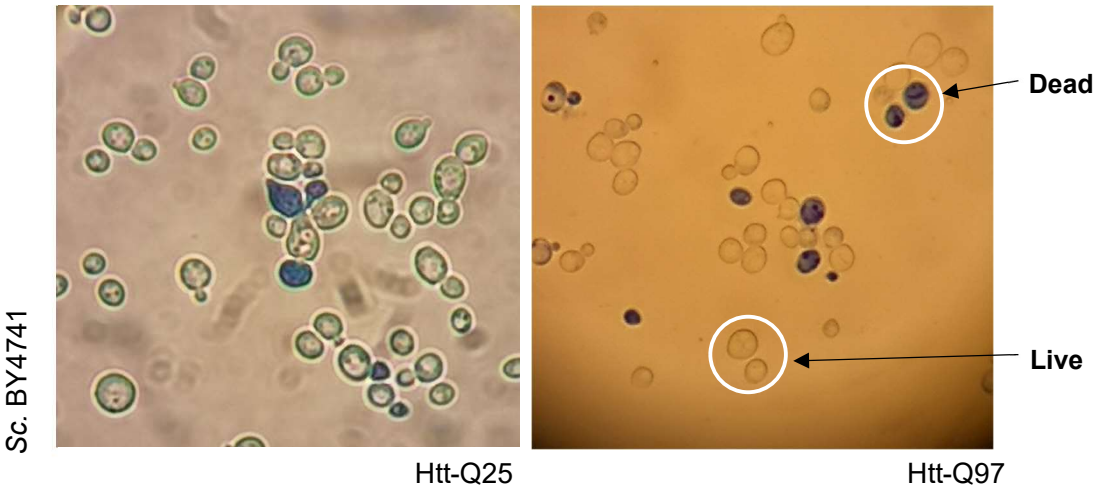

Figure 5.7: Methlyene blue staining for detecting dead cells. While living cells have an active dehydrogenase system which reduce methylene blue, dead cells cannot reduce the stain and therefore remain blue. In each strain, a minimum of 200 cells were manually counted across 3 independent biological experiments and labelled as blue (dead) or white (live).

In each strain, a minimum of 200 cells were manually counted across 3 independent experiments and labelled as blue (dead) or white (alive) following staining with methylene blue. Data shown reflects the average of these experiments. When analysing the percentage of viable cells following expression of Htt-Q97 and Htt-Q25, a statistically significant decrease in viable cells was seen in all strains and species, with the exception of the diploid strain Sc. BY4743 (**Figure 5.8**) suggesting that diploid strains have a higher resistance to Htt-Q97-mediated toxicity, consistent with the growth data (see **Figure 5.4**).

In summary, these data demonstrate that expression of Htt-Q97 has a clear impact on cell viability across all haploid strains of all *Saccharomyces* species tested, but not in the single diploid strain tested.

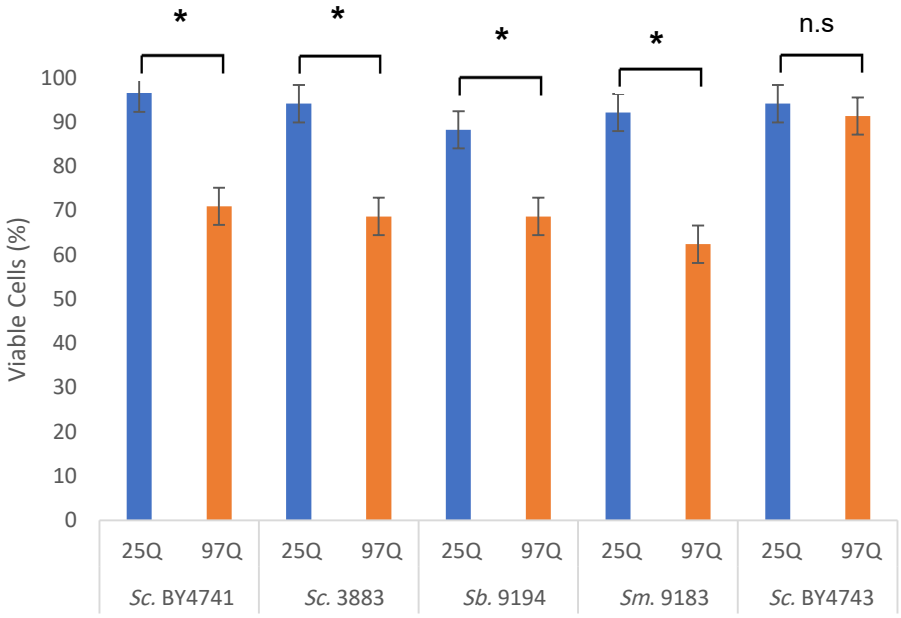

Figure 5.8: Expression of Htt-Q97 causes an increased cell death in different yeast strains and species following methlyene blue staining for detecting dead cells, where dead cells stain blue. While living cells have an active dehydrogenase system and stain white, dead cells cannot reduce the stain and therefore remain blue. In each strain, a minimum of 200 cells were manually counted across three independent biological experiments with two technical repeats, and labelled as blue (dead) or white (live). Statistics were performed on all of these replicates. Error bars denote standard deviation. Paired two tailed tests were carried out: *p<0.05, n.s. = not significant.

5.5.2.Assessing impact of Htt-Q97 expression on cell viability directly

Cell toxicity can also be observed using a spotting test assay as shown in **Figure 5.9**. In each case, expression of Htt-Q25 and Htt-Q97 was induced with galactose for 24 hours, and a dilution series of each culture was made and plated onto a rich glucose-based growth medium. Toxicity is evident in all strains expressing Htt-Q97, albeit at different levels. *Sc.* BY4741 shows the highest level of toxicity, compared to the visible development of colonies remaining in the highest dilution in all other strains. As expected, all strains induced to express the control Htt-Q25 grow without visible impairment. The observed toxicity of Htt-Q97 in all strains would be consistent with the presence of a [*PIN*$^+$]-like prion in all of the strains and species examined here.

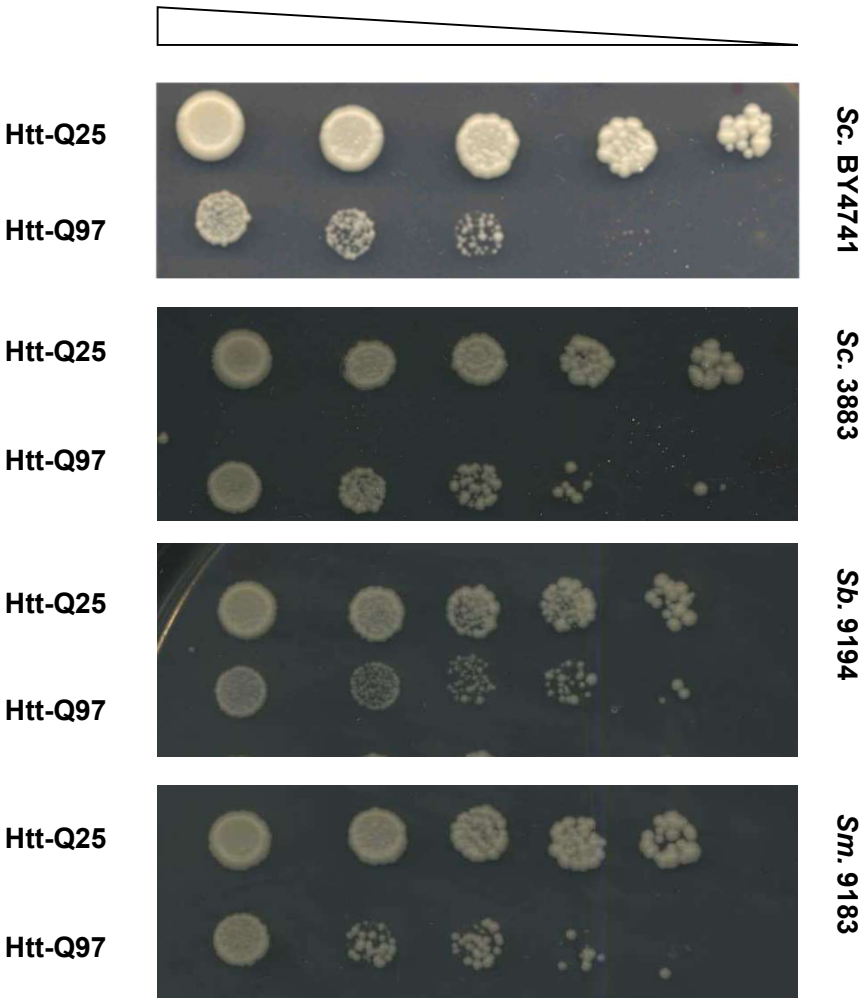

Figure 5.9: A plate assay to determine the effect of Htt-Q25 and Htt-Q97 expression on the growth and formation of colonies of all species on solid medium. In each case, expression of Htt-Q25 and Htt-Q97 was induced with galactose for 24 hours, and a dilution series of each culture was made and plated onto a rich glucose-based growth medium. The slope denotes serial dilution, with each step indicating a 1/10 dilution.

As with the earlier growth experiments, the spotting assay does not tell us whether the growth phenotype of the Htt-Q97 expressing strains is a cytostatic effect, where cells remain viable while halting division, or whether cells have died. Although visible growth impairment is apparent in all strains expressing Htt-Q97, this only indicates that those cells that remain are able to grow into a multicellular colony when plated onto a solid medium, and does not give any insight into cytostatic cells. Expression of Htt-Q97 may inhibit cell growth without impacting on viability, but cells may

still regrow once released from the effects of the toxic protein. In summary, it is evident that Htt-Q97 causes toxicity in all strains, but the exact mechanism remains unclear.

5.6. Visualisation of disease-associated amyloid aggregation in all *Saccharomyces* species using fluorescence microscopy

As described with the toxicity caused by Htt-Q97, this amyloid-forming protein has also been shown to form aggregates in *S. cerevisiae* cells carrying the [*PIN*$^+$] prion (Meriin et al., 2002). Detecting the formation of the Htt-associated proteins using fusions to a green fluorescent protein can be used to indicate whether a) aggregate formation occurs, and b) whether there are differing requirements for aggregation between each strain/species particularly with regard to the endogenous prion state. Detection of Aβ42 aggregation is also possible using fusions to mNeonGreen (Shaner et al., 2013).

5.6.1. Htt-Q97 and Aβ42 form aggregates in all strains and species of *Saccharomyces*

When Htt-Q97 was expressed, fluorescent foci indicative of amyloid aggregates were evident in all strains in stationary phase. Htt-Q25 expression resulted in diffuse fluorescence across all strains, as expected for the control. Haploid strains of *S. cerevisiae* displayed 1-2 foci in most cells, much like the diploid strain *Sc.* BY4743, however aggregate size (based on fluorescent intensity) appeared to vary. *S. mikatae* showed a much higher number of foci per cell, and most cells observed displayed 3+ foci per cell. When expressing fluorescent fusion proteins, strains of *S. bayanus* showed an alteration of cell size and shape, with elongated cells being particularly evident (**Figure 5.10**). The reason for this effect is unknown but may reflect some form of stress response.

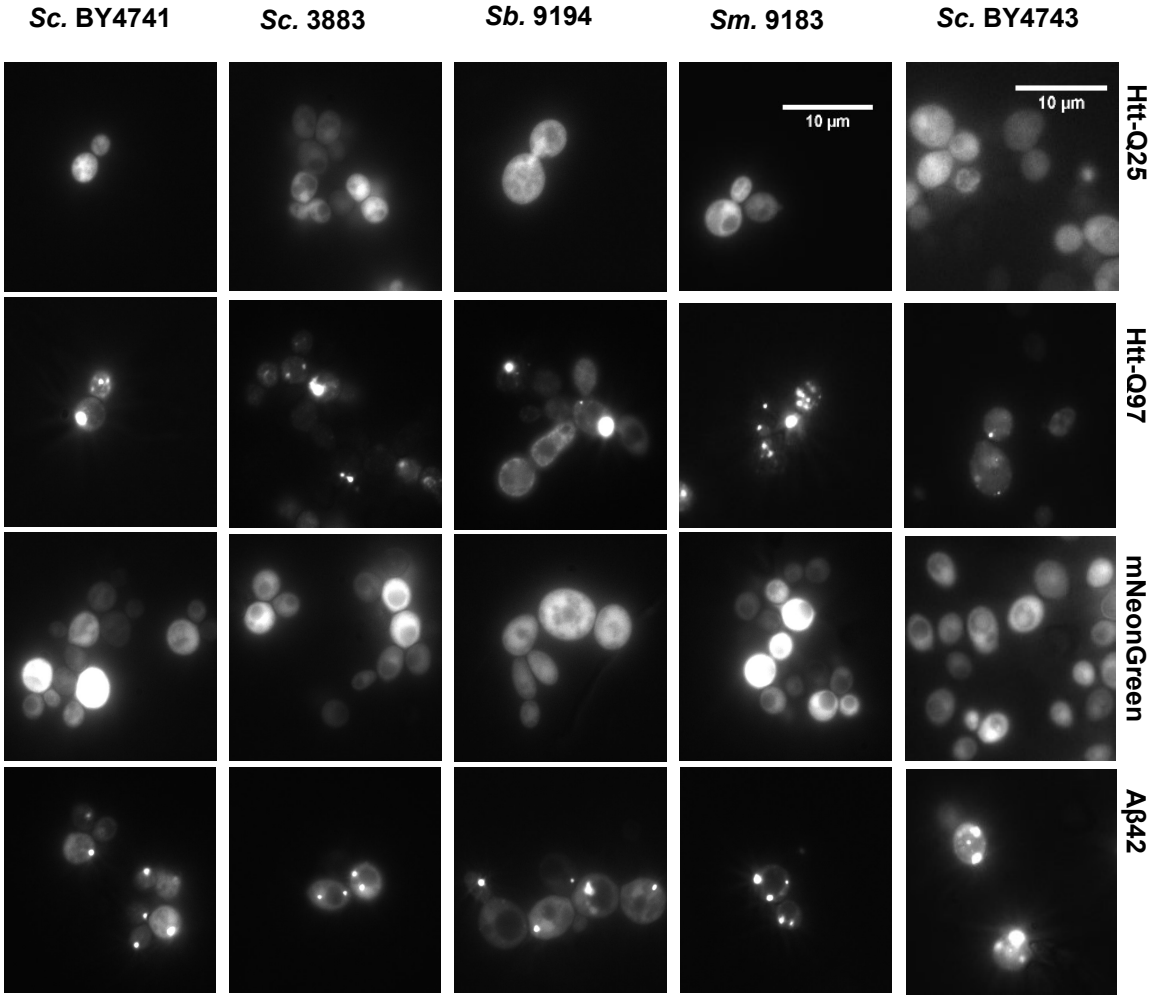

Figure 5.10: Cells expressing Htt-Q97 and Aβ42 form amyloid-associated aggregates in all species. Images shown were taken by fluorescent microscopy during stationary phase of growth, following 24 hours induction with galactose. Fluorescent signal represents the presence of the amyloid-forming proteins within cells, and vectors containing GFP alone to act as a control for each protein. Each strain was visualised in three independent experiments at 100x magnification, and at least 200 cells were visualised per condition. The scale bar represents 10 µm.

Aβ42 also formed aggregates in all strains tested as detected by the presence of fluorescent foci when compared to the diffuse fluorescence displayed in all strains expressing mNeonGreen alone. Aggregate size and number appeared to be consistent across strains and species, with an upper limit of 3 foci per cell and the majority of cells observed displaying 2 fluorescent foci per

cell. The only exception to this was the diploid strain *Sc.* BY4743, with the majority of cells containing 3 or more fluorescent aggregates per cell.

5.7. Visualisation of disease-associated amyloid aggregation in all species following treatment with GdnHCl

Following the visualisation of Htt-Q97 and Aβ42 aggregation in all strains, the [*PIN*$^+$] requirements for such aggregation was further by creating [*prion*$^-$] cells. As previously shown by Meriin et al. (2002), Htt-Q97 aggregation relies on the endogenous [*PIN*$^+$] prion in *S. cerevisiae*, so creating [*prion*$^-$] cells and revisiting the aggregation status of both Htt-Q97 and Aβ42 would be a means of establishing whether an endogenous [*PIN*$^+$]-like prion is required for disease-associated amyloid aggregation in all the *Saccharomyce*s species under test here.

Guanidine hydrochloride causes reversible inhibition of the chaperone activity of Hsp104 which is necessary for endogenous prion propagation (Ness et al., 2002) with exposure to 3-5 mM GdnHCl efficiently generating prion-free [including [*pin*$^-$] cells (Sondheimer & Lindquist, 2000).

5.7.1. Visualisation of disease-associated amyloid aggregation in [*prion*$^-$] strains

All strains were plated onto minimal media lacking uracil, supplemented with millimolar concentrations (5 mM) of GdnHCl for three independent rounds. Visualisation of all strains showed that fluorescent foci indicative of Htt-Q97 aggregation were no longer present, and diffuse fluorescence was seen across all cells in all strains (**Figure 5.11**). Interestingly, aggregates remained in *S. mikatae* until the concentration of GdnHCl used was increased to 8mM suggesting either reduced efficiency of uptake of GdnHCl or a reduced sensitivity of Hsp104 to GdnHCl (see Chapter 4).

In contrast, Aβ42 aggregates remained in all cells of all species following the same treatment with GdnHCl on solid medium. These findings suggest that aggregation of Htt-Q97 relies on [*PIN*$^+$] and Hsp104 (albeit indirectly) in all species, or an alternative [*PIN*$^+$]-like endogenous prion that also relies on Hsp104 for propagation. In contrast, the findings suggest that aggregation of Aβ42 does not rely on Hsp104 or an endogenous prion i.e. [*PIN*$^+$] in any species tested (**Figure 5.11**).

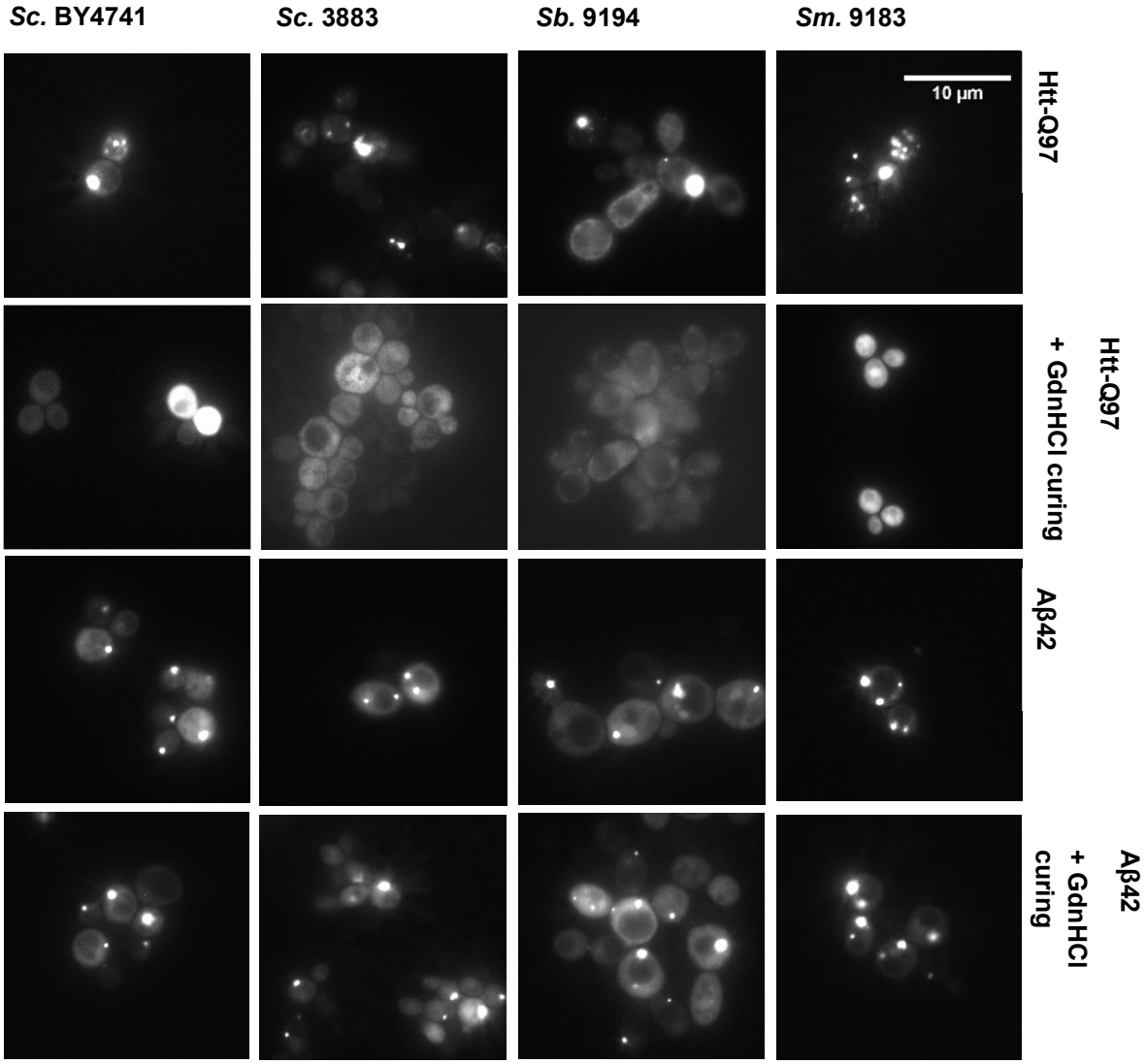

Figure 5.11*:* Visualisation of disease-associated amyloid aggregation in [*prion*$^-$] strains. Images shown were taken by fluorescent microscopy during stationary phase of growth, following 24 hours induction with galactose. Each strain was visualised at a magnification of 100x in three independent biological experiments, and at least 200 cells per condition were visualised. The scale bar represents 10 µm.

5.7.2. Visualisation of disease-associated amyloid aggregation in all strains following GdnHCl curing and continued inhibition of Hsp104

In the previous experiments (**Figure 5.11**) the presence or absence of aggregates was evaluated after the cells had been released from GdnHCl and hence Hsp104 activity would have been restored in these cells. In the next set of experiments, following three rounds of growth on solid medium supplemented with 5 mM millimolar concentrations of GdnHCl, strains were then transferred to a liquid medium containing 5 mM GdnHCl right up until the point of visualisation of aggregates via fluorescence microscopy thereby ensuring cells remained in a prion-free state and Hsp104 remained inactivated.

Visualisation of all strains showed that fluorescent foci indicative of Htt-Q97 aggregation were not observed in any strain (**Figure 5.12**), further supporting the reliance of Htt-Q97 on [*PIN*$^{+}$] and indirectly Hsp104 for aggregation. Following the prolonged inhibition of Hsp104, Aβ42 aggregates remained in all cells of all species (**Figure 5.12**). These findings further suggest that Aβ42 aggregation does not require Hsp104 or an endogenous prion i.e. [*PIN*$^{+}$] in any of the species tested.

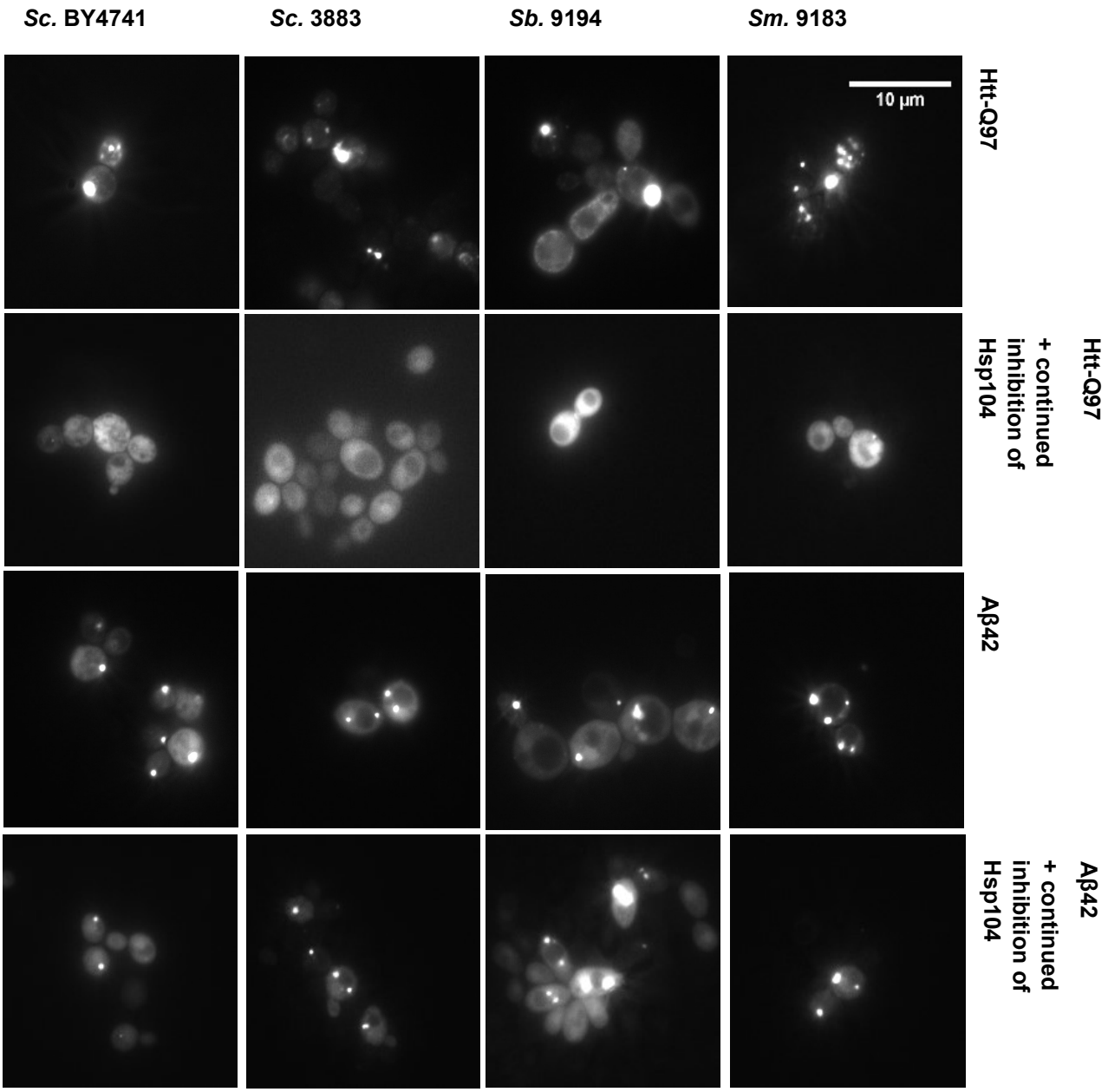

Figure 5.12: Visualisation of disease-associated amyloid aggregation in [*prion*$^{-}$] strains following continued inhibition of Hsp10 4 by GdnHCl. Images shown were taken by fluorescent microscopy during stationary phase of growth, following 24 hours induction with galactose supplemented with GdnHCl. Each strain was visualised at a magnification of 100x in three independent biological experiments, and at least 200 cells were visualised per condition. The scale bar represents 10 µm.

5.7.3. Confirming the requirement of Hsp104 for Htt-Q97 aggregation using *Sc. Δhsp104*

Although millimolar concentrations of GdnHCl are unlikely to affect the ability of either Htt-Q97 or Aβ42 to form aggregates, the requirement for Hsp104 for aggregation is best evaluated by deletion of the non-essential *HSP104* gene. Htt-Q25, Htt-Q97, mNeonGreen and Aβ42 were therefore expressed in the *Sc.* BY4741 *Δhsp104* strain. Visualisation of each disease-associated amyloid forming protein further supported the evidence that Htt-Q97 aggregation relies on Hsp104, whereas aggregation of Aβ42 does not (**Figure 5.13**).

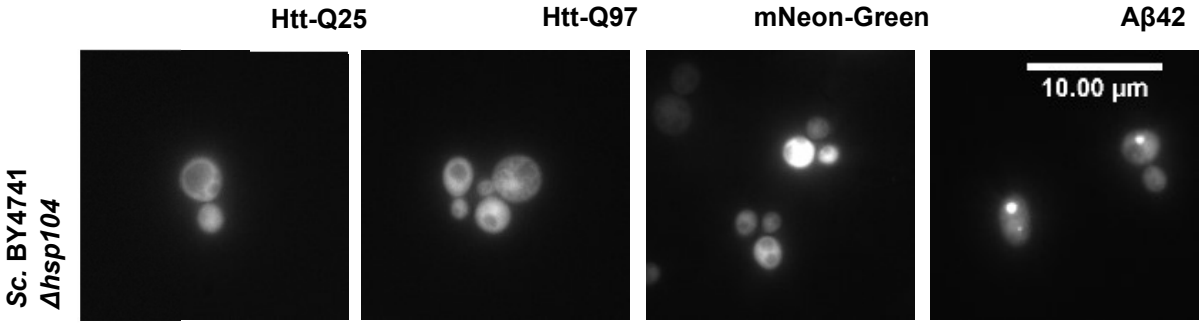

Figure 5.13: Confirming the requirement of Hsp10 4 for Htt-Q97 aggregation using *Sc. Δhsp104*. Images shown were taken by fluorescent microscopy during stationary phase of growth. Each strain was visualised at 100x magnification in three independent biological experiments, and at least 200 cells were visualised per condition. The scale bar represents 10 µm.

5.8. Exploring the impact of Htt-Q46 and Htt-Q72 expression in *S. cerevisiae*

We next investigated whether the length of the polyQ expansion had an impact on aggregates formed in *S. cerevisiae*. *Sc.* BY4741 was transformed with plasmids GAL46Q+ProGFPp416 and GAL72Q+ProGFPp416 and induced for gene expression using galactose. Duennwald et al. (2006) (Duennwald et al., 2006) have reported that Htt-Q46, Htt-Q72 and Htt-Q97 all form aggregates in *S. cerevisiae* compared to the Htt-Q25 control, and an increase in length of the polyQ region also increases toxicity in the cell. Thus, the expression of these proteins in *S.*

cerevisiae provides a model for the length-dependant aggregation and toxicity of polyQ expansions.

As discussed in Section 5.2.1, Htt-Q25 expression resulted in diffuse fluorescence in *Sc.* BY4741, as expected for the control. *Sc.* BY4741 expressing Htt-Q97 displayed 1-2 foci indicative of Htt-Q97 aggregation. [*PIN*$^+$] cells expressing Htt-Q46 and Htt-Q72 also formed fluorescent aggregates. With an increase in polyQ expansion, there was no observed difference in aggregate size or number per cell (**Figure 5.14**). Further analysis must be carried out in other species of *Saccharomyces* to comment on the aggregation status of Htt-Q46 and Htt-72 in these other closely related species. Expression of Htt-Q46 and Htt-Q72 following curing with GdnHCl must also be investigated across all species, in order to comment on the role of [*PIN*$^+$] and Hsp104 in the aggregation of these proteins, and any alternative requirements for maintenance.

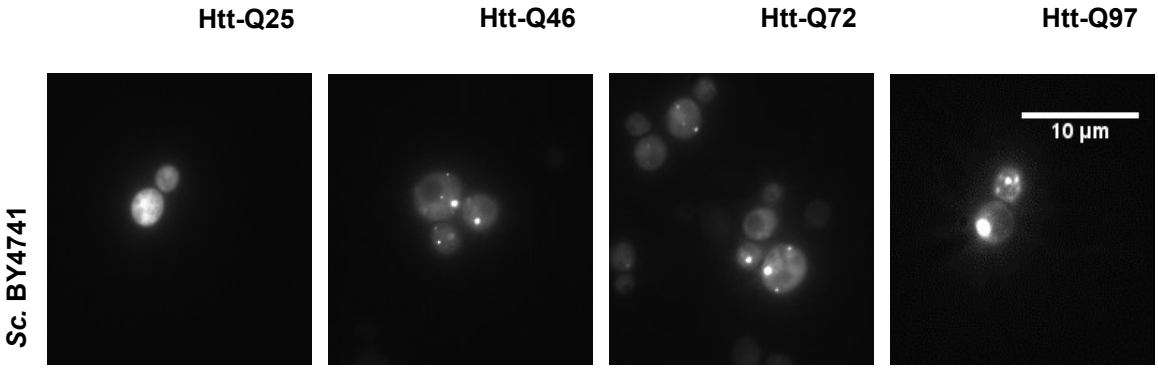

Figure 5.14: Analysis of Htt-Q46 and Htt-Q72 aggregation in *Sc.* BY4741. Images shown were taken by fluorescent microscopy during stationary phase of growth, following 24 hours induction with galactose. Each condition was visualised at a 100x magnification in three independent biological experiments, and at least 200 cells per condition were visualised. The scale bar represents 10µm**.**

5.9. Further analysis of Aβ42 aggregation in *S. cerevisiae* cells lacking a functional Hsp104

Observations suggest that Aβ42 aggregate number increased following treatment with GdnHCl in *Sc.* BY4741. Following Aβ42 expression, cells were put through three independent rounds of GdnHCl curing on solid medium, as well as continued growth in liquid media supplemented with

GdnHCl. Preliminary data involving manual counting of foci suggests that after both conditions, foci per cell increased. Cells with zero foci appeared to remain consistent across conditions, and cells containing either 2 foci or 3+ foci indicative of Aβ42 aggregates increased (**Figure 5.15**). These findings have only been made in one strain of *S. cerevisiae*, so it is not possible to comment on the impact GdnHCl has on Aβ42-associated aggregate number amongst other strains and species.

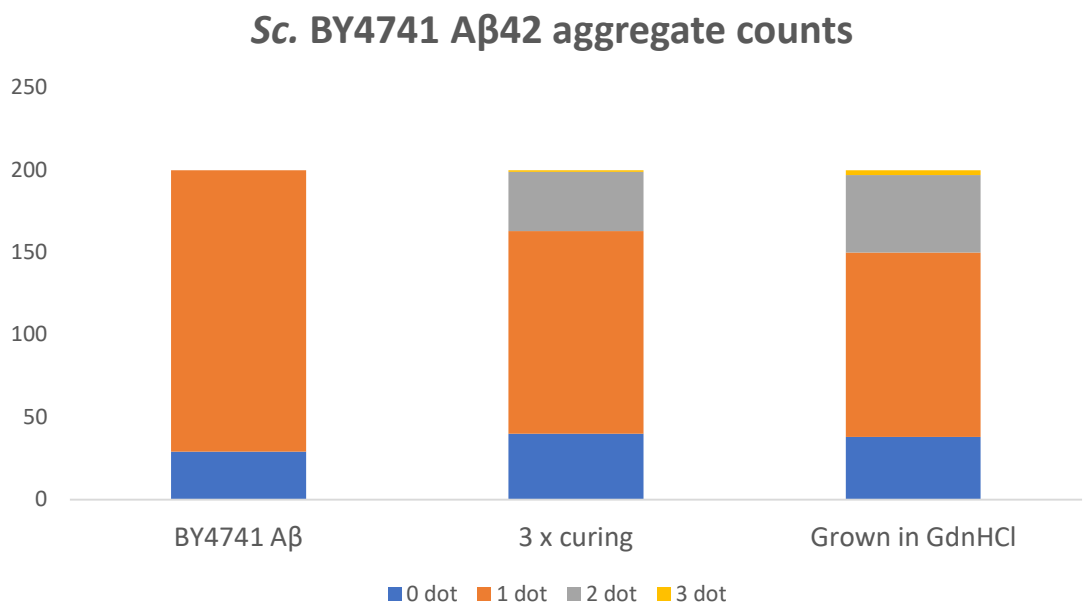

Figure 5.15: Analysis of Aβ42 aggregate number in *S. cerevisiae* cells lacking a functional Hsp104. In each condition, the foci in 200 cells were manually counted and an average was taken across three independent biological experiments, each with two technical replicates.

5.10. Exploring the requirement of Hsp90 for Aβ42 aggregation

Although the results presented above suggest that the aggregation of Aβ42 does not require Hsp104 in any species tested, the possibility remains that Aβ42 may require an alternative chaperone for aggregation and this was further investigated focusing on Hsp90. Hsp90 is an ATPase that associates directly with Hsp104. Hsp90 in *S. cerevisiae* exists as two near identical Hsp90 isoforms, Hsc82 and Hsp82, and only one must be maintained for viability (Newnam et al., 1999). The N-terminal domain of Hsp90 harbours an ATP/ADP binding site that specifically binds radicicol, an antifungal antibiotic originally isolated from *Monosporium bonorden* (Schulte

et al., 1998). We therefore use radicicol as a chemical inhibitor of Hsp90 function in *S. cerevisiae* to investigate the requirement of Hsp90 for Aβ42 aggregation in this species.

At increasing concentrations of radicicol (0-10 μg/ml) foci indicative of Aβ42 aggregates remained in *Sc.* BY4741 (**Figure 5.16**). The concentration of radicicol was increased to 15 μg/ml until cell growth stalled, observed by a lack of overnight growth in liquid culture. These results suggest that aggregation of Aβ42 does not rely on Hsp90 function in *S. cerevisiae*.

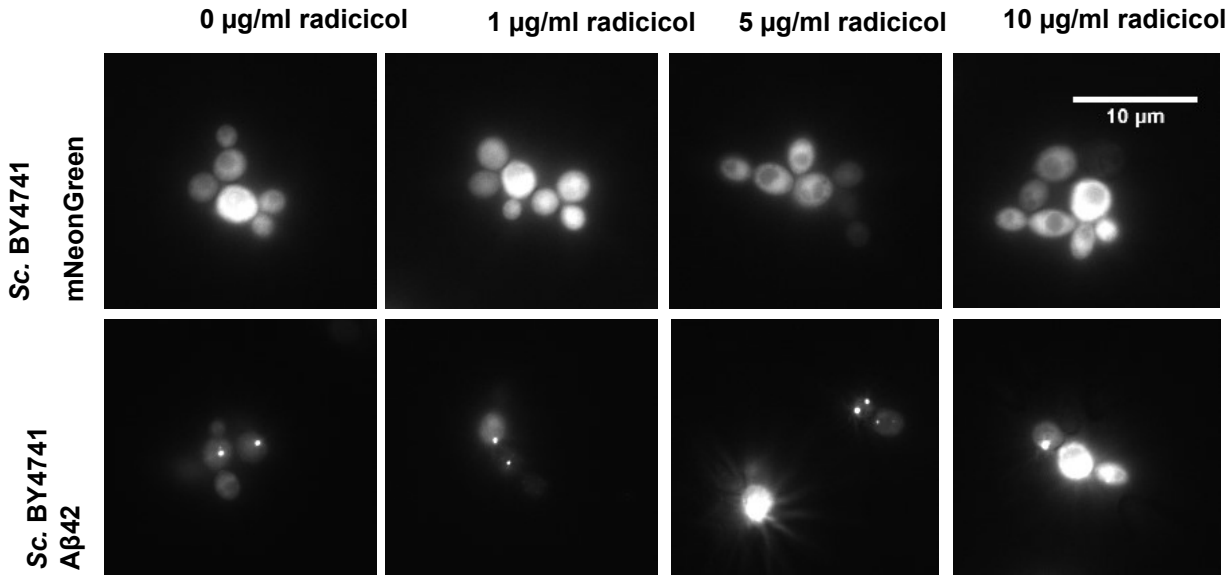

Figure 5.16: Exploring the requirement of Hsp90 for aggregation of Aβ42 by treatment with 0-10 μg/ml radicicol. Images shown were taken by fluorescent microscopy during stationary phase of growth, following 24 hours induction with galactose, then grown in radicicol. Each strain was visualised in three independent biological experiments at a magnification of 100x, and at least 200 cells per condition were visualised. The scale bar represents 10 μm.

Although relatively low concentrations of radicicol are unlikely to affect the ability of Aβ42 to form aggregates, the requirement of Hsp90 for aggregation was further evaluated by deletion of the *HSP82* gene. Control mNeonGreen and Aβ42 were each expressed in the *Sc.* BY4741 *Δhsp82* mutant. Continued appearance of these amyloid-forming proteins further support the evidence that Hsp90 is not required for aggregation of Aβ42 in *S. cerevisiae,* although it must be noted that Hsc82 is still present in the strain under test (**Figure 5.17**).

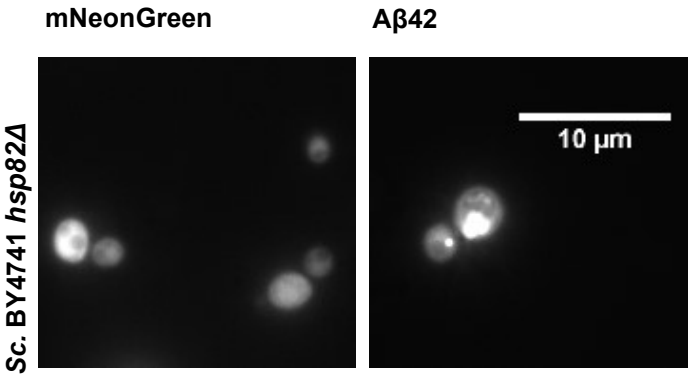

Figure 5.17: Exploring the requirement for Hsp90 in aggregation of Aβ42 using *Sc.* BY4741 *Δhsp82* expressing mNeonGreen and Aβ42. In each condition, at least 200 cells were visualised at 100x magnification in three independent biological experiments. The scale bar represents 10 µm.

5.11. Analysing the role of the *UPF1/2/3* genes in disease-associated amyloid aggregation

The Upf1/2/3 proteins form the nonsense-mediated decay (NMD) complex that recognises premature stop codons in mRNA transcripts at the ribosome, and Upf1p is responsible for shuttling mRNA transcripts containing premature stop codons to P-bodies for degradation (Mendell & Dietz, 2008). Both eRF1 (Sup45) and eRF3 (Sup35) interact with Upf proteins in yeast, and *UPF* gene deletions promote nonsense suppression (Wang et al., 2001).

Sc. BY4741 strains carrying either the *upf1Δ*, *upf2Δ* or *upf3Δ* gene deletions were transformed to express all Htt and Aβ associated amyloid-forming proteins. It was of interest to determine whether these proteins would suppress disease-associated amyloid aggregation, and whether any suppression of aggregation was due to the absence of Upf1p, or due to the function of the NMD complex as a whole.

Preliminary data by Gemma Staniforth in our laboratory showed that deletion of the *UPF1* gene suppressed both overexpression of Rnq1 and polyQ-mediated cytotoxicity (Staniforth, 2011).

Further work by Selena Li in our laboratory showed that deletion of the *UPF3* gene did not suppress the overexpression of Rnq1 and polyQ-mediated toxicity, suggesting that the suppression is not due to the function of the *UPF* genes as a complex, as Upf3 is involved in the core machinery.

5.11.1. Aggregation of Htt-Q97 relies on UPF1p, but aggregation of Aβ42 does not

In contrast to the results observed in *Sc.* BY4741 Δ*upf1*, aggregation of Htt-Q97 was not suppressed by *Δupf2* and *Δupf3* (**Figure 5.18**) These results indicate that Upf1p, but not Upf2p or Upf3p, is essential for the aggregation of Htt-Q97 in *S. cerevisiae*. This would also suggest that it is not the activity of each component of the NMD complex that plays a role in Htt-Q97 aggregation, but Upf1p specifically. It is known that proteins rich in glutamine and asparagine are required for P-body (processing body) assembly, so it could be that P-bodies act as 'seeding factors' for Htt-Q97 aggregation. These results may indicate that a reduction in P-body formation slows the rate of Htt-Q97 aggregate formation, so that the cell is able to maintain Htt-Q97 in a non-toxic state. Alternatively, it may simply be that Htt-Q97 expression levels are reduced in the *upf1*Δ strain. In contrast, **Figure 5.18** shows that Upf1p, Upf2p and Upf3p are not required for Aβ42 aggregation. This further highlights the differing requirements for maintenance of this disease-associated amyloid forming protein compared to Htt-Q97.

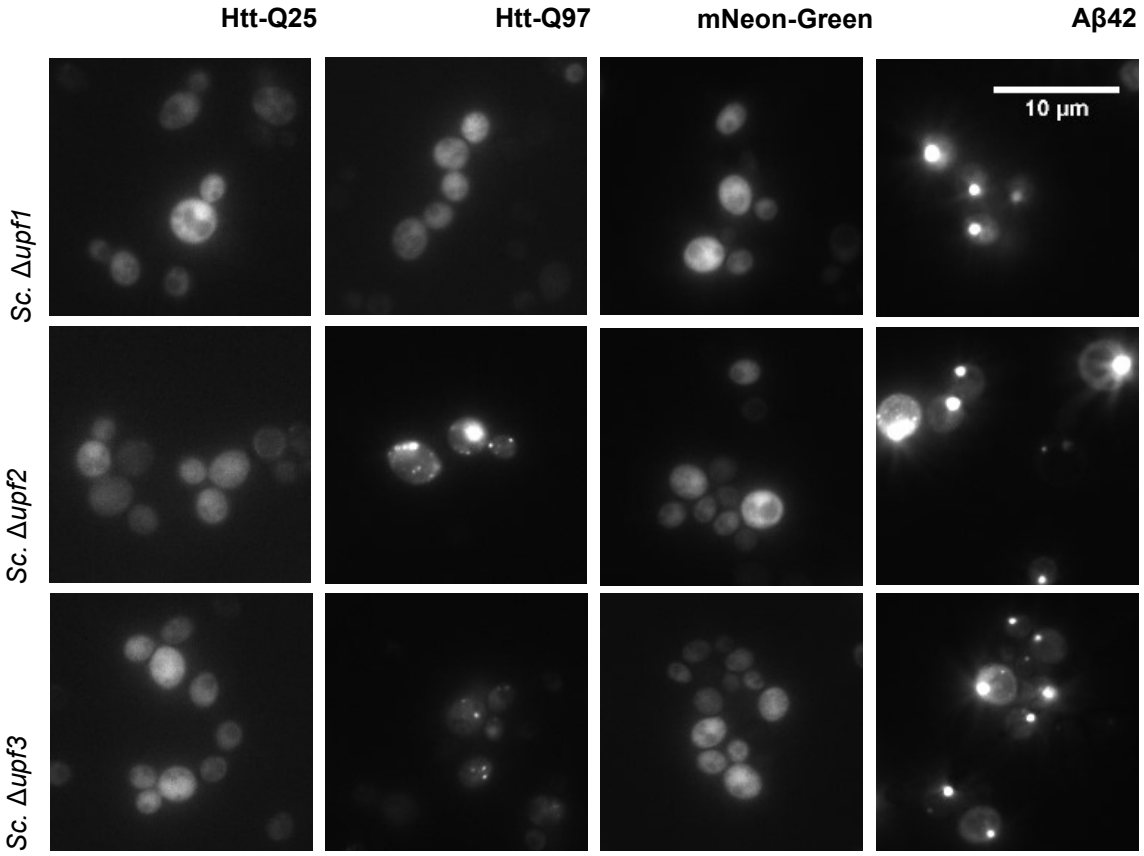

Figure 5.18: Exploring the requirement for UPF1p in disease-associated amyloid aggregation. Images shown were taken by fluorescent microscopy during stationary phase of growth, following 24 hours induction with galactose. Each condition was visualised at a 100x magnification in three independent biological experiments, and at least 200 cells were visualised in each condition. The scale bar represents 10 µm**.**

5.12. Discussion

In summary, both chemical inhibition of Hsp104 and the deletion of the gene show that Htt-Q97 aggregates are unable to form in all species, suggesting a requirement for a [*PIN*$^{+}$]-like prion and Hsp104 in Htt-Q97 aggregation. One explanation for this may be the need for an endogenous prion to act as a 'seeding factor' for polyglutamine expansion proteins, facilitating the formation of toxic amyloid. This is consistent with the idea that cross-seeding may be an important factor in the establishment of protein misfolding in yeast (Von Der Haar et al., 2007). By contrast, the same experiments showed that aggregation of Aβ42 does not require an endogenous prion or Hsp104 in any species tested. Chemical inhibition of Hsp90 using radicicol, and deletion of the *HSP82*

gene further suggested that Aβ42 does not require Hsp90 for aggregation in *S. cerevisiae.* Our findings suggest that although requirements for disease-associated amyloid aggregation differ between proteins, the requirements of each protein appear to be consistent across strains and species.

Similarly, our results indicate that Upf1p, but not Upf2p or Upf3p, is essential for the aggregation of Htt-Q97 in *S. cerevisiae*, but not for the aggregation of Aβ42. This further highlights the differing requirements for maintenance of this disease-associated amyloid forming protein compared to Htt-Q97. One possible reason is that the Upf1 protein may interact with Htt-Q97 directly, thus facilitating the aggregation of Htt-Q97, generating toxic aggregates in a [*PIN*$^+$] background. However, deletion of *upf1* may affect the protein-protein interaction and thus Htt-Q97 may form non-toxic inclusion bodies. Alternatively, such protein-protein interaction may be sequence-specific to *UPF1,* thus highlighting a role for this protein in the formation of toxic oligomers. This sequence may be incapable of interacting with Aβ42, thus explaining the differing requirements for maintenance of the proteins. **Table 5.1** summarises the differing behaviours of the two proteins in *Saccharomyces* species under test.

Table 5.1: A summary of the differing behaviours of the two proteins; Htt-Q97 and Aβ42 in *Saccharomyces* species.

	Htt-Q97	**Aβ42**
[*PIN*$^+$]-dependent	Yes	No
Hsp104-dependent	Yes	No
Upf1-dependent	Yes	No
Growth defect	Yes – in initial growth phases	Yes – in initial growth phases of *Sc*. BY4741 and *Sb*. 9194
Fluorescent foci	Multiple dot	Multiple dot

Chapter 6: Prion mediated phenotypic heterogeneity in *Saccharomyces* species

6. Chapter 6: Prion-mediated phenotypic heterogeneity in *Saccharomyces* species

6.1. Introduction

The phenotype of an organism is not only defined by its genotype; a significant contribution can also be made by several epigenetic factors. Such epigenetic factors are largely based on inherited changes in protein modification and/or structure as typified by the prion. Naturally-occurring prions in yeast promote heritable changes in protein conformation and function that can lead to the evolution of diverse new traits and survival in fluctuating environments (Chakrabortee, Byers, et al., 2016; Halfmann et al., 2012). Although we have learnt much about prions in *Saccharomyces cerevisiae*, we know almost nothing about the existence and/or function of prions in other evolutionarily-related yeast species (Nakayashiki et al., 2005). This chapter presents results exploring whether prions might act as novel epigenetic regulators of phenotype in species of *Saccharomyces.*

Near complete genome sequences and a collection of genetically marked haploid strains of *S. bayanus, S. mikatae* and *S. kudriavzevii* were made available for comparison to the *S. cerevisiae* reference genome (Scannell et al., 2011). Among these lineages, the divergence time relative to the origin of the genus, which coincides with the divergence of *S. bayanus,* was estimated using 106 genes spanning the yeast genome. For each species, relative divergence was expressed as a percentage. Respectively, the divergence of *S. kudriavzevii* and *S. mikatae* was 78% and 53% as old as the lineage, and the divergence of *S. cerevisiae* was 33% as old as the lineage (Scannell et al., 2011) (**Figure 6.1**). Thus, the discovery of well-established *S. cerevisiae* prions or novel prion-like proteins in these species would support the notion that prions are not simply 'laboratory artifacts' that arise through cultivation of fungal cells under conditions far removed from the environment, and instead exist in fungal lineages which diverged many years ago.

The ability to detect gene orthologues in the *Saccharomyces* lineages has allowed the identification of species-specific gains and losses at the genetic level, thus providing a means to review how

genetic networks have developed during the evolution of the genome. The conservation of *S. cerevisiae* genes that are essential for prion-forming proteins within these species would indicate the evolutionarily conservation of prion-like conformational switches and may imply the significance of such switches in a variety of common biological processes. Genetic losses were categorised into a) lineage-restricted losses i.e. lost in one or two species; b) widespread losses i.e. absent from more than two species; and c) duplicate gene losses i.e. losses of one paralogue of a duplicate gene pair descended from the whole-genome duplication. Genetic gains are categorised as genes that are present in one or more of the *Saccharomyces* species, but not in the *Saccharomyces* ancestor (Scannell et al., 2011). Such clear genetic diversity between these species may be an indication of naturally-occurring epigenetic diversity.

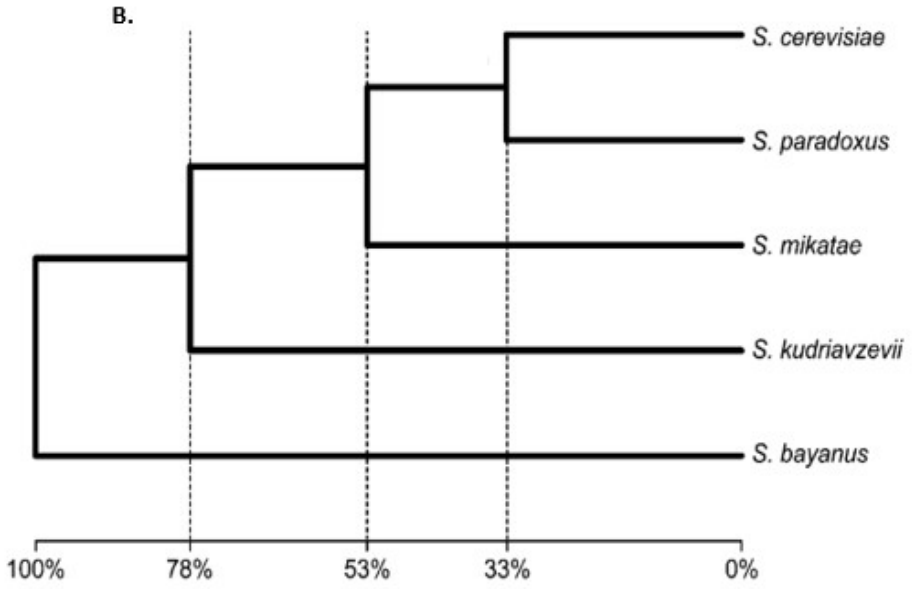

Figure 6.1: The phylogenetic tree of *Saccharomyces* species. The species divergence in percentage points relative to the origin of the genus, which coincides with the divergence of S. bayanus (taken from Scannell et al., 2011).

This chapter also describes a preliminary study on prion-related phenotypes using non-domesticated wild strains of *S. cerevisiae* that have been isolated from remote parts of the planet (Wang et al., 2012). The origin of such strains ranged from fruit, fruit trees and orchard soil in secondary forests to rotten wood and tree bark in primeval forests in Northern and

Southern China. Duan et al., (2018) showed that the genetic diversity of *S. cerevisiae* is contributed by the highly structured wild population under study, with greatly diverged lineages in China. Interestingly, neither the geographic nor ecological factors can explain the structure of the wild population. For example, wild isolates from the same locations may belong to greatly diverged lineages, or a single lineage has been shown to contain isolates from geographically separate regions (Duan et al., 2018). Further studies should focus on both genetic and proteomic profiling of these non-domesticated wild strains, with a particular focus on well-established prion-forming proteins.

Analysis in such non-domesticated wild strains of the same species allows us to account for the pan-genome; the concept of 'accessory' non-conserved genes across strains of the same species which contribute to intra-specific variability (McCarthy & Fitzpatrick, 2019). Accessory genes which differ between strains have been shown to make up approximately 15% of the pan-genome in *S. cerevisiae*. This chapter outlines the analysis of prion-mediated phenotypic heterogeneity in wild strains of yeast, as well as investigation into well-established yeast prions such as [*PIN*$^+$] and [*GAR*$^+$] in these strains, which reveals distinct individual differences between strains.

6.2. The generation of [*prion*$^-$] derivatives of *Saccharomyces* species

Guanidine hydrochloride (GdnHCl) is a chaotropic inhibitor of the chaperone activity of Hsp104, through a direct target of amino acid residue 184, inhibiting the ATPase activity of Hsp104 (Jung et al., 2002). This ATPase activity is necessary for the propagation of endogenous prion aggregates as Hsp104 actively fragments Sup35 prion fibrils, creating new propagons, thus increasing the availability of 'recruiting' ends (Chernoff et al., 1995; Glover et al., 1997). Exposure to millimolar concentrations of GdnHCl therefore generates prion-free [*prion*$^-$] cells (Tuite, Mundy and Cox, 1981; Ferreira et al., 2001).

Exposure to GdnHCl by addition to yeast growth media is a commonly used method for prion "curing" in *S. cerevisiae,* converting a [*PRION*$^{+}$] cell to a [*prion*$^{-}$] state (Ness et al., 2002). Cells are grown on solid medium supplemented with 3 – 5 mM GdnHCl for three independent rounds, to ensure continued inhibition of Hsp104, and to limit the possibility of GdnHCl-induced *petite* mutations which could impact the level of phenotypic heterogeneity. Naturally-occurring prions are not established in all species of *Saccharomyces,* so the conversion from [*PRION*$^{+}$] to [*prion*$^{-}$] is assumed in all strains. Additionally, any naturally-occurring prions in these strains may not be dependent on Hsp104 for propagation and therefore may not be eliminated by GdnHCl. Cured strains i.e. those that have undergone treatment with GdnHCl, and their non-cured derivatives are indicated throughout this chapter by a '-' or '+' respectively e.g. *Sk.* 9185^{-} and *Sk.* 9185^{+}.

As described in Chapter 1, Section 1.6.1, conformational conversion of the well-established prion protein Sup35p reduces the functional pool of Sup35p available for translation termination, resulting in the nonsense suppressor phenotype associated with the presence of [*PSI*$^{+}$] (Wickner, 1994). In the prion form, such proteins catalyse the conversion of homologous proteins in the [*prion*$^{-}$] state to the [*PRION*$^{+}$] state, allowing the protein conversion event to become conformationally dominant within the strain. In the *S. cerevisiae* strain 74D-694 (detailed in Materials and Methods) the *ADE1* gene required for adenine synthesis is represented by the *ade1-14* nonsense allele. Thus, [*psi*$^{-}$] cells are Ade^{-} due to termination of Ade1 synthesis at a premature UGA stop codon, causing an accumulation of a red intermediate of the adenine synthesis pathway, represented by red colony growth on solid medium (Patino et al., 1996). In [*PSI*$^{+}$] cells, the premature stop codon of *ade1-14* is suppressed, forming Ade^{+}, white-coloured colonies. In all rounds of GdnHCl-mediated curing described below, *Sc.* 74D-694 was used as a control strain, as a white to red colour change was indicative of the successful conversion of a [*PRION*$^{+}$] state to [*prion*$^{-}$], and confirmed the likelihood of the same event in all species of *Saccharomyces* (**Figure 6.2**).

To establish the optimal concentration of GdnHCl required for prion curing in all species of *Saccharomyces*, all strains were grown on glucose-rich media supplemented with varying concentrations of GdnHCl up to 10 mM for three independent rounds. *S. mikatae* showed a reduced sensitivity to GdnHCl, visualised by successful growth with several dilution series on media supplemented with 10 mM GdnHCl (**Figure 6.2**). This indicates GdnHCl-resistance relative to other species. In contrast, *S. kudriavzevii* was particularly sensitive to GdnHCl, with limited growth at 2.5 mM GdnHCl (**Figure 6.2**). This particular species is cryotolerant with an optimal growth temperature of ~24 °C and was thus incubated at a lower temperature than the other *Saccharomyces* species. The increased sensitivity of *S. kudriavzevii* to GdnHCl may be indicative of a more efficient uptake of this chemical, relative to *S. mikatae.* Furthermore, it is not clear whether visible growth impairment is suggestive of cytostatic cells or cytocidal cells; whether unprogrammed or natural.

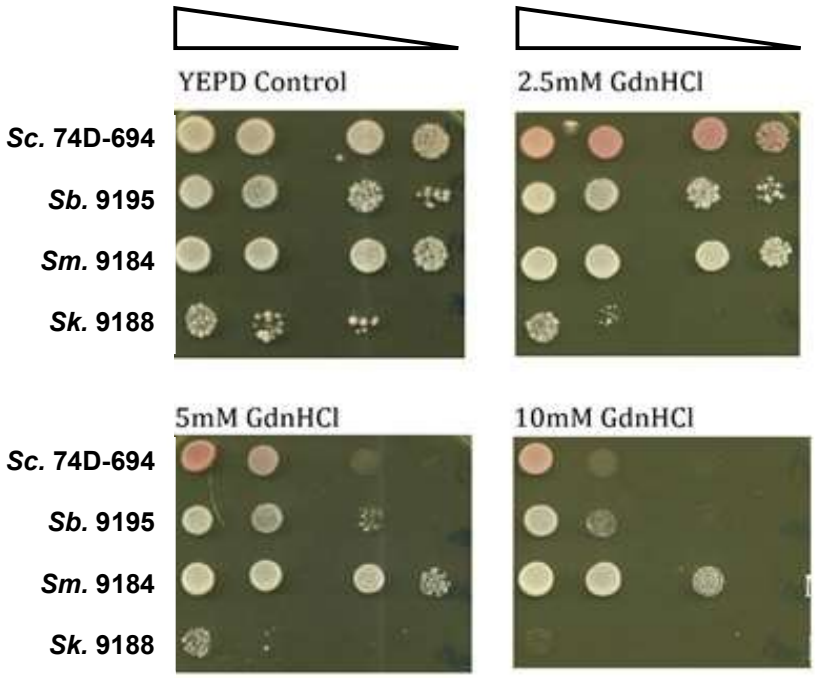

Figure 6.2: The effect of different concentrations of guanidine hydrochloride of the growth of *Saccharomyces* species. To establish the optimal concentration of GdnHCl required for prion curing in *Saccharomyces* species, all strains were grown on glucose-rich media supplemented with varying concentrations of GdnHCl for 3 days, for three independent rounds. Data shown represents one round of GdnHCl curing. Sc 74D-694 was used as a control. Each step indicates a 1/10 dilution within the dilution series.

The growth rate of all strains was analysed following three independent rounds of GdnHCl-mediated curing on solid medium, followed by continued growth in GdnHCl supplemented liquid medium. The growth profiles of [*PRION*$^{+}$] and [*prion*$^{-}$] derivatives of each species were overlaid to investigate the direct impact of GdnHCl on growth. The results indicated that the growth profiles of *S. bayanus* and *S. mikatae* are not directly impacted by GdnHCl, and a final OD_{600} after 28 hours above 2.5 confirmed the reduced sensitivity of *S. mikatae* to GdnHCl (**Figure 6.3**). By contrast, both the results of the growth experiment (**Figure 6.3**), and growth on solid medium (**Figure 6.2**) showed the detrimental impact of GdnHCl on the growth of *S. kudriavzevii* (**Figure 6.3**). Growth analysis was carried out at 24 ^{o}C to eliminate any growth defects caused by temperature, but in the [*prion*$^{-}$] state the growth of *S. kudriavzevii* was still impaired. This was particularly apparent by a significant reduction in the final OD_{600} of the cell population.

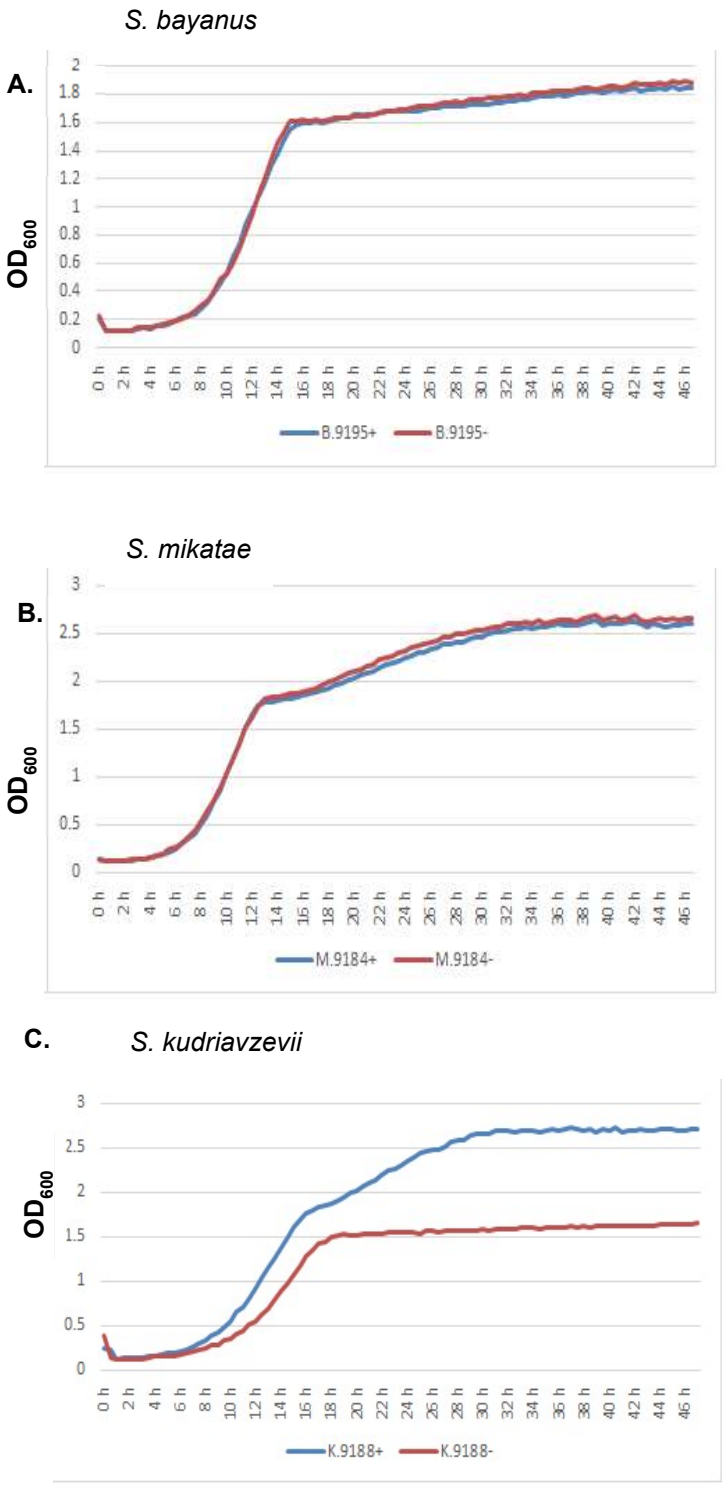

Figure 6.3: Growth profiles of [*PRION*$^{+}$] and [*prion*$^{-}$] derivates of each *Saccharomyces* species. Panel A. The growth profile of *S. bayanus*. **Panel B.** The growth profile of *S. mikatae*. **Panel C**. The growth profile of *S. kudriavzevii.* The growth profiles of *S. bayanus* and *S. mikatae* reveal no difference in growth profile when compared to the GdnHCl-cured derivative. The data reflects the average of three biological replicates, each with two technical repeats.

6.3. The impact of GdnHCl on prion-mediated phenotypic heterogeneity

To identify the level of phenotypic heterogeneity between [*prion*$^{-}$] and [*PRION*$^{+}$] strains of *Saccharomyces* species, the impact of osmotic stress on growth and the level of sensitivity to antifungal agent fluconazole were analysed. Observed growth defects in such fluctuating environments may be indicative of the presence of endogenous prions in these species. Prior to carrying out these phenotypic-based experiments, all species were grown on media containing glycerol as the sole carbon source, in order to eliminate *petite* mutants generated by GdnHCl and allow the selection of respiratory-efficient *grande* cells (see Chapter 4). It must also be noted that GdnHCl-induced *petite* mutants may still arise during these experimental procedures, thus impacting the growth of these strains.

6.3.1. Endogenous prions may provide a growth advantage to *Saccharomyces* species in conditions of hyper-osmolarity

In order to identify species of *Saccharomyces* with the ability to grow under conditions of high osmotic stress, both [*PRION*$^{+}$] and [*prion*$^{-}$] derivatives were grown on complete medium supplemented with varying concentrations of sodium chloride (NaCl) (0.4 - 0.8 M). Under conditions of hyper-osmolarity, yeast cells activate a stress pathway in which Msn2 and Msn4 bind to the stress-response elements (STREs) of stress-response genes, in turn activating their transcription (Li & Kowal, 2012). Deletion of *MSN2* leads to an increase in the frequency of [*PSI*$^{+}$] formation, indicating the involvement of stress-response proteins in prion formation (Li & Kowal, 2012). Although the exact role of endogenous prions in osmotic stress responses remains unclear, it may be that the endogenous [*PRION*$^{+}$] state is advantageous to cell survival during levels of high osmolarity.

Some [*PSI*$^{+}$]-associated phenotypes may be generated as a result of inactivating stop codon mutation (ISCMs) readthrough. Approximately 26,000 single nucleotide polymorphisms (SNPs) were identified in *S. cerevisiae* strain 74D-694 compared to reference strain S288C, some of

which cause potential ICSMs. These ICSMs were identified in genes with involvement in a variety of cellular processes, including oxidative stress response. Specifically, the presence of an ISCM in the *MSN4* gene could have major implications for 74D-694's ability to deal with high levels of NaCl, and may help to explain previously identified complex phenotypes associated with the presence of [*PSI*$^{+}$] (An et al., 2016).

In the presence of increasing concentrations of NaCl (0.4 - 0.8 M), a decrease in growth of *S. kudriavzevii* in a [*prion*$^{-}$] state was observed, compared to its wild type derivative (**Figure 6.4**). This may indicate the presence of an endogenous prion in this species, which is advantageous to the cell in conditions of hyper-osmolarity.

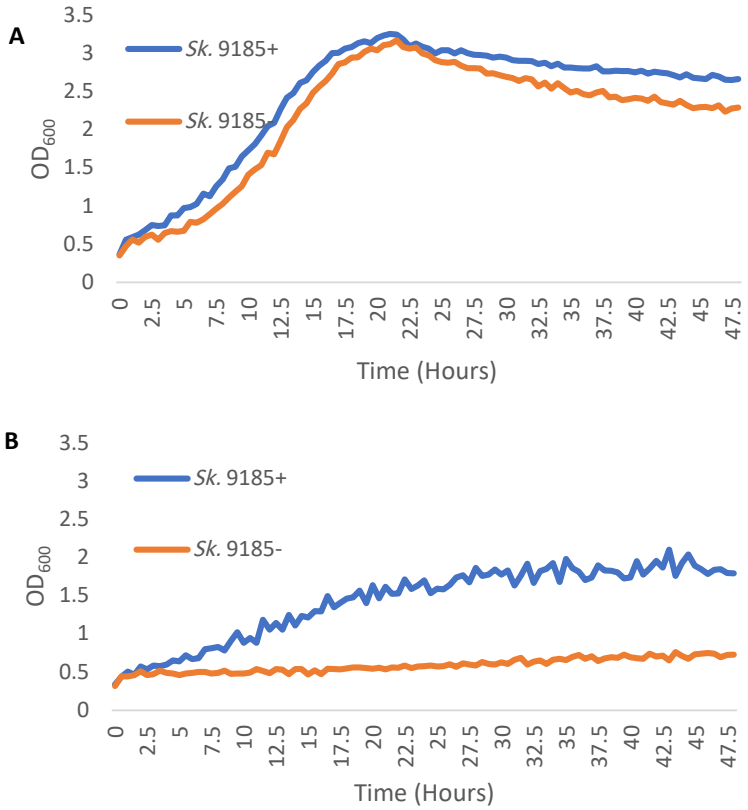

Figure 6.4: Growth profiles of Sk. 9185^{+} and Sk. 9185^{-} in YEPD + 0.4 M NaCl, following three rounds of GdnHCl-mediated curing on solid medium. Panel A) The growth profile of *S. kudriavzevii* in a [*PRION*$^{+}$] and [*prion*$^{-}$] state in glucose-containing medium. **Panel B**) The growth profile of *S. kudriavzevii* in a [*PRION*$^{+}$] and [*prion*$^{-}$] state in YEPD + 0.4 M NaCl. The data reflects the average of three biological repeats, each with two technical replicates.

6.3.2. Endogenous prions impact the survival of *Saccharomyces* species in the presence of fluconazole

Both [*PRION*$^{+}$] and [*prion*$^{-}$] derivatives of species were grown on complete medium supplemented with varying concentrations (1 – 5µg) of the ergosterol synthesis inhibitor fluconazole. Interestingly, prions have been shown to encode a natural resistance to fluconazole in laboratory strains of *S. cerevisiae.* [*MOD*$^{+}$] yeast contain a higher level of ergosterol than [*mod*$^{-}$] yeast, and an increased resistance to fluconazole (Suzuki & Tanaka, 2013). Fluconazole also caused selective pressure on [*mod*$^{-}$] yeast, which in turn increased the *de novo* appearance of [*MOD*$^{+}$]. This indicates the fitness advantage gained during Mod5p prion conversion, providing an increased chance of cell survival when faced with environmental stress (Suzuki & Tanaka, 2013). In addition, removal of fluconazole showed the loss of [*MOD*$^{+}$] over time, suggesting such prion conversion plays a critical role in fast cellular adaption to less advantageous environments (Suzuki & Tanaka, 2013). Bioinformatic studies should focus on identifying (a) the presence of *MOD5* in other *Saccharomyces* species and (b) the % identity and % similarity if this gene is present. Endogenous prions in non-laboratory strains of *S. cerevisiae* also provided cells with increased survival in the presence of fluconazole. One confirmed [*PSI*$^{+}$] wine strain was resistant to this antifungal agent (Byers & Jarosz, 2014), as was strain *Sc.* UCD#824 isolated from white wine (Halfmann et al., 2012). All observed phenotypes were prion dependant and eliminated by GdnHCl-mediated prion curing (Byers and Jarosz, 2014; Halfmann et al., 2012). In contrast to laboratory strains of *S. cerevisiae,* most of the observed prion-mediated phenotypes of wild strains were adaptive as opposed to neutral or detrimental to the cell (McGlinchey et al., 2011).

In contrast to the findings with *S. cerevisiae,* the non-cured [*PRION*$^{+}$] strain of *S. bayanus* showed a clear growth disadvantage in the presence of fluconazole, when compared to the cured [*prion*] derivative (**Figure 6.5**). A difference in growth profile may be indicative of the presence of an endogenous prion within this species that is detrimental to the cell in the presence of fluconazole, however further analyses into (a) the confirmed presence of an endogenous prion within this species, and (b) the impact of such a prion on the host must be carried out.

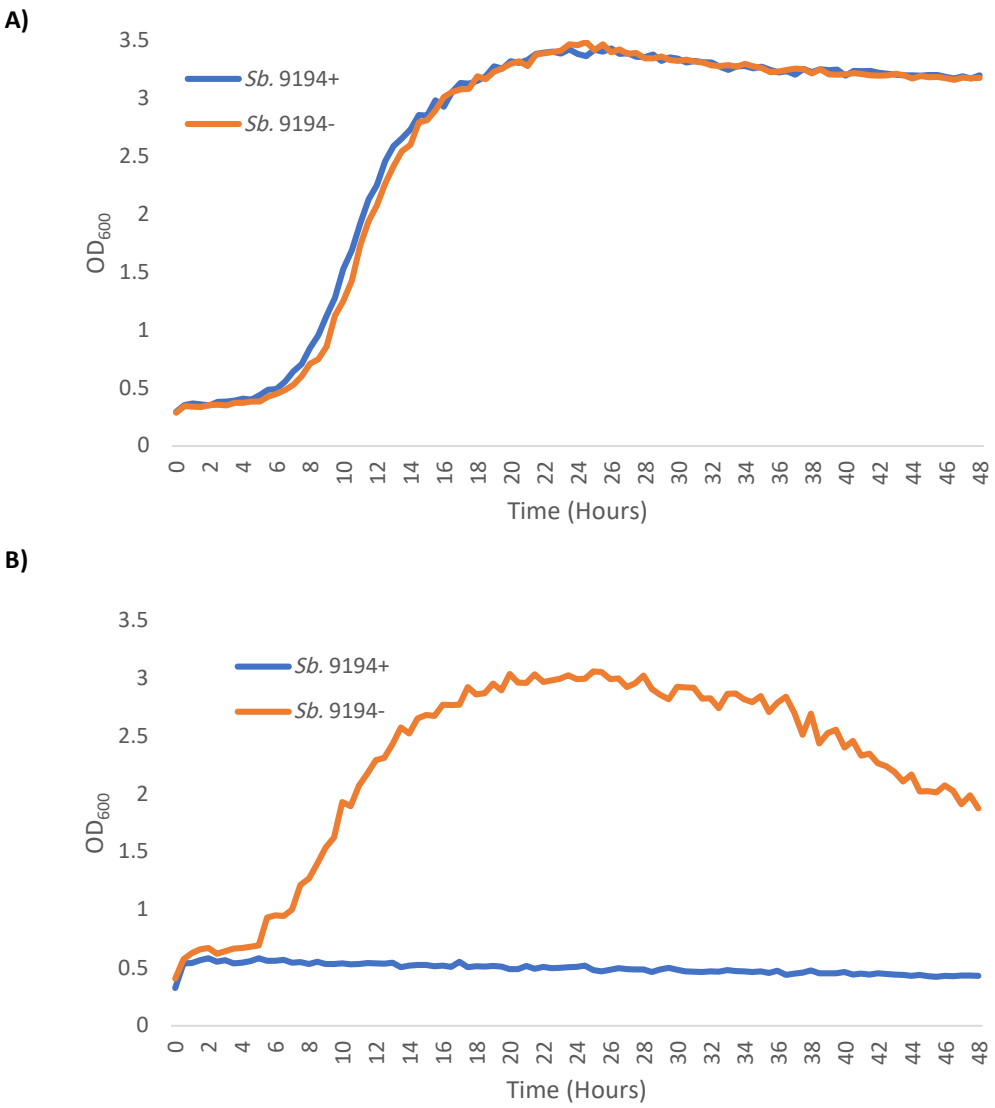

Figure 6.5: Growth profiles of *S. bayanus* in YEPD + fluconazole following three rounds of GdnHCl-mediated curing on solid medium. Panel A) The growth profile of *S. bayanus* in a [*PRION*$^{+}$] and [*prion*$^{-}$] state in glucose-containing medium. **Panel B)** The growth profile of *S. bayanus* in a [*PRION*$^{+}$] and [*prion*$^{-}$] state in YEPD + 1 µg fluconazole. The data reflects the average of three biological analyses**,** each with two technical replicates.

6.4. Preliminary studies with non-domesticated wild strains of *Saccharomyces cerevisiae*

As previously mentioned in Section 6, preliminary studies with wild strains of *S. cerevisiae* isolated from remote parts of the planet were also carried out, focussing on identifying prion-

mediated phenotypic heterogeneity in these strains. As with all species of *Saccharomyces,* exposure to GdnHCl by addition to yeast growth media was used to convert all wild strains of *S. cerevisiae* from a [*PRION*$^{+}$] cell to a [*prion*$^{-}$] state. Prior to the following experimental procedures, GdnHCl-induced *petite* mutants were not eliminated by growth on glycerol and therefore may be present in the analyses. Such mutants may impact the growth profiles of these strains, and further analyses into the frequency of both spontaneous and GdnHCl-induced *petite* mutants are required. Strains were grown on a solid rich (YEPD) medium supplemented with 5 mM GdnHCl for three consecutive rounds of sub-culturing. As with species of *Saccharomyces,* naturally-occurring prions have not yet been described in these non-domesticated wild strains of *S. cerevisiae.*

In an attempt to establish whether phenotypic heterogeneity between [*prion*$^{-}$] and [*PRION*$^{+}$] strains of wild yeast occurs; the levels of osmotic stress, antibiotic sensitivity, and the ability of the yeast to grow on alternative carbon sources were analysed. Observed differences in survival between strains during conditions of hyperosmolarity, exposure to antifungal agents, and a natural ability to utilise alternative sources of carbon may be indicative of the presence of endogenous prions in these strains.

6.4.1. Endogenous prions may be detrimental to wild strains of *S. cerevisiae* in conditions of hyper-osmolarity

In order to identify wild *S. cerevisiae* strains with the ability to grow under conditions of high osmotic stress, both [*PRION*$^{+}$] and [*prion*$^{-}$] derivatives were also grown on complete medium supplemented with varying concentrations of NaCl (0.4 - 0.8 M). In contrast with the findings by Li and Kowal (2012), Newnam, Birchmore and Chernoff (2011) suggested that prolonged incubation in the presence of NaCl for at least 24 hours caused an increase in [*PSI*$^{+}$] loss, which could be caused by an increased induction of Hsp104 (Newnam et al., 2011).

An increase in cell survival in a [*prion*$^{-}$] state was observed in the non-domesticated wild strain of *S. cerevisiae* HN11, isolated from a primeval forest in China (Wang et al., 2012). In this particular strain, increased cell growth on solid medium and a statistically significant improved growth profile was apparent in increasing concentrations of NaCl, following rounds of GdnHCl-mediated prion curing (**Figure 6.6**). This would suggest the presence of an endogenous prion in this strain, which is detrimental to the cell in conditions of hyper-osmolarity. Eleven other non-domesticated wild strains were tested for their levels of growth in conditions of hyper-osmolarity, but no other significant differences in the growth profile of [*PRION*$^{+}$] and [*prion*$^{-}$] derivatives were observed.

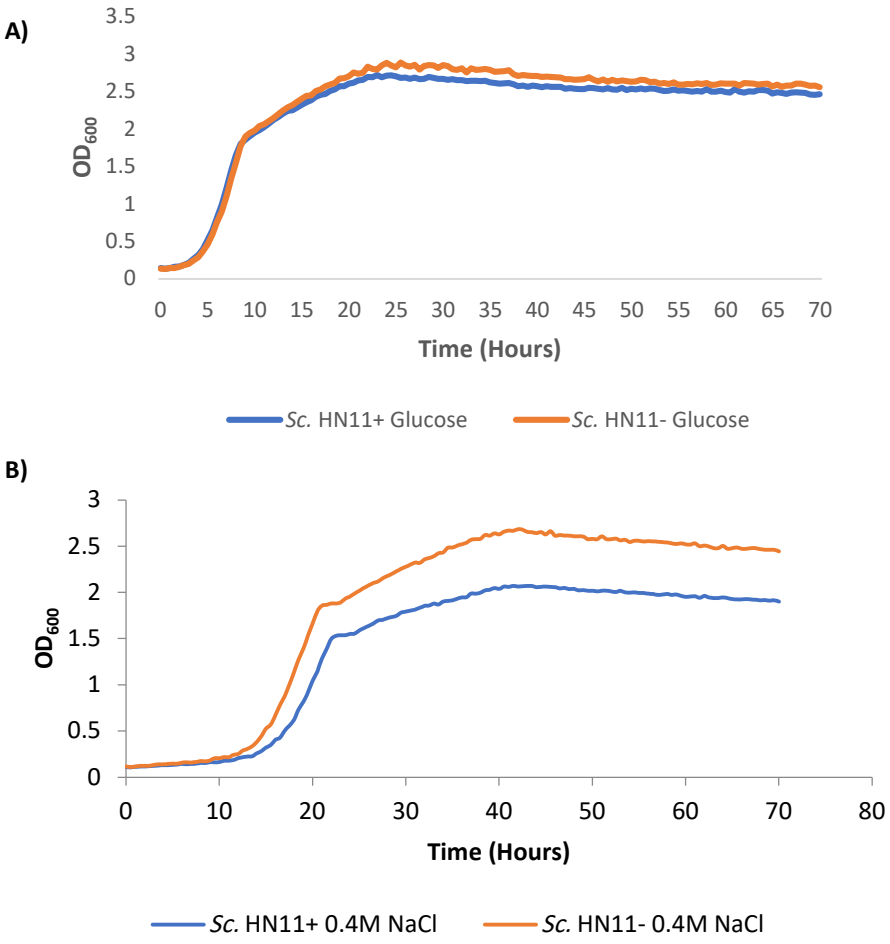

Figure 6.6: Growth profiles of Sc. HN11^{+} and Sc. HN11^{-} in YEPD + 0 .4M NaCl, following three rounds of GdnHCl-mediated curing on solid medium. Panel A) The growth profile of HN11 derivatives in glucose-containing medium. **Panel B)** The growth profile of *Sc*. HN11^{-} reveals a statistically significant increase in growth, when compared to the growth rate of its non-cured derivative. The data reflects the average of three biological repeats, each with two technical replicates.

6.4.2. Naturally-occurring prions affect the ability of wild strains of *S. cerevisiae* to utilise alternate carbon sources to glucose

Following GdnHCl-mediated prion curing, twelve strains of wild yeast were grown on galactose, fructose and maltose in order to distinguish any differences between [*PRION*$^{+}$] and [*prion*$^{-}$] states in their ability to utilise alternative fermentable carbon sources. Differences in the growth of [*PSI*$^{+}$] and [*psi*$^{-}$] *S. cerevisiae* cells originating from 7 different genetic backgrounds were observed, in the presence of dextrose, galactose and lactate (True & Lindquist, 2000). In each genetic background, fresh stable [*psi*$^{-}$] cells were generated using GdnHCl, to ensure that the observed phenotypic differences were due to the direct effects of the prion, rather than secondary genetic changes that may have occurred during long-term culture. In the presence of such fermentable carbon sources, [*PSI*$^{+}$] cells in several *S. cerevisiae* strains displayed a positive difference in growth when compared to their GdnHCl-cured derivative (True & Lindquist, 2000).

In support of these findings, non-domesticated wild strain *S. cerevisiae* SX2 isolated from a primeval forest in China showed impaired growth across several dilutions on solid fructose-containing medium following GdnHCl-mediated prion curing. This was also the case for *S. cerevisiae* HN15, also isolated from the Chinese primeval forest, which showed impaired growth on galactose when in the [*prion*$^{-}$] state. These findings are indicative of an endogenous prion in these two strains, which provides the cell with a mechanism of increased likelihood of cell survival in fluctuating environments. However, all conditions tested were only carried out on solid medium and scored for visual growth defects, and further analyses detailing the growth profile of each strain over time are required.

In contrast, *S. cerevisiae* strain BJ14 displayed an increase in the level of growth in galactose, fructose and maltose when in the cured [*prion*$^{-}$] state. This was also the case for *S. cerevisiae Sc.* HN11^{-} in the presence of galactose. The increased level of growth in these strains following GdnHCl-mediated prion curing may be due to an endogenous prion, which acts as a burden to cells and exhibits a measurable demand on cell function and survival. Interestingly,

the yeast [*SWI*$^{+}$] prion manifests as reduced growth on carbon sources other than glucose (Crow & Li, 2011). Specifically, poor growth of [*SWI*$^{+}$] *S. cerevisiae* is observed in medium containing raffinose, galactose, and glycerol, and mild growth defects were observed in medium containing sucrose (Du et al., 2008). Interestingly, growth of [*SWI*$^{+}$] cells improved on alternative carbon sources following 5 mM GdnHCl curing (Du et al., 2008). The phenotype of [*SWI*$^{+}$] cells displayed in such experiments may suggest the presence of [*SWI*$^{+}$] in these non-domesticated wild strains.

6.4.3. Endogenous prions may impact the survival of wild strains of *S. cerevisiae* in the presence of various antifungal agents

In order to identify strains of wild yeast where the ability to grow in the presence of various antifungal agents may be prion dependent, both [*PRION*$^{+}$] and [*prion*$^{-}$] derivatives were grown on complete medium supplemented with varying concentrations of protein synthesis inhibitors sordarin and cycloheximide, and fluconazole; an inhibitor of ergosterol biosynthesis. In certain conditions, the presence of an endogenous prion may be harmful to a cell's survival, as demonstrated by Radchenko et al., (2011). Their study suggests that when compared to the [*ISP*$^{+}$] strain of *S. cerevisiae,* its [*isp*$^{-}$] derivative displayed a higher level of resistance to the actions of cycloheximide (Radchenko et al., 2011).

Our investigations produced results in support of the findings by Radchenko et al*.,* (2011) with *Sc.* wild strain SX6 maintaining a higher level of cycloheximide resistance following GdnHCl-mediated prion curing, compared to its non-cured derivative. On solid medium, the zones of killing surrounding cycloheximide-infiltrated discs were significantly larger for *Sc.* SX6^{+} compared with the cured strain. This level of cycloheximide sensitivity was confirmed in liquid culture, indicating the detrimental effects of an endogenous prion in this strain for survival under such conditions (**Figure 6.7**).

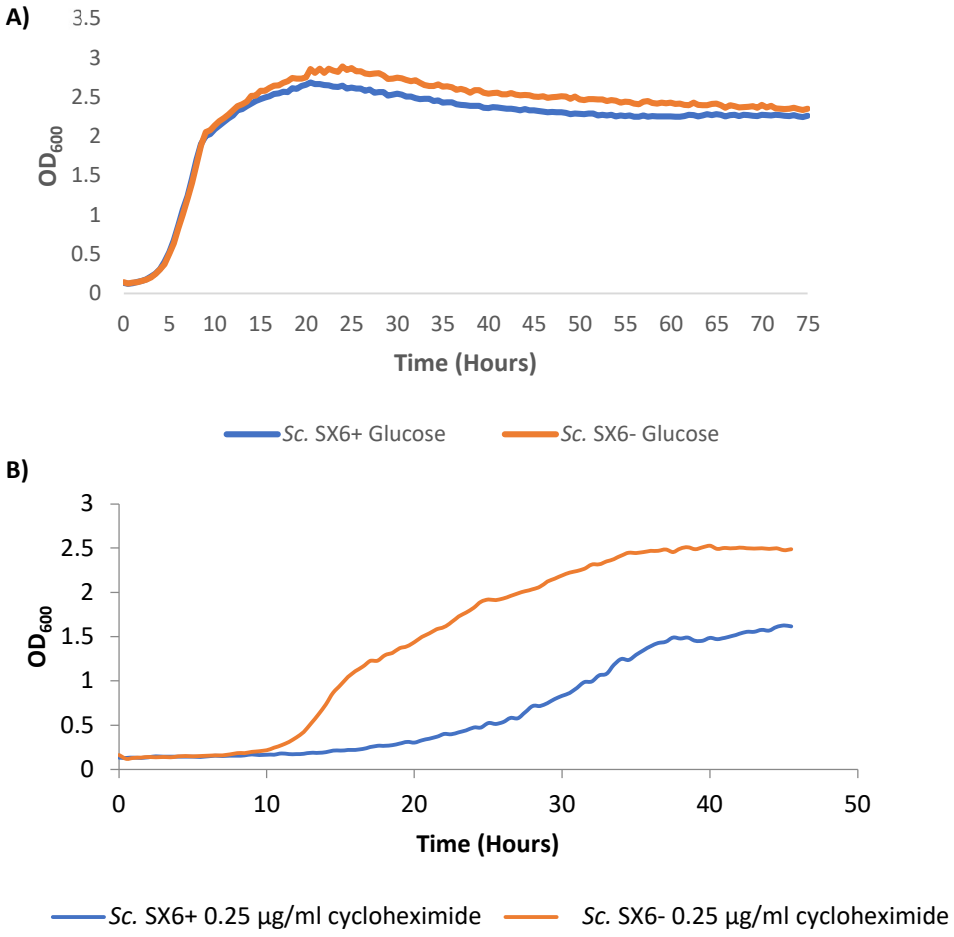

Figure 6.7: Growth profiles of *Sc.* SX6^{+} and *Sc.* SX6^{-} in YEPD + 0.25 µg/ml cycloheximide, following three rounds of GdnHCl-mediated curing on solid medium. Panel A) The growth profile of *Sc.* SX6 derivatives in glucose. **Panel B)** The growth profile of *Sc.* SX6^{-} reveals a statistically significant increase in growth, when compared to the growth rate of its non-cured derivate. The data reflects the average of three biological repeats, each with two technical replicates.

Interestingly, further investigations of the effects of cycloheximide specifically on [*PSI*$^{+}$] strains of *S. cerevisiae* revealed no significant loss of the prion, but instead an increase in bright, sharp foci indicative of Sup35-GFP seeds (Bailleul-Winslett et al., 2000). One explanation is that the inhibition of protein synthesis by cycloheximide prevents accumulation of both newly synthesised Sup35p and Sup35-GFP, thus leading to concentration of most of the Sup35-GFP in the aggregated structures (Bailleul-Winslett et al., 2000).

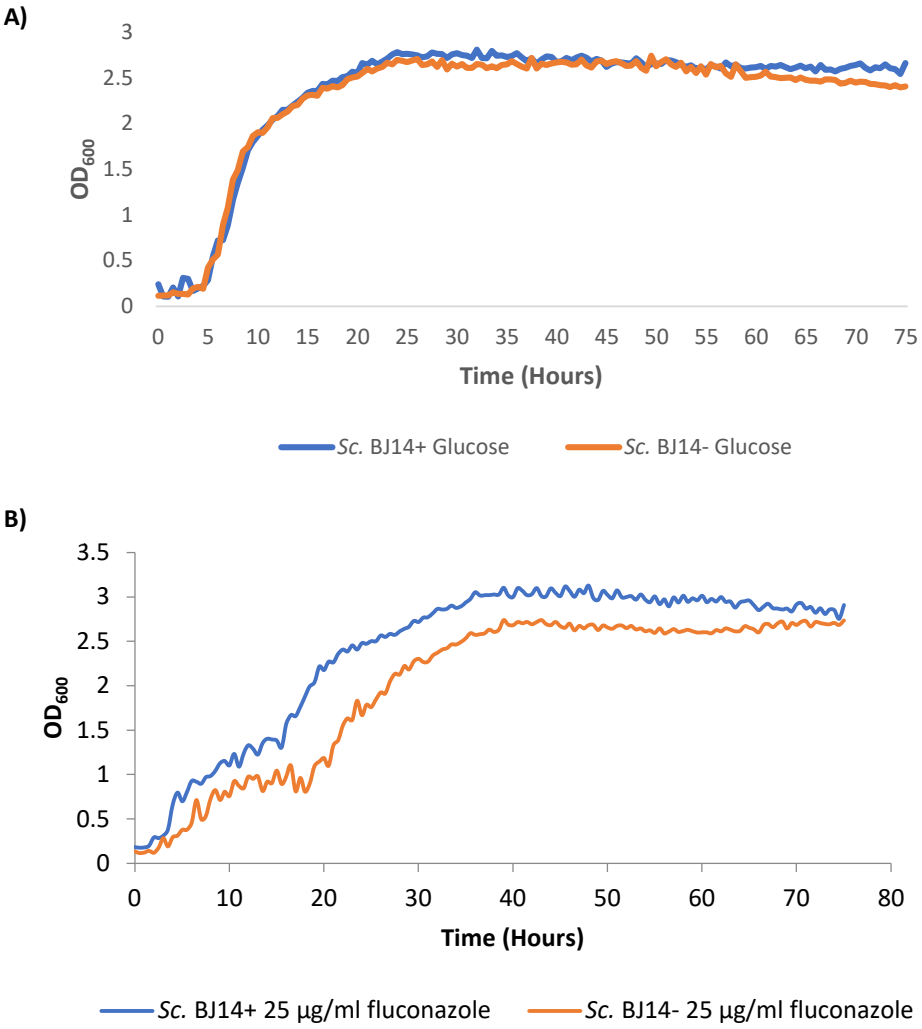

Figure 6.8: Growth profiles of Sc. BJ14+ and Sc. BJ14- in YEPD + 25 µg/ml fluconazole, following three rounds of GdnHCl-mediated curing on solid medium. Panel A) The growth profile of both *Sc.* BJ14 derivates in glucose. **Panel B)** The growth profile of *Sc.* BJ14^{-} reveals a statistically significant decrease in growth, when compared to the growth rate of its non-cured derivative. The data reflects the average of three biological replicates, each with two technical repeats.

In support of previous literature, our findings showed that the *Sc.* strain BJ14 was slightly more resistant to fluconazole in the wild type [*PRION*$^{+}$] state (**Figure 6.8**). It could be inferred that this particular strain has an increased chance of survival in the presence of fluconazole, which may be a trait encoded by a naturally-occurring prion.

Interestingly, *Sc*. BJ6 only showed resistance to sordarin at certain concentrations of the drug when in the [*PRION*$^{+}$] state. At concentrations of less than 0.5 µg/ml sordarin, the GdnHCl-cured version of *Sc*. BJ6 displayed a higher level of resistance, compared to its non-cured derivative. At 0.5 µg/ml to 1 µg/ml sordarin, *Sc.* BJ6 showed a reproducible higher growth and survival rate when in the [*PRION*$^{+}$] state (**Figure 6.9**). These results are indicative of a change in the level of resistance when a certain threshold is reached. It can be inferred that at increasingly harmful levels of sordarin, the *de novo* appearance of an endogenous prion is upregulated, thus increasing chances of survival in fluctuating, stressful environments.

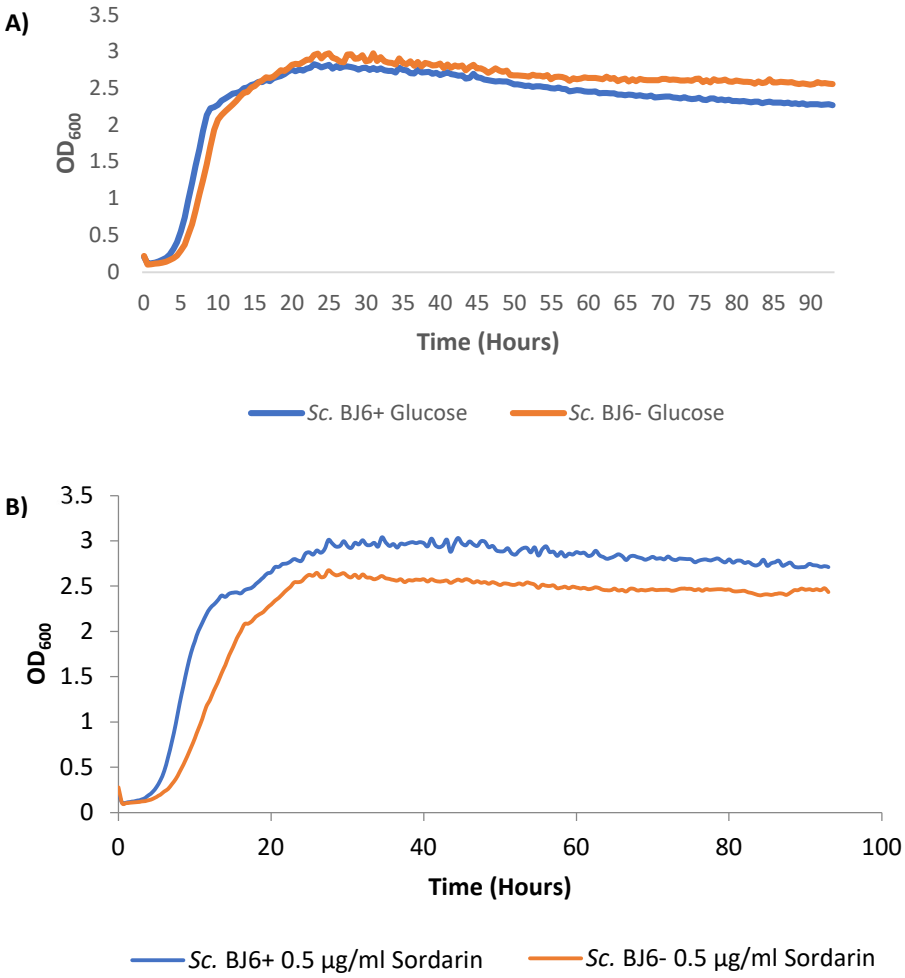

Figure 6.9: Growth profiles of *Sc.* BJ6^{+} and *Sc*. BJ6^{-} in YEPD + 0.5 µg/ml sordarin, following three rounds of GdnHCl-mediated curing on solid medium. Panel A) The growth of both BJ6 derivatives in glucose. **Panel B)** The growth profile of *Sc*. BJ6^{-} reveals a statistically significant decrease in growth, when compared to the growth rate of its non-cured derivative, in contrast with results at lower concentrations of sordarin. The data reflects the average of three biological replicates, each with two technical repeats.

6.5. All non-domesticated wild strains of *S. cerevisiae* are [*pin*$^-$]

The presence of an endogenous [*PIN*$^+$] state in wild strains of *S. cerevisiae* may indicate the biological relevance of prions occurring in non-laboratory strains and further highlight the requirement of advantageous prion-mediated phenotypes being maintained across generations. To evaluate this, in twelve wild strains of *S. cerevisiae*, the joining of a GFP-tagged Rnq1 fragment to endogenous prion aggregates made of the homologous Rnq1 protein was visualised by the formation of fluorescent foci, indicative of endogenous [*PIN*$^+$]. pAG426-RNQ1-GFP was expressed in all strains under the control of the *GAL1* promoter. In [*PIN*$^+$] *S. cerevisiae,* endogenous Rnq1p induces the exogenous *Sc*Rnq1-GFP to convert to the prion form, thus forming bright fluorescent foci, while the *Sc*Rnq1-GFP remains soluble and dispersed across the cell in a [*pin*$^-$] state (Derkatch et al., 2001).

In laboratory strains of *S. cerevisiae,* the presence of prions formed by Rnq1 was sufficient in making cells [*PIN*$^+$] (Derkatch et al., 2001). Deletion of the *RNQ1* gene in *Sc.* BY4741 caused the loss of the [*PIN*$^+$]-mediated phenotype, and [*PIN*$^+$] could not be transmitted to the Δ*rnq1* strain via cytoduction. Furthermore, *in vivo Sc*Rnq1-GFP aggregation analyses revealed Rnq1 in an aggregated state in [*PIN*$^+$] *Sc.* BY4741 (Derkatch et al., 2001). In support of these findings, *Sc*Rnq1-GFP was detected as bright fluorescent foci in the [*PIN*$^+$] control strain *Sc.* BY4741 (**Figure 6.10)**

In contrast, *Sc*Rnq1-GFP was expressed in twelve wild strains of *S. cerevisiae* using a plasmid conferring hygromycin B resistance to these strains. Yeast cells containing this plasmid were directly selected following transformation by growth on hygromycin B. All wild strains under test displayed *Sc*Rnq1-GFP as a soluble protein with fluorescence diffusely dispersed across all cells, confirming the [*pin*$^-$] state of all non-domesticated wild strains of *S. cerevisiae* (**Figure 6.10**).

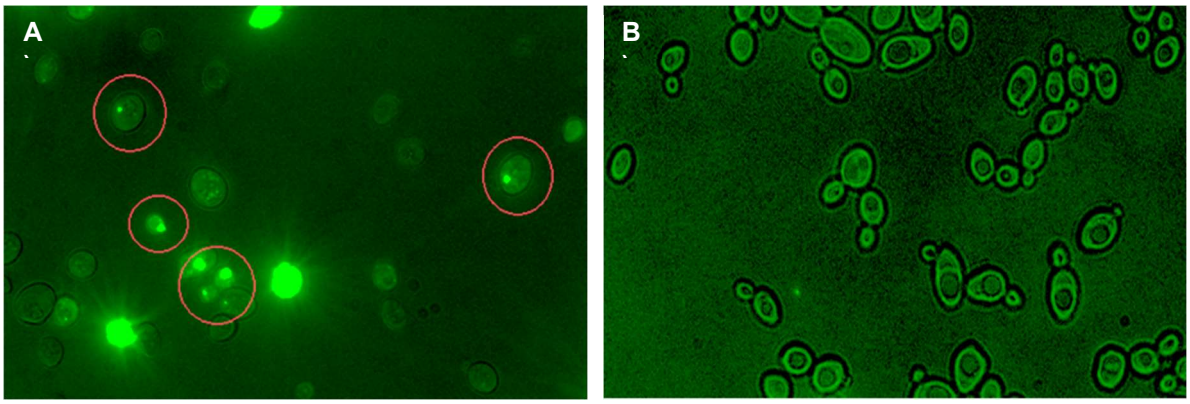

Figure 6.10: Expression of ScRnq1-GFP in both laboratory and wild strains of *S. cerevisiae*. Panel A) *Sc*Rnq1-GFP forms bright fluorescent foci in [*PIN*$^+$] control *Sc.* BY4741 highlighted by red circles. **Panel B)** *Sc*Rnq1-GFP forms diffuse dispersed fluorescence in *Sc.* HN11, representative of all wild strains of *S. cerevisiae*. All non-domesticated wild strains displayed diffuse fluorescence, confirming their [*pin*$^-$] state. Images shown were taken by fluorescent microscopy during both log and stationary phases of growth, following 24 hours induction with galactose. Each strain was visualised in three independent biological experiments, and at least 200 cells per condition were visualised.

The [*pin*$^-$] state revealed in all wild strains of *S. cerevisiae* in this study may contribute to the debate that prions in yeast are laboratory cultivated. However, in 70 alternative wild strains of *S. cerevisiae* originating from various geographical locations such as Belgium and West Africa, 11 were found to be strong [*PIN*$^+$] candidates, with clear formation of *Sc*Rnq1-GFP foci that was cured by growth on GdnHCl (Nakayashiki et al., 2005). This highlights the presence of [*PIN*$^+$] in individual wild strains of *S. cerevisiae.*

6.6. Characterisation of the [*GAR*$^+$] prion in *Saccharomyces* and non-domesticated wild strains of *S. cerevisiae*

As described in Chapter 1, Section 1.6.6 the [*GAR*$^+$] trait results in an override in the preference of carbon source in yeast, in contrast with [*gar*$^-$] cells which act as metabolic specialists primarily metabolising glucose. [*GAR*$^+$] cells are also resistant to glucosamine, a monosaccharide which structural similarity to glucose that cannot be metabolised by yeast (Jarosz, Lancaster, et al.,

2014). The [*GAR*$^{+}$] state creates a bacteria-friendly environment by reducing the ethanol output by >50%, and it has been suggested that such promotion of survival in less favourable environments comes from the secretion of chemical messengers from bacteria in close proximity to the yeast (Jarosz, Brown, et al., 2014). More recently, this chemical messenger was identified as lactic acid, which caused yeast cells to heritably bypass glucose repression on exposure (Garcia et al., 2016). Lactic acid also induced [*GAR*$^{+}$]-associated phenotypes in fungi with ~200 million years of evolutionary distance from *S. cerevisiae*, indicating the independent evolution of glucose repression and highlighting the significance of a bacterial metabolite with the ability to induce a yeast prion (Garcia et al., 2016)

6.6.1. *S. bayanus* is naturally [*GAR*$^{+}$], indicated by successful growth on GGM

To explore whether or not all species of *Saccharomyces* had the [*GAR*$^{+}$] phenotype, all species of *Saccharomyces* were grown on medium containing 2% glycerol and 0.05% glucosamine (GGM), to select for [*GAR*$^{+}$] strains with resistance to glucosamine and the ability to utilise glycerol as a carbon source. Previous studies have identified the laboratory strains *Sc.* BY4741 and *Sc.* 74D-694 as [*GAR*$^{+}$], as well as the genetically marked wild strains *Sc.* 3903, *Sc.* 3913 and *Sc.* 3923 (M.F.Tuite, unpublished data) taking these as suitable control strains for growth on GGM. Two strains of *S. bayanus* displayed a strong level of growth on GGM, indicative of a strong [*GAR*$^{+}$] phenotype in this species (**Figure 6.11**). However, further analyses are required to confirm the presence of the [*GAR*$^{+}$] prion as this prion is not Hsp104 dependent and hence would not be eliminated by GdnHCl-mediated curing (Brown & Lindquist, 2009).

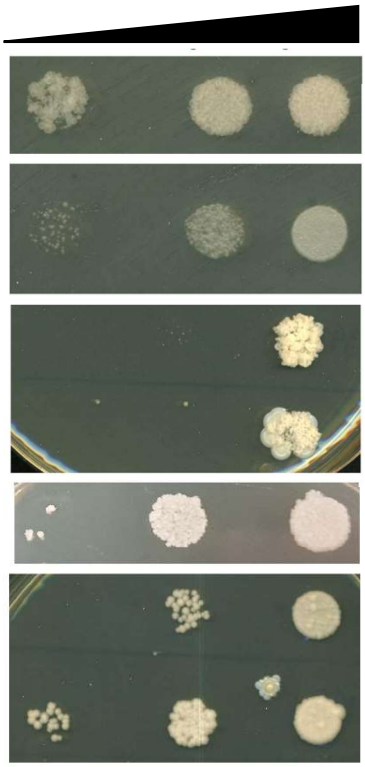

Figure 6.11: *S. bayanus* is [*GAR*$^+$], indicated by successful growth on GGM. Control strains of [*GAR*$^+$] *S. cerevisiae* are also shown, displaying a range of strong and weak [*GAR*$^+$] phenotypes by varying degrees of growth on GGM. The data shown are representative of three biologically independent experiments for each strain.

6.6.2.[*GAR*$^+$] is identified in non-domesticated wild strains of *S. cerevisiae*

As with strains of *Saccharomyces,* all wild strains of *S. cerevisiae* were grown on medium containing 2 % glycerol and 0.05 % glucosamine (GGM). All [*prion*$^-$] derivatives were also grown on GGM following GdnHCl-mediated prion curing, to confirm that [*GAR*$^+$] behaves the same in wild strains of *S. cerevisiae* i.e. does not rely on Hsp104 for propagation.

Seven wild strains of *S. cerevisiae* were found to be [*GAR*$^+$] by their ability to grow on GGM medium (**Figure 6.12**). Interestingly, in comparison with *Sc.* HN14 in its natural [*PRION*$^+$] state, the GdnHCl-cured [*prion*$^-$] derivative did not grow. This difference in growth between cured and non-cured derivatives of the same strain may suggest a differentiation in the level of the [*GAR*$^+$] phenotype, as suggested by Brown and Lindquist (2009). Weak and strong [*GAR*$^+$]-associated

phenotypes are shown by small and large colonies respectively, and weak [*GAR*$^{+}$] strains have been shown to convert to strong levels of [*GAR*$^{+}$]-associated growth, indicating a favourable selection of the strong phenotype (Brown & Lindquist, 2009). The 'strength' of this phenotype may be altered during GdnHCl-curing in certain strains, leading to varying levels of growth on GGM (**Figure 6.12**). This may imply either (a) a role for Hsp104 or an alternative target of GdnHCl in [*GAR*$^{+}$] yeast, or (b) a relationship between GdnHCl-induced *petite* mutants and the [*GAR*$^{+}$] trait. Furthermore, the presence of papillae observed in some strains in **Figure 6.12** may indicate 'stronger' [*GAR*$^{+}$] strains emerging in the cell population.

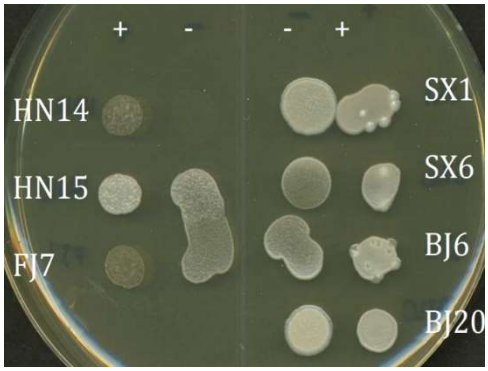

Figure 6.12: Identification of [*GAR*$^{+}$] strains of wild *S. cerevisiae* by successful growth on GGM, following three rounds of curing with GdnHCl. Seven wild strains of *S. cerevisiae* grow on GGM, indicative of the presence of the [*GAR*$^{+}$] prion in these strains. The data shown are representative of three biologically independent experiments for each strain.

6.7. Discussion

The findings reported in this chapter suggest the possible presence of endogenous prions in *Saccharomyces* species and non-domesticated wild strains of *S. cerevisiae* which may control phenotypic traits that impact on a cell's chance of survival in unfavourable and fluctuating environments. A summary of the experimental findings of this chapter can be found in **Table 6.1**, outlining both prions and prion-related phenotypes detected in the strains and species under test. Prion-related phenotypes may either be detrimental or advantageous to the strain in question, refer to relevant sections for details.

Table 6.1: Endogenous prion states and prion-related phenotypes detected in the strains and species under test. Ticks indicate both the prion state and prion-related phenotypes confirmed in each strain. Prion-related phenotypes may either be detrimental or advantageous to the strain in question, refer to relevant sections for details.

	S. bayanus	*S. mikatae*	*S. kudriavzevii*	*Sc.* HN11	*Sc.* SX2	*Sc.* HN15	*Sc.* BJ14	*Sc.* SX6	*Sc.* BJ6	*Sc.* HN14	*Sc.* FJ7	*Sc.* SX1	*Sc.* BJ20
NaCl			✓	✓									
Maltose							✓						
Fructose					✓		✓						
Galactose				✓		✓	✓						
Fluconzaole	✓						✓						
Sordarin									✓				
Cycloheximide								✓					
[*PIN*$^+$]													
[*pin*$^-$]	✓	✓	✓	✓	✓	✓	✓	✓	✓	✓	✓	✓	✓
[*GAR*$^+$]	✓					✓		✓	✓	✓	✓	✓	✓
[*gar*$^-$]		✓	✓	✓	✓		✓						

Notably, searching for prion-mediated phenotypic traits that are sensitive to GdnHCl-mediated curing only allows uncovering those yeast prions which rely on Hsp104 for their propagation. There has been no evidence that GdnHCl can inhibit any other molecular chaperones although some e.g. Hsp70 do have associated ATPase activity and are involved in prion propagation albeit indirectly (Newnam et al., 1999). While Hsp104 is the core chaperone involved in prion regulation

and propagation, its role is carried out in association with co-chaperones, such as members of the Hsp70 family (Kryndushkin & Wickner, 2007).

The presence of well-established *S. cerevisiae* prions such as [*PIN*$^+$] and [*GAR*$^+$] reveals distinct individual differences between strains and species. A number of proteins such as Pma1, Std1 and Hxt3 were identified as playing key roles in the [*GAR*$^+$]-associated phenotype in *S. cerevisiae,* and have different degrees of sequence conservation in other yeast species such as *S. bayanus* (Jarosz, Lancaster, et al., 2014). Further analyses into the % identities and % similarities of these proteins in other *Saccharomyces* species is required. Prion-based strategies as responses to metabolic stresses are therefore likely to extend across various *Saccharomyces* species and possibly wider afield.

[*GAR*$^+$] is an example of a yeast prion which is able to transmit its epigenetic state without Hsp104, and instead relies on Hsp70 (Jarosz, Lancaster, et al., 2014). This is also the case for the novel non-amyloid prion [*SMAUG*$^+$] which is responsible for delaying meiosis in response to starvation and formed by the RNA-binding protein Vts1 (Parfenova & Barral, 2020). Using a fluorescent reporter repressed by Vts1, [*SMAUG*$^+$] was found in several natural yeast isolates, enabling these yeasts to optimise sporulation efficiency depending on nutrient availability in their environment. The self-templating properties of this prion have denoted it as a ‘transgenerational memory element’, as [*SMAUG*$^+$] cells are able to ‘predict’ the duration of their next starvation period based on the history of the strain (Parfenova & Barral, 2020).

Chapter 7: Final Discussion

7. Chapter 7: Final Discussion

Prions are protein-based epigenetic determinants that undergo self-perpetuating, heritable changes in their structure, resulting in an alternative conformational form of a protein that typically assembles in cells into amyloid-based aggregates. To date, fungal prions have been almost exclusively studied in laboratory-bred strains of *S. cerevisiae,* and in this thesis I have broadened their study to wild strains i.e. non-laboratory strains of *S. cerevisiae* and three related *Saccharomyces* species: *S. bayanus, S. mikatae* and *S. kudriavzevii.*

7.1. The impact of guanidine hydrochloride on genetic and epigenetic determinants in *Saccharomyces species*

In order to identify prion-associated traits in each *Saccharomyces* species under examination, cells were exposed to low mM levels of GdnHCl in rich growth media. This is a commonly used method for prion "curing" in *S. cerevisiae,* converting a [*PRION*$^{+}$] cell to a [*prion*$^{-}$] state (Edskes et al., 1999; Tuite et al., 1981). Both treatment with GdnHCl and the concomitant loss of Hsp104 activity also leads a loss of mitochondrial function in *S. cerevisiae* (Juliani et al., 1973) raising the question of whether it is the loss of Hsp104 activity or some other facet of GdnHCl exposure that leads to the generation of *petite* mutants. Remarkably, GdnHCl still induced *petite* mutants in *S. cerevisiae* in the absence of Hsp104 (see Chapter 4), implicating the possibility of an alternative target of GdnHCl in *petite* generation. Hsp104 may therefore be a primary target of GdnHCl, but an alternative protein or proteins may play a role in *petite* mutant generation in the absence of this protein.

An alternate candidate for the target of GdnHCl in *petite* generation was hypothesised to be Hsp78; a disaggregase located in the mitochondrial matrix with similar activity to the cytosolic Hsp104. Hsp78 plays a key role in the translocation and initial stabilisation of proteins in the absence of Hsp70; a co-chaperone of Hsp104 (Schmitt et al., 1996). Thus, both the role

and location of Hsp70 in *S. cerevisiae* made this protein a likely candidate that mediated GdnHCl-induced *petite* generation.

However, the experimental findings reported in Chapter 4 suggest that the mitochondrially-located molecular chaperone Hsp78 is not directly impacted in GdnHCl-induced *petite* generation. An alternative protein target of GdnHCl may instead be one (or more) members of the Hsp70 chaperone protein family. This hypothesis is developed from the notion that both the integrity of the mitochondrial genome, and a sufficient mitochondrial membrane potential necessary for efficient protein import, requires at least one of Hsp70 and Hsp78, in the absence of Hsp104 (Moczko et al., 1995).

In the same manner in which GdnHCl may target Hsp70; an ATPase, this chemical agent was also shown to reactivate a dormant septin assembly pathway in *S. cerevisiae,* that was suppressed in this species during fungal evolution (Johnson et al., 2020). Septin proteins evolved from an ancestral GTPase, and co-assemble into hetero-oligomers, but subsequently lost the ability to hydrolyse GTP (Leipe et al., 2002). Johnson et al*.,* (2020) showed that GdnHCl occupies the site of an evolutionarily 'missing' arginine in *S. cerevisiae,* thus steering the protein towards the shape required to make the six-unit complex, reactivating the septin assembly pathway (Johnson et al., 2020). Moreover, Shu et al*.,* (2019) showed that GdnHCl inhibits the ATP hydrolysis and RNA helicase activities of Ebola virus (EBOV) VP35; an RNA polymerase cofactor which forms part of the EBOV ribonucleoprotein (RNP) complex (Shu et al., 2019). Such findings emphasise the additional targets of GdnHCl, and findings by Shu et al*.,* (2019) highlight the potential of this chemical to target helicases in *S. cerevisiae.* More specifically, one could hypothesise that Hmi1; a mitochondrially-localised helicase required for mitochondrial maintenance and function (Sedman et al., 2000), is a potential target of GdnHCl in *petite* generation.

7.2. Can prion-associated traits in other *Saccharomyces* species by identified by GdnHCl-mediated curing?

Using GdnHCl-mediated prion curing, prion-associated traits were identified in other *Saccharomyces* species. The experimental findings reported in Chapter 6 highlight the possible existence of phenotypes linked to one or more endogenous prions in *Saccharomyces* species other than *S. cerevisiae* as well as in genetically undefined wild strains of *S. cerevisiae*. These prions may control phenotypic traits that impact on a cell's chance of survival in unfavourable and fluctuating environments which these organisms are exposed to in their 'natural habitats', such as conditions of high osmolarity. However, searching for prion-mediated phenotypic traits that are sensitive to GdnHCl-mediated curing only allows us to reveal a class of prions which rely on Hsp104 for their propagation.

To date, there is no evidence that GdnHCl inhibits molecular chaperones other than Hsp104, although certain co-chaperones e.g. Hsp70, associate with Hsp104 ATPase activity and are indirectly involved in prion propagation (Newnam et al., 1999). Hsp70 is also thought to be responsible for the initial binding and stabilisation of mitochondria-imported misfolded substrate proteins, releasing them to Hsp78 for direct degradation in an ATP-dependent manner (Röttgers et al., 2002). Changes in the level of proteins by inhibition or overexpression can also remove prion traits, seen by inhibition and overproduction of Hsp104 (Ness et al., 2002; Ness et al., 2017), and overproduction of the chaperone Sse1, which eliminates the [*URE3*] yeast prion (Kryndushkin & Wickner, 2007). Sse1 together with a second co-chaperone Fes1 are nucleotide exchange factors which promote the release of ADP by Hsp70, thus allowing ATP to bind and thereby affecting the abilities of Hsp70 to bind, release and refold substrate proteins. Deletion of either the *SSE1* or *FES1* genes completely blocks [*URE3*] propagation (Kryndushkin & Wickner, 2007). Future studies should therefore employ the use of inhibitors of other chaperone proteins and relevant gene knockouts, such as *SSE1* or *FES1*, in order to uncover Hsp104-**in**dependent prion proteins in other *Saccharomyces* species.

7.3. Alternative mechanisms of protein inheritance in *Saccharomyces* species

In addition to the studies of Hsp104-independent prion proteins in other *Saccharomyces* species, future work should also broaden the search for prions in *Saccharomyces* and strains of *S. cerevisiae* to encompass prion-like elements that do not fulfil all the classic properties of a yeast prion e.g. mnemons (Caudron & Barral, 2013). An example of protein that can switch conformation to a mnemon form is Whi3 which encodes the 'memory' of a mating pheromone refractory state (Caudron & Barral, 2013). After prolonged exposure to a mating pheromone in the absence of a successful mating partner, budding yeast cells escape pheromone-induced cell cycle arrest through coalescence of the G1 cell cycle inhibitor Whi3 into a dominant, inactive super assembly, and resume their cell cycle (Caudron & Barral, 2013). Furthermore, these cells bud for the remainder of their life span even in the presence of mating pheromone, highlighting a memory state (Caudron et al., 2020). This pheromone refractory state remains stable over many cell cycles but is not passed on to daughter cells during mating. Mnemons share structural features with prions, yet the maintenance and asymmetric inheritance of $Whi3^{mnem}$ is unknown, and remains to be characterised in both *S. cerevisiae* and *Saccharomyces* species (Caudron et al., 2020). Preliminary studies into the sequence similarity of *WHI3* between *Saccharomyces* species reveals a relatively high degree of amino acid conservation between *S. cerevisiae* and *S. bayanus* and *S. mikatae,* at 81% and 85% respectively. The scores of *WHI3* sequence similarity could not be calculated for *S. kudriavzevii* as this particular gene sequence was only accessible as an incomplete shotgun sequence. Future work should focus on (a) the exact alignment of Whi3 between *Saccharomyces* species (b) key sequence features relative to the conformational switch to a mnemon, and (c) the possible production of mating pheromones in these species.

The molecular chaperone Hsp70 prevents the formation of Whi3 super-assemblies, while Hsp104 promotes their formation, thus highlighting a complex role for molecular chaperones in prion-like elements that also remains to be established in alternative *Saccharomyces* species (Caudron & Barral, 2013).

An alternative strategy with potential for uncovering protein-based epigenetic determinants in *Saccharomyces* species is the transient overexpression of proteins, used by Chakrabortee et al*.,* (2016) to uncover traits that remained heritable long after their relative protein expression returned to normal (Chakrabortee et al., 2016). Such protein overexpression uncovered a common type of protein-based inheritance in *S. cerevisiae,* through which intrinsically disordered proteins drive the emergence of novel phenotypes (Chakrabortee et al., 2016). Similarly, Sideri et al*.,* (2017) used a proteome-wide screen to identify the Ctr4 copper transporter subunit as a potential prion-forming candidate in *S. pombe,* with a predicted prion-like domain (Sideri et al., 2017). Overexpression of the *CTR4* gene resulted in large protein aggregates that were heritable in a non-Mendelian fashion, corresponding with other fungal prions (Sideri et al., 2017). This strategy uncovered the first transmissible protein-based determinant of trait in fission yeast, but naturally-occurring prion-like proteins in species of *Saccharomyces* are yet to be addressed using this method.

Moreover, Simpson-Lavy et al*.,* (2017) uncovered a controlled, non-pathological role of protein aggregation in the regulation of glucose response mechanisms. SNF1; responsible for the switch from respiration to fermentation in *S. cerevisiae,* is reduced by a reversible non-amyloid aggregation of Std1 (Simpson-Lavy et al., 2017). Std1 aggregation may function as short-term memory of prior nutrient status, thus regulating Snf1 function, leading to a change in phenotype in *S. cerevisiae* (Simpson-Lavy et al., 2017). The potential for this mechanism in species of *Saccharomyces* remains to be established.

7.4. The impact of natural genetic variation on protein aggregation in *Saccharomyces* species

In addition to searching for prion-related phenotypes in species of *Saccharomyces,* the ability of these genetically-related species to facilitate and perpetuate the formation of other amyloid-forming but heterologous proteins; in particular the Alzheimer's-related protein Aβ42 and Huntington's disease-associated Htt-polyQ, was examined. The results indicate that each of the

Saccharomyces species under test can propagate the aggregated forms of Aβ42 and polyQ, but these amyloid states were differentially impacted upon by the endogenous prion state of the host yeast species. Chemical inhibition of Hsp104 demonstrated that Htt-Q97 aggregates are unable to form in *Saccharomyces* species, namely *S. bayanus* and *S. mikatae.* Deletion of the *HSP104* gene in *S. cerevisiae* supported these findings, and the use of *HSP104* gene knockouts in other *Saccharomyces* species would further complement the strategy used here i.e. chemical inhibition of Hsp104 using GdnHCl. The inability of Htt-Q97 to aggregate in *Saccharomyces* species following Hsp104 inhibition suggests a requirement for a [*PIN*$^{+}$]-like prion and indirectly Hsp104 in Htt-Q97 aggregation, since Hsp104 is required for prion maintenance in yeast (Meriin et al., 2002). By contrast, the same experiments showed that aggregation of Aβ42 does not require an endogenous prion or Hsp104 in any species tested, as Aβ42 aggregates remained in all *Saccharomyces* species following GdnHCl-induced inhibition of Hsp104. Similarly, the results outlined in this thesis indicate that Upf1, but not Upf2 or Upf3, is essential for the aggregation of Htt-Q97 in *S. cerevisiae*, but not for the aggregation of Aβ42 and further highlights the differing requirements for maintenance of these amyloid-forming proteins.

The Upf1/2/3 proteins form the nonsense-mediated decay (NMD) complex that recognises premature stop codons in mRNA transcripts at the ribosome, and Upf1p is responsible for shuttling mRNA transcripts containing premature stop codons to P-bodies for degradation (Mendell & Dietz, 2008). Unlike in *S. cerevisiae,* an animal with a *UPF1* knockout is not viable, indicating the possibility of a further requirement of this protein separate to its role in NMD (Mendell & Dietz, 2008). Interestingly, mammals also have two Upf3 genes; *UPF3a* and *UPF3*b, highlighting subtle differences between the NMD complexes in mammals and *S. cerevisiae* (Mendell & Dietz, 2008). Despite these differences, our experimental findings highlight the role of *UPF1* in Htt-Q97 aggregation in *S. cerevisiae*, which may indicate a role of Upf1 in mammalian disease-associated amyloid aggregation and a potential as an anti-aggregation target.

Son and Wickner (2018) showed that Upf1 and Upf3 were frequently detected as anti-prion genes in a genetic screen (Son & Wickner, 2018). Interestingly, almost all [*PSI*$^{+}$] variants that arose in the absence of these proteins were eliminated by restoring the Upf1 and Upf3 protein levels back to normal (Son & Wickner, 2018). Upf1 and Upf3 may therefore act as anti-aggregation targets, by either (a) blocking the addition of new monomers to the Sup35 amyloid or (b) blocking the propagation of new [*PSI*$^{+}$] prion variants. Interestingly, Urakov et al*.,* (2018) showed that Upf1 only acted as an anti-[*PSI*$^{+}$] protein in the presence of Pub1; an RNA-binding protein (Urakov et al., 2018). The interplay between Upf1, Pub1, and [*PIN*$^{+}$] in *S. cerevisiae* is yet to be established, but [*PIN*$^{+}$]-associated aggregation may decrease in the absence of Upf1, thus inhibiting the aggregation of Htt-Q97.

Using Htt-72Q expressed in *S. cerevisiae,* Aktar et al*.,* (2019) also showed that Htt-GFP depends on Hsp104 for aggregation; with an inability to form inclusion bodies in a Δ*hsp104* strain (Aktar et al., 2019). Moreover, *rnq1*Δ strains expressing Htt-72Q were also unable to form inclusion bodies, small particles, aggregates or liquid assemblies, indicative of the requirement of Rnq1 for Htt-GFP aggregation (Aktar et al., 2019; Meriin et al., 2002; Peskett et al., 2018). Aktar et al*.,* (2019) also showed that Htt-GFP inclusions concentrate together with Hsp104, which is expressed significantly above cytoplasmic levels in the inclusion body. This may suggest a specific role for Hsp104 in catalysing Htt fibres in the cytoplasm, before unwinding them in the inclusion body (Aktar et al., 2019).

These findings, along with the experimental outcomes reported in this thesis indicate the possibility of either (a) a direct role for Hsp104 in Htt-polyQ aggregation or (b) an indirect role for Hsp104 in Htt-polyQ aggregation via an effect on an Hsp104 substrate that is in turn required for aggregation. However, the precise involvement in aggregation interaction remains to be established. It seems most likely that Htt-polyQ directly relies on a [*PIN*$^{+}$]-like factor for aggregation, much like the [*PSI*$^{+}$] prion. Htt-polyQ may use [*PIN*$^{+}$] as a template for initial seed formation, and co-localisation studies with Htt-polyQ, [*PIN*$^{+}$] and Hsp104 may help to uncover a more specific role of these proteins in Htt-polyQ aggregation. Following seed formation, it is possible that [*PIN*$^{+}$] may act as a 'distraction'

mechanism to Hsp104, reducing the clearance of Htt-Q97 by directly competing for Hsp104 binding, thus titrating its activity. The findings reported in this thesis extend the initial observations of the requirement of Hsp104 for Htt-polyQ aggregation into other species of *Saccharomyces,* as chemical inhibition of Hsp104 in these species demonstrated that Htt-Q97 aggregates are unable to form. Remarkably, some other less evolutionary-related fungi have apparently evolved powerful mechanisms to overcome the toxicity associated with aggregating and potentially toxic amyloid protein. This is demonstrated by the fungal pathogen *Candida albicans*, in which the expression of polyQ stretches up to 230Q have no effect on *C. albicans* growth and hence can withstand proteotoxic stress, despite having a glutamine-rich proteome similar to *S. cerevisiae* (Leach et al., 2017). This highlights the possibility that alternate fungal species have the ability to overcome the toxicity associated with Htt-polyQ aggregation, thus providing novel models for the investigation of disease-associated amyloid proteins.

7.5. The cross-species prion transmission barrier

The experimental findings presented in Chapter 3 highlight an inability of other *Saccharomyces* species to form fluorescent GFP foci following the expression of either ScSup35-GFP and ScRnq1-GFP. This finding is consistent with the existence of a cross-species prion transmission barrier rather than an intrinsic inability to form these prions (Chen et al., 2007). The cross-species barrier has been particularly well studied with the [*PSI*$^{+}$] prion in *Saccharomyces* species, where studies have revealed a high level of sequence divergence of the Sup35-PFD between these species resulting in asymmetric prion transmission (Bruce and Chernoff, 2011, see also Chapter 1, Section 1.4.3). [*PSI*$^{+}$] can be transferred between members of *Saccharomyces*, but this depends on the combination of Sup35-PFD sequences used, and the [*PSI*$^{+}$] conformational variant in the *S. cerevisiae* 'donor' strain (Afanasieva et al., 2011; Chen et al., 2007, 2010). It may be that the two related prion proteins are simply unable to interact; oligomers formed by one misfolded protein may be unable to promote the polymerisation of another, and are therefore responsible for the observed prion species barrier. However, the ability of non-*cerevisiae* Sup35 proteins to transform into a stable [*PSI*$^{+}$] conformation in their native cellular context remains to be

established. Remarkably, Nakayashiki et al., (2001) showed the potential of certain [PSI+] prions to overcome this cross-species barrier, with inter-species [PSI+] transmissibility and propagation between Kluyveromyces lactis and S. cerevisiae (Nakayashiki et al., 2001). Grizel, et al., (2016) summarised that the prion strain, amino acid sequence, cell environment, and conditions of the aggregation reaction all play a role in the cross-species prion transmission barrier (Grizel et al., 2016). Studies by Sharma et al., (2015) further highlighted that the major characteristics of the prion species barrier between members of *Saccharomyces* are determined by protein sequence, rather than intracellular environment, shown by transfection of cellular extract from one species to another (Sharma et al., 2015). Protein aggregation of both *S. bayanus* and *S. paradoxus* are also influenced by the type of anion present during the formation of the initial prion seed (Sharma et al., 2015). More specifically, salts present during seed formation determine the seed conformation, which in turn influences the efficiency of conformational adaptation of the added monomer to the preformed nuclei provided by the seed (Sharma et al., 2015). Salt present during amyloid formation can therefore alter the parameters of the species barrier, and a more pronounced barrier was apparent in the more divergent *S. bayanus* (Sharma et al., 2015). Future experimental work should therefore focus on overcoming the issue of the *Saccharomyces*-associated species barrier, by cloning *SUP35* and *RNQ1* genes from all *Saccharomyces* species, to create GFP fusions that can be expressed in each of the species. The corresponding expression of Sup35-GFP and Rnq1-GFP fusions in each of the *Saccharomyces* species may uncover more distinct barriers associated with certain species combinations.

7.6. Yeast models of neurodegenerative diseases

S. cerevisiae has served as a primary model for a variety of key cellular processes, including but not limited to the impact of oxidative stress on mitochondrial morphology (Rogov et al., 2018) and autophagy (Reggiori & Klionsky, 2013). The *Saccharomyces* Genome Database (https://www.yeastgenome.org/) is a readily available toolkit providing comprehensive biological information for *Saccharomyces cerevisiae,* making relevant material available to establish techniques for the genetic manipulation and modification of this species. *S. cerevisiae*-based models have therefore been used to unravel several human disease mechanisms including the molecular mechanisms underlying cancer (Ferreira et al., 2019). It has also provided an important

resource for characterising the ~17% of yeast genes which exist as members of orthologous gene families associated with human diseases (Foury, 1997). Using high-throughput screening methods, the expression of human proteins in yeast cells has also been significant for the discovery of chemical or protein inhibitors of their activity (Heinicke et al., 2007). *S. cerevisiae* has also been exploited as a suitable model for neurodegenerative disorders, due to the presence of a number of endogenous amyloid-forming proteins, including prions. To date, ~12 different prions have been identified in yeast, which are linked to either a loss of normal protein function, or a gain by that protein of a novel function (Wickner et al., 2018). *S. cerevisiae* has also provided a model for the discovery of alternative mechanisms of protein inheritance (Caudron & Barral, 2013; Chakrabortee et al., 2016) *S. cerevisiae* has therefore given us insight into amyloid protein-associated disease mechanisms, specific aspects of the pathobiology of neurodegenerative disorders, the role of cellular factors in protein-associated toxicity, and novel mechanisms of molecular memory.

Studies with *S. cerevisiae* has also contributed to the development of potential therapeutic strategies, by identifying molecular chaperones that disaggregate potentially toxic forms of disease-related proteins. Hsp104 has been identified as essential for the maintenance of several endogenous prions, as well as the aggregation of Huntington's disease-associated Htt-Q97 (see Chapter 5). Although there is no mammalian orthologue of Hsp104, this yeast chaperone can disaggregate and reduce levels of toxicity associated with several protein aggregates involved in neurodegenerative disorders (March et al., 2019).

There are however limitations in using *S. cerevisiae* as a disease model that must not be overlooked. Firstly, yeast cell-based neurodegenerative disease models typically involve expression of the target protein, and the evaluation of cell toxicity or protein aggregation. However, in their typical disease state, such proteins often interact with other proteins within the neuron for which there is no yeast orthologue, giving rise to the disease pathology. One example of this can be found with the AD-associated Tau protein, which is not toxic when expressed in

yeast, yet displays levels of toxicity when co-expressed with αsynuclein (Zabrocki et al., 2005). Further studies should therefore seek to replicate neuron-specific pathways in yeast; involving the correct expression and localisation of multiple heterologous proteins simultaneously. Secondly, in the majority of yeast cell-based disease models, the expression of the target protein is often regulated to be on or off. This limits studies into disease-associated proteins with an aggregation propensity that is concentration dependent.

On the other hand, throughout this thesis, species of *Saccharomyces* have been used to explore extrachromosomal regulators of phenotypic heterogeneity, and the ability of these species to facilitate and perpetuate the formation of other amyloid-forming proteins. However, using alternate species of yeast as model organism may provide unique challenges and limitations. Despite being included in the first genomic comparisons of the *Saccharomyces* group, there is only one strain of *S. mikatae* for which genomic data are available; limiting the levels of inter-strain variation to be uncovered in this species (Borneman & Pretorius, 2014). Moreover, the largest collection of *S. mikatae* strains all originate from environments in one country i.e. Japan, further limiting the potential levels of inter-strain variation. In contrast, studies using *S. kudriavzevii* have isolated strains from both Japan and Europe, representing a range of ecological niches. Furthermore, strains of *S. bayanus* are predominantly highly recombined, interspecific hybrids that comprise almost equal genomic contributions from *S. eubayanus* and *S. uvarum,* with minor input (70-80 kb) from *S. cerevisiae* (Libkind et al., 2011).

Despite the limitations faced by the use of *Saccharomyces* species, even a single representative strain of a species provides an additional point of comparison to other *Saccharomyces* species. Overall, yeast cell-based models remain as first-step models of neurodegenerative disorders (Tuite, 2019), and expanding studies into other species of *Saccharomyces* provides considerable potential to develop more disease-relevant models in the future.

References

Abrahão, J., Mokry, D. Z., & Ramos, C. H. I. (2017). Hsp78 (78 kDa heat shock protein), a representative AAA family member found in the mitochondrial matrix of *Saccharomyces cerevisiae. Frontiers in Molecular Biosciences*, *4*(AUG), 1–6. https://doi.org/10.3389/fmolb.2017.00060

Acta, B., Evans, I. H., Diala, E. S., Alison, E. A. R. L., & Wilkie, D. (1980). Mitochondrial control of cell surface characteristics in *Saccharomyces cerevisiae. Biochimica et Biophysica Acta. 602*, 201–206.

Afanasieva, E. G., Kushnirov, V. V., Tuite, M. F., & Ter-Avanesyan, M. D. (2011). Molecular basis for transmission barrier and interference between closely related prion proteins in yeast. *Journal of Biological Chemistry*, *286*(18), 15773–15780. https://doi.org/10.1074/jbc.M110.183889

Aktar, F., Burudpakdee, C., Polanco, M., Pei, S., Swayne, T. C., Lipke, P. N., & Emtage, L. (2019). The huntingtin inclusion is a dynamic phase-separated compartment. *Life Science Alliance*, *2*(5), 1–14. https://doi.org/10.26508/lsa.201900489

Alberti, S., Halfmann, R., King, O., Kapila, A., & Lindquist, S. (2009). A Systematic Survey Identifies Prions and Illuminates Sequence Features of Prionogenic Proteins. *Cell*, *137*(1), 146–158. https://doi.org/10.1016/j.cell.2009.02.044

An, L., Fitzpatrick, D., & Harrison, P. M. (2016). Emergence and evolution of yeast prion and prion-like proteins. *BMC Evolutionary Biology*, *16*(1), 1–13. https://doi.org/10.1186/s12862-016-0594-3

Baer, M., & Ross, E. (2020). Identifying the compositional features facilitating recruitment of prion-like domains to stress granules. *FASEB Journal*, *34*.

Bagriantsev, S., & Liebman, S. (2006). Modulation of Aβ42 low-n oligomerization using a novel yeast reporter system. *BMC Biology*, *4*, 1–12. https://doi.org/10.1186/1741-7007-4-32

Bailleul-Winslett, P. A., Newnam, G. P., Wegrzyn, R. D., & Chernoff, Y. O. (2000). An antiprion effect of the anticytoskeletal drug latrunculin A in yeast. *Gene Expression*, *9*(3), 145–156. https://doi.org/10.3727/000000001783992650

Baskakov, I. V., Legname, G., Baldwin, M. A., Prusiner, S. B., & Cohen, F. E. (2002). Pathway complexity of prion protein assembly into amyloid. *Journal of Biological Chemistry*,

277(24), 21140–21148. https://doi.org/10.1074/jbc.M111402200

Bharadwaj, P., Waddington, L., Varghese, J., & Macreadie, I. G. (2008). A new method to measure cellular toxicity of non-fibrillar and fibrillar Alzheimer's Aβ using yeast. *Journal of Alzheimer's Disease*, *13*(2), 147–150. https://doi.org/10.3233/JAD-2008-13204

Borneman, A. R., & Pretorius, I. S. (2014). Genomic insights into the *Saccharomyces sensu stricto* complex. *Genetics*, *199*(2), 281–291. https://doi.org/10.1534/genetics.114.173633

Brachmann, C. B., Davies, A., Cost, G. J., Caputo, E., Li, J., Hieter, P., & Boeke, J. D. (1998). Designer deletion strains derived from *Saccharomyces cerevisiae* S288C: A useful set of strains and plasmids for PCR-mediated gene disruption and other applications. *Yeast*, *14*(2), 115–132. https://doi.org/10.1002/(SICI)1097-0061(19980130)14:2<115::AID-YEA204>3.0.CO;2-2

Brown, J. C. S., & Lindquist, S. (2009). A heritable switch in carbon source utilization driven by an unusual yeast prion. *Genes and Development*, *23*(19), 2320–2332. https://doi.org/10.1101/gad.1839109

Bruce, K. L., & Chernoff, Y. O. (2011). Sequence specificity and fidelity of prion transmission in yeast. *Seminars in Cell and Developmental Biology*, *22*(5), 444–451. https://doi.org/10.1016/j.semcdb.2011.03.005

Brundin, P., Melki, R., & Kopito, R. (2010). Prion-like transmission of protein aggregates in neurodegenerative diseases. *Nature Reviews Molecular Cell Biology*, *11*(4), 301–307. https://doi.org/10.1038/nrm2873

Byers, J. S., & Jarosz, D. F. (2014). Pernicious Pathogens or Expedient Elements of Inheritance: The Significance of Yeast Prions. *PLoS Pathogens*, *10*(4), 0–3. https://doi.org/10.1371/journal.ppat.1003992

Byrne, L. J., Cole, D. J., Cox, B. S., Ridout, M. S., Morgan, B. J. T., & Tuite, M. F. (2009). The number and transmission of [*PSI*$^{+}$] prion seeds (propagons) in the yeast *Saccharomyces cerevisiae*. *PLoS ONE*, *4*(3). https://doi.org/10.1371/journal.pone.0004670

Byrne, L. J., Cox, B. S., Cole, D. J., Ridout, M. S., Morgan, B. J. T., & Tuite, M. F. (2007). Cell division is essential for elimination of the yeast [*PSI*$^{+}$] prion by guanidine hydrochloride.

Proceedings of the National Academy of Sciences of the United States of America, *104*(28), 11688–11693. https://doi.org/10.1073/pnas.0701392104

Caine, J., Sankovich, S., Antony, H., Waddington, L., Macreadie, P., Varghese, J., & Macreadie, I. (2007). Alzheimer's Aβ fused to green fluorescent protein induces growth stress and a heat shock response. *FEMS Yeast Research*, *7*(8), 1230–1236. https://doi.org/10.1111/j.1567-1364.2007.00285.x

Caudron, F, Lau, Y., Parfenova, I., Saarikangas, J., & Barral, Y. (2020). A mechanism to prevent transformation of the Whi3 mnemon into a prion. *BioRXRiv*

Caudron, Fabrice, & Barral, Y. (2013). A Super-Assembly of Whi3 encodes memory of deceptive encounters by single cells during yeast courtship. *Cell*, *155*(6), 1244–1257. https://doi.org/10.1016/j.cell.2013.10.046

Chakrabortee, S., Byers, J. S., Jones, S., Garcia, D. M., Bhullar, B., Chang, A., She, R., Lee, L., Fremin, B., Lindquist, S., & Jarosz, D. F. (2016). Intrinsically Disordered Proteins Drive Emergence and Inheritance of Biological Traits. *Cell*, *167*(2), 369-381.e12. https://doi.org/10.1016/j.cell.2016.09.017

Chakrabortee, S., Kayatekin, C., Newby, G. A., Mendillo, M. L., Lancaster, A., & Lindquist, S. (2016). Luminidependens (LD) is an Arabidopsis protein with prion behavior. *Proceedings of the National Academy of Sciences of the United States of America*, *113*(21), 6065–6070. https://doi.org/10.1073/pnas.1604478113

Chen, B., Bruce, K. L., Newnam, G. P., Gyoneva, S., Romanyuk, A. V., & Chernoff, Y. O. (2010). Genetic and epigenetic control of the efficiency and fidelity of cross-species prion transmission. *Molecular Microbiology*, *76*(6), 1483–1499. https://doi.org/10.1111/j.1365-2958.2010.07177.x

Chen, B., Newnam, G. P., & Chernoff, Y. O. (2007). Prion species barrier between the closely related yeast proteins is detected despite coaggregation. *Proceedings of the National Academy of Sciences of the United States of America*, *104*(8), 2791–2796. https://doi.org/10.1073/pnas.0611158104

Chen, X. J., & Clark-Walker, G. D. (1999). The petite mutation in yeasts: 50 years on. *International Review of Cytology*, *194*, 197–238. https://doi.org/10.1016/s0074-

7696(08)62397-9

Cheng, M. H. K., Hoffmann, P. C., Franz-Wachtel, M., Sparn, C., Seng, C., Maček, B., & Jansen, R. P. (2018). The RNA-Binding Protein Scp160p Facilitates Aggregation of Many Endogenous Q/N-Rich Proteins. *Cell Reports*, *24*(1), 20–26. https://doi.org/10.1016/j.celrep.2018.06.015

Chernoff, Y. O., Lindquist, S. L., Ono, B. I., Inge-Vechtomov, S. G., & Liebman, S. W. (1995). Role of the chaperone protein Hsp104 in propagation of the yeast prion-like factor [*PSI*$^{+}$]. *Science*, *268*(5212), 880–884. https://doi.org/10.1126/science.7754373

Chernova, T. A., Chernoff, Y. O., & Wilkinson, K. D. (2017). Prion-based memory of heat stress in yeast. *Prion*, *11*(3), 151–161. https://doi.org/10.1080/19336896.2017.1328342

Cohen, M., Appleby, B., & Safar, J. G. (2016). Distinct Prion-Like Strains of Amyloid Beta Implicated in Phenotypic Diversity of Alzheimer Disease. *National Library of Medicine.* 10 (1). 9-17 https://doi.org/10.1080/19336896.2015.1123371

Courchaine, E. M., Lu, A., & Neugebauer, K. M. (2016). Droplet organelles? *The EMBO Journal*, *35*(15), 1603–1612. https://doi.org/10.15252/embj.201593517

Coustou, V., Deleu, C., Saupe, S., & Begueret, J. (1997). The protein product of the het-s heterokaryon incompatibility gene of the fungus *Podospora anserina* behaves as a prion analog. *Proceedings of the National Academy of Sciences of the United States of America*, *94*(18), 9773–9778. https://doi.org/10.1073/pnas.94.18.9773

Cox, B. S. (1965). *A CYTOPLASMIC SUPPRESSOR OF SUPER-SUPPRESSOR IN YEAST*.

Coyne, L. P., & Chen, X. J. (2018). mPOS is a novel mitochondrial trigger of cell death – implications for neurodegeneration. *FEBS Letters*, *592*(5), 759–775. https://doi.org/10.1002/1873-3468.12894

Crow, E. T., & Li, L. (2011). Newly identified prions in budding yeast, and their possible functions. *Seminars in Cell and Developmental Biology*, *22*(5), 452–459. https://doi.org/10.1016/j.semcdb.2011.03.003

D'Angelo, F., Vignaud, H., Di Martino, J., Salin, B., Devin, A., Cullin, C., & Marchal, C. (2013). A yeast model for amyloid-β aggregation exemplifies the role of membrane trafficking and

PICALM in cytotoxicity. *DMM Disease Models and Mechanisms*, *6*(1), 206–216. https://doi.org/10.1242/dmm.010108

Danilov, L. G., Matveenko, A. G., Ryzhkova, V. E., Belousov, M. V., Poleshchuk, O. I., Likholetova, D. V., Sokolov, P. A., Kasyanenko, N. A., Kajava, A. V., Zhouravleva, G. A., & Bondarev, S. A. (2019). Design of a New [*PSI*$^{+}$]-No-More Mutation in SUP35 With Strong Inhibitory Effect on the [*PSI*$^{+}$] Prion Propagation. *Frontiers in Molecular Neuroscience*, *12*(November), 1–14. https://doi.org/10.3389/fnmol.2019.00274

Dehay, B., & Bertolotti, A. (2006). Critical role of the proline-rich region in Huntingtin for aggregation and cytotoxicity in yeast. *Journal of Biological Chemistry*, *281*(47), 35608–35615. https://doi.org/10.1074/jbc.M605558200

Deleault, N. R., Piro, J. R., Walsh, D. J., Wang, F., Jiyan, M., Geoghegan, J. C., & Supattapone, S. (2012). Isolation of phosphatidylethanolamine as a solitary cofactor for prion formation in the absence of nucleic acids. *Proceedings of the National Academy of Sciences of the United States of America*, *109*(22), 8546–8551. https://doi.org/10.1073/pnas.1204498109

DePace, A. H., Santoso, A., Hillner, P., & Weissman, J. S. (1998). A critical role for amino-terminal glutamine/asparagine repeats in the formation and propagation of a yeast prion. *Cell*, *93*(7), 1241–1252. https://doi.org/10.1016/S0092-8674(00)81467-1

Derkatch, I., Bradley, M., Zhou, P., Chernoff, Y., & Liebman, S. (1997). Genetic and Environmental Factors Affecting the de novo Appearance of the [*PSI*$^{+}$] Prion in *Saccharomyces cerevisiae Genetics Society of America*, *29*(7), 522–524. http://www.ncbi.nlm.nih.gov/pubmed/22215956

Derkatch, I. L., Bradley, M. E., Hong, J. Y., & Liebman, S. W. (2001). Prions Affect the Appearance of Other Prions: The Story of [*PIN*$^{+}$] *Cell*, *106*, 171–182. http://genome-www.stanford.edu

Du, Z., Park, K. W., Yu, H., Fan, Q., & Li, L. (2008). Newly identified prion linked to the chromatin-remodeling factor Swi1 in *Saccharomyces cerevisiae*. *Nature Genetics*, *40*(4), 460–465. https://doi.org/10.1038/ng.112

Duan, S. F., Han, P. J., Wang, Q. M., Liu, W. Q., Shi, J. Y., Li, K., Zhang, X. L., & Bai, F. Y.

(2018). The origin and adaptive evolution of domesticated populations of yeast from Far East Asia. *Nature Communications*, *9*(1). https://doi.org/10.1038/s41467-018-05106-7

Duennwald, M. L., Jagadish, S., Muchowski, P. J., & Lindquist, S. (2006). Flanking sequences profoundly after polyglutamine toxicity in yeast. *Proceedings of the National Academy of Sciences of the United States of America*, *103*(29), 11045–11050. https://doi.org/10.1073/pnas.0604547103

Eaglestone, S. S., Ruddock, L. W., Cox, B. S., & Tuite, M. F. (2000). Guanidine hydrochloride blocks a critical step in the propagation of the prion-like determinant [*PSI*$^{+}$] of *Saccharomyces cerevisiae*. *Proceedings of the National Academy of Sciences of the United States of America*, *97*(1), 240–244. https://doi.org/10.1073/pnas.97.1.240

Edskes, H. K., Gray, V. T., & Wickner, R. B. (1999). The [URE3] prion is an aggregated form of Ure2p that can be cured by overexpression of Ure2p fragments. *Proceedings of the National Academy of Sciences of the United States of America*, *96*(4), 1498–1503. https://doi.org/10.1073/pnas.96.4.1498

Edskes, H. K., Khamar, H. J., Winchester, C. L., Greenler, A. J., Zhou, A., Mcglinchey, R. P., Gorkovskiy, A., & Wickner, R. B. (2014). Sporadic distribution of prion-forming ability of Sup35p from yeasts and fungi. *Genetics*. 198 (2). 605-616

Edskes, H. K., McCann, L. M., Hebert, A. M., & Wickner, R. B. (2009). Prion variants and species barriers among *Saccharomyces* Ure2 proteins. *Genetics*, *181*(3), 1159–1167. https://doi.org/10.1534/genetics.108.099929

Fekete, V., Čierna, M., Poláková, S., Piškur, J., & Sulo, P. (2007). Transition of the ability to generate petites in the *Saccharomyces/ Kluyveromyces* complex. *FEMS Yeast Research*, *7*(8), 1237–1247. https://doi.org/10.1111/j.1567-1364.2007.00287.x

Ferreira, R., Limeta, A., & Nielsen, J. (2019). Tackling Cancer with Yeast-Based Technologies. *Trends in Biotechnology*, *37*(6), 592–603. https://doi.org/10.1016/j.tibtech.2018.11.013

Fitzpatrick, D. A., O'Brien, J., Moran, C., Hasin, N., Kenny, E., Cormican, P., Gates, A., Morris, D. W., & Jones, G. W. (2011). Assessment of inactivating stop codon mutations in forty *saccharomyces cerevisiae* strains: Implications for [*PSI*$^{+}$] prion- mediated phenotypes. *PLoS ONE*, *6*(12). https://doi.org/10.1371/journal.pone.0028684

Foury, F. (1997). Human genetic diseases: A cross-talk between man and yeast. *Gene*, *195*(1), 1–10. https://doi.org/10.1016/S0378-1119(97)00140-6

Garcia, D. M., Dietrich, D., Clardy, J., & Jarosz, D. F. (2016). A common bacterial metabolite elicits prion-based bypass of glucose repression. *ELife*, *5*(NOVEMBER2016), 1–17. https://doi.org/10.7554/eLife.17978

Giorgini, F., Guidetti, P., Nguyen, Q. V., Bennett, S. C., & Muchowski, P. J. (2005). A genomic screen in yeast implicates kynurenine 3-monooxygenase as a therapeutic target for Huntington disease. *Nature Genetics*, *37*(5), 526–531. https://doi.org/10.1038/ng1542

Glass, N. L., Jacobson, D. J., & Shiu, P. K. T. (2000). The genetics of hyphal fusion and vegetative incompatibility in filamentous *ascomycete* fungi. *Annual Review of Genetics.*34. 165-186

Glover, J. R., Kowal, A. S., Schirmer, E. C., Patino, M. M., Liu, J., & Lindquist, S. (1997). Self-Seeded Fibers Formed by Sup35 , the Protein Determinant of [*PSI*$^{+}$], a Heritable Prion-like Factor o*f S . cerevisiae*. *Cell.* 89, 811–819.

Goedert, M., & Spillantini, M. G. (2006). A century of Alzheimer's disease. *Science*, *314*(5800), 777–781. https://doi.org/10.1126/science.1132814

Goldfarb, L. G., Brown, P., McCombie, W. R., Goldgaber, D., Swergold, G. D., Wills, P. R., Cervenakova, L., Baron, H., Gibbs, C. J., & Gajdusek, D. C. (1991). Transmissible familial Creutzfeldt-Jakob disease associated with five, seven, and eight extra octapeptide coding repeats in the PRNP gene. *Proceedings of the National Academy of Sciences of the United States of America*, *88*(23), 10926–10930. https://doi.org/10.1073/pnas.88.23.10926

Goldring, E. S., Grossman, L. I., Krupnick, D., Cryer, D. R., & Marmur, J. (1970). The *petite* mutation in Yeast. Loss of mitochondrial deoxyribonucleic acid during induction of *petites* with ethidium bromide. *Journal of Molecular Biology*, *52*(2), 323–335. https://doi.org/10.1016/0022-2836(70)90033-1

Grizel, A. V., Rubel, A. A., & Chernoff, Y. O. (2016). Strain conformation controls the specificity of cross-species prion transmission in the yeast model. *Prion*, *10*(4), 269–282. https://doi.org/10.1080/19336896.2016.1204060

Halfmann, R., Jarosz, D. F., Jones, S. K., Chang, A., Lancaster, A. K., & Lindquist, S. (2012).

Prions are a common mechanism for phenotypic inheritance in wild yeasts. *Nature*, *482*(7385), 363–368. https://doi.org/10.1038/nature10875

Harjes, P., & Wanker, E. E. (2003). The hunt for huntingtin function: Interaction partners tell many different stories. *Trends in Biochemical Sciences*, *28*(8), 425–433. https://doi.org/10.1016/S0968-0004(03)00168-3

Harrison, B., & Zimmerman, S. B. (1984). Nucleic Acids Research Nucleic Acids Research. *Methods*, *12*(21), 8235–8251. https://doi.org/10.1007/978-3-642-04898-2_214

Harrison, L. B., Yu, Z., Stajich, J. E., Dietrich, F. S., & Harrison, P. M. (2007). Evolution of Budding Yeast Prion-determinant Sequences Across Diverse Fungi. *Journal of Molecular Biology*, *368*(1), 273–282. https://doi.org/10.1016/j.jmb.2007.01.070

Heinicke, S., Livstone, M. S., Lu, C., Oughtred, R., Kang, F., Angiuoli, S. V., White, O., Botstein, D., & Dolinski, K. (2007). The Princeton Protein Orthology Database (P-POD): A comparative genomics analysis tool for biologists. *PLoS ONE*, *2*(8). https://doi.org/10.1371/journal.pone.0000766

Hochschild, A., & Yuan, A. . (2017). Commentary: A bacterial global regulator forms a prion. *Frontiers in Microbiology*, *8*(APR), 198–201. https://doi.org/10.3389/fmicb.2017.00620

Hou, F., Sun, L., Zheng, H., Skaug, B., Jiang, Q. X., & Chen, Z. J. (2011). MAVS forms functional prion-like aggregates to activate and propagate antiviral innate immune response. *Cell*, *146*(3), 448–461. https://doi.org/10.1016/j.cell.2011.06.041

Hung, G. C., & Masison, D. C. (2006). N-terminal domain of yeast Hsp104 chaperone is dispensable for thermotolerance and prion propagation but necessary for curing prions by Hsp104 overexpression. *Genetics*, *173*(2), 611–620. https://doi.org/10.1534/genetics.106.056820

Itzhaki, R. F., Lin, W. R., Shang, D., Wilcock, G. K., Faragher, B., & Jamieson, G. A. (1997). Herpes simplex virus type 1 in brain and risk of Alzheimer's disease. *Lancet*, *349*(9047), 241–244. https://doi.org/10.1016/S0140-6736(96)10149-5

Iung, A. R., Coulon, J., Kiss, F., Ekome, J. N., Vallner, J., & Bonaly, R. (1999). Mitochondrial function in cell wall glycoprotein synthesis in *Saccharomyces cerevisiae* NCYC 625 (wild

type) and [rho^0] mutants. *Applied and Environmental Microbiology*, *65*(12), 5398–5402. https://doi.org/10.1128/aem.65.12.5398-5402.1999

Jarosz, D. F., Brown, J. C. S., Walker, G. A., Datta, M. S., Ung, W. L., Lancaster, A. K., Rotem, A., Chang, A., Newby, G. A., Weitz, D. A., Bisson, L. F., & Lindquist, S. (2014). Cross-kingdom chemical communication drives a heritable, mutually beneficial prion-based transformation of metabolism. *Cell*, *158*(5), 1083–1093. https://doi.org/10.1016/j.cell.2014.07.025

Jarosz, D. F., Lancaster, A. K., Brown, J. C. S., & Lindquist, S. (2014). An evolutionarily conserved prion-like element converts wild fungi from metabolic specialists to generalists. *Cell*, *158*(5), 1072–1082. https://doi.org/10.1016/j.cell.2014.07.024

Johnson, C. R., Steingesser, M. G., Weems, A. D., Khan, A., Gladfelter, A., Bertin, A., & McMurray, M. A. (2020). Guanidine hydrochloride reactivates an ancient septin hetero-oligomer assembly pathway in budding yeast. *ELife*, *9*, 1–31. https://doi.org/10.7554/eLife.54355

Jossé, L., Marchante, R., Zenthon, J., Von Der Haar, T., & Tuite, M. F. (2012). Probing the role of structural features of mouse PrP in yeast by expression as Sup35-PrP fusions. *Prion*, *6*(3), 201–210. https://doi.org/10.4161/pri.19214

Juliani, M. H., Costa, S. O. P., & Bacila, M. (1973). Non-chromosomal respiratory deficient mutants induced by guanidine hydrochloride in *Saccharomyces cerevisiae*. *Biochemical and Biophysical Research Communications*, *53*(2), 531–538. https://doi.org/10.1016/0006-291X(73)90694-3

Jung, G., Jones, G., & Masison, D. C. (2002). Amino acid residue 184 of yeast Hsp104 chaperone is critical for prion-curing by guanidine, prion propagation, and thermotolerance. *Proceedings of the National Academy of Sciences of the United States of America*, *99*(15), 9936–9941. https://doi.org/10.1073/pnas.152333299

Kadnar, M. L., Articov, G., & Derkatch, I. L. (2010). Distinct type of transmission barrier revealed by study of multiple prion determinants of Rnq1. *PLoS Genetics*, *6*(1), 31–34. https://doi.org/10.1371/journal.pgen.1000824

Kaufman, S. K., Sanders, D. W., Thomas, T. L., Sharma, A. M., Miller, T. M., Diamond, M. I.,

Kaufman, S. K., Sanders, D. W., Thomas, T. L., Ruchinskas, A. J., & Vaquer-alicea, J. (2016). Tau Prion Strains Dictate Patterns of Cell Pathology , Progression Rate , and Regional Vulnerability In Vivo Article Tau Prion Strains Dictate Patterns of Cell Pathology , Progression Rate , and Regional Vulnerability In Vivo. *Neuron*, 1–17. https://doi.org/10.1016/j.neuron.2016.09.055

Kelly, A. C., Shewmaker, F. P., Kryndushkin, D., & Wickner, R. B. (2012). Sex, prions, and plasmids in yeast. *Proceedings of the National Academy of Sciences of the United States of America*, *109*(40). https://doi.org/10.1073/pnas.1213449109

Kim, J. Il, Cali, I., Surewicz, K., Kong, Q., Raymond, G. J., Atarashi, R., Race, B., Qing, L., Gambetti, P., Caughey, B., & Surewicz, W. K. (2010). Mammalian prions generated from bacterially expressed prion protein in the absence of any mammalian cofactors. *Journal of Biological Chemistry*, *285*(19), 14083–14087. https://doi.org/10.1074/jbc.C110.113464

King, C.-Y., Tittmann, P., Gross, H., Gebert, R., Aebi, M., & Wuthrich, K. (1997). Prion-inducing domain 2 – 114 of yeast Sup35 protein transforms in vitro into amyloid-like filaments. *Proceedings of the National Academy of Sciences of the United States of America. 94*(June), 6618–6622.

Koski, L. B., & Golding, G. B. (2001). The closest BLAST hit is often not the nearest neighbor. *Journal of Molecular Evolution*, *52*(6), 540–542. https://doi.org/10.1007/s002390010184

Krishnan, R., & Lindquist, S. L. (2005). Structural insights into a yeast prion illuminate nucleation and strain diversity. *Nature*, *435*(7043), 765–772. https://doi.org/10.1038/nature03679

Kryndushkin, D., & Wickner, R. B. (2007). Nucleotide Exchange Factors for Hsp70s Are Required for [URE3] Prion Propagation in *Saccharomyces cerevisiae. Molecular Biology of the Cell*, *18*(June), 2149–2154. https://doi.org/10.1091/mbc.E07

Kushnirov, V. V., Kochneva-Pervukhova, N., Chechenova, M., Frolova, N., & Ter-Avanesyan, M. (2000). Prion properties of the Sup35 protein of yeast Pichia methanolica. *The EMBO Journal*, *19*(3), 324–331. https://doi.org/10.1093/emboj/19.3.324

LaFerla, F. M., Green, K. N., & Oddo, S. (2007). Intracellular amyloid-β in Alzheimer's disease. *Nature Reviews Neuroscience*, *8*(7), 499–509. https://doi.org/10.1038/nrn2168

Laurén, J., Gimbel, D. A., Nygaard, H. B., Gilbert, J. W., & Strittmatter, S. M. (2009). Cellular prion protein mediates impairment of synaptic plasticity by amyloid-B oligomers. *Nature*, *457*(7233), 1128–1132. https://doi.org/10.1038/nature07761

Lazarev, V. F., Mikhaylova, E. R., Guzhova, I. V., & Margulis, B. A. (2017). Possible function of molecular chaperones in diseases caused by propagating amyloid aggregates. *Frontiers in Neuroscience*, *11*(MAY), 1–8. https://doi.org/10.3389/fnins.2017.00277

Leach, M. D., Kim, T. H., DiGregorio, S. E., Collins, C., Zhang, Z., Duennwald, M. L., & Cowen, L. E. (2017). *Candida albicans* is resistant to polyglutamine aggregation and toxicity. *G3: Genes, Genomes, Genetics*, *7*(1), 95–108. https://doi.org/10.1534/g3.116.035675

Leipe, D. D., Wolf, Y. I., Koonin, E. V., & Aravind, L. (2002). Classification and evolution of P-loop GTPases and related ATPases. *Journal of Molecular Biology*, *317*(1), 41–72. https://doi.org/10.1006/jmbi.2001.5378

Leonhardt, S. A., Fearson, K., Danese, P. N., & Mason, T. L. (1993). HSP78 encodes a yeast mitochondrial heat shock protein in the Clp family of ATP-dependent proteases. *Molecular and Cellular Biology*, *13*(10), 6304–6313. https://doi.org/10.1128/mcb.13.10.6304

Li, L., & Kowal, A. S. (2012). Environmental Regulation of Prions in Yeast. *PLoS Pathogens*, *8*(11), 1–5. https://doi.org/10.1371/journal.ppat.1002973

Li, L., & Lindquist, S. (2000). Creating a Protein-Based Element of Inheritance. *Science*, *287*, 661–663.

Libkind, D., Hittinger, C. T., Valiero, E., Gonsalves, C., Dover, J., Johnston, M., Goncalves, P., & Sampaio, J. (2011). Microbe domestication and the identification of the wild genetic stock of lager-brewing yeast. *National Academy of Sciences*, *108*(35), 14539-44.

Liu, J. J., Sondheimer, N., & Lindquist, S. L. (2002). Changes in the middle region of Sup35 profoundly alter the nature of epigenetic inheritance for the yeast prion [*PSI*$^{+}$]. *Proceedings of the National Academy of Sciences of the United States of America*, *99*(SUPPL. 4), 16446–16453. https://doi.org/10.1073/pnas.252652099

Lum, R., Tkach, J. M., Vierling, E., & Glover, J. R. (2004). Evidence for an unfolding/threading mechanism for protein disaggregation by *Saccharomyces cerevisiae* Hsp104. *Journal of*

Biological Chemistry, *279*(28), 29139–29146. https://doi.org/10.1074/jbc.M403777200

Maclea, K. S., & Ross, E. D. (2011). Strategies for identifying new prions in yeast. *Prion*, 5 (4). 263-268. https://doi.org/10.4161/pri.17918

Madore, N. (1999). Functionally different GPI proteins are organized in different domains on the neuronal surface. *The EMBO Journal*, *18*(24), 6917–6926. https://doi.org/10.1093/emboj/18.24.6917

Malinovska, L., Palm, S., Gibson, K., Verbavatz, J. M., & Alberti, S. (2015). Dictyostelium discoideum has a highly Q/N-rich proteome and shows an unusual resilience to protein aggregation. *Proceedings of the National Academy of Sciences of the United States of America*, *112*(20), E2620–E2629. https://doi.org/10.1073/pnas.1504459112

March, Z. M., Mack, K. L., & Shorter, J. (2019). AAA+ Protein-Based Technologies to Counter Neurodegenerative Disease. *Biophysical Journal*, *116*(8), 1380–1385. https://doi.org/10.1016/j.bpj.2019.03.007

Marion, R. M., Regev, A., Segal, E., Barash, Y., Koller, D., Friedman, N., & O'Shea, E. K. (2004). Sfp1 is a stress- and nutrient-sensitive regulator of ribosomal protein gene expression. *Proceedings of the National Academy of Sciences of the United States of America*, *101*(40), 14315–14322. https://doi.org/10.1073/pnas.0405353101

Masino, L., Kelly, G., Leonard, K., Trottier, Y., & Pastore, A. (2002). Solution structure of polyglutamine tracts in GST-polyglutamine fusion proteins. *FEBS Letters*, *513*(2–3), 267–272. https://doi.org/10.1016/S0014-5793(02)02335-9

Matthews, C. G. (1914). On the Staining of Yeast Cells by Methylene Blue, etc. *Journal of the Institute of Brewing*, *20*(6), 488–496. https://doi.org/10.1002/j.2050-0416.1914.tb04728.x

McCarthy, C. G. P., & Fitzpatrick, D. A. (2019). Pan-genome analyses of model fungal species. *Microbial Genomics*, *5*(2). https://doi.org/10.1099/mgen.0.000243

McGlinchey, R. P., Kryndushkin, D., & Wickner, R. B. (2011). Suicidal [*PSI*$^{+}$] is a lethal yeast prion. *Proceedings of the National Academy of Sciences of the United States of America*, *108*(13), 5337–5341. https://doi.org/10.1073/pnas.1102762108

Mendell, J., & Dietz, H. (2008). Nonsense-mediated mRNA decay. *Biochemical Society*

Transactions, *36*(3), 514–516. https://doi.org/10.1042/BST0360514

Meriin, A. B., Zhang, X., He, X., Newnam, G. P., Chernoff, Y. O., & Sherman, M. Y. (2002). Huntingtin toxicity in yeast model depends on polyglutamine aggregation mediated by a prion-like protein Rnq1. *Journal of Cell Biology*, *157*(6), 997–1004. https://doi.org/10.1083/jcb.200112104

Moczko, M., Schönfisch, B., Voos, W., Pfanner, N., & Rassow, J. (1995). The mitochondrial ClpB homolog Hsp78 cooperates with matrix Hsp70 in maintenance of mitochondrial function. *Journal of Molecular Biology*, *254*(4), 538–543. https://doi.org/10.1006/jmbi.1995.0636

Moosavi, B., Wongwigkarn, J., & Tuite, M. (2017). Hsp70/Hsp90 co-chaperones are required for efficient Hsp104-mediated elimination of the yeast [*PSI*$^{+}$] prion but not for prion propagation. *Wiley Interscience*, *27*, 167–179.

Moriyama, H., Edskes, H. K., & Wickner, R. B. (2000). [URE3] Prion Propagation in *Saccharomyces cerevisiae*: Requirement for Chaperone Hsp104 and Curing by Overexpressed Chaperone Ydj1p. *Molecular and Cellular Biology*, *20*(23), 8916–8922. https://doi.org/10.1128/mcb.20.23.8916-8922.2000

Nagley, P., & Linnane, A. W. (1970). Mutants of Yeast. *Biochemical and Biophysical Research Communications*, *39*(5), 989–996.

Nakayashiki, T., Ebihara, K., Bannai, H., & Nakamura, Y. (2001). Yeast [*PSI*$^{+}$] "prions" that are crosstransmissible and susceptible beyond a species barrier through a quasi-prion state. *Molecular Cell*, *7*(6), 1121–1130. https://doi.org/10.1016/S1097-2765(01)00259-3

Nakayashiki, T., Kurtzman, C. P., Edskes, H. K., & Wickner, R. B. (2005). Yeast prions [URE3] and [*PSI*$^{+}$] are diseases. *Proceedings of the National Academy of Sciences of the United States of America*, *102*(30), 10575–10580. https://doi.org/10.1073/pnas.0504882102

Nan, H., Chen, H., Tuite, M. F., & Xu, X. (2019). A viral expression factor behaves as a prion. *Nature Communications*, *10*(1), 1–11. https://doi.org/10.1038/s41467-018-08180-z

Ness, F., Ferreira, P., Cox, B. S., & Tuite, M. F. (2002). Guanidine Hydrochloride Inhibits the Generation of Prion "Seeds" but Not Prion Protein Aggregation in Yeast. *Molecular and*

Cellular Biology, *22*(15), 5593–5605. https://doi.org/10.1128/mcb.22.15.5593-5605.2002

Ness, Frederique, Cox, B. S., Wongwigkarn, J., Naeimi, W. R., & Tuite, M. F. (2017). Over-expression of the molecular chaperone Hsp104 in *Saccharomyces cerevisiae* results in the malpartition of [*PSI*$^{+}$] propagons. *Molecular Microbiology*, *104*(1), 125–143. https://doi.org/10.1111/mmi.13617

Newnam, G. P., Birchmore, J. L., & Chernoff, Y. O. (2011). Destabilization and recovery of a yeast prion after mild heat shock. *Journal of Molecular Biology*, *408*(3), 432–448. https://doi.org/10.1016/j.jmb.2011.02.034

Newnam, G. P., Wegrzyn, R. D., Lindquist, S. L., & Chernoff, Y. O. (1999). Antagonistic Interactions between Yeast Chaperones Hsp104 and Hsp70 in Prion Curing. *Molecular and Cellular Biology*, *19*(2), 1325–1333. https://doi.org/10.1128/mcb.19.2.1325

Norremolle, A., Riess, O., Fenger, K., Haaholt, U., & Asger, S. (1994). Trinucleotide repeat elongation in the huntingtin gene in Huntington's disease patients from 85 French families. *Genetic Counseling*, *5*(4), 321–328.

Ogur, M., St. John, R., & Nagai, S. (1957). Tetrazolium overlay technique for population studies of respiration deficiency in yeast. *Science*, *125*(3254), 928–929. https://doi.org/10.1126/science.125.3254.928

Oishi, K., Kurahashi, H., Pack, C. G., Sako, Y., & Nakamura, Y. (2013). A bipolar functionality of Q/N-rich proteins: Lsm4 amyloid causes clearance of yeast prions. *MicrobiologyOpen*, *2*(3), 415–430. https://doi.org/10.1002/mbo3.83

Osherovich, L. Z., Cox, B. S., Tuite, M. F., & Weissman, J. S. (2004). Dissection and design of yeast prions. *PLoS Biology*, *2*(4). https://doi.org/10.1371/journal.pbio.0020086

Pan, K. M., Baldwin, M., Nguyen, J., Gasset, M., Serban, A., Groth, D., Mehlhorn, I., Huang, Z., Fletterick, R. J., Cohen, F. E., & Prusiner, S. B. (1993). Conversion of α-helices into β-sheets features in the formation of the scrapie prion proteins. *Proceedings of the National Academy of Sciences of the United States of America*, *90*(23), 10962–10966. https://doi.org/10.1073/pnas.90.23.10962

Pan, T., Colucci, M., Wong, B. S., Li, R., Liu, T., Petersen, R. B., Chen, S., Gambetti, P., & Sy,

M. S. (2001). Novel Differences between Two Human Prion Strains Revealed by Two-dimensional Gel Electrophoresis. *Journal of Biological Chemistry*, *276*(40), 37284–37288. https://doi.org/10.1074/jbc.M107358200

Papsdorf, K., Kaiser, C. J. O., Drazic, A., Grötzinger, S. W., Haeßner, C., Eisenreich, W., & Richter, K. (2015). Polyglutamine toxicity in yeast induces metabolic alterations and mitochondrial defects. *BMC Genomics*, *16*(1), 1–18. https://doi.org/10.1186/s12864-015-1831-7

Parfenova, I., & Barral, Y. (2020). Yeast Sporulation and [SMAUG+] Prion: Faster Is Not Always Better. *Molecular Cell*, *77*(2), 203–204. https://doi.org/10.1016/j.molcel.2019.12.017

Patel, B. K., & Liebman, S. W. (2007). "Prion-proof" for *[PIN*$^{+}$*]*: Infection with In Vitro-made Amyloid Aggregates of Rnq1p-(132-405) Induces [*PIN*$^{+}$]. *Journal of Molecular Biology*, *365*(3), 773–782. https://doi.org/10.1016/j.jmb.2006.10.069

Patino, M. M., Liu, J. J., Glover, J. R., & Lindquist, S. (1996). Support for the prion hypothesis for inheritance of a phenotypic trait in yeast. *Science*, *273*(5275), 622–626. https://doi.org/10.1126/science.273.5275.622

Paul, K. R., Hendrich, C. G., Waechter, A., Harman, M. R., & Ross, E. D. (2015). Generating new prions by targeted mutation or segment duplication. *Proceedings of the National Academy of Sciences of the United States of America*, *112*(28), 8584–8589. https://doi.org/10.1073/pnas.1501072112

Peskett, T. R., Rau, F., O'Driscoll, J., Patani, R., Lowe, A. R., & Saibil, H. R. (2018). A Liquid to Solid Phase Transition Underlying Pathological Huntingtin Exon1 Aggregation. *Molecular Cell*, *70*(4), 588-601.e6. https://doi.org/10.1016/j.molcel.2018.04.007

Pierce, M. M., Baxa, U., Steven, A. C., Bax, A., & Wickner, R. B. (2005). Is the prion domain of soluble Ure2p unstructured? *Biochemistry*, *44*(1), 321–328. https://doi.org/10.1021/bi047964d

Pious, D. A., & Hawley, P. (1972). Effect of antibiotics on respiration in human cells. *Pediatric Research*, *6*(8), 687–692. https://doi.org/10.1203/00006450-197208000-00007

Prusiner, S. B. (1982). Novel proteinaceous infectious particles cause scrapie. *Science*,

216(4542), 136–144. https://doi.org/10.1126/science.6801762

Radchenko, E., Rogoza, T., Khokhrina, M., Drozdova, P., & Mironova, L. (2011). SUP35 expression is enhanced in yeast containing [*ISP*+], a prion form of the transcriptional regulator Sfp1 . *Prion*, *5*(4), 317–322. https://doi.org/10.4161/pri.18426

Reggiori, F., & Klionsky, D. J. (2013). Autophagic processes in yeast: Mechanism, machinery and regulation. *Genetics*, *194*(2), 341–361. https://doi.org/10.1534/genetics.112.149013

Reidy, M., & Masison, D. C. (2010). Sti1 Regulation of Hsp70 and Hsp90 Is Critical for Curing of *Saccharomyces cerevisiae* [*PSI*$^{+}$] Prions by Hsp104. *Molecular and Cellular Biology*, *30*(14), 3542–3552. https://doi.org/10.1128/mcb.01292-09

Reidy, M., Miot, M., & Masison, D. C. (2012). Prokaryotic chaperones support yeast prions and thermotolerance and define disaggregation machinery interactions. *Genetics*, *192*(1), 185–193. https://doi.org/10.1534/genetics.112.142307

Resende, C. G., Outeiro, T. F., Sands, L., Lindquist, S., & Tuite, M. F. (2003). Prion protein gene polymorphisms in *Saccharomyces cerevisiae*. *Molecular Microbiology*, *49*(4), 1005–1017. https://doi.org/10.1046/j.1365-2958.2003.03608.x

Rizet, G. (1952). Les phénomènes de barrage chez *Podospora anserina*. I. Analyse génétique des barrages entre les souches S et s. *Rev Cytol Biol Veg*, *13*, 51–92.

Rogov, A. G., Ovchenkova, A. P., Goleva, T. N., Kireev, I. I., & Zvyagilskaya, R. A. (2018). New yeast models for studying mitochondrial morphology as affected by oxidative stress and other factors. *Analytical Biochemistry*, *552*, 24–29. https://doi.org/10.1016/j.ab.2017.04.003

Rogoza, T., Goginashvili, A., Rodionova, S., Ivanov, M., Viktorovskaya, O., Rubel, A., Volkov, K., & Mironova, L. (2010). Non-Mendelian determinant [ISP+] in yeast is a nuclear-residing prion form of the global transcriptional regulator Sfp1. *Proceedings of the National Academy of Sciences of the United States of America*, *107*(23), 10573–10577. https://doi.org/10.1073/pnas.1005949107

Röttgers, K., Zufall, N., Guiard, B., & Voos, W. (2002). The ClpB homolog Hsp78 is required for the efficient degradation of proteins in the mitochondrial matrix. *Journal of Biological*

Chemistry, *277*(48), 45829–45837. https://doi.org/10.1074/jbc.M207152200

Safar, J. G., Xiao, X., Kabir, M. E., Chen, S., & Kim, C. (2015). *Structural Determinants of Phenotypic Diversity and Replication Rate of Human Prions*. 1–17. https://doi.org/10.1371/journal.ppat.1004832

Saha, A., Wittmeyer, J., & Cairns, B. R. (2006). Chromatin remodelling: The industrial revolution of DNA around histones. *Nature Reviews Molecular Cell Biology*, *7*(6), 437–447. https://doi.org/10.1038/nrm1945

Santoso, A., Chien, P., Osherovich, L. Z., & Weissman, J. S. (2000). Molecular basis of a yeast prion species barrier. *Cell*, *100*(2), 277–288. https://doi.org/10.1016/S0092-8674(00)81565-2

Satpute-Krishnan, P., Langseth, S. X., & Serio, T. R. (2007). Hsp104-dependent remodeling of prion complexes mediates protein-only inheritance. *PLoS Biology*, *5*(2), 0251–0262. https://doi.org/10.1371/journal.pbio.0050024

Scannell, D. R., Zill, O. A., Rokas, A., Payen, C., Dunham, M. J., Eisen, M. B., Rine, J., Johnston, M., & Hittinger, C. T. (2011). The awesome power of yeast evolutionary genetics: New genome sequences and strain resources for the *Saccharomyces sensu stricto* genus. *G3: Genes, Genomes, Genetics*, *1*(1), 11–25. https://doi.org/10.1534/g3.111.000273

Schmitt, M., Neupert, W., & Langer, T. (1995). Hsp78, a Clp homologue within mitochondria, can substitute for chaperone functions of mt-hsp70. *The EMBO Journal*, *14*(14), 3434–3444. https://doi.org/10.1002/j.1460-2075.1995.tb07349.x

Schmitt, Matthias, Neupert, W., & Langer, T. (1996). The molecular chaperone Hsp78 confers compartment-specific thermotolerance to mitochondria. *Journal of Cell Biology*, *134*(6), 1375–1386. https://doi.org/10.1083/jcb.134.6.1375

Schulte, T. W., Akinaga, S., Soga, S., Sullivan, W., Stensgard, B., Toft, D., & Neckers, L. M. (1998). Antibiotic radicicol binds to the N-terminal domain of Hsp90 and shares important biologic activities with geldanamycin. *Cell Stress and Chaperones 3*(2) 100–108. https://doi.org/10.1379/1466-1268(1998)003<0100:ARBTTN>2.3.CO;2

Sedman, T., Kuusk, S., Kivi, S., & Sedman, J. (2000). A DNA Helicase Required for Maintenance of the Functional Mitochondrial Genome in *Saccharomyces cerevisiae. Molecular and Cellular Biology*, *20*(5), 1816–1824. https://doi.org/10.1128/mcb.20.5.1816-1824.2000

Shaner, N. C., Lambert, G. G., Chammas, A., Ni, Y., Cranfill, P. J., Baird, M. A., Sell, B. R., Allen, J. R., Day, R. N., Israelsson, M., Davidson, M. W., & Wang, J. (2013). A bright monomeric green fluorescent protein derived from Branchiostoma lanceolatum. *Nature Methods*, *10*(5), 407–409. https://doi.org/10.1038/nmeth.2413

Sharma, A., Bruce, K., Chen, B., Gyoneva, S., Behrens, S., Bommarius, A., & Chernoff, Y. (2015). Contributions of the Prion Protein Sequence, Strain and Environment to the Species Barrier. *Journal of Biological Chemistry*. 291 (3). 1277-88

Shattuck, J. E., Cascarina, S. M., Paul, K. R., & Ross, E. D. (2019). Sky1: at the intersection of prion-like proteins and stress granule regulation. *Current Genetics*, 66. 463-468 https://doi.org/10.1007/s00294-019-01044-z

Shu, T., Gan, T., Bai, P., Wang, X., Qian, Q., Zhou, H., Cheng, Q., Qiu, Y., Yin, L., Zhong, J., & Zhou, X. (2019). Ebola virus VP35 has novel NTPase and helicase-like activities. *Nucleic Acids Research*, *47*(11), 5837–5851. https://doi.org/10.1093/nar/gkz340

Sideri, T., Yashiroda, Y., Ellis, D. A., Rodríguez-López, M., Yoshida, M., Tuite, M. F., & Bähler, J. (2017). The copper transport-associated protein Ctr4 can form prion-like epigenetic determinants in *Schizosaccharomyces pombe*. *Microbial Cell*, *4*(1), 16–28. https://doi.org/10.15698/mic2017.01.552

Simpson-Lavy, K., Xu, T., Johnston, M., & Kupiec, M. (2017). The Std1 Activator of the Snf1/AMPK Kinase Controls Glucose Response in Yeast by a Regulated Protein Aggregation. *Molecular Cell*, *68*(6), 1120-1133.e3. https://doi.org/10.1016/j.molcel.2017.11.016

Soares, E. V. (2011). Flocculation in *Saccharomyces cerevisia*e: A review. *Journal of Applied Microbiology*, *110*(1), 1–18. https://doi.org/10.1111/j.1365-2672.2010.04897.x

Son, M., & Wickner, R. B. (2018). Nonsense-mediated mRNA decay factors cure most [*PSI*$^{+}$] prion variants. *Proceedings of the National Academy of Sciences of the United States of*

America, *115*(6), E1184–E1193. https://doi.org/10.1073/pnas.1717495115

Sondheimer, N., & Lindquist, S. (2000). Rnq1: An epigenetic modifier of protein function in yeast. *Molecular Cell*, *5*(1), 163–172.

Sparrer, J., Santoso, A., Szoka Jr, F., & Weissman, J. (2000). Evidence for the Prion Hypothesis: Induction of the yeast [*PSI*$^{+}$] Factor. *Science*, 289 (5479). 595-9

Speare, J. O., Offerdahl, D. K., Hasenkrug, A., Carmody, A. B., & Baron, G. S. (2010). GPI anchoring facilitates propagation and spread of misfolded Sup35 aggregates in mammalian cells. *EMBO Journal*, *29*(4), 782–794. https://doi.org/10.1038/emboj.2009.392

Stansfield, I., Jones, K. M., Kushnirov, V. V., Dagkesamanskaya, A. R., Poznyakovski, A. I., Paushkin, S. V., Nierras, C. R., Cox, B. S., Ter-Avanesyan, M. D., & Tuite, M. F. (1995). The products of the SUP45 (eRF1) and SUP35 genes interact to mediate translation termination in *Saccharomyces cerevisiae*. *The EMBO Journal*, *14*(17), 4365–4373. https://doi.org/10.1002/j.1460-2075.1995.tb00111.x

Su, T.-Y., & Harrison, P. M. (2019). Conservation of Prion-Like Composition and Sequence in Prion-Formers and Prion-Like Proteins of *Saccharomyces cerevisiae*. *Frontiers in Molecular Biosciences*, *6*(July), 1–9. https://doi.org/10.3389/fmolb.2019.00054

Suzuki, G., & Tanaka, M. (2013). Expanding the yeast prion world. *Prion*, *7*(2), 109–113. https://doi.org/10.4161/pri.22685

Taneja, V., Maddelein, M. L., Talarek, N., Saupe, S. J., & Liebman, S. W. (2007). A Non-Q/N-Rich Prion Domain of a Foreign Prion, [Het-s], Can Propagate as a Prion in Yeast. *Molecular Cell*, *27*(1), 67–77. https://doi.org/10.1016/j.molcel.2007.05.027

Ter-Avanesyan, M. D., Kushnirov, V. V., Dagkesamanskaya, A. R., Didichenko, S. A., Chernoff, Y. O., Inge-Vechtomov, S. G., & Smirnov, V. N. (1993). Deletion analysis of the SUP35 gene of the yeast *Saccharomyces cerevisiae* reveals two non-overlapping functional regions in the encoded protein. *Molecular Microbiology*, *7*(5), 683–692. https://doi.org/10.1111/j.1365-2958.1993.tb01159.x

Tetz, G., & Tetz, V. (2018). Prion-like Domains in Eukaryotic Viruses. *Scientific Reports*, *8*(1), 1–10. https://doi.org/10.1038/s41598-018-27256-w

Toombs, J. A., McCarty, B. R., & Ross, E. D. (2010). Compositional Determinants of Prion Formation in Yeast. *Molecular and Cellular Biology*, *30*(1), 319–332. https://doi.org/10.1128/mcb.01140-09

True, H. L., & Lindquist, S. L. (2000). True 2000 - A yeast prion provides a mechanism for genetic variation and phenotypic diversity. *Nature*, *407*, 477–483. papers3://publication/uuid/1B06DA1B-DA5E-4426-938A-A0C757FB67D8

Tuite, M. F., Mundy, C. R., & Cox, B. S. (1981). Agents that cause a high frequency of genetic change from [*PSI*$^{+}$] to [*psi*$^{-}$] in *Saccharomyces cerevisiae*. *Genetics*, *98*(4), 691–711.

Tuite, Mick F. (2013). The natural history of yeast prions. In *Advances in Applied Microbiology* (1st ed., Vol. 84). 85-137 Elsevier Inc. https://doi.org/10.1016/B978-0-12-407673-0.00003-5

Tuite, Mick F. (2019). Yeast models of neurodegenerative diseases. In *Progress in Molecular Biology and Translational Science* (1st ed., Vol. 168). Elsevier Inc. https://doi.org/10.1016/bs.pmbts.2019.07.001

Tuite, Mick F., & Koloteva-Levin, N. (2004). Propagating prions in fungi and mammals. *Molecular Cell*, *14*(5), 541–552. https://doi.org/10.1016/j.molcel.2004.05.012

Ueom, J., Kwon, S., Kim, S., Chae, Y., & Lee, K. (2003). Acquisition of heat shock tolerance by regulation of intracellular redox states. *Biochimica et Biophysica Acta - Molecular Cell Research*, *1642*(1–2), 9–16. https://doi.org/10.1016/S0167-4889(03)00081-8

Urakov, V. N., Mitkevich, O. V., Dergalev, A. A., & Ter-Avanesyan, M. D. (2018). The Pub1 and Upf1 proteins act in concert to protect yeast from toxicity of the [*PSI*$^{+}$] prion. *International Journal of Molecular Sciences*, *19*(11), 1–13. https://doi.org/10.3390/ijms19113663

Villali, J., Dark, J., Brechtel, T. M., Pei, F., Sindi, S. S., & Serio, T. R. (2020). Nucleation seed size determines amyloid clearance and establishes a barrier to prion appearance in yeast. *Nature Structural and Molecular Biology*, *27*(6), 540–549. https://doi.org/10.1038/s41594-020-0416-6

Von Der Haar, T., Jossé, L., Wright, P., Zenthon, J., & Tuite, M. F. (2007). Development of a novel yeast cell-based system for studying the aggregation of Alzheimer's disease-

associated Aβ peptides in vivo. *Neurodegenerative Diseases*, *4*(2–3), 136–147. https://doi.org/10.1159/000101838

Walsh, I., Giollo, M., Di Domenico, T., Ferrari, C., Zimmermann, O., & Tosatto, S. C. E. (2015). Comprehensive large-scale assessment of intrinsic protein disorder. *Bioinformatics*, *31*(2), 201–208. https://doi.org/10.1093/bioinformatics/btu625

Wang, Q. M., Liu, W. Q., Liti, G., Wang, S. A., & Bai, F. Y. (2012). Surprisingly diverged populations of *Saccharomyces cerevisiae* in natural environments remote from human activity. *Molecular Ecology*, *21*(22), 5404–5417. https://doi.org/10.1111/j.1365-294X.2012.05732.x

Wang, W., Czaplinski, K., Rao, Y., & Peltz, S. W. (2001). The role of Upf proteins in modulating the translation read-through of nonsense-containing transcripts. *EMBO Journal*, *20*(4), 880–890. https://doi.org/10.1093/emboj/20.4.880

Wang, X., Zuo, X., Kucejova, B., & Chen, X. J. (2008). Reduced cytosolic protein synthesis suppresses mitochondrial degeneration. *Nature Cell Biology*, *10*(9), 1090–1097. https://doi.org/10.1038/ncb1769

Wendland, B., & Emr, S. D. (1998). Pan1p, yeast eps15, functions as a multivalent adaptor that coordinates protein-protein interactions essential for endocytosis. *Journal of Cell Biology*, *141*(1), 71–84. https://doi.org/10.1083/jcb.141.1.71

Westermann, B., & Neupert, W. (2000). Mitochondria-targeted green fluorescent proteins: Convenient tools for the study of organelle biogenesis in *Saccharomyces cerevisiae*. *Yeast*, *16*(15), 1421–1427. https://doi.org/10.1002/1097-0061(200011)16:15<1421::AID-YEA624>3.0.CO;2-U

Wickner, R. B. (1994). [*URE3*] as an altered URE2 protein: Evidence for a prion analog in *Saccharomyces cerevisiae*. *Science*, *264*(5158), 566–569. https://doi.org/10.1126/science.7909170

Wickner, R. B., Edskes, H. K., Bateman, D. A., Kelly, A. C., Gorkovskiy, A., Dayani, Y., & Zhou, A. (2013). Amyloids and yeast prion biology. *Biochemistry*, *52*(9), 1514–1527. https://doi.org/10.1021/bi301686a

Wickner, R. B., Kryndushkin, D., Shewmaker, F., McGlinchey, R., & Edskes, H. K. (2018). Study of amyloids using yeast. *Methods in Molecular Biology*, *1779*, 313–339. https://doi.org/10.1007/978-1-4939-7816-8_19

Yue, J. X., Li, J., Aigrain, L., Hallin, J., Persson, K., Oliver, K., Bergström, A., Coupland, P., Warringer, J., Lagomarsino, M. C., Fischer, G., Durbin, R., & Liti, G. (2017). Contrasting evolutionary genome dynamics between domesticated and wild yeasts. *Nature Genetics*, *49*(6), 913–924. https://doi.org/10.1038/ng.3847

Yun, S., Urbanc, B., Cruz, L., Bitan, G., Teplow, D. B., & Stanley, H. E. (2007). Role of electrostatic interactions in amyloid β-protein (Aβ) oligomer formation: A discrete molecular dynamics study. *Biophysical Journal*, *92*(11), 4064–4077. https://doi.org/10.1529/biophysj.106.097766

Zabrocki, P., Pellens, K., Vanhelmont, T., Vandebroek, T., Griffioen, G., Wera, S., Van Leuven, F., & Winderickx, J. (2005). Characterization of α-synuclein aggregation and synergistic toxicity with protein tau in yeast. *FEBS Journal*, *272*(6), 1386–1400. https://doi.org/10.1111/j.1742-4658.2005.04571.x

Zajkowski, T., Mondal, S., Dunin-Horkawicz, S., Lee, M. ., Bense, N. B., & Rothschild, L. (2019). The hunt for ancient prions. *NASA*.

Zenthon, J. F., Ness, F., & Tuite, M. F. (2006). The [*PSI*$^{+}$] Prion of *Saccharomyces cerevisiae* Can Be Propagated by an Hsp104 Orthologue from *Candida albicans*. *5*(2), 217–225. https://doi.org/10.1128/EC.5.2.217

Zhouravleva, G., Frolova, L., Le Goff, X., Le Guellec, R., Inge-Vechtomov, S., Kisselev, L., & Philippe, M. (1995). Termination of translation in eukaryotes is governed by two interacting polypeptide chain release factors, eRF1 and eRF3. *The EMBO Journal*, *14*(16), 4065–4072. https://doi.org/10.1002/j.1460-2075.1995.tb00078.x